

**Novel Traditional Chinese Medicine-Platinum
Compound that Bypasses Mitotic DNA Damage
Checkpoints in Cancer Cells**

GUAN, Huaji

A Thesis Submitted in Partial Fulfillment of
The Requirement for the Degree of Doctor of Philosophy in Pharmacy

The Chinese University of Hong Kong

May 2010

UMI Number: 3445954

All rights reserved

INFORMATION TO ALL USERS

The quality of this reproduction is dependent upon the quality of the copy submitted.

In the unlikely event that the author did not send a complete manuscript and there are missing pages, these will be noted. Also, if material had to be removed, a note will indicate the deletion.



UMI 3445954

Copyright 2011 by ProQuest LLC.

All rights reserved. This edition of the work is protected against unauthorized copying under Title 17, United States Code.



ProQuest LLC
789 East Eisenhower Parkway
P.O. Box 1346
Ann Arbor, MI 48106-1346

Thesis/ Assessment Committee

Professor CHOW, Hee Lum Albert (Chair)

Professor LEE, Vincent Hon Leung (Thesis Supervisor)

Professor AU-YEUNG, Steve Chik Fun (Co-supervisor)

Professor HO, Yee Ping (Co-supervisor)

Professor TO, Kin Wah (Co-supervisor)

Professor BAUM, Lawrence William (Committee Member)

Professor HONKANEN, Richard E. (External Examiner)

Professor WONG, Wing-tak (External Examiner)

Acknowledgements

My deepest gratitude will be given to my four supervisors: Prof. Vincent H.L. Lee, Prof. Yee-ping Ho, Prof. Kenneth K.W. To, and Prof. Steve C.F. Au-yeung. They are great inspirations, devoting scientists, and unconditional friends that I will always look up to.

I would like to express my thankfulness to all the staffs and students of School of Pharmacy. I find help, knowledge, consolations and joy when working with them.

The last place will always be saved for my mother. All the things I do, if there is a reason, are to make her feel proud.

Abstract

Background: A common procedure in current cancer chemotherapy is to induce genomic stress in cancer cells, leading to irreparable DNA damage and eventually cell death. However, there are several DNA repair mechanisms in cancer cells to maintain genomic stability, which require cell cycle checkpoints to stop cell proliferation for DNA damage repair, thereby avoiding errors in cellular events like DNA replication, transcription and mitosis. Among these cell cycle checkpoints, antepause and G2 checkpoints are two gate checkpoints for mitosis. Abrogation of G2 checkpoint has been reported to give rise to synergistic cytotoxic effect with DNA damaging agents, representing a means of circumventing drug resistance in chemotherapy.

Aim: Cisplatin is the first platinum drug that shows promising anti-tumor effect clinically. Oxaliplatin, a third-generation platinum drug that incorporates a diaminocyclohexane (DACH) structural entity, can overcome cisplatin resistance. *R,R*-5, a novel platinum compound that integrates the DACH entity with a demethylcantharidin (DMC) component that is derived from a traditional Chinese medicine (TCM), can also overcome cisplatin resistance. The principal objectives

of this study was to investigate in detail, the effect of these compounds at the antephase and G2 checkpoints of the cell cycle, and to establish the relationship (if any) between different structural entities with checkpoint activation. The ultimate aim of the study was to ascertain the potential for the development of novel checkpoint abrogators as anti-tumor agents.

Methods: Microarray analysis was used to detect gene transcription profiles after drug treatments. The activation of mitotic checkpoints was inspected by counting mitotic cells and utilizing flow cytometry. Using Western blotting, the activation of certain key players in the antephase and G2 checkpoint was revealed. MTT assays were performed to show the outcome of checkpoint activation.

Results: In HCT116 cells, 35 genes that facilitate G2/M transition were found to be up-regulated after *R,R*-5 treatment compared with oxaliplatin in the microarray analysis, implying the bypass of mitotic checkpoints by *R,R*-5 rather than oxaliplatin. Acute stress (2 hour) of cisplatin activated the antephase checkpoint, resulting in a rapid decrease in mitotic index and phosphorylation of histone H1, which avoided mitotic catastrophe and promoted cell survival in HeLa cells. Further experiments demonstrated that this antephase checkpoint could be abrogated by c-Abl and

p38MAPK inhibitors, or siRNAs against c-Abl or MEKK1, suggesting that this checkpoint may be controlled by an MMR/c-Abl/MEKK1/p38MAPK pathway. In contrast, oxaliplatin and *R,R*-5 did not activate this antepause checkpoint. Moreover, after 24 hour oxaliplatin treatment in HeLa cells, the mitotic index and CDK1 activity were decreased, which could be restored by concomitant treatment with ATM/ATR inhibitor and DMC. This indicated the activation of G2 checkpoint by oxaliplatin and implied that DMC can abrogate oxaliplatin-activated G2 checkpoint by restoring CDK1 activity. Cisplatin could also activate G2 checkpoint, whereas *R,R*-5 apparently bypassed this G2 checkpoint.

Conclusions: Acute stress to cisplatin can activate the MMR/c-Abl/MEKK1/p38MAPK pathway, leading to the activation of antepause checkpoint, and stop cells from entering mitosis immediately. DACH-containing platinum compound oxaliplatin fails to activate this antepause checkpoint. However, both cisplatin and oxaliplatin can activate the G2 checkpoint, which can be abrogated by DMC. In contrast, *R,R*-5 can bypass both the antepause and G2 checkpoints. In summary, novel TCM-platinum compound *R,R*-5 can bypass mitotic DNA damage checkpoints in cancer cells and thus has the potential for further development as an anti-cancer drug.

摘要

新型傳統中藥-鉑類化合物躍過腫瘤細胞周期有絲分裂基因 損傷檢查點之研究

研究背景：在腫瘤細胞造成不可修復的基因損傷而致使其死亡，是現時化療的一大策略。然而腫瘤細胞內存在著幾種基因損傷修復機制來維持基因穩定性，這些機制要求激活基因損傷檢查點來停止細胞周期，創造出時間間隔進行基因修復，從而避免在諸如基因複製、轉錄以及有絲分裂等重要細胞事件中出現錯誤。在這些細胞周期檢查點中， antephase和G2 phase是進入有絲分裂前的兩個守衛檢查點。而抑制G2 檢查點已經被報道能增強基因損傷化療藥物的活性，也是化療中對抗腫瘤細胞抗藥性的一種策略。

研究目的：順鉑是臨床試驗中首個顯示抗腫瘤活性的化療藥物。奧沙利鉑是第三代鉑類藥物，其結構中引入了環己二胺對映異構體，能對抗順鉑抗藥性。*R, R*-5 是融合了環己二胺對映異構體和從傳統中藥斑蝥中衍生出來的去甲基斑蝥素的新型鉑類化合物，它同樣能對抗順鉑抗藥性。研究這些化合物對 antephase 和 G2 檢查點可能揭開

結構改造與檢查點激活的關係，甚至導致新型細胞周期檢查點抑制劑的發現。

研究方法: 藥物作用后的細胞基因轉錄譜用生物芯片技術來檢測。細胞周期檢查點的激活用數有絲分裂細胞和流式細胞儀來分析。再用蛋白免疫印跡方法可找出 antephase 和 G2 檢查點信號通路中相關蛋白的激活。MTT 試驗可顯示出檢查點激活和細胞死亡之間的關係。

研究結果: 在HCT116 細胞中，生物芯片檢測結果顯示相比于奧沙利鉑，*R, R-5* 上調了 35 個能促使有絲分裂的基因，說明了*R, R-5* 躍過了有絲分裂檢查點而非奧沙利鉑。在HeLa細胞受順鉑短暫作用兩小時后，出現顯著的有絲分裂細胞數目和組蛋白H1 磷酸化減少，標誌著antephase檢查點的激活，從而阻止有絲分裂錯誤並增加細胞存活。順鉑只能在錯配修復(MMR)陽性的HCT116+ch3 細胞而不能在MMR陰性的HCT116+ch2 細胞中激活antephase檢查點。進一步實驗證明antephase檢查點的激活可以被c-Abl抑制劑和siRNA，MEKK1 siRNA所抑制，但不受ATM/ATR或蛋白磷酸化酶 1/2A抑制劑影響，說明這個檢查點是經由MMR/c-Abl/MEKK1/p38MAPK信號通路被激活。然而奧沙利鉑和*R, R-5* 沒有激活antephase檢查點。當HeLa細胞經過 24 小時奧

沙利鉑作用后，有絲分裂細胞和CDK1 活性明顯減少，而這種現象能被ATM/ATR抑制劑和去甲基斑蝥素所抑制，說明去甲基斑蝥素通過恢復CDK1 活性拮抗了奧沙利鉑激活的G2 檢查點。順鉑也被證實能激活G2 檢查點，而*R, R*-5 則躍過G2 檢查點。

結論：短暫的順鉑作用可以激活 MMR/c-Abl/MEKK1/p38MAPK 信號通路，來激活 antephase 檢查點，從而迅速抑制細胞進入有絲分裂。含有環己二胺對映異構體的奧沙利鉑沒有激活 antephase 檢查點。然而順鉑和奧沙利鉑都能激活 G2 檢查點，但此激活可以被去甲基斑蝥素所抑制。相比之下，*R, R*-5 沒有激活 antephase 或 G2 檢查點。綜而述之，新型傳統中藥-鉑化合物 *R, R*-5 能躍過腫瘤細胞有絲分裂基因損傷檢查點，從而有潛力被開發成新型抗腫瘤藥物。

Publication

Pang, S.K.; Yu, C.W.; **Guan, H.J.**; Au-Yeung, S.C.F.; Ho, Y.P. Impact of oxaliplatin and a novel DACH-platinum complex in the gene expression of HCT116 colon cancer cells. *Oncology Reports*, **2008**; *20*, 1269-76.

Table of Contents

Acknowledgement	II
Abstract	III
Abstract (Chinese)	VI
Publication	IX
Table of Contents	X
Table of Figures	XVII
List of Tables	XXIII
List of Abbreviations	XXIV

Chapter One	Introduction	1
1.1	Traditional Platinum-Based Anti-Tumor Drugs	2
1.2	Design of Novel Traditional Chinese Medicine (TCM)-Platinum Compounds	5
1.3	Previous Studies of Novel TCM-Platinum Compounds	8
1.3.1	Anti-Tumor Activities <i>in vitro</i> and <i>in vivo</i>	8
1.3.2	Pharmacokinetics	9
1.3.3	Biological Evaluation of Compound <i>R,R-5</i>	11
1.4	Protein Phosphatase 2A Inhibitors as Anti-Tumor Agents	14
1.4.1	Biological Properties of PP2A	14
1.4.2	Structure and Function of PP2A	15
1.4.3	Role of PP2A Inhibitors in DNA Damage Repair	19
1.4.4	Role of PP2A Inhibitors in Cell Cycle Regulation	20
1.4.5	Role of PP2A Inhibitors in Apoptosis	27
1.4.6	Potential Use of PP2A Inhibitors in Cancer Chemotherapy	29
1.4.7	Proposed Characteristics of <i>R,R-5</i> as a PP2A Inhibitor	30
1.5	Signal Transduction of DNA Damaging Agents: From Damage Repair to Mitogen-Activated Protein Kinase	31
1.5.1	<i>c-Abl</i> forms the Link between Mismatch Repair and MAPK	33
1.5.2	BRCA1 May Link Homologous Recombination to MAPK	34
1.5.3	Lyn Links the Inhibition of NHEJ to MAPK	36
1.5.4	GADD45 May Link NER to MAPK	40
1.5.5	The Sequential DNA Repair-“Linker”-MAPK Binding Determines Cell Fate	42

1.5.6 Predicted Effect of <i>R,R</i> -5 as a DNA Damaging Agent	44
1.6 Study Objectives	45
Chapter Two cDNA Microarray Analysis	46
2.1 Introduction	46
2.2 Materials and Methods	50
2.2.1 Chemicals and Reagents	50
2.2.2 Cell Lines and Cell Cultures	50
2.2.3 Preparation of RNA Samples	51
2.2.4 RNA Purity	52
2.2.5 Microarray Analysis with the Human HG-U133A GeneChip (Affymetrix Inc.)	53
2.3 Results and Discussions	55
2.3.1 Cell Cycle Regulation	58
2.3.1.1 Genes Related to G1 to S Transition	59
2.3.1.2 Genes Related to G2 to M Transition	63
2.3.2 DNA Replication	72
2.3.3 DNA Damage Repair	73
2.3.4 Other Up-regulated Genes with Miscellaneous Functions and the Down- Regulated Genes	73
2.4 Conclusions	76

Chapter Three c-Abl Activates the Antephase Checkpoint and Promotes Cancer Cell Survival in Response to Acute Stress of Cisplatin

-----Effect of <i>R,R</i>-5 at the Antephase Checkpoint	78
3.1 Introduction	78
3.2 Objectives	89
3.3 Experimental Design	90
3.4 Materials and Methods	92
3.4.1 Chemicals	92
3.4.2 Cell Lines and Cell Cultures	92
3.4.3 Mitotic Index Assay and Examination of Mitotic Catastrophe	93
3.4.4 Immunoblotting (Western Blot) and Immunoprecipitation	94
3.4.4.1 Solutions and Reagents	94
3.4.4.2 Total Protein (Whole Cell Lysate) Extraction	96
3.4.4.3 Histone Extraction	97
3.4.4.4 Protein Electrophoresis	98
3.4.4.5 Membrane Transfer	99
3.4.4.6 Antibody Probing	99
3.4.4.7 Antibodies	100
3.4.4.8 Immunoprecipitation	100
3.4.5 siRNA Transfection	100
3.4.6 Flow Cytometry Analysis	103
3.4.7 MTT Assay and Crystal Violet Staining	108
3.5 Results and Discussions	109
3.5.1 Antephase Checkpoint Was Activated by Cisplatin But Not Oxaliplatin or	

<i>R,R</i> -5	109
3.5.2 Abrogation of Antephase Checkpoint by <i>c</i> -Abl Inhibitor and siRNA	117
3.5.3 Antephase Checkpoint is Absent in Mismatch Repair Deficient Cell Line	122
3.5.4 Abrogation of Antephase Checkpoint Led to Prolonged and Aberrant	
Mitosis	132
3.6 Conclusions	140

Chapter Four Demethylcantharidin Abrogates Oxaliplatin-Activated G2 Checkpoint by Restoring CDK1 Activity, Independent of CHK1/CHK2 Activation -----Effect of *R,R*-5 at the G2 Checkpoint

	142
4.1 Introduction	142
4.2 Objectives	149
4.3 Experimental Design	150
4.4 Materials and Methods	152
4.4.1 Chemicals	152
4.4.2 Cell Lines and Cell Cultures	152
4.4.3 Mitotic Index Assay and Examination of Mitotic Catastrophe	152
4.4.4 Cell Cycle Synchronization and Flow cytometry Analysis	153
4.4.5 Real-time RT-PCR	154
4.4.6 Western Blotting Analysis	155
4.4.7 siRNA Transfection	155
4.4.8 MTT Assay and BrdU Incorporation Assay	156

4.5 Results and Discussions	158
4.5.1 DMC Abrogated Oxaliplatin-Stimulated G2 Checkpoint in HCT116 Cells	158
4.5.2 DMC Restored Oxaliplatin-Decreased Mitotic Index Without Altering G2/M Arrest or DNA Synthesis	162
4.5.3 DMC Restored Oxaliplatin-Crippled CDK1 Activity Independent of CHK1/CHK2 Activation	170
4.5.4 DMC Abrogated Oxaliplatin-stimulated G2 Checkpoint without Up-Regulating CDK1	174
4.5.5 DMC Abrogated Oxaliplatin-Stimulated G2 Checkpoint by Restoring CDK1 Activity	177
4.5.6 DMC Abrogated Oxaliplatin-Stimulated G2 Checkpoint, Leading to Aberrant Mitosis and Failure at Mitotic Exit, and Consequently Inhibition of Cell Survival	185
4.6 Conclusions	194
Chapter Five Conclusions	197
5.1 Effect of <i>R,R</i> -5 at the Antephase Checkpoint (Chapter Three)	200
5.2 Effect of <i>R,R</i> -5 at the G2 checkpoint (Chapter Four)	203
5.3 Summary of the Thesis	207
5.4 Future Work	210

Attachment

Pang, S.K.; Yu, C.W.; Guan, H.J.; Au-Yeung, S.C.F.; Ho, Y.P. Impact of oxaliplatin and a novel DACH-platinum complex in the gene expression of HCT116 colon cancer cells. *Oncology Reports*, **2008**; *20*, 1269-76.

Table of Figures

Figure 1.1	Chemical structures of cisplatin, carboplatin, oxaliplatin and UCN-01.	3
Figure 1.2	DNA damage checkpoints in a cell cycle.	4
Figure 1.3	Chemical structures of cantharidin, demethylcantharidin and novel TCM-Platinum compounds.	7
Figure 1.4	Demethylcantharidin is derived from traditional Chinese medicine blister beetles.	7
Figure 1.5	Hydrolysis reactions of a) cisplatin and b) compound 5.	10
Figure 1.6	Chemical structures of <i>R,R</i> -, <i>S,S</i> -, <i>trans</i> -(±)- and <i>cis</i> -compound 5 and oxaliplatin.	12
Figure 1.7	Chemical structures of PP2A inhibitors.	15
Figure 1.8	The structure and function of PP2A.	16
Figure 1.9	Proposed mechanisms for the effect of PP2A inhibitors on the G1→S cell cycle transition.	18
Figure 1.10	Effect of okadaic acid and TGF-β on G1→S cell cycle entry.	23
Figure 1.11	Effect of okadaic acid on mitosis.	27
Figure 1.12	Effect of okadaic acid on apoptosis.	29
Figure 1.13	Mismatch repair transmits death signal to MAPK via c-Abl.	34
Figure 1.14	Proposed mechanism for inhibition of NHEJ and initiation of death signal transduction by MAPK.	39
Figure 1.15	GADD45 links nucleotide excision repair to MAPK in	41

	response to UV stimulation.	
Figure 1.16	Proposed "linkers" transmit cellular signals from DNA damage repair mechanisms to MAPK.	44
Figure 2.1	Protocol of microarray analysis in HCT116 cells.	48
Figure 2.2	Results from the microarray analysis in HCT116 cells (<i>R,R</i> -5 v.s. oxaliplatin at IC ₅₀).	56
Figure 2.3	Genes related to cell cycle regulation in the microarray analysis (<i>R,R</i> -5 vs. oxaliplatin at respective IC ₅₀ in HCT116 cells).	58
Figure 3.1	Illustration of the proposed checkpoint bypass effect of <i>R,R</i> -5.	79
Figure 3.2	Figures (adapted from Matsusaka <i>et al.</i>) demonstrating the activation of antephasic checkpoint by microtubule disassembly.	82
Figure 3.3	Mitotic catastrophe induced by DNA damage.	84
Figure 3.4	Proposed pathway of antephasic checkpoint activation by cisplatin.	87
Figure 3.5	Inhibitors used in the experiments.	93
Figure 3.6	c-Abl siRNK effectively knocked down c-Abl mRNA level in HeLa cells.	102
Figure 3.7	Cell cycle synchronization using double-thymidine block in HeLa cells	104
Figure 3.8	Mitotic index assay showing that activation of antephasic checkpoint by cisplatin treatment but not oxaliplatin or <i>R,R</i> -5.	111

- Figure 3.9** Mitotic index assay showing that cisplatin did not activate the antephasis checkpoint in c-Abl non-functional HCT116 cells. 112
- Figure 3.10** Western blotting analysis showing the activation of the c-Abl/p38MAPK pathway by cisplatin. 116
- Figure 3.11** Mitotic index assay showing c-Abl and p38MAPK inhibitors abrogated cisplatin-induced antephasis checkpoint activation in HeLa cells. 118
- Figure 3.12** Western blotting analysis showing that the abrogation of cisplatin-induced antephasis checkpoint activation by c-Abl and p38MAPK inhibitors in HeLa cells. 119
- Figure 3.13** Western blotting analysis showing that the abrogation of cisplatin-induced activation of the antephasis checkpoint by c-Abl and MEKK1 siRNAs in HeLa cells. 120
- Figure 3.14** Immunoprecipitation analysis showing that association of c-Abl and p38MAPK with MEKK1 after 1 hr cisplatin treatment in HeLa cells. 121
- Figure 3.15** Mitotic index assay showing that MMR/c-Abl is indispensable for cisplatin-induced antephasis checkpoint activation. 125
- Figure 3.16** Western blotting analysis showing that c-Abl is essential for cisplatin-induced antephasis checkpoint activation in HCT116+ch3 cells. 126
- Figure 3.17** Flow cytometry analysis showing that antephasis arrest 127

	contributed to the G2/M arrest induced by cisplatin.	
Figure 3.18	MTT assay showing that activation of the antephasis checkpoint promoted cancer cell survival after acute stress to cisplatin.	128
Figure 3.19	MTT and crystal violet-staining assay showing that acute cisplatin treatment promoted cell survival in HCT116+ch3 cells but sustain cisplatin treatment led to cell death.	130
Figure 3.20	Mitotic index assay showing that abrogation of antephasis checkpoint led to prolonged mitosis and failure at mitotic exit.	134
Figure 3.21	Flow cytometry analysis showing that abrogation of cisplatin-activated antephasis checkpoint led to failure at mitotic exit.	135
Figure 3.22	Abrogation of antephasis checkpoint activation could lead to mitotic catastrophe.	138
Figure 3.23	Mechanism of antephasis checkpoint activation in response to acute stress of cisplatin.	141
Figure 4.1	Mechanism of G2 checkpoint activation via ATM/ATR.	144
Figure 4.2	A proposed mechanism for the promotion of mitosis by okadaic acid.	148
Figure 4.3	Chemical structures of cisplatin, oxaliplatin, <i>R,R</i> -5 and DMC.	159
Figure 4.4	cDNA microarray analysis showing the up-regulated genes related to G2→M transition after <i>R,R</i> -5 treatment compared with oxaliplatin (at respective IC ₅₀ in HCT116 cells).	160

- Figure 4.5** Cell cycle analysis showing the oxaliplatin-induced G2/M 161
arrest due to G2 checkpoint activation in HCT116 cells.
- Figure 4.6** Mitotic index assay showing that cisplatin and oxaliplatin, but 166
not *R,R*-5, DMC or okadaic acid, could decrease mitotic index
in HCT116 cells.
- Figure 4.7** Mitotic index assay showing that cisplatin and oxaliplatin, but 167
not *R,R*-5 or DMC+oxaliplatin, decreased mitotic index due
to G2 checkpoint activation in HeLa cells.
- Figure 4.8** Cell cycle analysis showing that DMC did not affect 168
oxaliplatin-induced G2/M arrest in HeLa cells.
- Figure 4.9** BrdU incorporation assay showing that DMC did not affect 169
oxaliplatin-inhibited DNA synthesis.
- Figure 4.10** Western blotting analysis showing that activation of G2 173
checkpoint by oxaliplatin was accompanied by CHK1 and
CHK2 activation, and histone H1 dephosphorylation.
- Figure 4.11** Real-time RT-PCR analysis showing that DMC abrogated 176
oxaliplatin-stimulated G2 checkpoint without requirement of
CDK1 transcription.
- Figure 4.12** Western blotting analysis showing that DMC and *R,R*-5 181
maintained histone H1 phosphorylation by restoring CDK1
activity.
- Figure 4.13** Mitotic index assay showing that DMC and *R,R*-5 promoted 183
mitotic entry by restoring CDK1 activity.

- Figure 4.14** Cell cycle assay showing that CDK1 activity was required in 187
DMC- and *R,R*-5-induced mitosis.
- Figure 4.15** Aberrant mitosis cell-counting demonstrating that DMC 190
abrogated oxaliplatin-stimulated G2 checkpoint and led to
mitotic catastrophe.
- Figure 4.16** MTT assay showing that DMC abrogated 193
oxaliplatin-stimulated G2 checkpoint and led to inhibition of
cancer cell survival.
- Figure 4.17** DMC abrogates oxaliplatin-activated G2 checkpoint by 196
restoring CDK1 activity, independent of CHK1/CHK2
activation.
- Figure 5.1** Effect of platinum compounds at mitotic DNA damage 209
checkpoints.

List of Tables

Table 2.1	Microarray analysis of <i>R,R</i> -5 against oxaliplatin at respective IC_{50} in HCT116 cells.	57
Table 2.2	Genes related to G1→S transition that were found up-regulated (<i>R,R</i> -5 vs. oxaliplatin at respective IC_{50} in HCT116 cells).	60
Table 2.3	Genes related to G2→M transition that were found up-regulated (<i>R,R</i> -5 vs. oxaliplatin at respective IC_{50} in HCT116 cells).	67
Table 3.1	Relationship between cell genotype and antephasis checkpoint activation.	115

List of Abbreviations

5-FU	5-aminouracil
ATM	Ataxia telangiectasia mutated
ATR	ATM and Rad3-related
BRCA1	Breast cancer 1
CDC2	Cell Division Cycle 2, also CDK1
CDC6	Cell Division Cycle 6 Homolog
CDC25C	Cell Division Cycle 25C
CDK1	Cyclin-Dependent Kinase 1, also CDC2
DACH	Diaminocyclohexane
DEPC	Diethyl Pyrocarbonate
DMC	Demethylcantharidin
GADD45	Growth Arrest and DNA Aamage-Inducible Gene 45
HMG	High Mobility Group Box
IR	Ionzing Radiation
JNK	c-Jun N-Terminal Kinase
MAD2L1	MAD2 Mitotic Arrest Deficient-Like 1
MCM4	Minichromosome Maintenance Deficient 4
MCM5	Minichromosome Maintenance Deficient 5, cell division cycle 46
MCM7	Minichromosome Maintenance Deficient 7
MCM10	Minichromosome Maintenance Deficient 10
MLH1	MutL Homolog 1

MMR	Mismatch Repair
MMS	Methyl-methanesulfonate
MNNG	N-methyl-N'-nitro-N-nitrosoguanidine
MSH2	MutS Homolog 2
MSH4	MutS Homolog 4
MSH6	MutS Homolog 6
MTT	3-(4,5-Dimethylthiazoly-2)-2,5-Diphenyltetrazolium Bromide
NEK2	NIMA (Never in Mitosis Gene A)-Related Kinase 2
NER	Nucleotide Excision Repair
NMR	Nuclear Magnetic Resonance
NSCLC	Non-Small Cell Lung Cancer
PBS	Phosphate Buffered Saline
PCNA	Proliferating-Cell Nuclear Antigen
PI	Propidium Iodide
PP1	Protein Phosphatase 1
PP2A	Protein Phosphatase 2A
RAD54B	RAD54 Homolog B
RFC	Replication Factor C
SAPK	Stress-Activated Protein Kinase
SCLC	Small Cell Lung Cancer
SMC1	Structural Maintenance of Chromosomes 1-like 1
TBE	Tris-Borate-EDTA
TCM	Traditional Chinese Medicine

TEM	Tail-Extent-Moment
TGF-β	Transforming Growth Factor β
TMZ	Temozolomide
TOP2A	Topoisomerase 2A
WEE1	WEE1 Homolog

Chapter One

Introduction

Cancer is one of the major lethal diseases in U.S.A., which killed 559,888 people (23.1% of mortality) in 2006 (American Cancer Society, Inc., 2009). The three most common cancers are lung/bronchus, prostate, and colon/rectum in male; and lung/bronchus, breast, and colon/rectum in female, respectively. The lifetime probability of developing cancer is 1 in 2 (men), and 1 in 3 (women) (American Cancer Society, Inc., 2009). Some breakthrough in cancer research has been achieved as scientists continued to unlock the mechanisms contributing to the development of cancer. The top 3 curable cancers (>5-year survival after treatment from 1996 to 2004) in American Caucasians are: breast cancer (91% survival), colon cancer (66% survival), and esophagus cancer (18% survival) (National Cancer Institute, 2008). Despite these progresses, cancer metastasis and drug resistance are still major problems facing the cancer patients. A variety of anti-cancer drugs are commonly employed for cancer chemotherapy. However, they may not be effective in certain cancer types and their effectiveness can further be compromised by the emergence of drug resistance. The development of novel anti-tumor agents with distinct mode of action is strongly warranted for this unmet medical need.

1.1 Traditional Platinum-Based Anti-tumor Drugs

Cisplatin, carboplatin and oxaliplatin (Figure 1.1) are three clinically acclaimed platinum-based anti-tumor drugs. Cisplatin was approved by The Food and Drug Administration (FDA) in U.S.A. in 1978 (Wiltshaw *et al.*, 1979; Chabner and Roberts Jr., 2005), and is still commonly used for the treatment of solid tumors, such as testicular, ovarian, bladder, cervical, head and neck, esophageal, and small cell lung cancers (Giaccone, 2000). The acknowledged anti-tumor mechanism of cisplatin is that it can bind to DNA with covalent bonding and consequently induce DNA damage (Lippard and Hoeschele, 1979). However, cisplatin can lead to serious side effects such as nausea and vomiting, nephrotoxicity, ototoxicity, neuropathy and myelosuppression (Krakoff, 1979). Moreover, intrinsic and acquired resistance to cisplatin has also posed a threat to its successful clinical use in the treatment of cancer. Carboplatin, a second-generation platinum drug with similar mechanism as cisplatin, is more soluble in water and less nephrotoxic (Calvert *et al.*, 1982). However, it is cross-resistant to cisplatin. Oxaliplatin, a third-generation platinum compound, was able to overcome the problem of resistance and was the first platinum-based anti-tumor drug approved by the FDA in the mid-90s for the treatment of advanced colorectal cancer (Jakupec *et al.*, 2003). Unfortunately, it was reported to generate neurotoxicity (Extra *et al.*, 1990; Spunt *et al.*, 2007). As a result,

developing novel anti-tumor drugs with high potency and low adverse effects remains a challenging goal for cancer research.

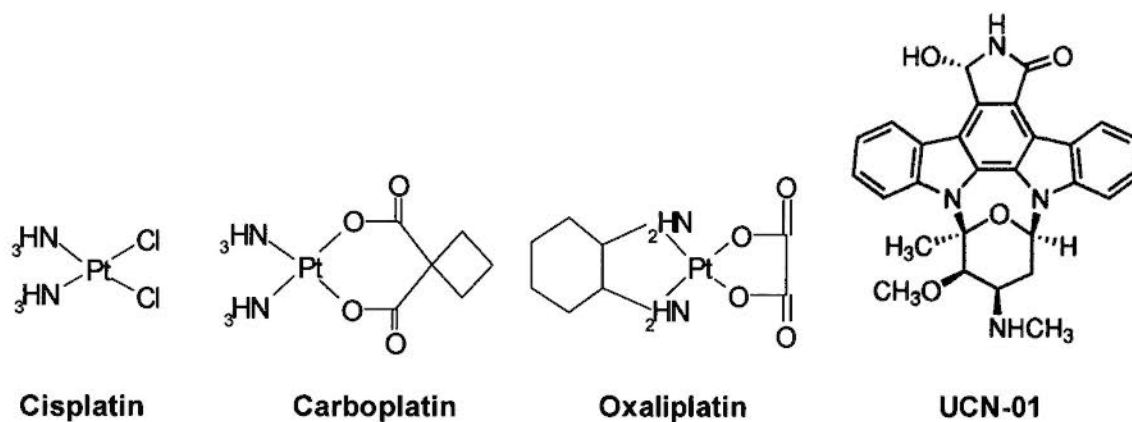


Figure 1.1: Chemical structures of cisplatin, carboplatin, oxaliplatin and UCN-01.

A common strategy in current cancer chemotherapy is to induce DNA damage in cancer cells, thereby leading to cell death. However, this will activate the DNA damage checkpoints of the cell cycle, including the extensively studied G1, S, G2, checkpoints (Dasika *et al.*, 1999), mitotic spindle checkpoint (Gorbsky, 2001), the newly discovered antephasic checkpoint (Mikhailov *et al.*, 2005) and the post-mitotic checkpoint (Tritarelli *et al.*, 2004) (Figure 1.2). Activation of these DNA damage checkpoints facilitates DNA damage repair before cell cycle progression, thereby avoiding errors in cellular events such as DNA replication, transcription and mitosis. As a result, the efficacy of chemotherapy can be greatly compromised due to the activation of these DNA damage checkpoints. In fact, it has been reported that abrogation of the G2 checkpoint can sensitize cancer cells to irradiation (Russell *et*

al., 1995; Terzoudi *et al.*, 2005). It is therefore hypothesized that G2 checkpoint abrogators may represent a new strategy for cancer therapy to sensitize cancer cells to DNA damaging agents and to circumvent drug resistance (Kawabe, 2004). To date, a number of G2 checkpoint abrogators have been discovered. For example, UCN-01 (Figure 1.1), a CHK1 inhibitor, has entered phase I trial in combination with fluorouracil and leucovorin for the treatment of patients with metastatic or unresectable solid tumors (ClinicalTrials.gov identifier: NCT00042861), and with carboplatin for patients with advanced solid tumors (ClinicalTrials.gov identifier: NCT00036777).

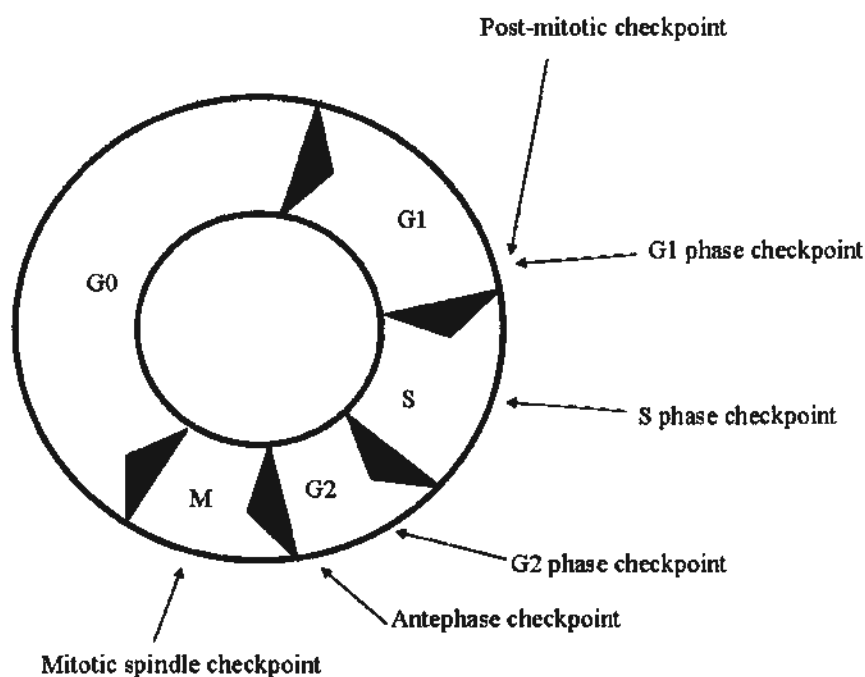


Figure 1.2: DNA damage checkpoints in a cell cycle.

1.2 Design of Novel Traditional Chinese Medicine (TCM)-Platinum Compounds

Platinum anti-tumor agents typically consist of a platinum moiety, two fairly labile leaving ligands, and two non-leaving ammine ligands that are inert to substitution under biological conditions. The leaving ligand is hydrolyzed in aqueous solution and biological medium (Figure 1.4). Cisplatin and carboplatin share the same diammino non-leaving group; hence they exhibit similar anti-cancer mechanisms of action. Oxaliplatin has a novel bidentate diaminocyclohexane (DACH) carrier ligand, replacing the two amino groups in cisplatin. Importantly, oxaliplatin forms DNA adducts that are poorly recognized by the mismatch repair (MMR) protein MutS (Zdraves *et al.*, 2002), enabling the circumvention of drug resistance to cisplatin (Espinosa *et al.*, 2005; Wong and Giandomenico, 1999). While the MMR system is required for cell death induced by cisplatin, cancer cells deficient in MMR are still susceptible to oxaliplatin with the incorporation of the DACH functionality in its structure (Fink *et al.*, 1997). Therefore, the DACH ligand has become the backbone structure for the design of novel platinum-based anticancer drugs for the circumvention of cisplatin resistance. The next opportunity for novel design of Pt anti-cancer drugs is to find an appropriate leaving group to introduce additional biological activities into the compounds.

Expanding on the conceptual framework of the use of bioactive ligands, and based on an “East meets West” philosophy, our research team has designed a novel series of platinum compounds with anti-cancer activity. We focused on traditional Chinese medicine due to its acknowledged effectiveness and low toxicity based on its clinical practice on human bodies for thousands of years. Cantharidin (Figure 1.3), a small molecule isolated from traditional Chinese medicine blister beetles (Figure 1.4), is widely used in the treatment of various kinds of cancers (Rauh *et al.*, 2007). It could be a favorable leaving group ligand due to the composition of two potential carboxylic acid groups. The major mechanism for anti-tumor activity of cantharidin is believed to be the inhibition of protein phosphatase 1 and 2A (PP1 and PP2A) (Rauh *et al.*, 2007). The incorporation of cantharidin in Pt drugs may be beneficial because okadaic acid (a PP2A inhibitor) (Figure 1.3) has been reported to disrupt DNA damage checkpoint induced by thymidine incorporation into DNA (Ghosh *et al.*, 1996) and inhibit DNA damage repair (Ariza *et al.*, 1996). However, cantharidin is highly toxic and it is a powerful vesicant (Brimfield, 1995). Therefore, demethylcantharidin (DMC, also known as norcantharidin, Figure 1.3), a derivative of cantharidin demonstrating PP1 and PP2A inhibitory activity but with less side effects, was finally chosen as the leaving group for a novel series of Pt-based anti-tumor agents (Ho *et al.*, 2001). It is hypothesized that by combining DMC with a

platinum moiety, the novel Pt compound could exhibit dual mechanisms of actions:

(1) the Pt moiety introduces DNA damage and, (2) the released DMC ligand after hydrolysis inhibits DNA damage checkpoint and DNA damage repair. Five novel TCM-Pt complexes were synthesized (Ilo *et al.*, 2001; Figure 1.3), by combining various platinum moieties with DMC, as the leaving group (US Patent #6,110,907 Aug 2000; PRC Patent #2197102796X June 2001).

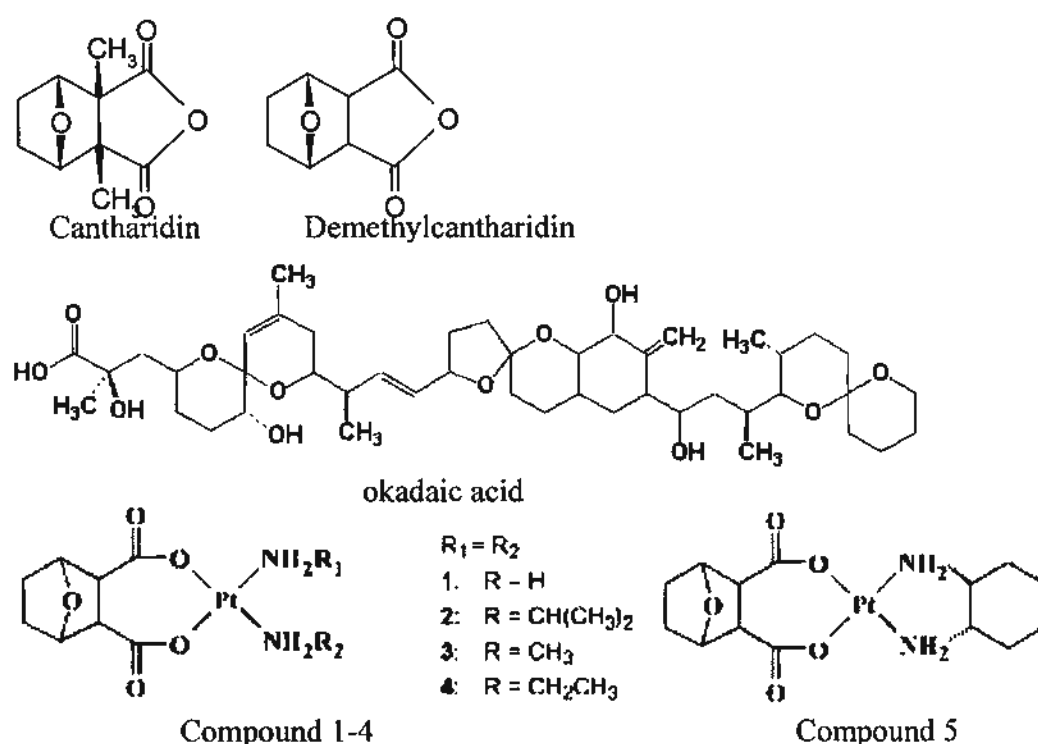


Figure 1.3: Chemical structures of cantharidin, demethylcantharidin and novel

TCM-Platinum compounds.

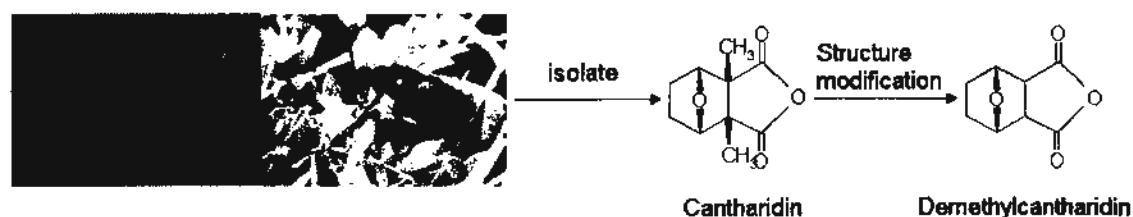


Figure 1.4: Demethylcantharidin is derived from traditional Chinese medicine blister

beetles.

1.3 Previous Studies on Novel TCM-Platinum Compounds (1-5)

1.3.1 Anti-Tumor Activities *in vitro* and *in vivo*

Previous studies by our research group have demonstrated that the novel TCM-Platinum compounds (compounds 1 to 5) have strong cytotoxic effects against various cancer cell lines: L1210 (mouse leukemia), COLO320DM (human colon cancer), SK-Hep-1 (human liver cancer), Hep-G2 (human liver cancer), MDA-MB-231 (human breast cancer), NCI:H460 (human non-small cell lung cancer), SK-OV-3 (human ovarian cancer), NTERA-S cl D1 (human testicular cancer), and two primary cultures of human gastric cancer. Among all tested compounds (compounds 1 to 5, DMC, cisplatin, carboplatin and oxaliplatin), compound 5 showed the strongest anti-tumor activity (To *et al.*, 2004). Compounds 1 to 5 also exhibit PP2A inhibitory activity, presumably ascribed to the presence of the DMC leaving ligand (To *et al.*, 2001; Ho *et al.*, 2004). The fact that DMC could inhibit Pt-DNA adduct removal and synergize cisplatin cytotoxicity (To *et al.*, 2004) may explain the higher cytotoxicity of these PP2A-containing novel compounds than traditional Pt compounds. More importantly, all of these novel compounds were found to be lack of cisplatin cross resistance *in vitro* and *in vivo* (To *et al.*, 2004; To *et al.*, 2005), once again pointing

towards the usefulness of incorporation of DMC in circumventing cisplatin resistance. The novel TCM-Pt compounds also demonstrated favorable anti-tumor activity in animal studies. In a SK-Hep-1 sc-inoculated xenograft model, the most potent compound 5 at a dose of 50 mg/kg could decrease tumor volume by 14.6% (mean value) compared with the control, without causing lethal effects in mice, which was significantly more effective than cisplatin, oxaliplatin or compounds 1 to 4 (Ho *et al.*, 2001).

1.3.2 Pharmacokinetics

It is well known that Pt-based anti-tumor drugs have to be hydrolyzed into an active aqueous form before interacting with DNA. For cisplatin, the chloride leaving groups will be released and replaced by two hydroxide groups upon hydrolysis (Figure 1.5). All novel DMC-Pt compounds share similar behavior in aqueous solutions. When compounds 1 to 5 were incubated in normal saline at 37 °C for up to 24 hrs, slow hydrolysis occurred, which released the DMC and the corresponding Pt moiety, as determined by gas chromatography (To *et al.*, 2001). The released Pt moiety can then interact with DNA directly and DMC could function as a PP2A inhibitor.

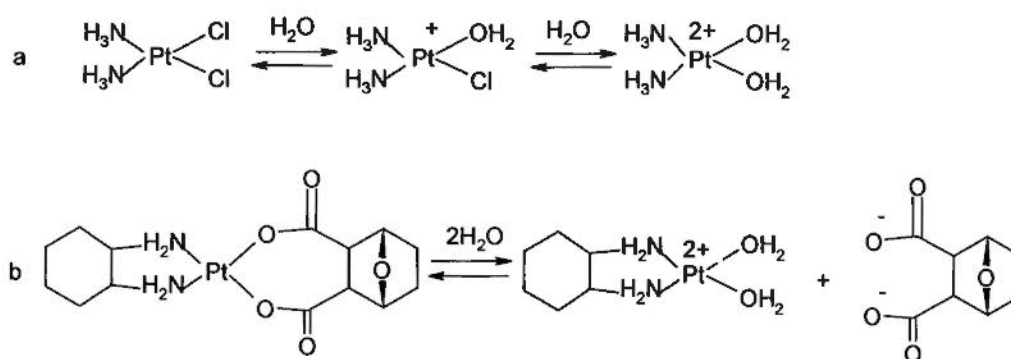


Figure 1.5: Hydrolysis reactions of a) cisplatin and b) compound 5.

The pharmacokinetics and tissue distribution of the novel compounds in Sprague–Dawley rats have also been studied. Compared with cisplatin, the novel TCM-Pt compounds exhibited a longer elimination half-life, larger dose-normalized area under the curve (AUC/D), larger volume of distribution at steady-state (Vd), slower clearance of free platinum and higher percentage of cumulative urinary excretion (CUE) (Wang *et al.*, 2007), which can be attributed to their lower chemical reactivity (To *et al.*, 2006). In various organs, the highest Pt concentrations were found in the kidney, followed by the liver and the heart; no Pt was detected in the brain (Wang *et al.*, 2007). Since the novel compounds are mainly accumulated in the kidney, it is possible that they may cause nephrotoxicity. By using a MTT assay in quiescent LLC-PK1 kidney cells, the nephrotoxicity was found to rank as follows: cisplatin > compound 5 > carboplatin (To *et al.*, 2006). However, compound 5 did not cause animal mortality at doses up to 50 mg/kg, the dose at which significantly

cytotoxic effect was observed in the xenograft mice model. In contrast, there was lethal incidence observed in mice treated with cisplatin at 8 mg/kg or above, where antitumor activity was not prominent.

1.3.3 Biological Evaluations of Compound *R,R*-5

The DACH-containing Pt drug oxaliplatin can process different stereo-isomers: *R,R*- (Figure 1.6), *S,S*-, or *cis*- isomers, depending on the conformations of the diaminocyclohexane (DACH) ring. *R,R*-oxaliplatin is used in the clinic because it is more effective in treating cisplatin-sensitive and resistant cell lines than other isomers of oxaliplatin (Pendyala *et al.*, 1995; Di Francesco *et al.*, 2002). Since compound 5 also contains a DACH structure, the corresponding conformational isoforms of compound 5 may show different biological behaviors. As a result, *R,R*-, *S,S*-, *trans*-(±)- and *cis*-isomers of compound 5 were synthesized and evaluated *in vitro* for cytotoxicity (Figure 1.6) (Yu *et al.*, 2006).

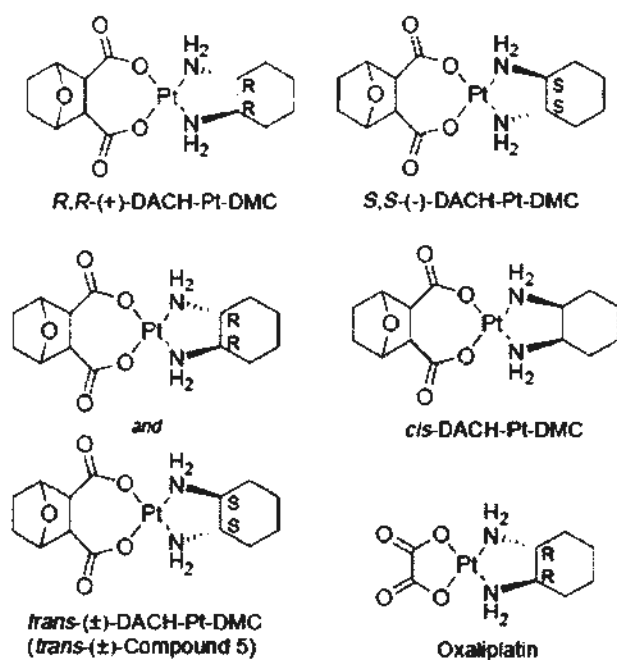


Figure 1.6: Chemical structures of R,R -, S,S -, $trans(\pm)$ - and *cis*-compound 5 and oxaliplatin. $Trans(\pm)$ -compound 5 is a mixture of R,R - and S,S -compound 5.

Similar to the conformational isomers of oxaliplatin, compound R,R -5 exhibited the strongest anti-tumor activity among cisplatin, carboplatin, oxaliplatin, and R,R -, S,S -, $trans(\pm)$ -, *cis*-compound 5, in colon cancer cell lines HCT116, HT29 and Colo320DM, as well as in pairs of cisplatin sensitive and resistant Huh-7 and SK-Hep-1 cell lines (Yu *et al.*, 2006). By using a comet assay, the ability of the novel TCM-Pt compounds (50 μ M for 3 hrs) to induce DNA strand breaks in HCT116 cells, reflected as the length of comet tails, were found to follow this order: compound R,R -5 > compound 1 > oxaliplatin > DMC > carboplatin > carboplatin > control \approx cisplatin (Pang *et al.*, 2007). Furthermore, the formation of DNA adduct of

these compounds (at 50 μ M in HCT116 cells) were ranked as below: carboplatin > compound 1 > *R,R*-5 > oxaliplatin > cisplatin (Pang *et al.*, 2007). These results imply that compared with other compounds, *R,R*-5 can induce the most severe DNA damage in cancer cells per amount of DNA-Pt adducts formed. Collectively, this may explain the higher cytotoxicity of *R,R*-5 than all other Pt compounds tested.

Flow cytometry analysis of the novel compounds was also carried out. At a concentration of $5 \times IC_{50}$ in HCT116 cells, *R,R*-5 could lead to G0/G1 and G2/M cell cycle arrests after 72 hrs treatment, which is similar to the cell cycle profile of oxaliplatin-treated HCT116 cells (Yu *et al.*, 2006).

Taken together, *R,R*-5 showed the strongest anti-tumor activity *in vitro*, probably by inducing more severe DNA damage in cells, and was lack of cisplatin resistance. Consequently, we chose *R,R*-5 for more extensive study in this thesis because it seems to be the most promising candidate suitable for further development into an useful anti-tumor agent. In this thesis, the biological behavior of *R,R*-5 will be explored, with an aim to unravel the mechanisms of anti-tumor activity of this novel compound.

We hypothesize that *R,R*-5 has a dual mechanism of action: (1) PP2A inhibitory effect from the leaving ligand DMC (the gradual release of DMC from compound 5 is extrapolated to *R,R*-5 causing PP2A inhibition) (To *et al.*, 2002), and

(2) DNA damaging effect from the DACH-Pt moiety. Prior to studying the mechanisms of anti-tumor action of *R,R*-5, it is necessary to review previous studies on PP2A inhibitors (Chapter 1.4) and the relevant cellular signal pathways that DNA damaging agents may activate (Chapter 1.5). This will be beneficial to propose a possible anti-tumor mechanism of *R,R*-5.

1.4 Protein Phosphatase 2A Inhibitors as Anti-Tumor Agents

1.4.1 Biological Properties of PP2A

Protein phosphatase 2A (PP2A) is a widely expressed member of the protein serine/threonine phosphatase family, which is involved in numerous cellular events, such as DNA replication (Chou *et al.*, 2002), cell cycle progression (Kawabe *et al.*, 2004; Messner *et al.*, 2001), apoptosis (Goldbaum *et al.*, 2002; Boudreau *et al.*, 2002), MAP kinase signaling (Boudreau *et al.*, 2002; Liu *et al.*, 2004), calcium channel regulation (Herman *et al.*, 2002), Wnt signaling (Seeling *et al.*, 1999) and cytoskeleton formation (Mistry *et al.*, 1998; Sontag *et al.*, 1996). Some of these cellular signaling pathways are critical for cellular survival, therefore it is expected that inhibitors of PP2A could prevent cell proliferation and exhibit anti-tumor activity.

Okadaic acid, microcystin LR, nodularin, tautomysin, calyculin A (Figure 1.7) and cantharidin (Figure 1.3) are all potent naturally occurring PP2A inhibitors.

Okadaic acid is isolated from a group of polyether toxins produced by marine microalgae (Takai *et al.*, 1987; Bialojan *et al.*, 1988; Cohen *et al.*, 1990). It is a useful research tool for the study of PP2A function in cellular signal transduction, which may help advance our understanding about the anti-tumor mechanisms of PP2A inhibitors.

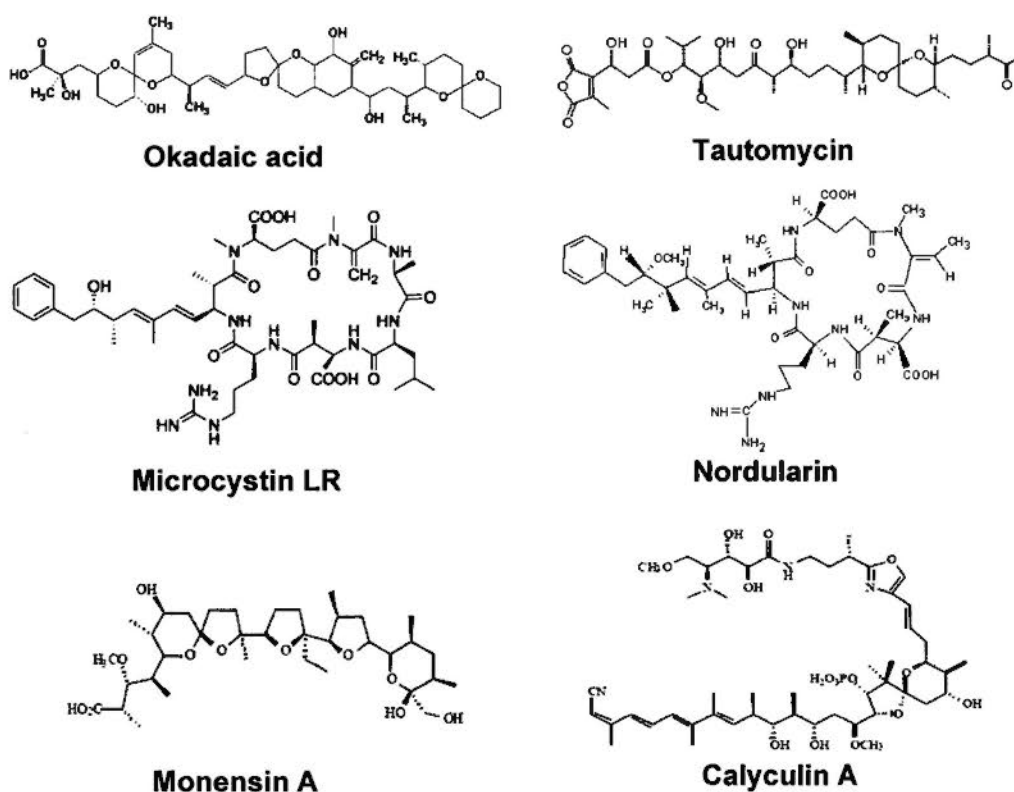


Figure 1.7: Chemical structures of PP2A inhibitors.

1.4.2. Structure and Function of PP2A

The structure of PP2A contains a catalytic subunit, a scaffold subunit and a wide variety of regulatory subunits. The functional diversity of PP2A in various cellular pathways is believed to be determined by the three different regulatory

subunits (R2, R3 and R5) (Figure 1.8).

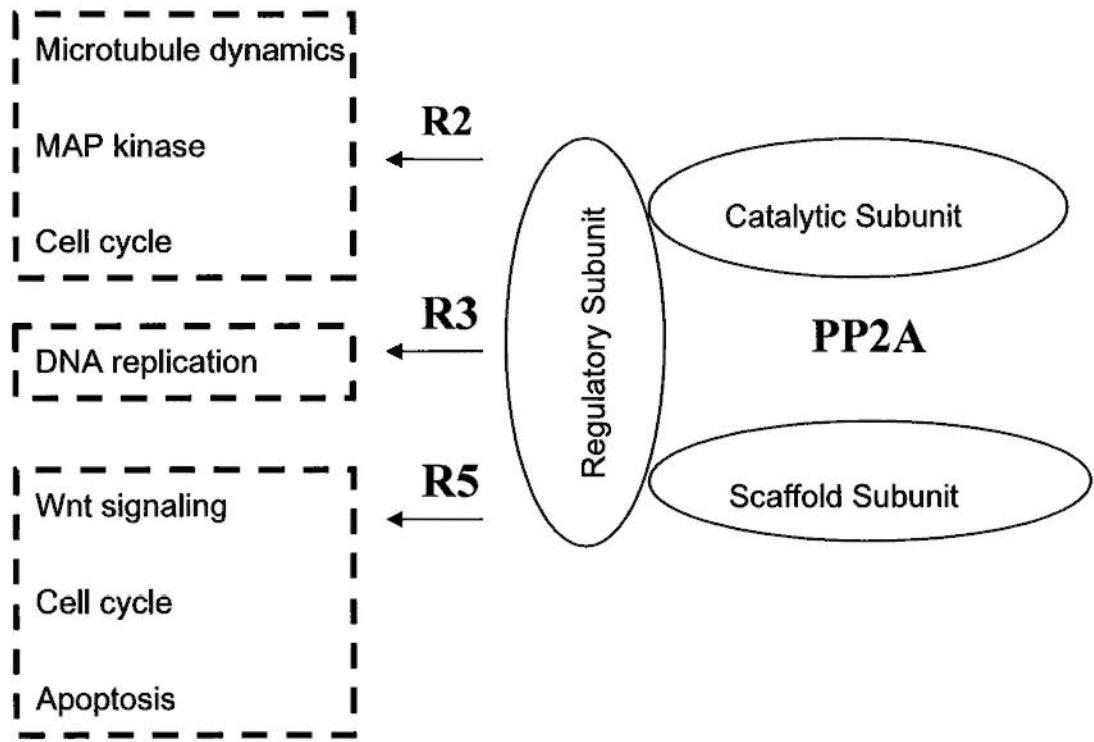


Figure 1.8: The structure and function of PP2A. The structure of PP2A contains a catalytic subunit, a scaffold subunit and a wide variety of regulatory subunits. The three regulatory subunits R2, R3 and R5 control the biological functions of PP2A in different cellular pathways.

The R2 regulatory subunit is involved in the maintenance of hypophosphorylation of microtubule-associated protein tau, leading to the binding of tau to microtubule and an increase in microtubule stability (Sontag *et al.*, 1996). It can also suppress the Ras-Raf-MAPK (mitogen activated protein kinase) pathway.

Mutation in the R2 subunit has been shown to enhance the Raf protein kinase activity in *C. elegans* (Abraham *et al.*, 2000). Moreover, the R2 subunit participates in the activation of mitotic kinetocore/spindle checkpoint (M phase cell cycle checkpoint) in *S. cerevisiae* by regulating the phosphorylation status of Cyclin B/CDC28, a key component of the mitotic promoting factor crucial for the G2→M cell cycle transition (Healy *et al.*, 1991; Minshull *et al.*, 1996; Wang *et al.*, 1997).

The R3 subunit of PP2A is involved in the initiation of DNA replication. In a yeast two-hybrid system, R3 β (PR59) protein was found to interact with p107 (Voorhoeve *et al.*, 1999), a protein that binds to E2F and inhibit E2F-induced transcription critical for G1→S entry. Overexpression of R3 β lead to the hypophosphorylation of p107 and increased binding to E2F (Voorhoeve *et al.*, 1999). Moreover, results from a yeast two-hybrid screening suggested that R3 γ (PR48) bind to CDC6. The phosphorylation of CDC6 triggers its dissociation from the chromatin and is required for the initiation of DNA replication. Further evidence demonstrates that overexpression of R3 γ could arrest cells at G1 phase (Yan *et al.*, 2000). These results suggest that PP2A may inhibit G1→S entry, either by inhibiting E2F-mediated transcription via p107 hypophosphorylation, or by inhibiting CDC6 phosphorylation to avoid the initiation of DNA replication. In contrast, PP2A inhibitors (such as okadaic acid and DMC) may promote G1→S entry (Figure 1.9;

will be further discussed in Chapter 1.4.4), thereby explaining their possible role in carcinogenesis. *R,R*-5 is not likely to be carcinogenic as other PP2A inhibitors (including DMC) because it can arrest cells in the quiescent G0/G1 phase (Yu *et al.*, 2006; also in Chapter 4.5.1, Figure 4.5).

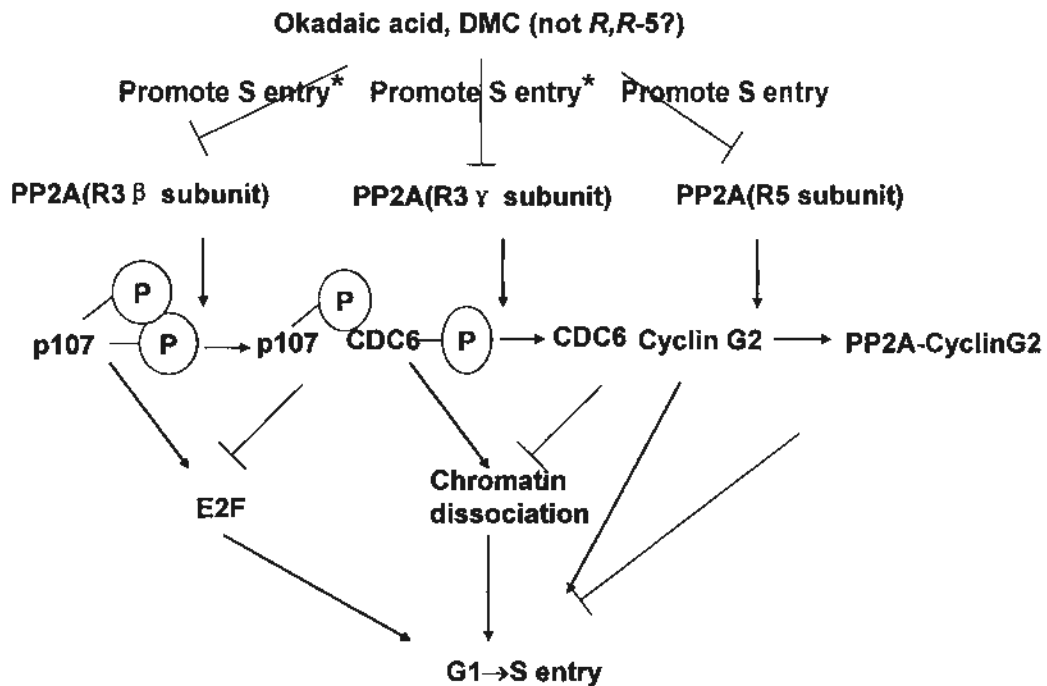


Figure 1.9: Proposed mechanisms for the effect of PP2A inhibitors on the G1→S cell cycle transition. PP2A may inhibit G1→S transition by: (1) inhibiting E2F mediated transcription that is required for G1→S transition via dephosphorylation of p107; or (2) promoting CDC6 phosphorylation to avoid initiation of DNA replication; or (3) inhibiting Cyclin G2 function by binding to it directly. Therefore, PP2A inhibitors (such as okadaic acid and DMC) are able to inhibit these processes and promote G1→S entry, giving rise to their carcinogenic effect. *R,R*-5 is not expected to promote G1→S progression because the DACH moiety can activate G1 cell cycle

checkpoint and counteract this S phase-promoting effect induced by the leaving ligand DMC. * suggests that there is no direct evidence demonstrating that the downstream pathways can promote G1→S transition.

The R5 regulatory subunit of PP2A controls cell transformation, apoptosis and cell cycle progression. The interactions of R5 subunit with adenomatous polyposis coli (APC) protein have been demonstrated in a yeast two-hybrid system (Seeling *et al.*, 1999), illustrating an important role for PP2A in the cell transformation through the regulation of the Wnt signaling pathway. Furthermore, R5 subunit can bind to cyclin G2, which forms a complex that can be isolated from cultured cells (Figure 1.9). This R5-cyclin G2 complex can inhibit cell cycle progression and arrest cells in the G1 phase (Bennin *et al.*, 2002). The depletion of the R5 subunit by RNA interference in *Drosophila* cells resulted in apoptosis (Silverstein *et al.*, 2002), hence suggesting that PP2A may participate in apoptosis signaling.

1.4.3. Role of PP2A Inhibitors in DNA Damage Repair

Most anti-cancer drugs such as doxorubicin, cisplatin and 5-fluorouracil kill proliferating cancer cells by causing DNA damage. Failure to repair DNA damage would lead to cancer cell death. The involvement of PP2A in DNA damage repair is

still not fully understood, though increasing evidence demonstrates that treatment with PP2A inhibitors can reduce DNA damage repair in cancer cells. Microcystin-LR, a PP2A inhibitor, has been reported to inhibit gamma-radiation-induced DNA damage repair, probably due to its involvement in the regulation of DNA-dependent protein kinase (DNA-PK) in the non-homologous end joining (NHEJ) repair pathway (Lankoff *et al.*, 2006). Moreover, microcystin-LR also inhibits nucleotide excision repair (NER) in CHO-K1 cells after UV radiation (Lankoff *et al.*, 2006). Besides microcystin-LR, other PP2A inhibitors like okadaic acid and tautomycin, were also found to inhibit UV-induced NER (Ariz *et al.*, 1996). DMC, a derivative of cantharidin that exhibits PP2A inhibitory activity, has been reported to reduce the removal of DNA-Pt adducts in L1210 cells after cisplatin treatment (To *et al.*, 2005). Inhibition of PP2A by RNAi or okadaic acid resulted in a longer persistence of γ -H2AX after camptothecin, hydroxyurea and H₂O₂-induced DNA double strand breaks, suggesting that inhibition of PP2A (by RNAi or okadaic acid) can attenuate the process of DNA damage repair (Chowdhury *et al.*, 2005). In short, all these studies demonstrated that PP2A inhibitors are able to inhibit DNA damage repair and therefore are expected to sensitize cancer cells to DNA damaging agents.

1.4.4. Role of PP2A Inhibitors in Cell Cycle Regulation

PP2A inhibitors were found to have profound effect on cell cycle regulation. In G1→S transition, as discussed in Chapter 1.4.2, the PP2A inhibitors okadaic acid and calyculin A were reported to prevent dephosphorylation of the retinoblastoma family proteins (RB) and p107 (Figure 1.9; Figure 1.10), resulting in the dissociation of these two proteins from E2F. E2F is subsequently activated to drive the transcription of genes necessary for DNA synthesis (Cicchillitti *et al.*, 2003). Overexpression of SV small t antigen (a commonly used protein to inhibit PP2A R2 subunit) abrogates the inhibition of DNA synthesis induced by H₂O₂ (Cicchillitti *et al.*, 2003), suggesting that PP2A inhibition has a positive role in the regulation of DNA synthesis. Previous study also reported that okadaic acid could prevent the inhibition of AP-1, an important G1→S transcription factor, induced by all-trans retinoic acid in CA-OV3 cells (Ramírez *et al.*, 2005). Likewise, okadaic acid was found to restore AP-1-mediated cyclin D1 transcription that was inhibited by leptomycin B in NIH3T3 cells (Tsuchiya *et al.*, 2006). Further mechanistic study found that okadaic acid inhibits dephosphorylation of the β 1 subunit of AP-1 in the mouse L cells (Ghosh *et al.*, 2003). Taken together, all these studies demonstrate that PP2A inhibitors could promote G1→S transition and therefore carcinogenesis. However, in another study, okadaic acid was found to prevent the loading of CDC45 onto the

pre-replication complex, resulting in the inhibition of DNA synthesis (Chou *et al.*, 2002; Petersen *et al.*, 2006). This observation implies that PP2A inhibitors facilitate gene transcription for G1→S progression but inhibit DNA synthesis at the onset of S phase. For example (Figure 1.10), the binding of TGF-β (transforming growth factor β) to the TGF-β receptor activates PP2A and stimulates the PP2A-p70s6k association, leading to G1 arrest (Petritsch *et al.*, 2000), whereas inhibition of PP2A (in T51B cells by okadaic acid) also leads to G1 arrests (Messner *et al.*, 2001), suggesting that both activation and inhibition of PP2A will lead to G1 arrest. In fact, this okadaic acid-induced G1 arrest is believed to be the net effect of PP2A inhibition: promote gene transcription for G1 → S progression but inhibit DNA synthesis.

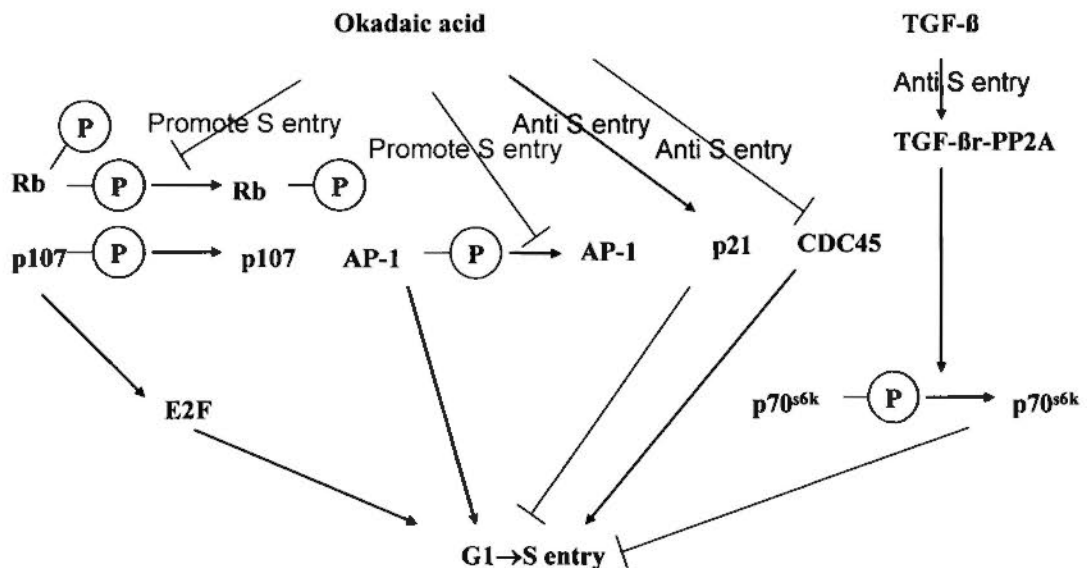


Figure 1.10: Effect of okadaic acid and TGF-β on G1→S cell cycle entry. Okadaic acid can inhibit the binding and inhibition of Rb and p107 to E2F, subsequently

releasing E2F, to transcribe genes required for S phase entry. It can also activate AP-1, also a transcription factor to prepare for S phase entry. However, okadaic acid can accumulate p21 and prevent the loading of CDC45 onto the pre-replication platform, attenuating S phase entry. TGF- β can lead to the association of TGF- β receptor with PP2A, resulting in the deactivation of p70^{s6k}, inhibiting S phase progression.

In a normal cell cycle, when DNA damage is detected during and after DNA replication, the ATM/ATR-dependent DNA damage checkpoints (S and G2 checkpoints) will be activated. Cells will be arrested at the S and/or G2 phase without progression into mitosis, thereby allowing time for DNA damage repair. Abrogation of the G2 check point is believed to prevent DNA damage repair and facilitate apoptosis. Many anti-tumor drugs are non-cell cycle specific and they cannot differentiate between cancer cells (proliferating cells) and other normal cells (non-proliferating cells), which will generate adverse side effects due to the disturbed physiological functions of healthy cells. Since G2 check point abrogators can selectively inhibit G2 DNA damage check point and DNA repair in proliferating cells (laboring at G2 phase) without affecting stationary cells (most normal cells are stationary cells in G0 phase), they may cause less side effects in cancer therapy. Some cell cycle-associated proteins, including ATM/ATR, CHK1/CHK2 and Wee1,

are critical components of the G2 checkpoint. Their inhibitors, caffeine (Mante *et al.*, 1990; Sarkaria *et al.*, 1996; Cortez, 2003), UCN-01 (Jackson *et al.*, 2000; Yu *et al.*, 2002; Graves *et al.*, 2000; Sato *et al.*, 2002), and PD0166285 (Wang *et al.*, 2001), respectively, have been used to abrogate this G2 cell cycle checkpoint.

PP2A inhibitors were known to abrogate G2 DNA damage check point and facilitate cells entering mitosis. Okadaic acid was reported to disrupt thymidine-activated G2 checkpoint (Ghosh *et al.*, 1996); fostriecin can also abrogate DNA damage check point and facilitate cells entering mitosis (Kawabe *et al.*, 2004; Roberge *et al.*, 1994). In other reports, the evidence is more circumstantial. PP2A inhibitors were usually found to promote mitotic entry. Okadaic acid was proved to arrest cells in a premature mitosis status (characterized by cytoskeletal rearrangements, nuclear envelope breakdown, DNA condensation but failure in separation) (Ghosh *et al.*, 1998; Ghosh *et al.*, 1992), either by activating the mitosis promoting factor CDK1/Cyclin B1 (Yamashita *et al.*, 1990), or Nek2 (NIMA (never in mitosis gene a)-related kinase 2) (Ghosh *et al.*, 1998). Fostriecin, another PP2A inhibitor, was also reported to arrest cells at mitosis, which is not dependent on CDK1 or histone H1 hyperphosphorylation. The effect is associated with enhanced histone H2A and H3 phosphorylation (Guo *et al.*, 1995). Histone H3 is a known substrate of aurora A. Since PP1 and PP2A have been reported to inhibit the

activation of aurora A (Eyers *et al.*, 2003), drug treatment with PP2A inhibitors may therefore facilitate aurora A hyperactivation and histone H3 phosphorylation and subsequently mitosis. Collectively, these studies suggest the PP2A inhibitors can promote mitosis through CDK1/Cyclin B1, NIMA, and/or aurora A (Figure 1.11).

Interestingly, besides promoting cell cycle progression to mitosis by regulating cell cycle checkpoint associated proteins, PP2A inhibitors were also found to regulate chromatid separation and microtubule dynamics (Figure 1.11). Recent studies demonstrate that Sgo1 recruits PP2A to kinetochore to antagonize the POLO-induced phosphorylation of cohesin, and therefore inhibiting the cell cycle transition from prophase to metaphase. Okadaic acid has been shown to increase the phosphorylation of cohesin and facilitate progression to mitosis (Nasmyth, 2002; Rivera and Losada, 2006; Kitajima *et al.*, 2006). Also, okadaic acid was reported to activate separase and promote chromosome separation. Under physiological conditions, the metaphase→anaphase transition requires anaphase promoting complex (APC)-dependent destruction of securin and consequently the release and activation of separase, thereby allowing the separation of chromosomes. However, in okadaic acid-treated cells, securin was found to be hyperphosphorylated and was rapidly degraded, and the separation of sister chromosomes was therefore triggered by the released separase (Gil-Bernabe *et al.*, 2006). The mitotic arrest induced by

PP2A inhibitors may also involve a change in microtubule stability. Okadaic acid is reported to maintain the phosphorylated state of stathmin, resulting in the inhibition of stathmin and increased stability of microtubule, and subsequently CDK1 phosphorylation and the progression into mitosis (Mistry *et al.*, 1998). Furthermore, the inhibition of PP2A R2 subunit by SV small t antigen overexpression has been shown to disrupt the PP2A-tau interaction, leading to the hyperphosphorylation of tau and its dissociation with microtubule. This would cripple the formation and stability of microtubule (Sontag *et al.*, 1996). Collectively, PP2A inhibitors could promote mitotic entry by regulating the process of chromosome separation and microtubule formation.

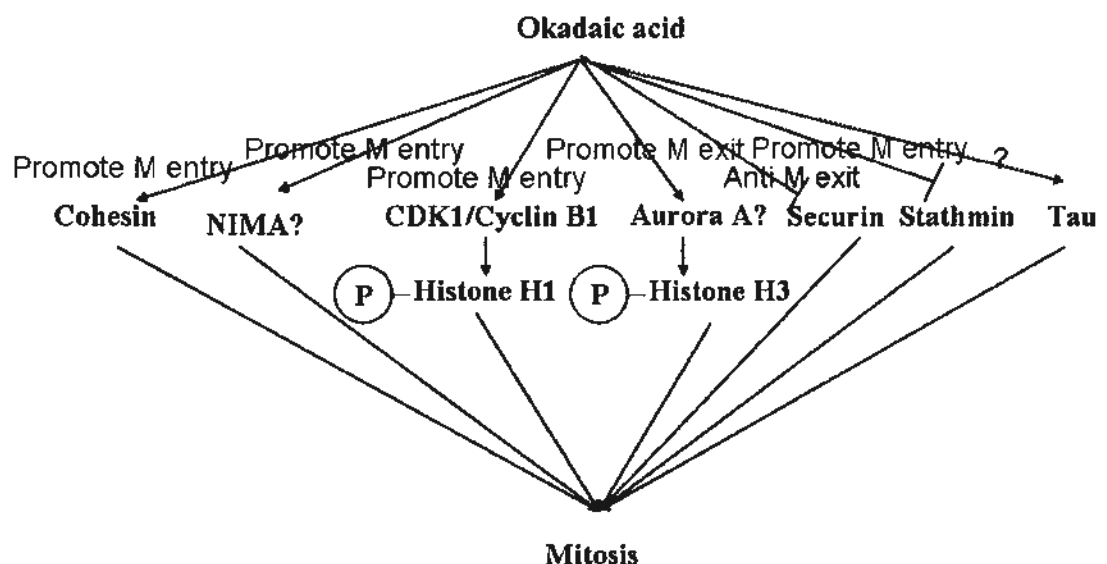


Figure 1.11: Effect of okadaic acid on mitosis. Okadaic acid can activate cohesin, possibly NIMA and aurora A, to promote mitotic entry. Also, it can inhibit securin and promote chromatid separation. It can inhibit stathmin, resulting in increased

microtubule stability and promote mitotic entry. However, okadaic acid can decrease microtubule stability by activating tau, which may inhibit mitotic events (though no direct evidence has been reported).

1.4.5. Role of PP2A Inhibitors in Apoptosis

PP2A is involved in the dephosphorylation of many proteins in cells, including those related to apoptosis, thus PP2A inhibitors are also found to have profound influence on apoptosis (Figure 1.12). In general, treatment of cells with PP2A inhibitors triggers apoptosis. Inhibition of PP2A by okadaic acid has been shown to activate both mitochondria-dependent and death receptor Fas-mediated apoptotic pathways, resulting in the loss of mitochondria membrane potential, cleavage-induced activation of caspase-3, -8, and -9, and DNA fragmentation in T leukemia cells (Boudreau *et al.*, 2007). Moreover, the pro-apoptotic function of p53 may also contribute to the cell death caused by PP2A inhibitors because p53 was found to be activated in okadaic acid treated T51B cells (Messner *et al.*, 2004). Furthermore, inactivation of the tumor promoter Bcl-2 may also be involved in the apoptosis induced by okadaic acid. In fact, okadaic acid has been reported to overcome the resistance to apoptosis that was caused by PP2A-mediated dephosphorylation of Bcl-2 (Simizu *et al.*, 2004). However, activation of the p38MAPK pathway by okadaic

acid has been reported to oppose its apoptotic effect (Boudreau *et al.*, 1996). PP2A was known to dephosphorylate Bax and enhance its pro-apoptotic function, which could be readily inhibited by okadaic acid (Xin *et al.*, 2006). PP2A inhibitors have also been found to prevent stress-induced apoptosis. Fostriecin and calyculin A were reported to antagonize cell death induced by the tumor necrosis factor α (TNF α), owing to the inhibition of Bax through activation of the MEK-ERK pathway (Grethe and Poörn-Ares, 2006). Similarly, PP2A inhibition by okadaic acid was found to attenuate H₂O₂-induced apoptosis and reduce heat shock-induced DNA fragmentation, due to the activation of MEK-ERK pathway (Liu *et al.*, 2004, Goldbaum *et al.*, 2002). These observations imply that the mechanisms of apoptosis induced by PP2A inhibitors and other stresses (such as TNF and H₂O₂) are different but interrelated, in which Bax and mediators in the MEK-ERK pathway play an important role (Figure 1.12).

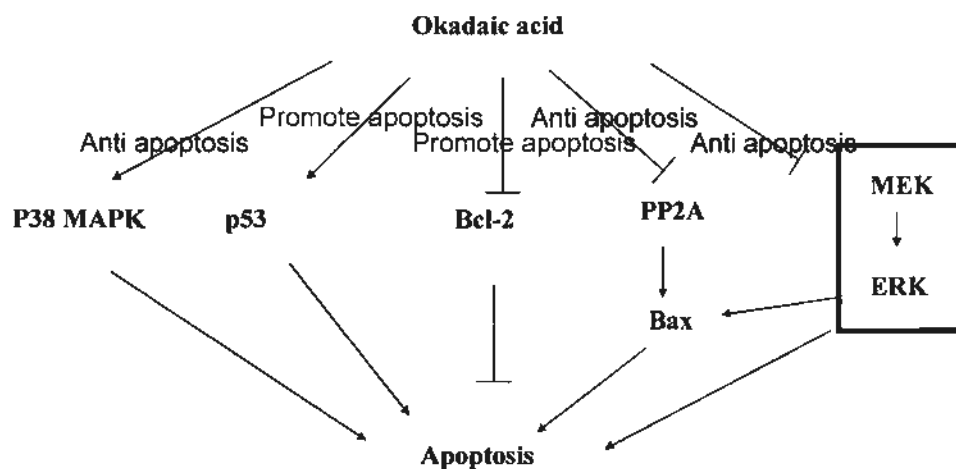


Figure 1.12: Effect of okadaic acid on apoptosis. Okadaic acid can activate p53 and

inhibit Bcl-2 to induce apoptosis. However, it can activate p38 MAPK and antagonize ERK (when ERK is activated by other stresses) to inhibit apoptosis. It can also dephosphorylate Bax and attenuate Bax-mediated apoptosis.

1.4.6. Potential Use of PP2A Inhibitors in Cancer Chemotherapy

The involvement of PP2A in cellular signal transduction is complicated. As a result, PP2A inhibitors can exhibit numerous biological effects, including those on cell cycle and apoptosis regulations as discussed above. Inhibition of PP2A was known to: (1) up-regulate genes promoting G1→S entry; (2) inhibit DNA synthesis at the very beginning when the pre-replication complex is formed; (3) abrogate G2 DNA damage check point and inhibit DNA damage repair; (4) induce apoptosis via both mitochondria and Fas pathways; (5) inhibit apoptosis induced by stresses like TNF and H₂O₂. The most extensively studied PP2A inhibitor, okadaic acid, is actually considered as a food poison and tumor promoter. Another PP2A inhibitor, fostriecin, has been used in cancer chemotherapy for a number of years with few reported side effects. Taken together, PP2A inhibitors exert their anti-tumor activity through multiple mechanisms and are a novel class of promising anti-tumor agents. The development of novel PP2A inhibitors with high selectivity towards the different regulatory subunits may provide another suitable candidate anti-tumor agent in

chemotherapy.

1.4.7 Proposed Characteristics of *R,R*-5 as a PP2A Inhibitor

Since *R,R*-5 is expected to release DMC upon hydrolysis in aqueous solution, we hypothesized that *R,R*-5 could have biological activities akin to those of PP2A inhibitors. Similar to the disruption of thymidine-activated G2 checkpoint by okadaic acid (Ghosh *et al.*, 1996), we proposed that *R,R*-5 may abrogate cell cycle DNA damage checkpoint, which will be discussed in Chapter Four. Importantly, this hypothesized effect (G2 checkpoint abrogation by *R,R*-5) may explain the higher ability to induce DNA damage and cytotoxicity of *R,R*-5, than cisplatin, carboplatin and oxaliplatin.

1.5 Signal Transduction of DNA Damaging Agents: From Damage Repair to Mitogen-Activated Protein Kinase

Our previous study suggested that the DACH-Pt moiety of *R,R*-5 endows the novel compound with the ability to induce DNA damage (Pang *et al.*, 2007). To propose the biological functions of *R,R*-5 as a DNA damaging agent, an appropriate signal transduction pathway, the mitogen-activated protein kinase (MAPK) pathway, was chosen for detailed investigation. This is due to emerging evidence suggesting

that cellular signals for cell cycle regulation and apoptosis are transmitted, at least partially, via the mitogen-activated protein kinase (MAPK) when cells are subjected to DNA damage. For example, the mismatch repair (MMR)/c-Abl/p38MAPK signaling is an important pathway mediating cell cycle arrest and apoptosis in response to DNA alkylating agent TMZ (temozolomide) (Hirose *et al.*, 2003). Therefore, c-Abl represents a mediator linking DNA repair and MAPK activation, which determines the cellular response to DNA damaging agents.

In current cancer therapy, the prevailing strategy of causing cancer cell death is to induce DNA damage by genotoxic drugs or radiation. DNA damage can take the form of single/double DNA strand breaks, DNA adducts, thymidine dimers, base-pair mismatch, etc. Cancer cells utilize different DNA damage repair mechanisms to maintain genomic stability. Five DNA damage repair mechanisms have been suggested, including nucleotide excision repair (NER), mismatch repair (MMR), homologous recombination (HR), non-homologous end joining (NHEJ), and base excision repair (BER). Failure to repair DNA damage is known to cause cell death. However, the signal transduction pathways linking DNA damage repair to the downstream cell cycle and apoptotic regulation remain largely unknown.

MAPK contain three subfamilies: extracellular signal-regulated protein kinase (ERK), p38MAPK, and c-Jun N-terminal kinase/stress-activated protein kinase

(JNK/SAPK). p38MAPK and JNK/SAPK were shown to participate in apoptosis induced by some genotoxic stresses. However, the mechanisms leading to p38MAPK and JNK/SAPK activation by DNA damage are not fully-understood. Mounting evidence suggested that DNA damage repair pathways are the upstream activators of the MAPK pathways in response to DNA damages (Hirose *et al.*, 2003). In other words, there must be some signaling “linkers” that transmit the DNA damage signal to MAPK to execute the down-stream effect on cell cycle and apoptosis regulation. Despite their important biological functions, understanding of these “linkers” is still obscure. Therefore, our review on this topic will focus on the DNA damage repair-“linkers”-MAPK signaling pathway, which allows us to propose the cellular pathways that *R,R-5* may participate in.

1.5.1. c-Abl forms the Link between Mismatch Repair and MAPK

The proto-oncogene c-Abl is well-known for its contribution to the etiology of chronic myelogenous leukemia (CML), where the formation of the transforming Bcr-Abl fusion protein leads to continuous activation of c-Abl kinase activity (Goff *et al.*, 1980). c-Abl is also required for cisplatin-induced apoptotic signaling (Mansouri *et al.*, 2003) (Figure 1.13). It has been reported that c-Abl is activated by MLH1 (also by MSH2) from the mismatch repair (MMR) pathway in response to cisplatin

treatment (Nehmé *et al.*, 1999). The activated c-Abl interacts directly with MEKK1, an up-stream activator of JNK/SAPK, and leads to immediate activation of JNK (Kharbanda *et al.*, 2000). Interestingly, this JNK/SAPK activation, and p38MAPK signaling, are required for cisplatin-induced cell death (Mansouri *et al.*, 2003). Therefore, c-Abl is indispensable for MMR to transmit death signal to MAPK. c-Abl knocked-down mouse embryo fibroblasts fail to activate p38MAPK and trigger cell death upon cisplatin exposure (Pandey *et al.*, 1996). Transfection of c-Abl was also found to induce apoptosis through MKK6, a p38MAPK upstream activator (Wei *et al.*, 2005). These findings demonstrate that c-Abl links MMR to MAPK, and triggers apoptosis after cisplatin treatment. Moreover, c-Abl was reported to stabilize p73 through a c-Abl/p38MAPK pathway (Gong *et al.*, 1999), while JNK/SAPK was also reported independently to stabilize p73 (Toh *et al.*, 2004). Activation of p73 leads to the up-regulation of Puma and Bax, resulting in mitochondria-dependent apoptosis (Thottassery *et al.*, 2006).

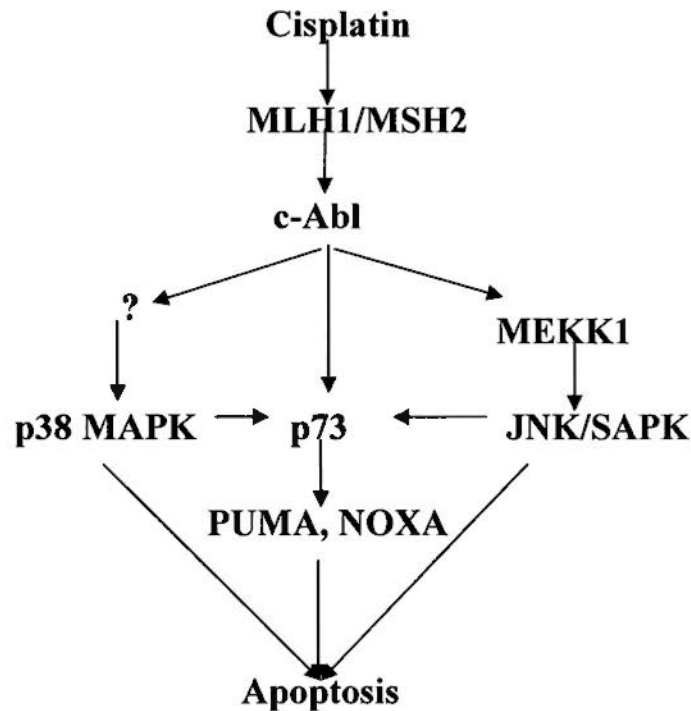


Figure 1.13: Mismatch repair transmit death signal to MAPK via c-Abl. Cisplatin can activate c-Abl via mismatch repair proteins MLH1 and MSH2, which subsequently activate p38MAPK and/or JNK/SAPK to trigger apoptosis.

1.5.2 BRCA1 May Link Homologous Recombination to MAPK

Another important DNA repair mechanism that may activate MAPK is homologous recombination (HR). A possible “linker” that passes down cellular signals from HR to MAPK is the breast cancer susceptibility gene 1 (BRCA1). BRCA1 is indispensable for the DNA binding of HR components (Powell *et al.*, 2003) and is able to bind to MAPK kinase kinase 3 (MAPKKK3, MEKK3) after paclitaxel treatment (Gilmore *et al.*, 2004). Moreover, BRCA1 has been shown to

increase the cytotoxic effect of paclitaxel (Quinn *et al.*, 2003; Gilmore *et al.*, 2004), suggesting that the association of BRCA1 and MEKK3 may induce MAPK-dependent cell death. Also, MEKK4, one of the MAPKKs, is activated in a Ras-dependent manner when cells are over-expressed with BRCA1 (Thangaraju *et al.*, 2000). In fact, over-expression of BRCA1 leads to apoptosis via MEKK4 activation (Thangaraju *et al.*, 2000). Despite that BRCA1 can reinforce the toxicity of doxorubicin (Foulkes, 2006), inhibitory effect of BRCA1 on IR-induced apoptosis (Abbott *et al.*, 1999; Quinn *et al.*, 2003; DelloRusso *et al.*, 2007), and on cisplatin-induced cell death (Quinn *et al.*, 2003), are also reported, suggesting the proposed HR/BRCA1/MAPK pathway can either inhibit or promote cell death under different settings, which can be reflected by the differential regulation on DNA damage-induced cell death of BRCA1 (reviewed by Kennedy *et al.*, 2004).

Since BRCA1 interacts with kinases to mediate its downstream biological activities, the binding partners of BRCA1 are also actively studied. A proline-rich sequence (PXXP sequence, Src-homolog 2, SH2) is found in BRCA1, which is believed to mediate its binding to Src-homolog 3- (SH3-) containing proteins. For instance, BRCA1 is reported to bind to the non-receptor tyrosine kinase c-Abl, which contains the SH3 domain (Foray *et al.*, 2002). As mentioned in Chapter 1.5.1, c-Abl can bind to MEKK1 upon MMR initiation after cisplatin exposure, leading to JNK

activation (Kharbanda *et al.*, 2000), but the signaling pathway for c-Abl to activate p38MAPK is unknown. We hypothesize that a potential mediator for this c-Abl/p38MAPK pathway is MEKK1 because it is both a p38MAPK and JNK activator (this is confirmed in Chapter Three). Since c-Abl can constitutively bind to BRCA1 (Foray *et al.*, 2002), it is also possible that c-Abl may be associated with the proposed HR/BRCA1/MAPK pathway to activate p38MAPK (or JNK).

1.5.3. Lyn Links the Inhibition of NHEJ to MAPK

DNA-dependent protein kinase (DNA-PK) is a crucial component in non-homologous end joining (NHEJ) for recruiting the DNA repair machinery, which consists of a Ku70 and Ku86 heterodimer, and a DNA-PK catalytic subunit (DNA-PKcs). Unlike MMR, NHEJ increases cell survival after ionizing radiation (IR) treatment rather than causing MAPK-dependent apoptosis. It has been shown that Ku70^{-/-} mice (NHEJ non-functional) are more sensitive to IR than wildtype Ku70 baring (NHEJ functional) mice (Narasimhaiah *et al.*, 2005). Cisplatin has been demonstrated to enhance IR-induced cell death by inhibiting NHEJ (Boeckman *et al.*, 2005). These observations imply that repair of DNA damage by NHEJ promotes cell survival rather than apoptosis. Interestingly, DNA-PKcs is responsible for the delayed (6 hr drug treatment before JNK could be soundly activated) JNK/SAPK

activation after treatment with alkylating agents such as MMS (Methyl methanesulfonate) or MNNG (N-methyl-N'-nitro-N-nitrosoguanidine) (Fritz *et al.*, 2006), suggesting a “linker” must have connected NHEJ with MAPK. The tyrosine kinase Lyn has been shown to associate with DNA-PKcs constitutively, with or without exposure to IR (Kumar *et al.*, 1998). Since Lyn activates the MEKK1/MKK4/JNK pathway in response to Ara-C, cisplatin and IR (Yoshida *et al.*, 2000), Lyn may be a mediator transmitting the (apoptosis) signal from NHEJ to MAPK. However, current evidence suggests that NHEJ (and indirectly the proposed NHEJ/Lyn/MAPK pathway) apparently triggers a survival signal (not an apoptotic signal). Our thinking (Figure 1.14) is that NHEJ can repair DNA damage and promote cell survival. However, unreparable DNA damage (such as strong ionizing radiation) will “turn off” NHEJ and “turn on” NHEJ-Lyn-MAPK association for apoptosis. As a result, the outcome of genotoxic stress depends on the balance between the activation of NHEJ (survival) and its inactivation (apoptosis). A possible mechanism to inactivate NHEJ, is the ATM/c-Abl signaling (Figure 1.14). c-Abl is activated after IR in an ATM-dependent but MMR-independent manner (Brown *et al.*, 2003; Shafman *et al.*, 1997). c-Abl can also phosphorylate DNA-PKcs after IR, resulting in the dissociation of DNA-PKcs from DNA (Kharbanda *et al.*, 1997). These observations suggest that ATM/c-Abl is activated by IR to inhibit

DNA-PK, leading to its dissociation from DNA damage sites (Figure 1.14). The dissociated DNA-PKcs could then trigger Lyn-MEKK1 association and activate MAPK to induce apoptosis. In fact, it was found that JNK/SAPK activation by IR requires the presence of ATM (Lee *et al.*, 1998, 2001).

The hypothesis that ATM/c-Abl inactivates NHEJ and initiate death signal via MAPK may explain the balance between cell survival and death in different experimental settings. Gao reported that DNA-PKcs null fibroblast exhibit increased IR sensitivity but not DNA-PKcs null ES cells (Gao *et al.*, 1998); Zhang reported that silencing of DNA-PKcs in WTK human lymphoblastoid cells with siRNA increases IR-induced cell killing (Zhang *et al.*, 2007); Jin reported that DNA-PKcs can promote the cytotoxicity of Topoisomerase II inhibitor Etoposide (Jin *et al.*, 1998). Taken together, Lyn may function as the death signal transducer to initiate the MAPK pathway after NHEJ is inhibited by ATM/c-Abl.

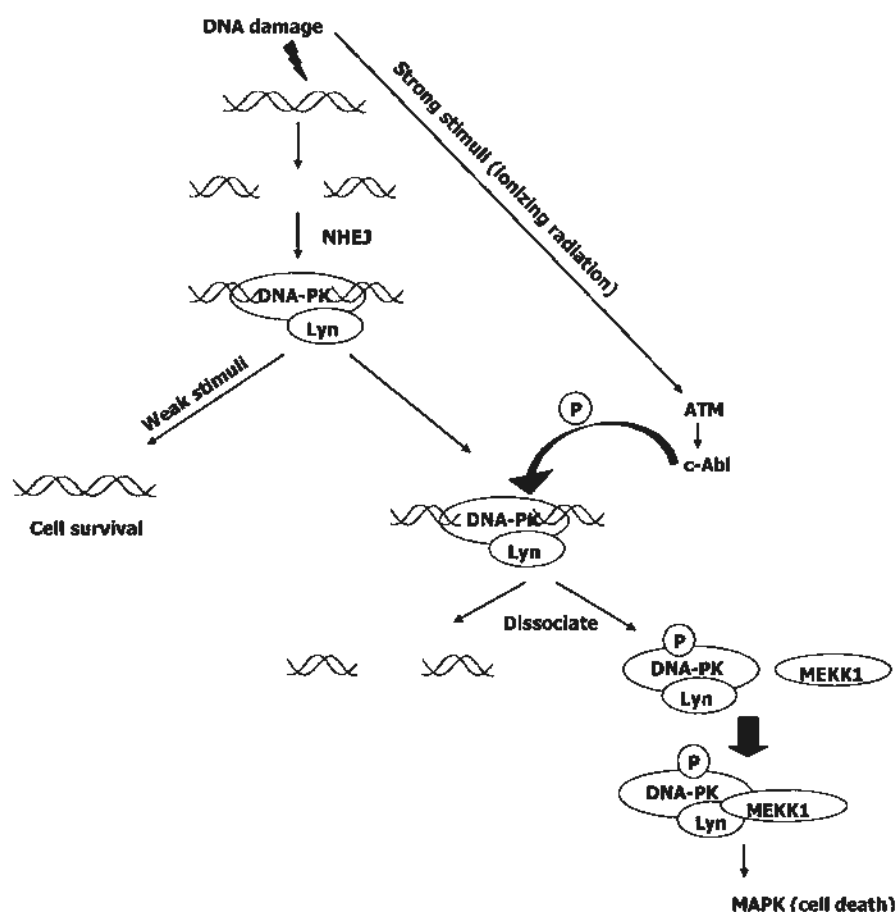


Figure 1.14: Proposed mechanism for inhibition of NHEJ and initiation of death signal transduction by MAPK. DNA-PK complex recognizes and binds to the end of double DNA strand breaks induced by IR, recruiting other DNA repair machineries like DNA ligase IV and XRCC4. On the other hand, DNA damage activates ATM, which consequently activates non-receptor tyrosine kinase c-Abl. Activated c-Abl binds to and phosphorylates DNA-PKcs, resulting in the dissociation of the DNA-PK complex from DNA. This process will probably activate Lyn, a constitutive component of DNA-PK, leading to its binding to MEKK1, which activates the MAPK pathway and initiates the downstream apoptotic signal transduction.

1.5.4. GADD45 May Link NER to MAPK

Growth arrest and DNA-damage-inducible 45 (GADD45) is required for UV-induced NER to remove thymine dimers (Maeda *et al.*, 2005). On the other hand, GADD45 has been indicated to bind to the N-terminal segment of MEKK4 with its C-terminal segment, leading to the auto-phosphorylation of MEKK4 at Thr1493 (Miyake *et al.*, 2007). This finding implies that GADD45-dependent NER may link to MAPK through GADD45/MEKK4 interaction (Figure 1.15). In fact, co-transfection of GADD45 and MEKK4 has been shown to activate JNK/SAPK and p38MAPK, and induce apoptosis (Takekawa *et al.*, 1998). Hyperosmotic stress was also shown to induce cell death via this GADD45/MEKK4 pathway (Mak *et al.*, 1998). Over-expression of GADD45 stops cell proliferation through direct binding and inhibition of CDK1 (Jin *et al.*, 2000), but activation of p38MAPK by GADD45 may possibly contribute to this process (Takekawa *et al.*, 1998). However, it was reported that the presence of GADD45 could inhibit UV-induced cell death (Smith *et al.*, 2000), which is contrary to the mounting evidences of the major pro-apoptotic effect of GADD45 discussed above. In conclusion, the NER/GADD45/MAPK pathway participates in DNA damage-induced apoptosis and/or cell cycle regulation.

Interestingly, JNK/SAPK and p38MAPK activation by the proposed NER/GADD45/MEKK4 pathway only occurs as a late response (5 hrs after UV

treatments to activate JNK) to DNA damage (Wang *et al.*, 1999). This may account for the time needed for the induction of GADD45 by p53 and direct binding to GADD45 promoter by BRCA1 from HR (Jin *et al.*, 2000) (Figure 1.15). The up-regulation of GADD45 by BRCA1 also suggests that HR is responsible, at least in part, for the activation of NER, which is supported by the fact that BRCA1 can transcribe NER genes XPC, DDB2 and GADD45 regardless of the p53 status (Hartman *et al.*, 2002).

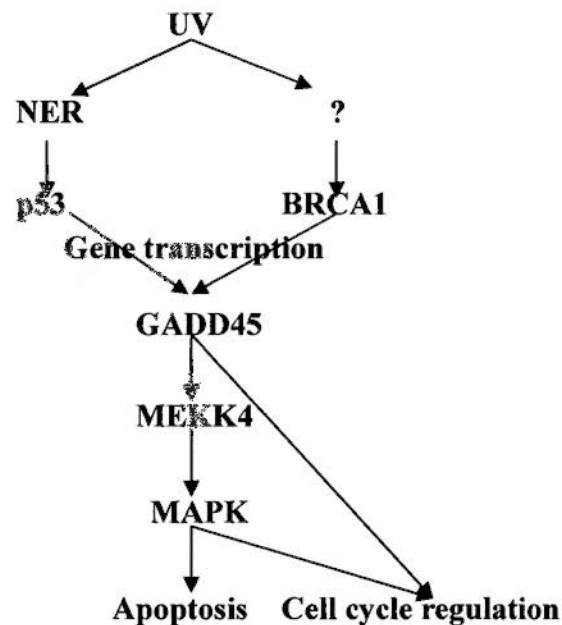


Figure 1.15: GADD45 links nucleotide excision repair to MAPK in response to UV stimulation. UV exposure can induce thymidine dimer, which is repaired by NER. NER can activate p53, which joins BRCA1 to transcribe GADD45, leading to the binding of GADD45 to MEKK4, and subsequently initiating MAPK.

1.5.5. The Sequential DNA Repair-“Linker”-MAPK Binding Determines Cell Fate

MMR, HR, NHEJ, NER and BER are the five identified DNA damage repair mechanisms. MMR, HR, NHEJ and NER all seem to directly or indirectly participate in the initiation or inhibition of apoptosis and/or cell cycle regulation via their effects on the MAPK pathway (Figure 1.16). In contrast, BER pathway is less understood. GADD45a derived from the NER pathway is likely to be required in methyl methanesulfonate (MMS)-triggered BER (Jung *et al.*, 2007), yet it is not known whether BER-induced cell death depends on GADD45a or MAPK. In all DNA repair mechanisms discussed above (Figure 1.16), the modulators (or the “linkers”) that transmit the DNA repair signals to the activation of MAPK, are all non-receptor tyrosine kinases (c-Abl and Lyn) except GADD45 (BRCA1 has a SH2-domain that may bind to the SH3- region of non-receptor tyrosine kinases, and this may be required for the down-stream MAPK activation).

Interestingly, the time needed for the initiation of MAPK signal varies according to different genomic stresses and repair mechanisms. Cisplatin can activate p38MAPK and JNK/SAPK via MMR/c-Abl in an hour (Pandey *et al.*, 1996). IR also activates JNK/SAPK via a proposed NHEJ/DNA-PK/Lyn/MEKK1 pathway in one hour (Lee *et al.*, 1998). In contrast, MMS (an alkylating agent) can only

activate DNA-PK/JNK after 6 hrs of treatment (Fritz *et al.*, 1998), suggesting that NHEJ can be either a rapid (IR, 1 hr) and a delayed (MMS, 6 hr) mechanism for activation of MAPK, depending on the types of stimuli. UV and MMS activate JNK/SAPK and p38MAPK by the proposed NER/GADD45/MEKK4 pathway only after 5 hrs of treatment (Wang *et al.*, 1999), implying that NER is a mechanism for late activation of MAPK, probably due to the extra time needed for induction of GADD45 expression before NER can be activated. Currently, there is no data demonstrating the time needed for the MAPK initiation by HR. These results suggest that cell death induced by DNA damage may be sequential when handled by different DNA repair mechanisms.

This sequential DNA repair-“linker”-MAPK binding mode discussed above may explain why excess DNA damage leads to apoptosis while limited damage does not. Excessive DNA damage activates “linkers” such as c-Abl, BRCA1, Lyn and GADD45 for processing DNA repair. These activated “linkers” can then recruit more MAPKKs, leading to increased activation of downstream effectors. As a result, the transition from DNA damage to apoptosis, is actually a phenomenon caused by excessive association of these “linkers” with MAPKKs. Evidence supporting this hypothesis is that over-expression of BRCA1 (Thangaraju *et al.*, 2000), GADD45 (Mak *et al.*, 2004) or c-Abl (Theis and Roemer, 1998) alone could

lead to cell death independent of DNA damage.

In conclusion, a number of "linkers" have been identified that can activate the downstream MAPK pathways in response to DNA damage repair signals, leading to cell death. Loss of these "linkers" is believed to cause resistance to DNA damaging agents. Clinically, these "linkers" may represent useful biomarkers for the prediction of patient response in chemo- or radio-therapy.

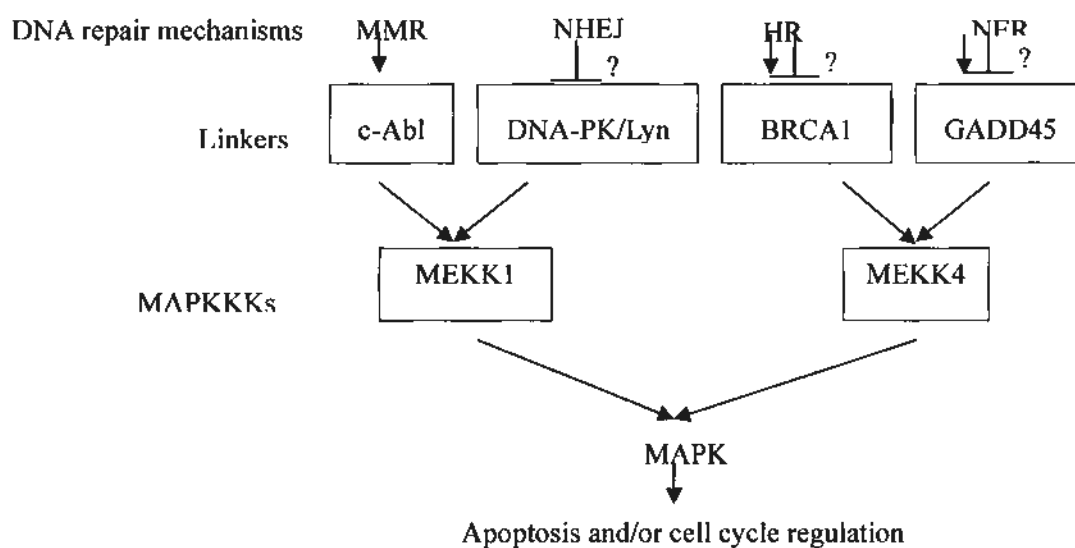


Figure 1.16: Proposed "linkers" transmit cellular signals from DNA damage repair mechanisms to MAPK. c-Abl, Lyn, BRCA1 and GADD45 may link MMR, NHEJ, HR and NER, respectively, to the MAPK pathway, consequently leading to apoptosis and/or cell cycle regulation.

1.5.6 Proposed Effect of *R,R*-5 as a DNA Damaging Agent

From the discussion above (Chapter 1.5.1), cisplatin can activate MMR/c-Abl/p38MAPK signaling pathway after 1 hr treatment (Pandey *et al.*, 1996), to

mediate the downstream effect on cell cycle regulation and apoptosis. Importantly, this signal transduction pathway is not shared by oxaliplatin (Nehmé *et al.*, 1999). With the DACH moiety, *R,R*-5 is believed to behave similarly to oxaliplatin. *R,R*-5 may also bypass the MMR pathway and fail to activate p38MAPK after 1 hr treatment. The evidence demonstrating the lack of effect of oxaliplatin and *R,R*-5 at the antephase cell cycle checkpoint, a known downstream pathway of p38MAPK, will be presented in Chapter Three.

1.6 Study Objectives

To further our understanding about the dual mechanisms of action of the novel Pt compound *R,R*-5, the aims of this thesis work are:

- a) To differentiate the biological behavior of *R,R*-5 from oxaliplatin (using cDNA microarray analysis; Chapter Two);
- b) To study the effect of *R,R*-5 at the antephase cell cycle checkpoint (Chapter Three);
- c) To study the effect of *R,R*-5 at the G2 cell cycle checkpoint (Chapter Four).

Chapter Two

cDNA Microarray Analysis

2.1 Introduction

In our continued quest for a superior Pt-based anticancer drug that is distinct from cisplatin and carboplatin, we have constructed a novel DACH-Pt-DMC analogue (*R,R*-5) having the same conformation as oxaliplatin (Chapter 1.3.3; Yu *et al.*, 2006). Oxaliplatin is the only DACH-containing Pt-based anticancer drug currently in clinical use. *R,R*-5 has the closest structural resemblance to oxaliplatin, with DMC replacing oxalic acid in oxaliplatin as the leaving group ligand. It was shown to be the most potent amongst our novel series of TCM-Pt compounds and is also devoid of cisplatin cross-resistance. A potential dual mechanism of drug action has been proposed for *R,R*-5: (1) the DACH platinum moiety alkylates DNA; and (2) the leaving ligand DMC produces additional DNA damage and/or cell cycle distortion (Pang *et al.*, 2007). To better understand the role played by DMC in the superior antitumor activity of *R,R*-5 over oxaliplatin, the differences in gene regulation in cells treated by the two compounds were explored by cDNA microarray analysis. As described in Chapter 1.3.2 (Figure 1.4), *R,R*-5 can be hydrolyzed to

give the PP2A inhibiting DMC as the leaving ligand. Results from the cDNA microarray analysis could reveal the specific cellular pathways targeted by DMC and could also explain the higher cytotoxicity and capability to induce DNA damage of *R,R*-5 than oxaliplatin (Pang *et al.*, 2007).

The cDNA microarray analysis was performed in total RNAs obtained from a human colon cancer cell line HCT116 treated with *R,R*-5 or oxaliplatin. Oxaliplatin is the first Pt-based drug approved by Food and Drug Administration (FDA) in the U.S.A. for the treatment of advanced colorectal cancer, where cisplatin or carboplatin was found to have compromised anti-cancer activity (Simpson *et al.*, 2003). Therefore, the study is expected to demonstrate the biological difference between *R,R*-5 and oxaliplatin and the functional role of DMC in a clinically relevant tumor type.

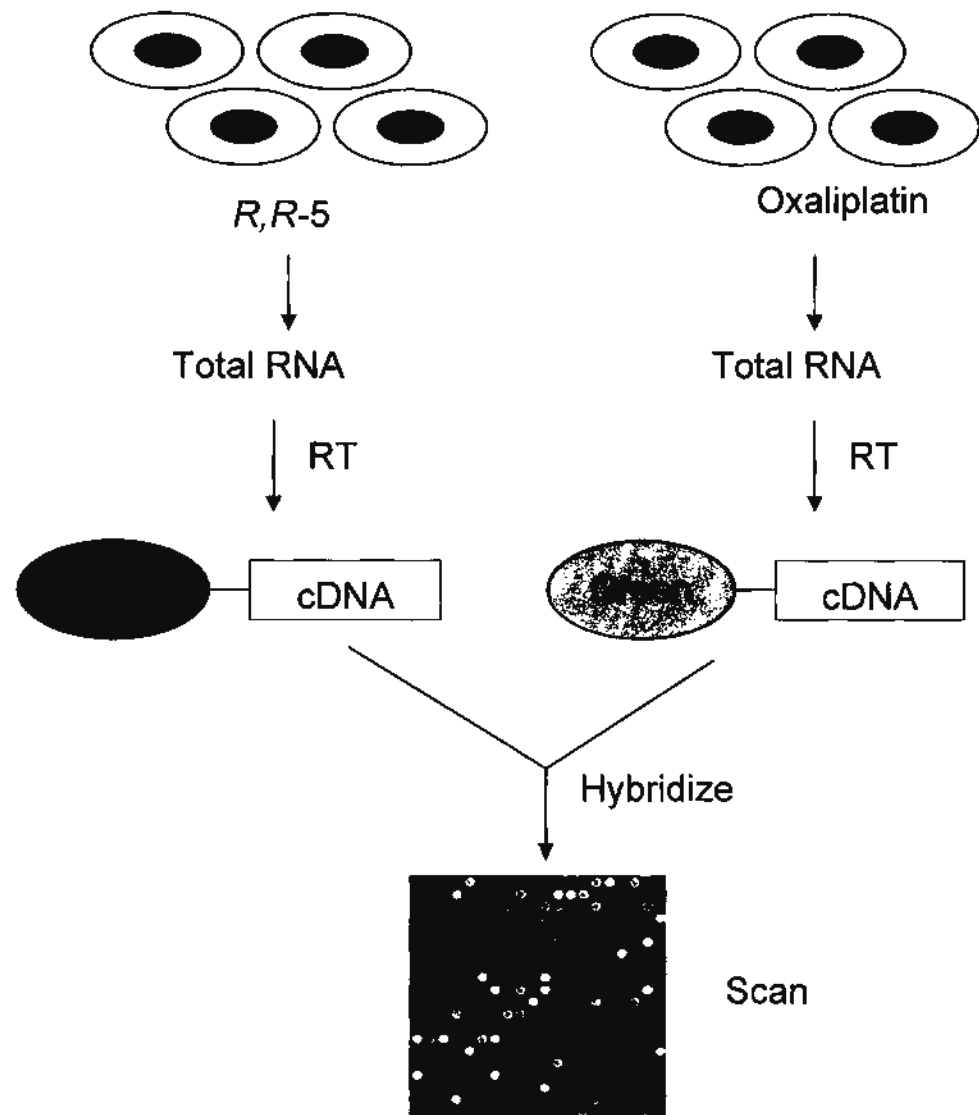


Figure 2.1: Protocol of microarray analysis in HCT116 cells.

The protocol for the microarray analysis is illustrated in Figure 2.1. Total RNA from the human colon cancer cell line HCT116 was extracted after exposure to *R,R*-5 or oxaliplatin, respectively. The RNA was then reverse-transcribed into fluorescence-labeled cDNA. The sample of *R,R*-5 treated HCT116 cells was labeled

in red, and oxaliplatin in green. Then the cDNA was hybridized to a set of known oligonucleotide probes, representing most of the well-characterized human genes in the human genome, arrayed on a gene chip. Unbound and non-specific cDNA was washed away, and the fluorescence signals were then captured and processed by a detector. By comparing the relative intensity of the red and green fluorescence on each oligonucleotide probe, the difference in mRNA level of each gene in *R,R-5* and oxaliplatin treated HCT116 cells can be estimated. In order to avoid false positive and negative results in the microarray assay, the experiments were conducted twice and only genes that were 200% higher and 50% lower in both trials were considered to be positive and negative, respectively.

2.2 Materials and Methods

2.2.1 Chemicals and Reagents

Oxaliplatin and ethidium bromide were obtained from Aldrich-Sigma Chemical Company (St. Louis, MO, U.S.A.). *R,R*-5 was synthesized by the School of Pharmacy at the Chinese University of Hong Kong, identified by elemental analysis, mass spectrum and ¹H-NMR (nuclear magnetic resonance) (Yu *et al.*, 2006). Agarose was purchased from Gene Company Limited (Hong Kong, China); TriReagent from Molecular Research Center, Inc. (Cincinnati, OH, U.S.A.); diethyl pyrocarbonate (DEPC) from ICN Biomedicals, Inc. (Aurora, OH, U.S.A.); RNeasy MinElute Cleanup Kit from Qiagen, Inc. (Valencia, CA, U.S.A.); GeneChip® Human Genome U133A Set for microarray analysis from Affymetrix Inc. (Santa Clara, CA, U.S.A.); GeneTools software from Syngene (Cambridge, UK). 100-bp DNA ladder and DNA/*Hind* III fragments ladder were purchased from Invitrogen (Carlsbad, California, U.S.A.). All other chemicals and solvents used were of analytical grade.

2.2.2 Cell Line and Cell Culture

Human colorectal cancer cell line HCT 116 was obtained from the American Type Culture Collection (ATCC), cultured in RPMI1640 medium (Hyclone, South

Logan, UT, Africa), supplemented with 10% fetal bovine serum (v/v) (Hyclone, South Logan, UT, Africa), 100 U/mL penicillin and 100 U/mL streptomycin (Hyclone, South Logan, UT, Africa) in a humidified CO₂ incubator (5% CO₂/95% air) at 37 °C. The cell line was split every 3-4 days.

2.2.3 Preparation of RNA Samples

4×10^5 HCT116 cells were seeded onto 10 cm² culture plates. 24 hours later, cells were exposed to either oxaliplatin or *R,R*-5 at their IC₅₀ concentrations for 72 hrs (i.e., 1.24 μM for oxaliplatin and 0.40 μM for *R,R*-5) (Yu *et al*, 2006). After drug treatment, the cells were washed with PBS and trypsinized. Total RNA was extracted by TriReagent (1 mL), following a standard protocol (Molecular Research Center, TRI Reagent Protocol). Cells were lysed by repetitive pipetting and the homogenate was stored for 5 minutes at room temperature to permit complete dissociation of the nucleoprotein complexes. Chloroform (0.2 mL) was added and the sample mixture was shaken vigorously for 15 seconds. The resulting mixture was stored at room temperature for 2–15 minutes and centrifuged at 12,000 g for 15 minutes at 4 °C. RNA remained exclusively in the upper aqueous phase, which was transferred to a fresh tube and mixed with isopropanol (0.5 mL) in order to precipitate out the RNA. Afterwards, the sample mixture was stored at room

temperature for 5–10 minutes and centrifuged at 12,000 g for 8 minutes at 4 °C. A white pellet (RNA sample) was formed at the bottom of the tube after centrifugation and the supernatant was removed. The RNA pellet was then washed (by vortexing) in 75% ethanol (1 mL) (prepared in DEPC-water) and subsequently centrifuged at 7,500 g for 5 minutes at 4 °C. The ethanol was removed and the RNA pellet was briefly air-dried. The RNA was dissolved in DEPC treated water and then incubated for 10–15 minutes at 55–60 °C to ensure complete dissolution. The RNA samples were purified by using Qiagen RNeasy MinElute Cleanup Kit (Hilden, Germany).

2.2.4 RNA Purity

The purity of RNA samples used is crucial for the success of microarray experiments. Impurities could inhibit reverse transcription and the subsequent DNA-probe binding. RNA purity was determined by the UV absorption method and further confirmed by electrophoresis examination. By using the UV-2550 spectrophotometer (Shimazu, Tokyo, Japan), the ratio of the absorbances at wavelengths 260/280 ($A_{260/280}$) were measured for RNA samples. Acceptable $A_{260/280}$ ratios fall in the range of 1.8 to 2.1 (ratios < 1.8 indicates possible protein contamination whereas ratios > 2.1 indicates the presence of degraded RNA, truncated cRNA transcripts, and/or excess free nucleotides) as described by

Affymetrix (Affymetrix, GeneChip® Expression Analysis, Data Analysis Fundamentals).

Normal agarose (1.5 g) was allowed to dissolve completely in 1× Tris-Borate-EDTA (TBE) buffer (100 mL) by using a microwave oven. Ethidium bromide (50 µg) was added to the mixture and allowed to solidify at room temperature. Total RNA was then analyzed by gel electrophoresis (1.5% agarose) in 1 × TBE buffer. Bands corresponding to the ribosomal RNA (rRNA) can be visualized by ethidium bromide staining. The intensity of the bands was analyzed by GeneTools software. For eukaryotic samples, intact RNA should give clear 28S and 18S rRNA bands. The 28S rRNA band should be about 2 times more intense than the 18S rRNA band. This 2:1 ratio (28S:18S) is a good indicator of purity of the RNA samples.

2.2.5 Microarray Analysis with the Human HG-U133A GeneChip (Affymetrix Inc.)

The human HG-U133A GeneChip containing ~54,000 probe sets including 38,500 well-characterized human genes (Affymetrix Inc.) was used in our microarray analysis. The microarray analysis was contracted to Gene Company Limited, Hong Kong. Each probe on the GeneChip® uses a 25-mer complementary DNA sequence targeting one gene in the genome. Each probe was designed to have the optimal

balance between sensitivity and specificity to the target gene. 22 probes are usually used for each expression measurement and this multiple probes design provides high sensitivity and reproducibility. Apart from those probes that match perfectly with their target sequence, paired “mismatch” probes were also built in the GeneChip to detect and eliminate false or contaminating fluorescence signals within the measurement (Affymetrix Webpage).

2.3 Results and Discussions

The effect on gene expression in HCT116 cells treated with either oxaliplatin or *R,R*-5 was compared by cDNA microarray analysis. The results are expected to distinguish the cellular responses specific to *R,R*-5 and to indicate the contribution by the DMC ligand to the overall cytotoxicity of this novel TCM-Pt compound. The criterion for gene selection was a fold-change of ≥ 2.0 (or < 0.5) in both replicate experiments. According to this criterion, 137 genes were found to be up-regulated in HCT116 cells treated with *R,R*-5 compared with oxaliplatin, while only 4 genes were found to be down-regulated (Table 2.1). Since *R,R*-5 has DMC as the leaving ligand in place of oxalic acid in oxaliplatin, the results suggested that the DMC component may generally activate pathways and gene transcription (137 genes up-regulated), rather than suppressing cell signaling transduction (only 4 genes down-regulated), under the condition when cells were consistently exposed to genotoxic stress from the DACH-Pt moiety.

To illustrate the potential biological functions of DMC, the 137 up-regulated genes were categorized into five groups according to their gene function: cell cycle regulation (51 genes), DNA replications (25 genes), DNA repair (6 genes), and others (55 genes) (Figure 2.2).

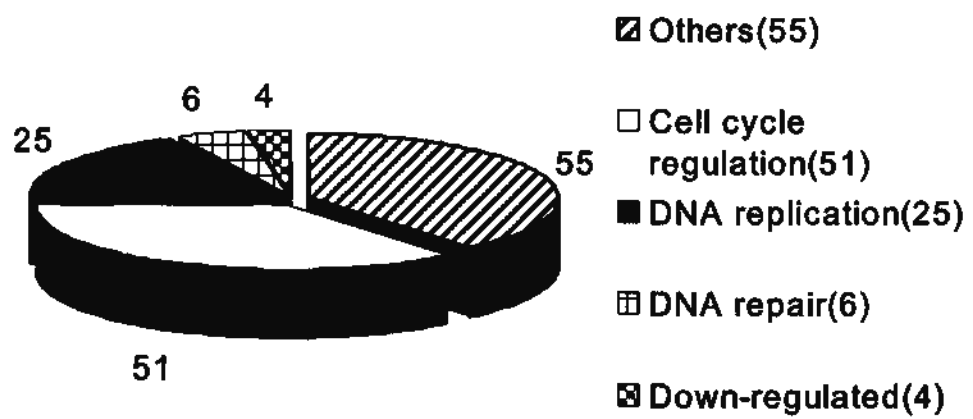


Figure 2.2: Results from the microarray analysis in HCT116 cells (*R,R*-5 v.s. oxaliplatin at IC_{50}). 137 genes were found up-regulated, which were categorized into five sub-groups as shown. Only 4 genes were found down-regulated.

Table 2.1: Microarray analysis of *R,R*-5 against oxaliplatin at respective IC₅₀ in HCT116 cells.

Up-regulated (Total 137)				Down-regulated (Total 4)	
Cell Cycle Regulation (Total 51)	DNA Replication (Total 25)	DNA Repair (Total 6)	Other genes (Total 55)		
SMC4L1	TOP2A	MSH6	stathmin	GINS2	SERPINE1
PLK1	RRM1	RAD51	H2AFZ	FAM64A	NR4A2
KIAA0101	MCM6	RAD51AP1	ID2	CCDC99	MSH4
cyclinB2	MCM2	MSH2	ID2B	PRC1	SNAI2
CDC20	TK1	RAD54B	PSRC1	LOC146909	
UBE2C	DHFR	BRCA1	USP1	RACGAP1	
SPAG5	FOXM1		PRKACB	GINS3	
CDC20	PRPS2		FBXO11		
MAD2L1	RFC4		DCK		
cyclinA2	RFC3		EZH2		
DLG7	FEN1		TMPO		
CDC6	PRIM1		GGH		
ZWINT	ORC1L		PRKAR2B		
AURKA	ITGB3BP		DBF4		
CDKN2C	POLE2		FKBP5		
KNTC2	HMGB2		MELK		
CKS2	DUT		STIL		
GTSE1	RRM2		NMU		
KIF11	MCM7		CYP24A1		
CDC7	MCM4		KITLG		
NEK2	MCM5		HMMR		
KIF23	HMGB1		PIR		
TTK	HMG1L1		WHSC1		
CENPA	ASF1B		SPBC25		
CENPF	MCM10		GINS1		
CSPG6			TAF5		
AURKB			SLC19A1		
BUB1B			TMEM97		
CDKN3			PAQR4		
cyclinE2			OIP5		
WEE1			PSMC3IP		
BRRN1			NUSAP1		
cyclinB1			CEP55		
DLEU2			DTL		
DLEU2L			DKFZp762E1312		
geminin			C22orf18		
HCAP-G			ATAD2		
ASPM			FBXO5		
E2F8			MLF1IP		
ESPL1			PBK		
KIF14			SHCBP1		
KIF2C			C16orf60		
PLK4			LUZP50		
KIF22			C11orf75		
KIAA1794			DEP domain containing 1		
KIF4A			CDCA3		
KIF20A			CDCA8		
KIF18A					
KIF23					
TPX2					
survivin					

2.3.1 Cell Cycle Regulation

51 genes related to cell cycle regulation were found to be up-regulated (Figure 2.3). These genes can be further divided into two sub-categories according to their role in the cell cycle transition: genes related to G1 to S transition (9 genes) and genes related to G2 to M transition (42 genes).

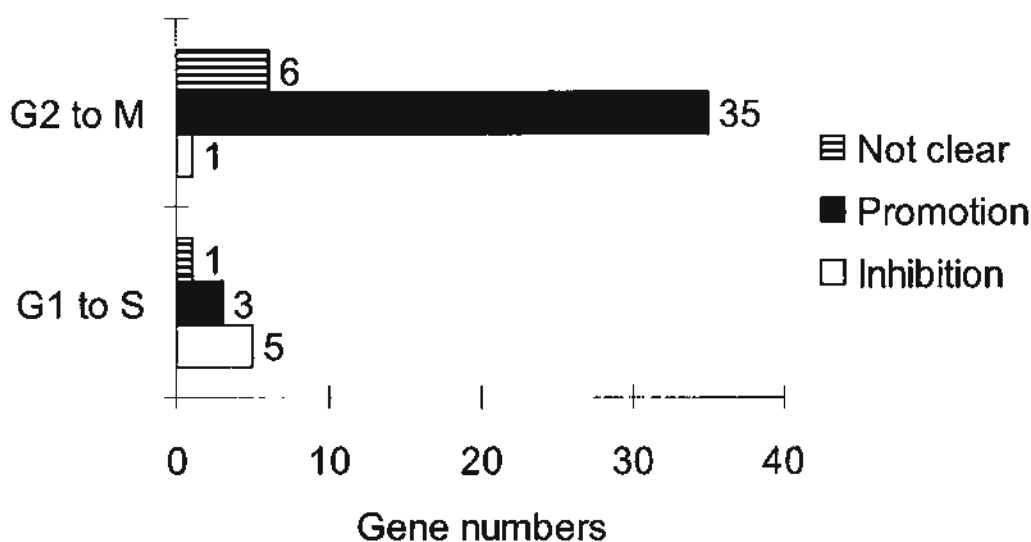


Figure 2.3: Genes related to cell cycle regulation in the microarray analysis (*R,R-5* vs. oxaliplatin at respective IC_{50} in HCT116 cells). 51 cell cycle regulating genes were found to be up-regulated, which were categorized into two groups: genes related to G1 to S transition (9 genes) and G2 to M transition (42 genes).

2.3.1.1 Genes Related to G1 to S Transition

9 genes among the 51 up-regulated cell cycle genes are critical for the G1 to S phase transition: 5 of them inhibit this transition; 3 of them cause a promotion; and the remaining gene is functionally unknown but predicted to be involved in G1 to S transition (Figure 2.3, Table 2.2).

The 5 up-regulated genes causing an inhibition of G1 to S transition were KIAA0101, geminin, CDKN2C, CDKN3 and E2F8, in which KIAA0101 and geminin are more extensively studied than the others. KIAA0101 can bind to proliferating cell nuclear antigen (PCNA) (Guo *et al.*, 2006) and prevent the formation of PCNA ring trimer as the DNA replication enzyme loading platform. Geminin can bind to DNA replication initiating protein Cdt1 and inhibit the formation of origin replication complex (ORC), thereby hindering DNA synthesis (Pitulescu *et al.*, 2005). Recently, CDKN2C (Bai *et al.*, 2006), CDKN3 (Chinami *et al.*, 2005) and E2F8 (Maiti *et al.*, 2005) have been shown to inhibit cell cycle transition from G1 to S phase, though the precise mechanism is not clear.

Table 2.2: Genes related to G1→S transition that were found up-regulated (*R,R*-5 vs. oxaliplatin at respective IC_{50} in HCT116 cells).

	Gene Title	Gene Symbol	Description	Fold (trial 1)	Fold (trial 2)	References
Inhibition (5)	geminin, DNA replication inhibitor	GMNN	Inhibit DNA synthesis	2.46	2.63	Pitulescu <i>et al.</i> , 2005
	KIAA0101	KIAA0101	Bind to PCNA, inhibit G1→S transition	2.29	2.46	Guo <i>et al.</i> , 2006
	cyclin-dependent kinase inhibitor 2C (p18, inhibits CDK4)	CDKN2C	Inhibit G1→S transition	3.24	3.48	Bai <i>et al.</i> , 2006
	cyclin-dependent kinase inhibitor 3 (CDK2-associated dual specificity phosphatase)	CDKN3	Inhibit G1→S transition	2.29	2.46	Chinami <i>et al.</i> , 2005
	E2F transcription factor 8	E2F8	Inhibit G1→S transition	2.14	2.63	Maiti <i>et al.</i> , 2005
Promotion (3)	CDC6 cell division cycle 6 homolog (<i>S. cerevisiae</i>)	CDC6	DNA replication initiation	3.03 2.63	2.63 2.46	Ayad, 2005
	CDC7 cell division cycle 7 (<i>S. cerevisiae</i>)	CDC7	DNA replication initiation	2	3.03	Masai and Arai, 2002
	CCNE2	Cyclin E2	Promote G1→S transition	2.11	2.82	Hwang and Clurman, 2005
Not Clear (1)	KIAA1794	KIAA1794	Required in the S checkpoint (inhibit G1→S transition)	2.29 3.28	2.29 2.29	Miki <i>et al.</i> , 2001

The 3 up-regulated genes that promotes G1 to S transition were CyclinE2, CDC6 (*S. cerevisiae*) and CDC7 (*S. cerevisiae*). CDC6 and CDC7 were originally cloned from *S. cerevisiae* but highly resembled to human CDC6 (Ayad, 2005) and CDC7 (Masai and Arai, 2002), hence used (and universally considered) as human genes. This suggests that *R,R-5* may have a positive role in regulating DNA synthesis (compared with oxaliplatin), owing to the fact that CDC6 (Ayad, 2005) and CDC7 (Masai and Arai, 2002) participate in the DNA replication initiation. This result is consistent with the finding that 25 genes related to DNA replication were also found to be up-regulated in the microarray analysis. Cyclin E2, the other up-regulated gene that promote G1 to S transition was reported to function closely to the more extensively studied Cyclin E1 (Hwang and Clurman, 2005), which can bind to CDK2 and promote G1 to S transition.

The functionally unclear gene KIAA1794 has been recently confirmed to be FANCI (Fanconi anemia, complementation group I) (Miki *et al.*, 2001), a gene required in the S phase checkpoint in response to DNA damaging agents. It is believed to inhibit G1 to S transition.

Since we have identified five genes up-regulated by *R,R-5* that can inhibit G1 to S phase transition, it will be reasonable to predict that *R,R-5* can arrest more

HCT116 cells in G1 phase than oxaliplatin. HCT116 cells have a wild-type p53 gene and therefore they should have a functional G1 checkpoint. In fact, our previous study demonstrated that, at the concentration of $5 \times IC_{50}$ of these two drugs, *R,R*-5 could lead to G1 arrests in HCT116 cells after 72 hrs treatment (Yu *et al.*, 2006). In terms of therapeutic effect of DNA damaging agents in patients, it is desirable to activate the G1 checkpoint to prevent apoptosis of the G0/G1 phase cells. Since most normal cells in the human body stay in G0 phase, a functional G1 checkpoint can protect normal cells from chemotherapy and maintain genomic stability from DNA damage. Anti-cancer drugs that cause a G1 to S arrest could selectively kill the proliferating cancer cells but spare the normal healthy cells, thereby avoiding toxic side effect. From the microarray data we can predict that *R,R*-5 may have less side effect on the normal cells. Our previous study has demonstrated that no lethal effect was observed in male nude mice after treatment with compound 5 (a mixture of conformational isomers containing *R,R*-5) at up to 50mg/kg, a dose at which prominent anti-tumor activity can be achieved. In contrast, remarkable mice mortality was observed upon cisplatin treatment at 8mg/kg and above (Ho *et al.*, 2001).

2.3.1.2 Genes Related to G2 to M Transition

42 genes related to G2 to M transition were found to be up-regulated according to the microarray analysis: 35 of them can promote G2 to M transition; 1 gene can inhibit this transition; and the remaining 6 genes are functionally unclear but have been reported to be associated with G2 to M transition (Table 2.3).

Upon a closer look at the 35 up-regulated genes that promote G2 to M transition, most of them played an essential role in mitosis and are considered mitotic markers (such as Cyclin B1, CDK1, AURKA, CENPF and TPX2, etc). Since so many mitotic genes were up-regulated by *R,R-5* compared to oxaliplatin, we believe that *R,R-5* did not promote just one or two particular mitotic pathways but it may accelerate cells entering mitosis compared with oxaliplatin.

The anti-apoptosis gene survivin is an interesting gene among the 35 up-regulated genes that promote G2 to M transition. Survivin has been extensively studied. It inhibits mitochondria-mediated apoptosis by preventing the activation of caspase 9 (Mita *et al.*, 2008), which is also implicated in anti-cancer drugs resistance. Based on this reported function of survivin, it should therefore be categorized into genes related to apoptosis. However, survivin is also an important component in the mitotic chromosomal passenger complex, regulating microtubule dynamics in mitosis and cytokinesis (Mita *et al.*, 2008). Therefore, survivin can be categorized as

both anti-apoptotic genes and mitotic genes. Regarding there were already 34 other mitotic genes up-regulated without transcriptional change in any other apoptotic genes, survivin is more reasonable to participate in the mitotic events rather than apoptosis, thus it is classified as cell cycle regulation genes. Since oxaliplatin and *R,R*-5 were used at their IC_{50} for microarray analysis, there should be equally 50% of cell death in both *R,R*-5 and oxaliplatin treated cells. This may explain that no apoptotic genes were found up- or down-regulated.

It is commonly believed that DNA damage checkpoints are activated when cancer cells are exposed to various DNA damages, which stops cell cycle progression and allow time for DNA repair. This is crucial for the cells because errors can be avoided, especially in important cellular activities such as DNA replication, transcription and mitosis. Errors in these cellular events may be detrimental to cell survival. For example, if one cell bearing DNA damage fails to repair DNA damage and enter mitosis, it will lead to mitotic catastrophe, where sister chromatids are unable to separate and be equally divided into two daughter cells, chromosomes are irregularly packed, and the cell fails to exit mitosis and eventually dies. As a result, cancer cells often utilize cell cycle checkpoints to attenuate cell cycle progression for DNA damage repair and then re-enter cell proliferation,

thereby leading to drug resistance and improved cancer cell survival after chemotherapy.

Based on this working model, the disruption of DNA damage checkpoints could be used as a strategy in cancer chemotherapy, to elicit mitotic catastrophe and finally cancer cell death. Several DNA damage checkpoints have been identified in a cell cycle: G1 checkpoint, S phase checkpoint, G2 checkpoint (late S checkpoint), mitotic spindle checkpoint, antephasis checkpoint (late G2 checkpoint), and the post-mitotic checkpoint (Figure 1.2). Among these checkpoints, G2 and antephasis checkpoints are critical for the regulation of G2 to M transition. According to our microarray data, *R,R*-5 seems to be able to bypass these two checkpoints and facilitate cells entering mitosis compared with oxaliplatin, because 35 genes promoting the G2 to M transition were found to be up-regulated. Since the microarray analysis is performed with an aim to reveal the distinct biological effects contributed by the leaving ligand DMC, more extensive studies have been performed to compare the effect of *R,R*-5, cisplatin and oxaliplatin on the G2 to M transition (at the antephasis and G2 checkpoint). The results will be discussed in Chapter 3 (antephasis checkpoint) and Chapter 4 (G2 checkpoint).

The only up-regulated gene that inhibits the G2 to M transition was WEE1 homolog (*S. pombe*). WEE1 is expressed in G1, S and G2 phases but not in mitosis,

which protects immature activation of the major mitotic promoting factor CDK1/Cyclin B1 (Lim and Surana, 2003). The biological meaning of the up-regulation of WEE1 is not clear but it may suggest a higher proportion of cells in the G1, S or G2 phases upon *R,R*-5 treatment, compared with oxaliplatin. .

Table 2.3: Genes related to G2→M transition that were found to be up-regulated (*R,R-5* vs. oxaliplatin at respective IC₅₀ in HCT116 cells).

	Gene Title	Gene Symbol	Description	Fold (trial 1)	Fold (trial 2)	References
Promotion (35)	SMC4 structural maintenance of chromosomes 4-like 1 (yeast)	SMC4L1	Part of condensin; promote chromatid segregation	2.46 2.14	2.46 2.63	Yen <i>et al.</i> , 2005
	chromosome condensation protein G	HCAP-G	Non-SMC subunit of condensin, promote chromatid segregation	2 2.46	2.82 2.82	Yeong <i>et al.</i> , 2005
	barren homolog 1 (Drosophila)	BRRN1	Part of condensin; promote chromatid segregation	2.63	2.46	Cabello <i>et al.</i> , 2005
	polo-like kinase 1 (Drosophila)	PLK1	Inhibit Emil (mitotic inhibitor), activate CDC25C	2.14	2.14	Eckerdt and Strebhardt, 2006
	polo-like kinase 4 (Drosophila)	PLK4	Inhibit Emil (mitotic inhibitor), promote chromatid segregation	2.42	2.29	Habedanck <i>et al.</i> , 2005
	cyclin B1	CCNB1	Promote G2 →M	3.03	3.24	Ohi and Gould <i>et al.</i> , 1999
	cyclin B2	CCNB2	Promote G2 →M	4	3.24	Ohi and Gould <i>et al.</i> , 1999
	CDC20 cell division cycle 20 homolog (<i>S. cerevisiae</i>)	CDC20	Bind to APC, promote chromatid segregation	2.63	2.46	Fang <i>et al.</i> , 1998
	cell division cycle 2, G1 to S and G2 to M	CDC2	Part of MPF complex (CDC2-cyclinB), Promote G2 →M	3.03 2.82	3.73 3.48	Gowdy <i>et al.</i> , 1998
	BUB1 budding uninhibited by benzimidazoles 1 homolog beta (yeast)	BUB1B	Motosis check point protein, inhibit APC	3.03	3.73	Davenport <i>et al.</i> , 1999

Table 2.3 (continued): Genes related to G2→M transition that were found to be up-regulated (*R,R-5* vs. oxaliplatin at respective IC₅₀ in HCT116 cells).

	Gene Title	Gene Symbol	Description	Fold (trial 1)	Fold (trial 2)	References
Promotion (35)	BUB1 budding uninhibited by benzimidazoles 1 homolog (yeast)	BUB1	Motosis check point protein, inhibit APC	4 2.46	3.48 3.24	Davenport <i>et al.</i> , 1999
	ZW10 interactor	ZWINT	Promote chromatid segregation	2.82	3.03	Wang <i>et al.</i> , 2004
	aurora kinase A	AURKA	Spindle formation, centrosome maturation, chromatid segregation	2.82 3.03	2.82 3.24	Yang <i>et al.</i> , 2005
	aurora kinase B	AURKB	Spindle formation, centrosome maturation, chromatid segregation	3.24	2	Yang <i>et al.</i> , 2005
	kinetochore associated 2	KNTC2	Promote chromatid segregation	2.82	4	Not clear
	CDC28 protein kinase regulatory subunit 2	CKS2	Promote chromatid segregation	2	2	Spruck <i>et al.</i> , 2005
	kinesin family member 11	KIF 11	Promote chromatid segregation	3.48	4.28	Miki <i>et al.</i> , 2001
	kinesin family member 14	KIF 14	Promote chromatid segregation	2.46	3.73	Miki <i>et al.</i> , 2001
	kinesin family member 22	KIF 22	Promote chromatid segregation	2	2.14	Miki <i>et al.</i> , 2001
	kinesin family member 23	KIF 23	Promote chromatid segregation	2.46	3.48	Miki <i>et al.</i> , 2001

Table 2.3 (continued): Genes related to G2→M transition that were found to be up-regulated (*R, R-5* vs. oxaliplatin at respective IC₅₀ in HCT116 cells).

	Gene Title	Gene Symble	Description	Fold (trial 1)	Fold (trial 2)	References
Promotion (35)	kinesin family member 2C	KIF 2C	Promote chromatid segregation	3.03 2.14	2.82 2.82	Miki <i>et al.</i> , 2001
	kinesin family member 4A	KIF 4A	Promote chromatid segregation	2.14	2.82	Miki <i>et al.</i> , 2001
	kinesin family member 18A	KIF 18A	Promote chromatid segregation	3.73	2.82	Miki <i>et al.</i> , 2001
	kinesin family member 20A	KIF 20A	Promote chromatid segregation	3.24	2.82	Miki <i>et al.</i> , 2001
	NIMA (never in mitosis gene a)-related kinase 2	NEK2	Promote chromatid segregation	3.24	3.73	Hayward <i>et al.</i> , 2006
	TTK protein kinase	TTK	Mitotic spindle checkpoint	4.59	4.28	Fisk <i>et al.</i> , 2006
	centromere protein A, 17kDa	CENPA	Mitosis progression	4	3.48	Saxena <i>et al.</i> , 2006
	centromere protein F, 350/400ka (mitosin)	CENPF	Mitosis progression	2.46	2.82	Ma <i>et al.</i> , 2006
	chondroitin sulfate proteoglycan 6 (bamacan)	CSPG6	SMC3 or Bamacan; Promote chromatid segregation	2.29	2.63	Potts <i>et al.</i> , 2006
	asp (abnormal spindle)-like, microcephaly associated (<i>Drosophila</i>)	ASPM	Control centrosome unction	2.82	2.82	Zhong <i>et al.</i> , 2005
	MAD2 mitotic arrest deficient-like 1 (yeast)	MAD2L1	Mitotic spindle check point	3.73	3.2	Percy <i>et al.</i> , 2000

Table 2.3 (continued): Genes related to G2→M transition that were found to be up-regulated (*R,R-5* vs. oxaliplatin at respective IC₅₀ in HCT116 cells).

	Gene Title	Gene Symble	Description	Fold (trial 1)	Fold (trial 2)	References
Promotion (35)	extra spindle poles like 1 (<i>S. cerevisiae</i>)	ESPL1	Seperase, promote G2-M	2	2	Terret and Jallepalli, 2006
	cyclin A2	CCNA2	Promote G1→S transition	3.03	3.48	Wolgemuth <i>et al.</i> , 2004
	survivin	survivin	Mitotic chromosomal passenger complex	2.84	2.19	Mita <i>et al.</i> , 2008
	TPX2, microtubule-associated, homolog (<i>Xenopus laevis</i>)	TPX2	Control Aurora localization	2.46	2.29	Kufer <i>et al.</i> , 2002
Inhibition (1)	WEE1 homolog (<i>S. pombe</i>)	WEE1	Inhibit G2 →M transition	2.82	3.03	Lim <i>et al.</i> , 2003
Not clear (6)	G-2 and S-phase expressed 1	GTSE1	Present in S/G2 cells	2.46	3.03	Utrera <i>et al.</i> , 1998
	sperm associated antigen 5	SPAG5		2.46	2.14	Not clear
	discs, large homolog 7 (<i>Drosophila</i>)	DLG7	Tumor suppressor	2.82	3.73	Not clear
	deleted in lymphocytic leukemia, 2	DLEU2		2.82 2.29	4.28 3.48	Corcoran <i>et al.</i> , 2004
	deleted in lymphocytic leukemia 2-like	DLEU2L		2.82	4.28	Corcoran <i>et al.</i> , 2004
	ubiquitin-conjugating enzyme E2C	UBE2C		2.63	2.14	Not clear

The 6 functionally-unknown genes that may be related to G2 to M transition are SPAG5, DLG7 (Drosophila), DLEU2, DLEU2L, UBE2C and GTSE1. It is interesting to have identified GTSE1 (G2 and S-phase expressed 1) because GTSE1 is normally expressed in S and G2 phase, which promotes p53 degradation in physiological condition and maintains a balance in p53 level (Utrera *et al.*, 1998). Thus far, there is no direct evidence to prove that GTSE1 inhibits G2 to M transition, but it is clear that GTSE1 does not express in M phase cells. Considering that 25 genes related to DNA replication were found up-regulated (see later at Chapter 2.3.2.), the transcription of GTSE1 may be due to the presence of more cells in S phase (or S phase onset), rather than inhibition of G2 to M transition. Very little information is available for the remaining genes sperm associated antigen 5 (SPAG5) (Shao *et al.*, 2001), Discs, Large Homolog 7 (DLG7) (Drosophila) (Gudmundsson *et al.*, 2007), Deleted in lymphocytic leukemia, 2 (DLEU2) (Corcoran *et al.*, 2004), DLEU2L (Corcoran *et al.*, 2004), Ubiquitin-conjugating enzyme E2C (UBE2C) (Lin *et al.*, 2007). They may participate in mitosis or meiosis.

2.3.2 DNA Replication

25 genes related to DNA replication were found to be up-regulated after *R,R*-5 treatment compared with oxaliplatin. They are known to be indispensable components for DNA synthesis, such as TOP2A, MCM2, MCM7, etc. Some of these genes, such as TOP2A, also participate in the DNA damage repair pathways. After removal of damaged DNA bases, the DNA replication machinery is needed to fill in the opened DNA strands. We considered these functionally-overlapping genes as DNA replication genes rather than DNA damage repair genes, because most of DNA replication genes (total 25) were found to be up-regulated in our microarray analysis. These 25 genes exert their functions in diverse areas: recognition of DNA replication origin (ORC1L), formation of enzyme loading platform (MCM2), controlling the topological change of DNA (TOP2A), stabilizing the open DNA strand (HMGB1), etc. Based on this finding, *R,R*-5 may enhance DNA replication compared with oxaliplatin. Therefore, *R,R*-5 may probably bypass the S phase cell cycle checkpoint besides the mitotic DNA damage checkpoints as discussed above (Chapter 2.3.1.2). However, this possibility will not be explored in this thesis.

2.3.3 DNA Damage Repair

6 genes related to DNA damage repair were found to be up-regulated in the microarray analysis (Table 2.1). MSH2 and MSH6 belong to the mismatch repair (MMR) pathway and RAD51, RAD51AP1, RAD54B and BRCA1 (BRCA1 also regulates nucleotide excision repair) are critical genes from the homologous recombination (HR) pathway. This result suggests that the incorporation of DMC into DACH-Pt moiety may lead to the activation of both MMR and HR pathways. This agrees with our earlier finding that *R,R*-5 can induce more severe DNA damage than oxaliplatin (Pang *et al.*, 2007). However, the activation of MMR by *R,R*-5 may be contradictory because another MMR gene MSH4, was found to be down-regulated in the microarray analysis (Table 2.1). Besides, DACH-containing drug oxaliplatin has been reported to bypass MMR recognition (Zdraves *et al.*, 2002).

2.3.4 Other Up-regulated Genes with Miscellaneous Functions and the Down-Regulated Genes

From the microarray analysis, there were another 55 up-regulated genes that cannot be categorized into a specific functional class (i.e. cell cycle regulation, DNA replication or DNA repair) (Table 2.1). Most of these genes are newly discovered whose biological functions are still yet to be defined. *Stathmin* is one of these genes

that deserve some discussion. Recently, it has been demonstrated that over-expression of stathmin leads to microtubule disassembly in mitosis (Iancu *et al.*, 2004). The PP2A inhibitor okadaic acid has also been reported to cause microtubule disassembly (Gurland *et al.*, 1993). Further mechanistic study demonstrated that PP2A maintains the hypophosphorylation of microtubule-associated protein tau, leading to the binding of tau to microtubule and an increase in microtubule stability (Sontag *et al.*, 1996). As PP2A inhibitors, DMC and *R,R*-5 may also lead to microtubule disassembly by: a) inhibition of PP2A, maintaining the phosphorylation of tau and consequently microtubule disassembly; and/or b) up-regulating stathmin (according to the microarray analysis result). Given that the disruption of microtubule assembly may activate the antephasic checkpoint via Chfr (Matsusaka and Pines, 2004), DMC and *R,R*-5 as PP2A inhibitors may activate the antephasic checkpoint through a similar mechanism. However, the antephasic checkpoint can be activated promptly within one hour of drug treatment, which therefore may not involve stathmin transcription. In Chapter Three, we will discuss activation of the antephasic checkpoint by cisplatin-induced DNA damage in greater detail. Since HCT116 cells do not express Chfr, this stathmin-mediated mechanism should not be functional to facilitate the activation of the antephasic checkpoint by *R,R*-5.

Although most of the genes are up-regulated by *R,R*-5 relative to oxaliplatin, we have also identified 4 significantly down-regulated genes (Table 2.1). Among them, only MSH4 is more extensively studied. MSH4 is known to participate in the mismatch repair (MMR) pathway. As discussed earlier, two other members of the MMR pathway (MSH2 and MSH6) were found to be up-regulated in the microarray analysis. Therefore, the down-regulation of MSH4 might be a false positive result, or suggest that MMR does not require MSH4 to repair *R,R*-5 induced DNA damage.

2.4 Conclusions

The goal of the microarray analysis is to reveal the distinct biological activity, if any, contributed by the DMC leaving ligand in *R,R*-5. Based on the microarray data and from our knowledge about DMC as a PP2A inhibitor, the following hypotheses can be generated:

- a) *R,R*-5 may activate the G1 DNA damage checkpoint and avoid damaging normal cells (5 genes that inhibit G1 to S transition were found to be up-regulated).
- b) *R,R*-5 may bypass the two mitotic DNA damage checkpoints: antephase checkpoint (will be discussed in Chapter Three) and G2 checkpoint (will be discussed in Chapter Four) (35 genes promoting G2 to M transition were found to be up-regulated). This may explain why *R,R*-5 is more cytotoxic than oxaliplatin.
- c) *R,R*-5 may also bypass the S phase checkpoint (25 genes regulating DNA replication were found to be up-regulated).
- d) *R,R*-5 may activate mismatch repair and homologous recombination to repair DNA damage (compared with oxaliplatin).
- e) *R,R*-5 may lead to microtubule disassembly by decreasing phosphorylation of tau and up-regulating stathmin.

The second hypothesis mentioned above, i.e. *R,R-5* may be able to bypass both antephasis and G2 DNA damage checkpoints, will be examined in more detail in Chapter Three (antephasis checkpoint) and Chapter Four (G2 checkpoint). We found that cisplatin is able to activate both checkpoints and oxaliplatin could activate the G2 but not the antephasis checkpoint, and *R,R-5* could bypass both checkpoints. The results may explain the superior anti-cancer activity demonstrated by *R,R-5* over oxaliplatin and cisplatin.

Chapter Three

c-Abl activates the antephase checkpoint and promotes cancer cell survival in response to acute stress of cisplatin

-----Effect of *R,R*-5 at the Antephase Checkpoint

3.1 Introduction

When cancer cells are exposed to DNA damage, DNA damage checkpoints are activated, which stops cell cycle progression and allows time for DNA damage repair, thereby avoiding errors in some important cellular activities such as DNA replication, transcription and mitosis. There are two gate checkpoints in the G2→M cell cycle transition: (1) G2 checkpoint and (2) the recently discovered antephase checkpoint. As discussed in Chapter Two, our cDNA microarray analysis revealed that 35 genes promoting G2→M transition were differentially up-regulated in HCT116 cells treated with *R,R*-5 compared to oxaliplatin (Table 2.3). Since *R,R*-5 was found to be more cytotoxic than oxaliplatin to cancer cells (Yu *et al.*, 2006), we hypothesized that *R,R*-5 may enable cancer cells to bypass G2 and/or antephase checkpoints, undergo aberrant mitosis and subsequently die from mitotic catastrophe

(Figure 3.1). In this Chapter, the biological behavior of *R,R*-5 at the antephase checkpoint will be discussed. Effect of *R,R*-5 at the G2 checkpoint will be discussed in Chapter Four.

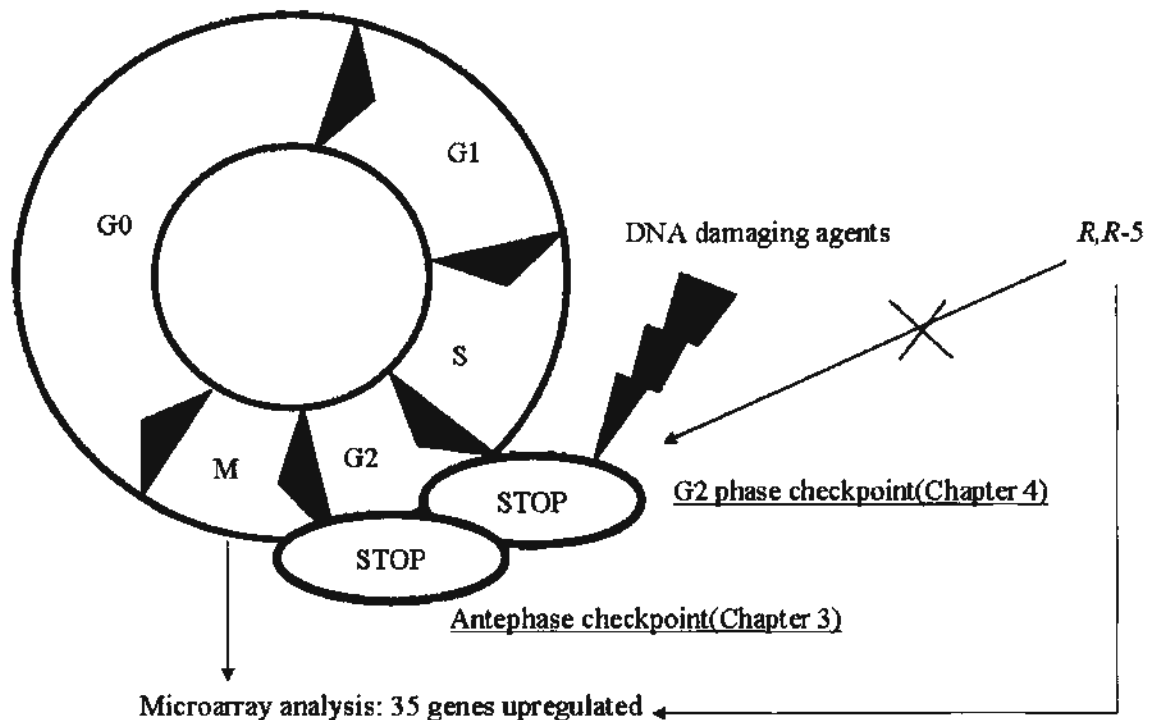


Figure 3.1: Illustration of the proposed checkpoint bypass effect of *R,R*-5. *R,R*-5 may bypass G2 and/or antephase checkpoints because 35 genes promoting G2→M transition were found to be up-regulated in HCT116 cells after *R,R*-5 treatment compared with oxaliplatin.

Antephase describes a short period in the late G2 phase of a cell cycle, when the first visible sign of chromosome condensation becomes evident under a microscope, preceding nuclear envelope break-down. When cells at the antephase are exposed to various kinds of stresses, such as osmotic shock (Dmitrieva *et al.*, 2002), cold shock (Rieder, 1981), UV or ionizing radiation (Rieder and Cole, 1998), microtubule disassembly (Rieder and Cole, 2000) (Figure 3.2), a p38 mitogen-activated protein kinase (p38MAPK)-mediated checkpoint, known as the antephase checkpoint, will be activated (Figure 3.2). This stops the DNA condensation process immediately (in less than an hour), and facilitate the cell to resolve the stresses, thereby avoiding mitotic catastrophe (Figure 3.3) and promoting cell survival after stresses (for a review, see Mikhailov *et al.*, 2005). To date, the signaling transduction of antephase checkpoint in response to DNA damaging agents is not well defined. It has been demonstrated that cisplatin can activate p38MAPK in an hour via a mismatch repair (MMR)/c-Abl dependent pathway (Sanchez-Prieto *et al.*, 2000), which may serve as an initial signal for the activation of the antephase checkpoint (Figure 3.4C). Furthermore, it was also reported that cisplatin activates p38MAPK in a c-Myc-dependent manner, though this pathway requires 4 hrs to activate p38MAPK (Desbiens *et al.*, 2003), which therefore may not contribute to the rapid response (about 1 hr) of antephase checkpoint. Extra time might be needed for the

transactivation of the apoptosis signal-regulating kinase 1 (ASK1) via the c-myc pathway after cisplatin treatment, which activates MKK3/6 and subsequently p38MAPK. This c-Myc/ASK1/MKK3&6/p38MAPK pathway may be involved in apoptotic response rather than antephasic checkpoint regulation.

In this study, we sought to elucidate the signaling pathway for the activation of the antephasic checkpoint in response to Pt-based DNA damaging agents. Since bypass of the antephasic checkpoint may result in cell death from mitotic catastrophe, our second goal was to establish whether the use of antephasic checkpoint inhibitors could give rise to synergistic cytotoxic effect with cisplatin or other DNA damaging agents.

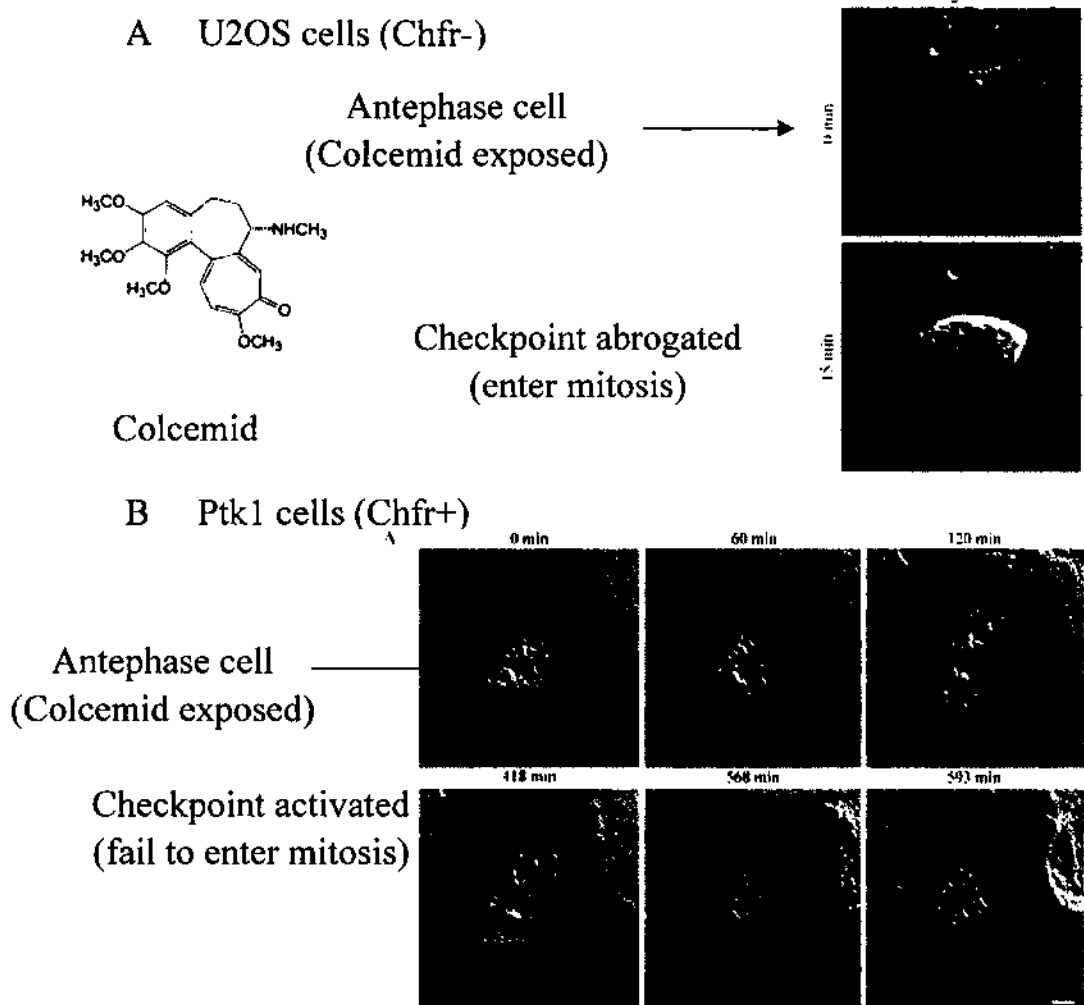


Figure 3.2: Figures (adapted from Matsusaka *et al.*) demonstrating the activation of antephase checkpoint by microtubule disassembly. Colcemid can lead to microtubule disassembly, which activates the Chfr/p38MAPK pathway and subsequently the antephase checkpoint. A) U2OS cells (Chfr-) were exposed to 15 μ M colcemid at 0min. U2OS cells have a defective antephase checkpoint in response to microtubule disassembly because of the absence of Chfr. As observed under the microscope, the stressed U2SO cell entered enter mitosis at 15min,

reflected as the round-up and shrinkage of the cell, which would split into two daughter cells subsequently. B) Ptk1 cells (Chfr+) were exposed to 15 μ M colcemid at 0min. Ptk1 cells have a functional antepause checkpoint in response to microtubule disruption due to Chfr expression. The stressed Ptk1 cell in the picture failed to enter mitosis even at 593 minutes after treatment because of the activation of antepause checkpoint.

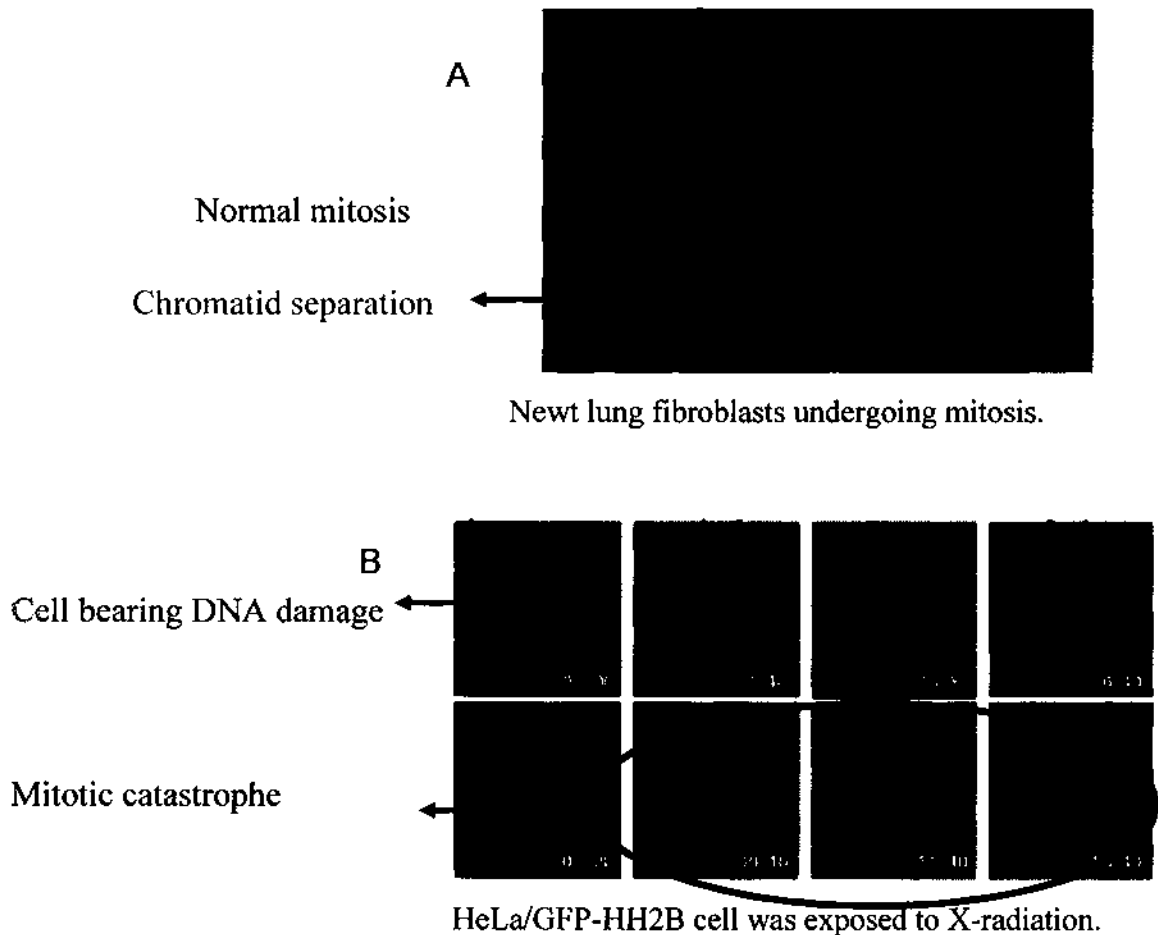
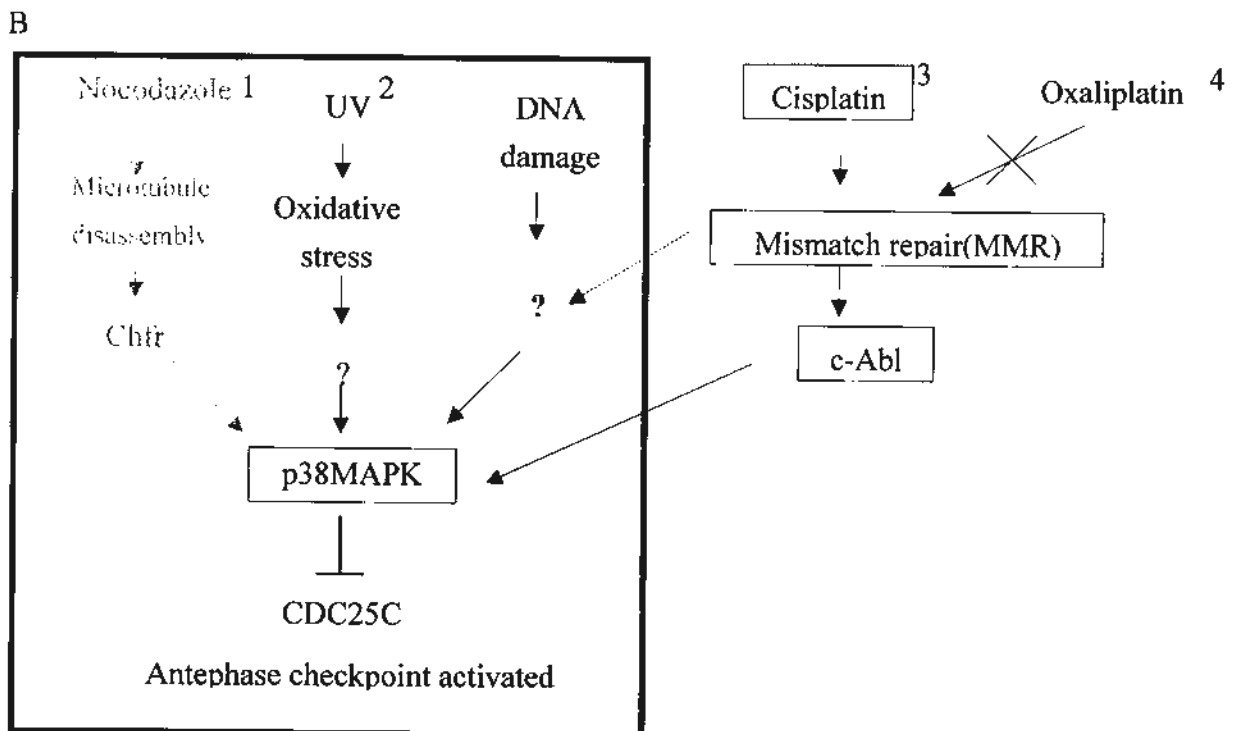
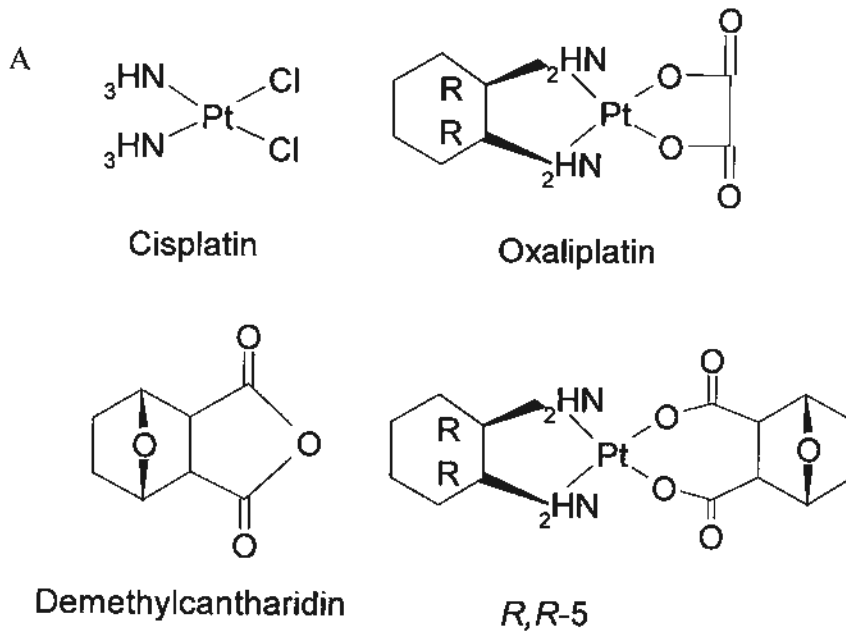


Figure 3.3: Mitotic catastrophe induced by DNA damage. A) Newt lung fibroblasts undergoing mitosis (figures adapted from Warwick Prospective Undergraduate web site <http://www2.warwick.ac.uk/fac/sci/bio/ug/courses/biolsci/> accessed June 2009). In normal mitosis, chromosomes (stained in blue) are able to separate and equally distributed into two daughter cells. B) HeLa/GFP-HH2B cells were exposed to X-radiation (Nitta *et al.*, 2004). When the cells bearing unreparable DNA damage enter mitosis, the cells will die from mitotic catastrophe: failure of the chromatids (in green) to separate, irregular distribution of the chromosomes and the failure of cells to exit mitosis. Activation of mitotic DNA damage checkpoint before mitosis can

facilitate cells repairing DNA damage, avoid mitotic catastrophe and promote cancer cell survival after genomic stress.



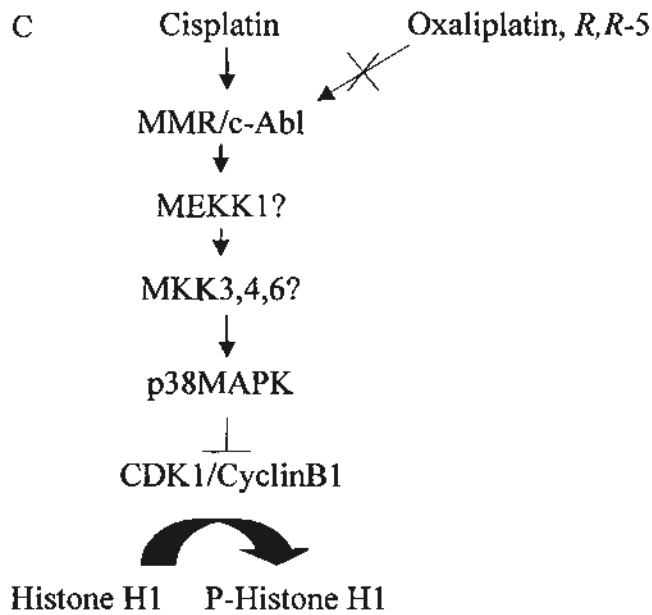


Figure 3.4: Proposed pathway of antephase checkpoint activation by cisplatin. A) Structures of cisplatin, oxaliplatin, DMC and *R,R-5*. B) Previous studies about the various mechanisms for the activation of the antephase checkpoint, including cisplatin-induced p38MAPK activation. On the left panel, various studies had indicated that p38MAPK controls the antephase checkpoint activation under stresses. On the right panel, we hypothesize that cisplatin (but not oxaliplatin) may act through the MMR/c-Abl pathway to stimulate p38MAPK (as previously reported), and consequently activate the antephase checkpoint (highlighted in yellow). C) Proposed pathway of antephase checkpoint activation by cisplatin but not oxaliplatin or *R,R-5*. Cisplatin may activate the antephase checkpoint by MMR/c-Abl/MEKK1/p38MAPK pathway, while oxaliplatin and *R,R-5* may not activate this pathway or checkpoint.

1. Scolnick *et al.*, 2000
2. Bulavin *et al.*, 2001
3. Pandey *et al.*, 1996
4. Nehmé *et al.*, 1999

3.2 Objectives

The objectives of the work reported in this chapter are:

- a) To examine, if any, the precise mechanism by which cisplatin, as a DNA damaging agent, activates the antephasic checkpoint (via a proposed MMR/c-Abl/MEKK1/p38MAPK pathway);
- b) To evaluate if DACH-containing Pt compounds oxaliplatin and *R,R*-5 activate this proposed pathway and the antephasic checkpoint;
- c) To search for and verify whether antephasic checkpoint inhibitors could sensitize cancer cells to platinum anti-cancer drugs (or other DNA damaging agents) and help circumvent drug resistance.

3.3 Experimental Design

As discussed in Chapter 3.1, antephasis checkpoint is a checkpoint with rapid response, which can be activated within an hour. Since the antephasis checkpoint is the closest checkpoint to mitosis, activation of this checkpoint should decrease the proportion of mitotic cells (by inhibiting mitotic entry) immediately, which can be readily measured by the mitotic index assay (Bulavin *et al.*, 2004).

Activation of the antephasis checkpoint is known to repress kinase activity of the major mitotic promoting factor CDK1/Cyclin B1, leading to decreased phosphorylation of its substrate histone H1. Phosphorylation of histone H1, a widely-used mitotic marker, was therefore utilized as our second indicator of antephasis activation (examined by Western blot analysis). The phosphorylation status of c-Abl and p38MAPK was also examined by Western blot analysis, which could reflect their importance in the activation of the antephasis checkpoint.

Cell cycle analysis by flow cytometry was also employed to further ascertain the activation of the antephasis checkpoint. An increase in G2/M arrest (unsynchronized cells) or a decrease in mitotic exit (increase in G0 phase cells in synchronized model) could indicate the activation of antephasis checkpoint.

To verify if cisplatin activate the antephasis checkpoint via our proposed MMR/c-Abl/MEKK1/p38MAPK pathway, cisplatin-induced antephasis checkpoint

was examined in cells treated with or without chemical inhibitors or siRNA against c-Abl. Moreover, the absolute requirement of c-Abl in antephasis activation was also illustrated using a pair of c-Abl functional and non-functional cell lines. As the outcome of antephasis checkpoint abrogation, mitotic catastrophe was quantified by cell counting under a microscope. Lastly, MTT and crystal violet-staining assays were used to reveal the biological significance of the checkpoint activation in terms of drug cytotoxicity.

3.4 Materials and Methods

3.4.1 Chemicals

Cisplatin was purchased from Strem Chemicals (Newburyport, MA, USA); oxaliplatin, caffeine, thymidine, okadaic acid, SB202190, SP600125, crystal violet and Tetrazolium MTT (3-(4,5-dimethylthiazolyl-2)-2, 5-diphenyltetrazolium bromide) were products from Aldrich-Sigma Chemical Company (St. Louis, MO, USA). DMC, *R,R*-5 were synthesized by the School of Pharmacy and Department of Chemistry at the Chinese University of Hong Kong. STI571 was a kind gift from Novartis Pharmaceuticals. All other chemicals and solvents used were of analytical grade. The chemical structure of the various inhibitors used in the experiments are illustrated in Figure 3.5.

3.4.2 Cell Lines and Cell Cultures

HeLa, HCT116, HT29 and Colo320 cells were obtained from the American Type Culture Collection. The cell lines were maintained in complete RPMI1640 medium (supplemented with 10% fresh bovine serum (v/v) (Hyclone), 100U/ml penicillin and 100 U/ml of streptomycin (Hyclone) in a humidified CO₂ incubator (5% CO₂/95% air) at 37 °C. HCT116+ch3 and HCT116+ch2 cells were kind gifts from National Institute of Health U.S.A., and cultured in complete RPMI1640

medium supplemented with 400ug/ml G418 (Roche). Cells were split every three or four days.

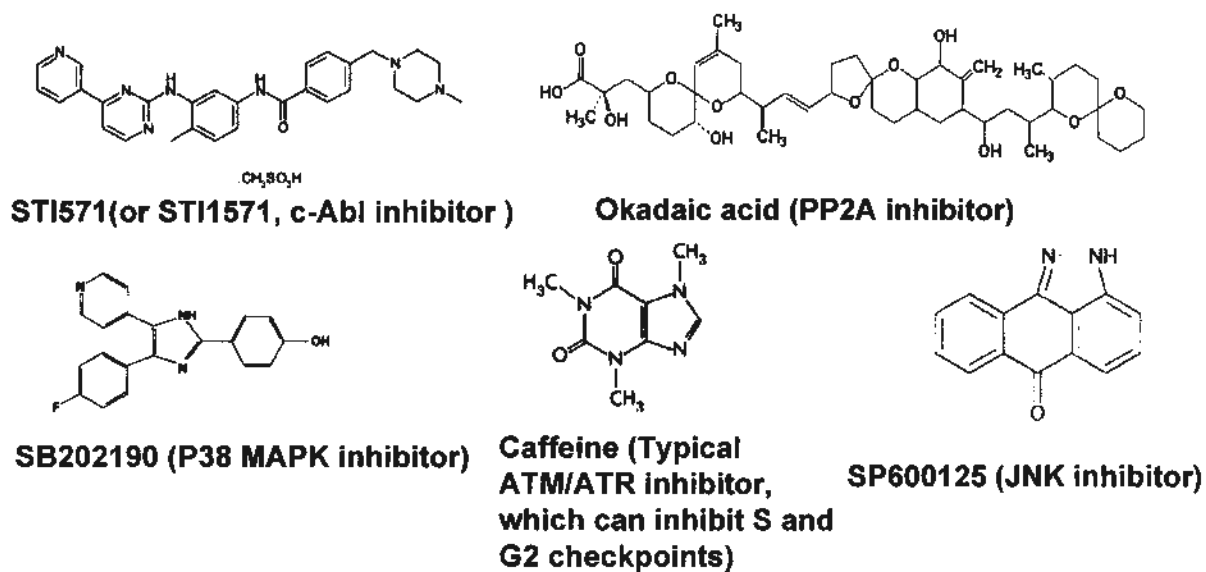


Figure 3.5: Inhibitors used in the experiments. STI571, okadaic acid, SB202190, caffeine and SP600125 were used as specific inhibitors, respectively, to c-abl, PP2A, p38MAPK, ATM/ATR, and JNK.

3.2.3 Mitotic Index Assay and mitotic catastrophe quantification

The assay was adapted with modification from Bulavin *et al.* 2×10^4 cells/well were seeded in a 96-well plate. All platinum drugs were added 24 hrs later. In experiments involving combination of cisplatin with inhibitors against the different

pathways, the various inhibitors were added 0.5 hr before cisplatin treatment. Cells were fixed overnight with 4% paraformaldehyde after drug treatment for various durations and then stained with 10% Giemsa. Mitotic cells (prophase, pro-metaphase, metaphase, anaphase, telophase and cytokinesis) were counted among over 600 cells randomly picked from each well. For mitotic catastrophe quantification, HeLa cells were treated with various drugs for 2 hrs, washed with PBS, and maintained in fresh medium for another 20 hrs to accumulate aberrant mitotic cells. Then cells were fixed with 4% paraformaldehyde overnight and stained with 10% Giemsa. Aberrant mitotic cells (mitosis with irregularly arrayed and/or unequally distributed chromosomes) were counted among over 600 cells randomly picked from each well, under a microscope. Inhibitors were added 0.5 hr before cisplatin treatment and stayed present during the 24 hr incubation.

3.4.4 Immunoblot (Western Blot) Analysis and Immunoprecipitation

3.4.4.1 Solutions and Reagents

Lysis buffer (for whole cell lysate): 0.15 M NaCl, 5 mM EDTA, 1% Triton X100, 10 mM Tris-Cl, pH 7.4. 1:1000 5 M DTT, 1:1000 100 mM PMSF (in isopropanol). 1 mM NaF and 2 mM $(\text{NH}_4)_3\text{VO}_4$ were added fresh to the lysis buffer immediately before use.

Lysis buffer (for histones): 10 mM HEPES, 1.5 mM MgCl₂, 10 mM KCl, adjust pH to 7.9. 0.5 mM DTT, 1.5 mM PMSF in isopropanol. 1 mM NaF and 2 mM (NH₄)₃VO₄ were added fresh to the lysis buffer immediately before use.

5×Sample Buffer: 0.3125 M Tris pH 6.8, 10% SDS, 50% (V/V) glycerol, 0.005% (W/V) bromophenol blue, 2% (W/V) DTT.

8×Resolving gel buffer (100 ml): 36.3 g Trizma base, 0.8 g SDS were diluted in distilled water and pH value was adjusted to 8.8 with concentrated HCl, then the volume was made up to 100 ml.

4×stacking gel buffer (100 ml): 6.05 g Trizma base, 0.4 g SDS were diluted in distilled water and pH value was adjusted to 6.8 with concentrated HCl, then the volume was made up to 100 ml.

10×Running buffer (1 L): 30.3 g Trizma base, 144 g Glycine, 10 g SDS were diluted in distilled water, and then the volume was made up to 1 L.

10×Blotting buffer (1 L): 30.3 g Trizma base, 144 g Glycine were diluted in distilled water, and then the volume was made up to 1 L.

1×Blotting buffer (1 L): 200 ml methanol, 100 ml 10×Blotting buffer were mixed, and then the volume was adjusted to 1 L with distilled water.

Resolving gel (6 ml for 9%): 1.35 ml 40% acrylamide/bisacrylamide (29:1 mix), 0.75 ml 8×Resolving gel buffer, 3.9 ml water, 3 µl TEMED, 15 µl 20% ammonium

persulfate.

Resolving gel (6.9345 ml for 15%): 2.624 ml 40% acrylamide/bisacrylamide (29:1 mix), 0.7875 ml 8×Resolving gel buffer, 3.502 ml water, 3.5 µl TEMED, 17.5 µl 20% ammonium persulfate.

Stacking gel (4.0148 ml for 5%): 0.5 ml 40% acrylamide/bisacrylamide (29:1 mix), 1 ml 4×Stacking gel buffer, 2.5 ml water, 4 µl TEMED, 10.8 µl 20% ammonium persulfate.

10×TBS (concentrated TBS): 24.23 g Trizma HCl, 80.06 g NaCl were mixed in 800 ml distilled water, then pH was adjusted to 7.6 with pure HCl. Volume was topped up to 1 L with distilled water.

TBST (1 L): 100 ml of 10×TBS + 900 ml ultra distilled water + 1ml Tween20. TBST was kept at 4 °C to prevent contamination and discarded if stored for more than 1 week.

Blocking buffer (0.5 L): 3% Bovine serum albumin (Fraction V) was diluted in TBST and sterile filtered. Then 0.05% Tween 20 was added. Blocking buffer was kept at 4 °C to prevent bacterial contamination.

3.4.4.2 Total Protein (Whole Cell Lysate) Extraction

a) Drain the medium, wash cells in 10 cm dish with phosphate buffered saline

(Sigma).

b) Lyse the cells in 10 cm dish with 300 μ l lysis buffer on ice for 10 minutes, scrape the cells off, transfer lysate into a 1.5 ml centrifuge tube, vortex and then sonicate for 3 minutes to aid complete cell lysis.

c) Cool and centrifuge to collect cell pellets.

d) Protein is quantified using the Bio-rad protein assay (Bio-Rad Laboratories Inc., Hercules, CA) and stored at -20 °C.

3.4.4.3 Histone Extraction

a) Drain the medium, wash cells in 10 cm dish with phosphate buffered saline (Sigma).

b) Lyse the cells in 10 cm dish with 300 μ l lysis buffer (for histones only) on ice for 1 minutes, scrape the cells off, transfer lysate into a 1.5 ml centrifuge tube.

c) Add hydrochloric acid to a final concentration of 0.2 M (0.2N). Use polypropylene tubes. Vortex and then sonicate for 3 minutes to aid complete lysis of cell and protein extraction.

d) Incubate on ice for 4 hrs for acid extraction of histones.

e) Centrifuge at 11,000 \times g for 10 minutes at 4 °C.

f) Keep the supernatant fraction, which contains the acid soluble proteins, and

discard the acid-insoluble pellet.

g) Add 6 volume of acetone (pre-chilled at -20 °C), gently mix and store at -20 °C over night.

h) Centrifuge at 11,000 × g for 10 minutes at 4 °C.

i) Drain the supernatant fraction.

j) The centrifuge tube containing histone pellet at the bottom was placed in a fume hood at room temperature for 10 minutes for evaporation of acetone.

k) Reconstitute the histone pellet in 200 ul distilled water containing 0.5 mM DTT, 1.5 mM PMSF in isopropanol, 1 mM NaF and 2 mM (NH₄)₃VO₄.

l) Histones were quantified using the Bio-rad protein assay and stored at -20 °C.

m) Before electrophoresis, if pH value of the sample appears to be low because of the remaining acid, do either of these: i) Dialyze three times against 200 ml H₂O for 1 hour, 3 hours, and overnight, respectively. ii) Wash histones with acetone until pH is about 7. Usually none of these two steps are necessary when using this method for histone extraction.

3.4.4.4 Protein Electrophoresis

Protein samples prepared above were subjected to SDS-PAGE (sodium dodecyl sulfate polyacrylamide gel electrophoresis) using Bio-Rad Mini-Protean 3 Cell (Bio-

Rad Laboratories Inc., Hercules, CA) following the instructions. Gel was developed with constant current (8~18mA with voltage set <300V).

3.4.4.5 Membrane Transfer

After gel SDS-PAGE, proteins were transferred onto a piece of PVDF membrane (Millipore Immobion-P) (Millipore Corp., Temecula, CA) using the GE hoefer TE77 semi-dry transfer unit (GE Healthcare, Sioux Falls, SD) following the instructions. Gel was transferred with constant current (34mA for 2 hours).

3.4.4.6 Antibody Probing

a) Incubate the membrane with primary antibody diluted in Blocking buffer over night at 4 °C.

b) Wash 3×10 minutes with TBST.

c) Incubate with secondary antibody diluted in Blocking buffer for 4 hours at 4°C.

d) Wash 3 ×10 minutes with TBST.

e) Detect with Enhanced Chemiluminescence kit (Pierce, Rockford, IL).

3.4.4.7 Antibodies

Blotted membranes were incubated with antibodies against P^{Tyr245}-c-Abl and p^{Thr180/Tyr182}-p38MAPK (Cell Signaling Tech., Beverly, MA), phospho-histone H1 (Upstate Biotechnology, Lake Placid, NY), beta-Tubulin (Santa Cruz Biotechnology, Santa Cruz, CA), c-Abl, MEKK1 (Invitrogen, Carlsbad, CA) or histone H1 (Abnova, Heidelberg, Germany). Phosphorylation of c-Abl at Tyrosine245 indicates c-Abl activation. Similarly, phosphorylation of p38MAPK at Threonine180 and Tyrosine182 is used as the marker for p38MAPK activation. Anti-rabbit and anti-mouse antibodies (Cell Signaling Tech., Beverly, MA) were served as secondary antibodies according to the animal source of the primary antibodies.

3.4.4.8 Immunoprecipitation

Whole cell lysates were incubated with anti-MEKK1 (Invitrogen) for 2 hrs at 4 °C, and then the immune complexes were captured by protein A beads (Sigma) for 0.5 hr before separation by SDS-PAGE for immunoblotting.

3.4.5 siRNA Transfection

Human c-Abl (sense r(CCAAGCCUUUGAAACA AUG)dTdT, anti-sense r(CAUUGUUUCA AAGGCUUGG)dTdT) (catalog number SI00299103), or

MEKK1 (sense r(CCGGGUGUUUCAACUAGAA)dTdT, anti-sense r(UUCUAGUUGAAACACCCGG)dTdG) (catalog number SI02659965) siRNAs and a scrambled siRNA (Alexa Fluor 488[®] labeled siRNAs, catalog number 1027280) that does not match any known gene sequences, were purchased from Qiagen. siRNA was provided as frozen powder, which was reconstituted in siRNA dilution buffer (Qiagen). Then the solution was heated at 92 °C for 10 seconds and followed by another 1 hr incubation at 37°C. This will remove all the secondary structures of siRNA formed during lyophilization without disrupting the siRNA. HeLa cells were transfected with these siRNAs using Hi-PerFect transfection reagent (Qiagen). 20,000 HeLa cells per well were seeded onto a six-well plate. Cells must be proliferating in the exponential phase healthily without contamination. 0.5 hr before transfection, cells were washed twice with warm (37°C) serum-free medium, and 2ml/well fresh medium with serum (but without any antibiotics) was then added. The optimal confluence for the cells at the time of transfection is about 40-50%. For each transfection condition), siRNA cocktail was prepared using 24 µL of siRNA solution (2 µM), 12 µl of Hi-perfect transfection reagent (Qiagen) and 64 µL of serum-free medium. After a 10min-incubation at room temperature (25 °C), the transfection cocktail containing siRNA was added dropwisely to the cells. A final concentration at 20 nM of siRNA was used. 6 to 8 hrs later, transfection efficiency

was monitored under a fluorescence microscope. About 80% to 90% of HeLa cells were transfected with the negative control siRNA, which were emitting green fluorescence (Alexa Fluor 488[®]) upon UV excitation. Knock-down efficiency was further confirmed by real-time PCR (Figure 3.6) and Western blotting (Figure 3.13).

Twenty-four hours after transfection, when target gene expression was reduced by about 60%, as confirmed by real-time RT-PCR (Figure 3.6) and Western blot analysis (Figure 3.13), fresh medium was added and cells were treated with drugs for 1 hr or 4 hr, before extraction for whole cell lysates and histones for Western blotting, respectively.

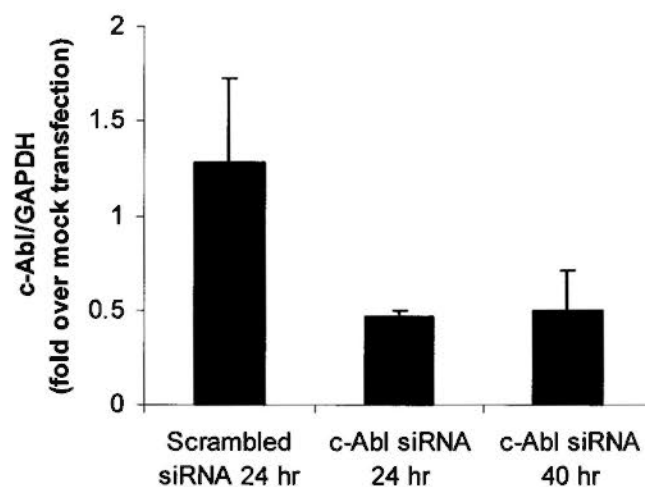


Figure 3.6: c-Abl siRNK effectively knocked down c-Abl mRNA level in HeLa cells.

HeLa cells were transfected with culture medium (mock), scrambled or c-Abl siRNA (20 nM), and harvested at 24 hr or 40 hr after transfection for RNA extraction using

RNeasy Mini Kit (Qiagen). The Transcriptor First Strand cDNA Synthesis Kit (Roche, South San Francisco, CA) was used for the reverse transcription of RNA samples into cDNA. Real-time RT-PCR detection of human c-Abl (forward primer 5'-CCCAACCITTTTCGTTCGCACTGT-3', reverse primer 5'-CGGCTCTCGGAGGAGACGTAGA-3') and GAPDH (forward primer 5'-ACCACAGTCCATGCCATCAC-3', reverse primer 5'-TCCACCACCCTGTTGCTGTA-3'), were performed on the Light Cycler 480 (Roche) using the Light Cycler 480 SYBR Green I Master Mix (Roche). Mean±SD of three PCR replicates from one representative transfection experiment is shown.

3.4.6 Flow Cytometry Analysis

Since the proportion of cells at the antepase is fairly low (about 10%), it is necessary to accumulate antepase cells for flow cytometry analysis in order to show changes in G2/M cell cycle arrest. A double-thymidine block method (Cude *et al.*, 2007) (Figure 3.7) was used to synchronize and accumulate antepase HeLa cells. HeLa cells have a very low p53 level and therefore a defective p53→apoptosis checkpoint response (i.e. HeLa cells will not trigger G1 checkpoint and mediate apoptosis in response to thymidine because of the absence of p53). When HeLa cells

was treated with thymidine at a high concentration (2 mM), thymidine will replace deoxythymidine and incorporate into the DNA during DNA replication, which can signal the activation of the S phase checkpoint and cells will be arrested at the onset of S phase. However, this will not lead to apoptosis after 19 hrs because of the low p53 level in the cells. Early S phase cells can therefore be accumulated and synchronized using this method. Subsequently, when HeLa cells are released into fresh medium (without thymidine) again, the early S phase-arrested HeLa cells will start progressing into S phase at the same time. In our assays, two consecutive thymidine blocks were performed to maximize the synchronization effect.

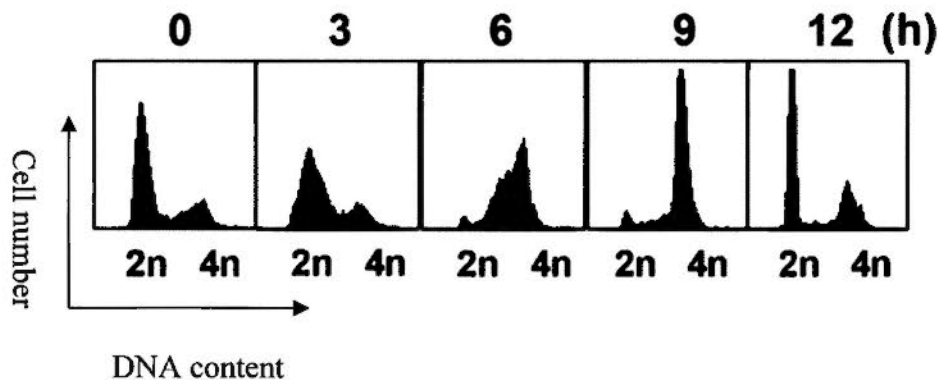


Figure 3.7: Cell cycle synchronization using double-thymidine block in HeLa cells (figure adapted from Cude *et al.*). Double-thymidine block can arrest about 85% of cells in the G1 phase (0 hr) with 2n chromosomes (2 sets of chromosomes from each of the parents); 3 hrs after release to fresh medium, cells have started DNA replication and enter S phase, leading to an increase in S phase cells (cells with DNA content between 2n and 4n); 6 hrs after release, cells are entering mitosis, as

illustrated by the accumulation of G2/M cells with 4n chromosomes; 9 hr after release, about 90% of cells are in G2/M phase (cells with 4n chromosomes after DNA replication), preparing for or undergoing mitosis; 12 hrs after release, about 80% cells have exited mitosis and return to G0 phase (one mitotic cell bearing 4n chromosomes is divided into two daughter cells each bearing 2n chromosomes).

Six hours after released from thymidine, HeLa cells were synchronized and they are laboring at the antephase (where cells were proceeding into G2/M phase, Figure 3.21). These cells were exposed to cisplatin for 2 hr, then washed with PBS (phosphate buffered saline) once and fresh medium without cisplatin was added. In experiments involving combination treatments, the various inhibitors were added 0.5 hr before cisplatin exposure, stayed throughout cisplatin treatment, and added again after the 2 hr-cisplatin treatment when medium was changed, and remained present until fixation for flow cytometry analysis at 14 hr. After fixation (with 70% ethanol), cells were stained with 50 $\mu\text{g/ml}$ propidium iodide (containing 10 mg/ml RNase A). Propidium iodide can bind to DNA groves and label DNA with red fluorescence upon laser excitation. Accordingly, DNA content of one cell can be determined by the fluorescence intensities: cells in the G0/G1 phase have 2n chromosomes from each of the parents; cells in G2 and M phase possess 4n chromosomes after DNA

replication; cells in the S phase should have DNA content between $2n$ and $4n$; apoptotic and necrotic cells will undergo DNA-degradation or DNA-leakage, which consequently contain DNA content less than $2n$, termed as sub-G1 cells. By quantifying cells bearing different DNA contents, the percentage of cells in each cell cycle phase can be estimated. Antephase locates in the late G2 phase of a cell cycle; hence antephase cells will have $4n$ chromosomes and be calculated as G2/M cells. Abrogation of the antephase checkpoint by inhibitors (proposed to be c-Abl and p38MAPK inhibitors) can be reflected by a decrease in G2/M cells, or an increase in G0 cells (increase in mitotic exit). In addition, G2 checkpoint activation may also contribute to cisplatin-induced G2/M arrests, which however, could be theoretically restored by ATM/ATR inhibitor caffeine. Mitotic transition under the same treatment mentioned above were also recorded using the mitotic index assay (Figure 3.20), where cells were fixed with 4% paraformaldehyde and stained with 10% Giemsa, as described in Chapter 3.4.3.

For unsynchronized cell cycle analysis, HCT116+ch3 and HCT116+ch2 cells were treated with cisplatin for 2 hrs, washed once with PBS and recovered in fresh medium for another 48 hrs before fixation for flow cytometry analysis. HCT116+ch3 cells are c-Abl functional while HCT116+ch2 cells are c-Abl non-functional. They have functional p53 and G1 checkpoint and cannot be synchronized

using double-thymidine block. The use of these two cell lines can reveal the contribution of antephase checkpoint activation to MMR-mediated G2/M arrest. In fact, the MMR-mediated G2/M arrest may consist of: a) antephase arrest; b) the MMR/p38MAPK/p53/p21 pathway-induced G2 arrest (Mikhailov *et al.*, 2005); c) the G2 arrest accumulated via the ATM/ATR pathway (G2 checkpoint, which usually require longer drug exposure than 2 hr and will be discussed in Chapter Four, Figure 4.1); and less likely, d) mitotic arrest due to the activation of mitotic spindle checkpoint. Just for clarification, the MMR/p38MAPK/p53/p21 pathway-induced G2 arrest should not be confused with the antephase arrest because antephase checkpoint does not require p53 activation or p21 transcription (2 hr-cisplatin treatment can activate antephase arrest but may not be adequate to turn on p21 expression for G2 arrest; our findings in Table 3.1).; but it is a sequential checkpoint after the activation of antephase checkpoint, which reinforces the G2 arrest after DNA damage. Hence compared to the synchronized HeLa cell model, this unsynchronized cell cycle analysis is less specific for the investigation of the antephase checkpoint because other checkpoints are also involved.

Flow cytometry analysis was carried out using a BD FACSAria™ flow cytometer (BD Biosciences, Becton Drive Franklin Lakes, NJ). Data were processed using the WinMDI 2.9 software (free software downloaded from

<http://facs.scripps.edu/software.html>; accessed on 28 July, 2009).

3.4.7 MTT Assay and Crystal Violet Staining

For acute drug treatment (2 hrs of drug incubation), 2,000 cells/well were seeded in a 96-well plate. Twenty-four hours later, cells were treated with different platinum compounds for 2 hrs, and then washed with PBS once and incubated in fresh medium for another 6-day recovery before MTT assay. Medium was changed 48 hrs after drug treatment. In experiments involving drug combinations, the various inhibitors were added 0.5 hr before cisplatin exposure, stayed throughout cisplatin treatment, and added again after the 2 hr-cisplatin treatment when medium was changed, and remained present until at 48 hr when medium was changed again. Cells were then incubated for another 4 days before MTT assay. For sustain drug treatment (24 hrs of drug incubation), 10,000 cells/well were seeded in a 96-well plate. Twenty-four hours later, cells were treated with different platinum compounds for 24 hrs before MTT assay or Crystal Violet staining. For Crystal Violet staining (Kim *et al.*, 2002), cells after treatment were fixed with 4% paraformaldehyde overnight, stained with 0.1% crystal violet for 0.5 hr, washed with PBS for three times before 10% acetic acid was added. Plates were detected with a microplate reader (Bio-rad) at 595nm.

3.5 Results and Discussions

3.5.1 Antephase checkpoint was activated by cisplatin but not oxaliplatin or *R,R*-5

When HeLa (MMR+, p53-, Chfr-) cells were exposed to cisplatin, the proportion of mitotic cells decreased rapidly from 2.83% (untreated control, 0 hr) to 0.39% (5 μ M) or to 0.061% (25 μ M) at 2 hr, indicating the antephase checkpoint activation (Figure 3.8). The same phenomenon was also observed in HT29 (MMR+, p53-, Chfr+) and Colo320 (MLH1+, MSH2+, p53+, Chfr+), but not HCT116 cells (MMR-, p53+, Chfr-; Figure 3.9). Therefore, activation of the antephase checkpoint by cisplatin seems to depend on MMR status (but not p53 or Chfr). To this end, Chfr has been reported to contribute to antephase checkpoint activation in response to microtubule disassembly (Scolnick *et al.*, 2000). Oxaliplatin, which induces cell death in an MMR-independent manner due to the incorporation of the DACH moiety (Fink *et al.*, 1997), failed to activate this checkpoint, as reflected by the minimal change in mitotic index after drug treatment at 2 hr (Figure 3.8). The novel DACH-containing platinum compound *R,R*-5, which contains a DMC moiety derived from the traditional Chinese medicine, also did not affect the antephase checkpoint (as evidenced by the minimal change in mitotic index shown in Figure 3.8). The concentration used in our assays were 5 μ M and 25 μ M of each Pt compounds,

which may differentiate the biological behaviors of diamino-Pt groups (cisplatin) and DACH-Pt (oxaliplatin and *R,R*-5) at equal Pt level. As a reference, the IC₅₀ of cisplatin in HeLa for 48 hrs is around 0.4 to 0.7 μM (Reithofer *et al.*, 2007; Bannon *et al.*, 2007). IC₅₀ of cisplatin in HT29, Colo320 and HCT116 for 72 hrs treatment were 6.47 μM, 4.14 μM, 1.97 μM, respectively (Yu *et al.*, 2006). The cisplatin treatment mainly used in our assays is 5 μM for 2 hrs, which is close to the unbound-cisplatin blood concentration in patients (around 4 μM) before complete clearance from blood (<2 hrs, Urien and Lokiec, 2004). Interestingly, Compound 5 (a mixture of *S,S*- and *R,R*-5) has been demonstrated to have very limited hydrolysis after 2 hr incubation in normal saline (To *et al.*, 2002), which may affect the behavior of *R,R*-5 at the antephasic checkpoint in HeLa cells, except that enzymes in cancer cells may change/accelerate the hydrolysis of *R,R*-5.

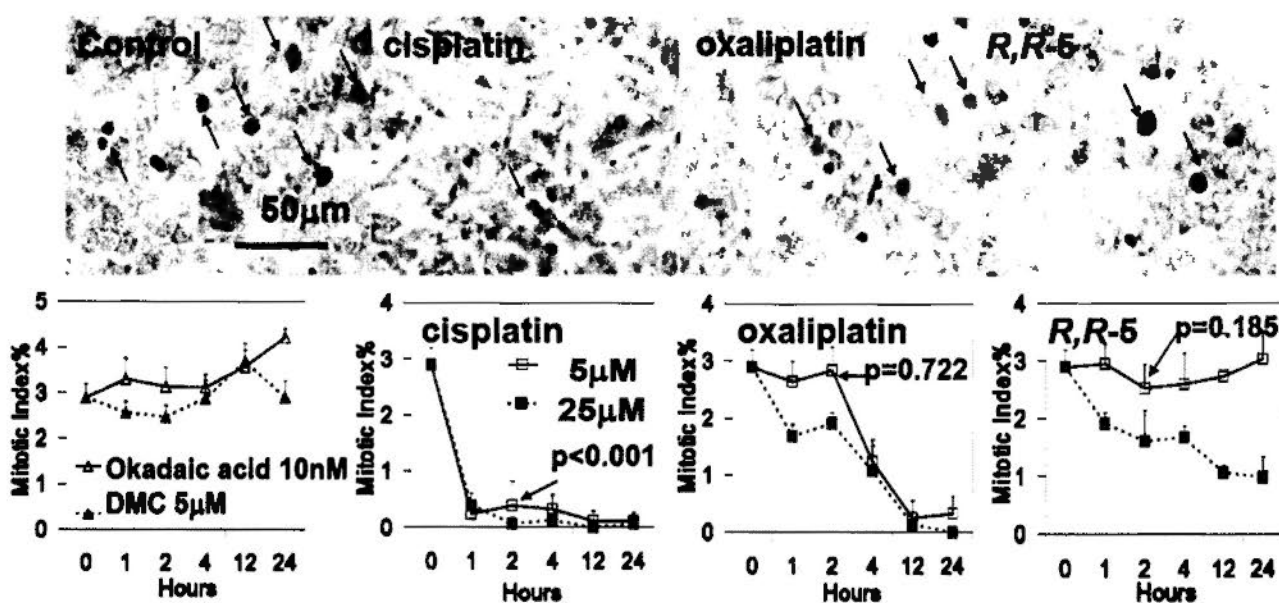


Figure 3.8: Mitotic index assay showing that activation of antepause checkpoint by cisplatin treatment but not oxaliplatin or *R,R-5*. Cisplatin could decrease mitotic index in 2 hrs, which is considered due to the activation of antepause checkpoint. This effect was absent in HeLa cells treated with oxaliplatin or the PP2A inhibitors *R,R-5*, DMC and okadaic acid. Representative images of Pt compounds (5 μ M at 2 hr), and mean \pm SD of 9 replicates from 3 independent experiments are shown. Student's t test is used to compare the mitotic indices of HeLa cells treated with various compounds at 2 hr with control (0 hr). At 12 hr after drug treatment, a decrease in the number of mitotic cells in both cisplatin and oxaliplatin-treated HeLa cells was observed, but not in PP2A inhibitors-treated cells. This observation was considered due to the activation of G2 checkpoint by cisplatin and oxaliplatin, but not PP2A inhibitors. The modulation of the G2 checkpoint of PP2A inhibitors will be discussed in Chapter Four.

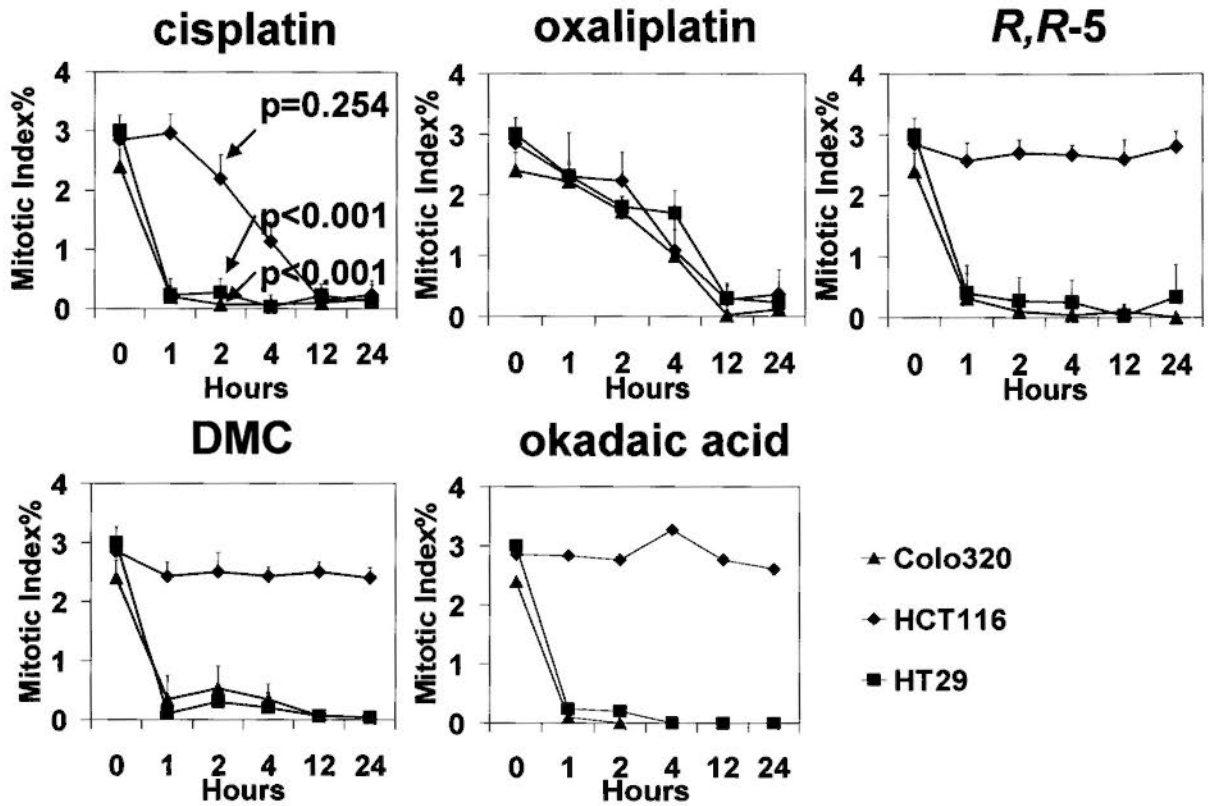


Figure 3.9: Mitotic index assay showing that cisplatin did not activate the antephrase checkpoint in c-Abl non-functional HCT116 cells. HT29, Colo320 and HCT116 cells were treated with cisplatin (5 μ M), oxaliplatin (5 μ M), *R,R*-5 (5 μ M), DMC (5 μ M) or okadaic acid (10 nM). Mean \pm SD of 9 replicates from 3 independent experiments are shown. Student's t test is used to compare the mitotic indices of each cell line treated with cisplatin for 2 hr with respective control (0 hr).

The results for the mitotic index assay in different cell lines are summarized in Table 3.1. Cisplatin was found to activate the antepause checkpoint in cells with functional c-Abl, regardless of the p53 and Chfr status. Oxaliplatin did not activate the antepause checkpoint in all cell lines tested. DMC, okadaic acid and *R,R*-5 activates the antepause checkpoint only in cell lines having Chfr expression (i.e. HT29 and Colo320). Since Chfr can trigger antepause checkpoint activation in response to microtubule disassembly (Scolnick *et al.*, 2000), this result suggests that DMC, okadaic acid and *R,R*-5 may lead to instability of microtubule. In fact, it has been reported that the PP2A inhibitor okadaic acid can disrupt microtubule formation (Gurland *et al.*, 1993). PP2A has also been shown to maintain the hypophosphorylation of microtubule-associated protein tau, leading to the binding of tau to microtubule and an increase in microtubule stability (Sontag *et al.*, 1996). This may explain why these PP2A inhibitors can activate the antepause checkpoint in Chfr-positive cell lines. Moreover, from our cDNA microarray analysis, *R,R*-5 was found to up-regulate the microtubule destabilizing gene *stathmin* (Iancu *et al.*, 2004) (Table 2.1) compared with oxaliplatin. However, since the increased transcription of *stathmin* may take time to occur, the increase in *stathmin* expression may not contribute to the rapid activation of the antepause checkpoint (within 1 hr).

We also explored the mechanism by which cisplatin activates the antepause

checkpoint. c-Abl and p38MAPK activation, as well as dephosphorylation of the CDK1/CyclinB1 substrate histone H1, were observed, accompanying the checkpoint activation by cisplatin (Figure 3.10). The results suggest that cisplatin activated the antephase checkpoint via a c-Abl/p38MAPK pathway, leading to inhibition of the kinase activity of the major mitotic complex CDK1/CyclinB1 and consequently a decrease in phosphorylation of histone H1. In HeLa cells, both DACH-containing Pt compounds oxaliplatin and *R,R*-5 did not activate this c-Abl/p38MAPK pathway (Figure 3.10), which may explain why these two compounds did not activate the antephase checkpoint. PP2A inhibitors (DMC, okadaic acid and *R,R*-5) may activate the antephase checkpoint via the Chfr/p38MAPK pathway only in Chfr⁺ cell lines (such as HT29 and Colo320) but not Chfr⁻ HeLa cells (Table 3.1), hence no rapid p38MAPK activation or histone H1 dephosphorylation was observed in *R,R*-5 treated HeLa cells in Figure 3.10. In our study, this Chfr pathway was not further investigated.

Table 3.1: Relationship between cell genotype and antephasis checkpoint activation.

Cell lines	Cell genotype			Antephasis checkpoint activation		
	c-Abl	p53	Chfr	Cisplatin	Oxaliplatin	R,R-5
HeLa	+	- (low protein level)	-	+	-	-
HT29	+	-	+	+	-	+
Colo320	+?	+	+	+	-	+
HCT116	- (non-functional)	+	-	-	-	-

The activation of the antephasis checkpoint was examined by the mitotic index assay. Cisplatin activated the antephasis checkpoint only in cells with functional c-Abl (HT29, Colo320 and HeLa). The MMR/c-Abl status in Colo320 has not been reported before, but Colo320 has intact MMR genes *MLH1* and *MSH2*. HCT116 cells have mutated (defective) *MLH1* gene and therefore a deficient MMR status. Hence, as an MMR substrate in response to cisplatin treatment (Sanchez-Prieto *et al.*, 2000), c-Abl is non-functional in HCT116 cells and cannot be activated by MMR. Oxaliplatin did not activate the antephasis checkpoint in all cell lines tested. R,R-5 and the PP2A inhibitors (DMC and okadaic acid) activated the antephasis checkpoint in cell lines with Chfr expression (HT29 and Colo320).

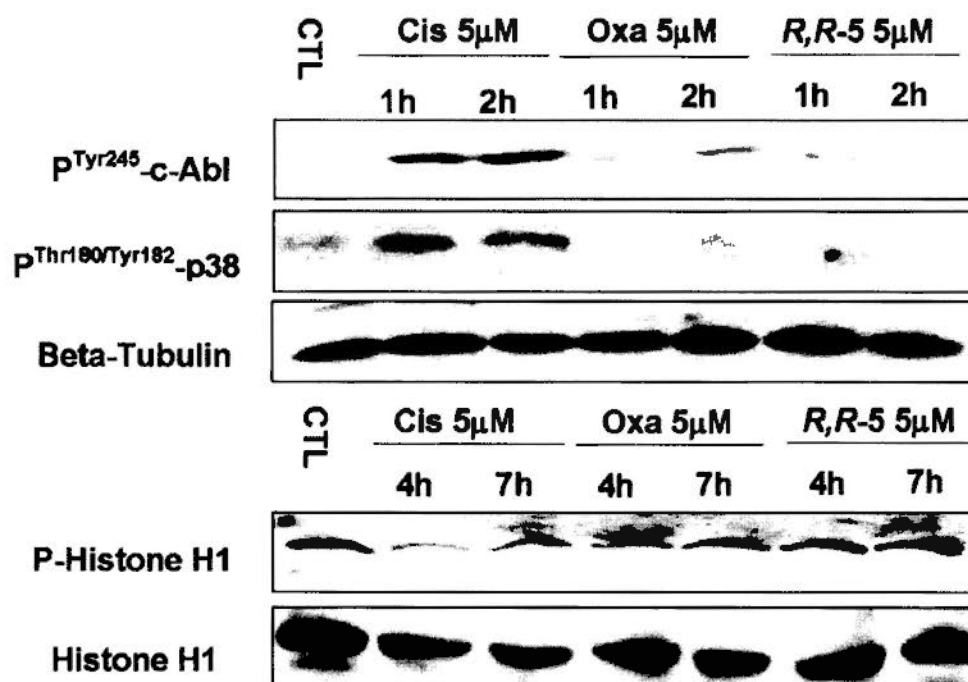


Figure 3.10: Western blot analysis showing activation of the c-Abl/p38MAPK pathway by cisplatin. HeLa cells were treated with cisplatin, oxaliplatin or *R,R*-5 for the indicated period of time before extraction of whole cell lysate or histones. Cisplatin could lead to c-Abl/p38MAPK activation (1 hr) and histone H1 dephosphorylation (4 hr) but this effect was either absent or weak in oxaliplatin or *R,R*-5 treated HeLa cells. A representative set of result from three independent experiments is shown.

3.5.2 Abrogation of Antephase Checkpoint by c-Abl Inhibitor and siRNA.

Based on the results from the Western blot analysis in Figure 3.10, we proposed that the activation of the c-Abl/p38MAPK pathway is crucial for cisplatin-induced antephase activation. This was further confirmed by the use of chemical inhibitors against c-Abl (STI571) or p38MAPK (SB202190) because these inhibitors could prevent cisplatin induced c-Abl/p38MAPK activation and phosphorylation of histone H1 (Figure 3.12), and abrogate the decrease in mitotic index (Figure 3.11). Inhibitors against ATM/ATR (caffeine) or PP2A (okadaic acid and DMC) did not attenuate cisplatin-induced rapid decrease in mitotic index (Figure 3.11). Therefore, ATM/ATR and PP2A may not be involved in antephase checkpoint activation by cisplatin. Silencing of c-Abl and MEKK1 in HeLa by siRNA were also found to abrogate the antephase checkpoint activation by cisplatin (Figure 3.13), suggesting that the involvement of the c-Abl/MEKK1/p38MAPK pathway. In fact, kinase active c-Abl and p38MAPK were observed to bind to MEKK1 after cisplatin exposure (Figure 3.14). Consistent with this finding, it has been reported that c-Abl binds to MEKK1 and activates JNK after cisplatin exposure (Kharbanda *et al.*, 2000). Interestingly, cisplatin treatment combined with SB202190 (Figure 3.12) or MEKK1 siRNA (Figure 3.13) failed to activate c-Abl, implying that activation of c-Abl may require p38MAPK and MEKK1.

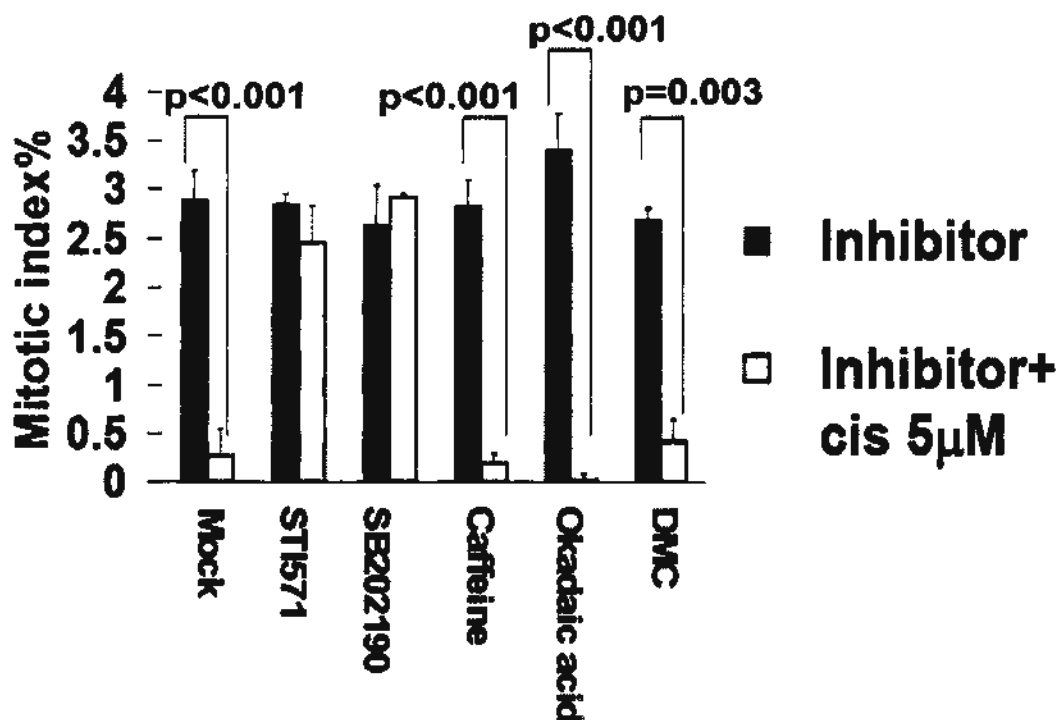


Figure 3.11: Mitotic index assay showing c-Abl and p38MAPK inhibitors abrogated cisplatin-induced antephasic checkpoint activation in HeLa cells. Mitotic indices of HeLa cells after exposure to cisplatin 5 µM for 2 hrs, concomitantly treated with water (mock) or inhibitors against c-abl, p38MAPK, ATM/ATR, and PP2A, respectively: STI571 (5 µM), SB202190 (20 µM), caffeine (5 mM), okadaic acid (10 nM) and DMC (5 µM). Inhibitors were added 0.5 hr before cisplatin treatment. Mean±SD of 9 replicates from 3 independent experiments is shown. Student's t test was used for statistical analysis to compare the various treatment groups. Cisplatin was shown to activate the antephasic checkpoint and decrease the mitotic index after 2 hr treatment, which was inhibited by c-Abl and p38MAPK inhibitors but not ATM/ATR and PP2A inhibitors.

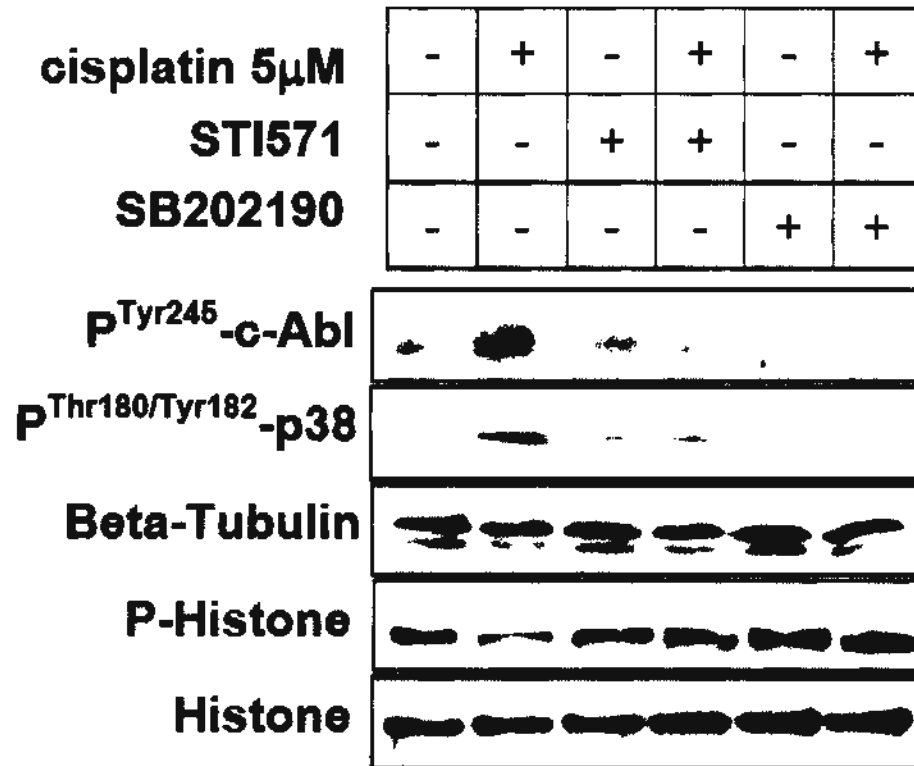


Figure 3.12: Western blot analysis showing the abrogation of cisplatin-induced antepause checkpoint activation by c-Abl and p38MAPK inhibitors in HeLa cells. c-Abl and p38MAPK inhibitors attenuated cisplatin-induced c-Abl and p38MAPK activation (1 hr treatment), and therefore dephosphorylation of histone H1 (4 hr treatment). A representative set of result from three independent experiments is shown. Beta-tubulin and histone were used as loading controls.

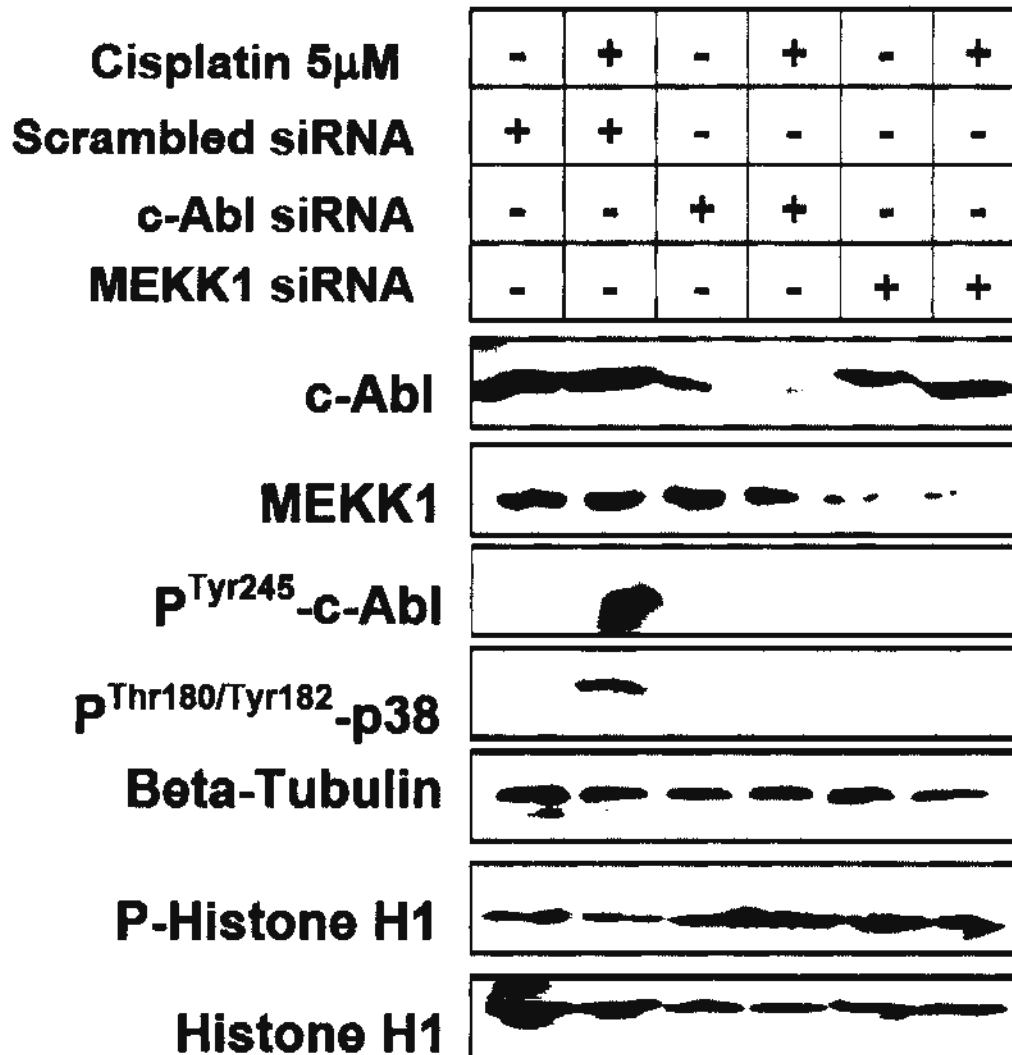


Figure 3.13: Western blot analysis showing that the abrogation of cisplatin-induced activation of the antepause checkpoint by c-Abl and MEKK1 siRNAs in HeLa cells. Silencing of c-Abl and MEKK1 inhibited cisplatin-induced c-Abl and p38MAPK activation (1 hr treatment), and dephosphorylation of histone H1 (4 hr treatment). A representative set of result from three independent experiments is shown. Beta-tubulin and histone were used as loading controls.

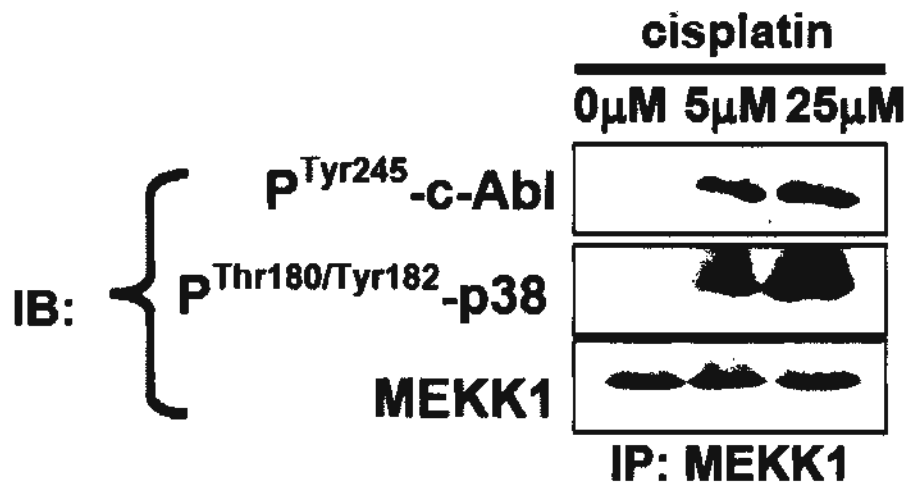


Figure 3.14: Immunoprecipitation analysis showing the association of c-Abl or p38MAPK with MEKK1 after 1 hr cisplatin treatment in HeLa cells. Cell lysates were probed with anti-MEKK1, and then the immune complexes were isolated for immunoblotting. The active forms of c-Abl and p38MAPK were found to bind to MEKK1 only after cisplatin treatment. A representative set of result from three independent experiments is shown. MEKK1 were used as the loading control.

3.5.3 Antephase Checkpoint is Absent in Mismatch Repair Deficient Cell Line.

We have observed earlier that cisplatin cannot activate the antephase checkpoint in the MMR-deficient and c-Abl non-functional HCT116 cell line (Table 3.1). HCT116 cells are *MLH1* mutated and therefore exhibit a defective MMR phenotype (MMR non-functional). To establish the critical role of the MMR status in the regulation of the antephase checkpoint, a pair of MMR-proficient (HCT116+ch3) and MMR-deficient (HCT116+ch2) cell lines were introduced. In HCT116+ch3 cells (*MLH1+*), MMR is restored to HCT116 by introduction of a normal human chromosome 3 (residing the *MLH1* gene) via viral infection. As a negative infection control, HCT116+ch2 cells (*MLH1-*) were also used, where an irrelevant normal human chromosome 2 was introduced by viral infection and therefore the cells are still MMR deficient.

Since cisplatin was reported to activate c-Abl via MMR genes, such as *MLH1* and *MSH2* (Desbiens *et al.*, 2003), studies to understand the function of c-Abl are often performed in pair of HCT116+ch3 (MMR/c-Abl functional) and HCT116+ch2 (or non-transfected HCT116) (MMR/c-Abl non-functional) cells. After cisplatin treatment, the activation of c-Abl and p38MAPK, phosphorylation of histone H1 (Figure 3.16), and the reduction in mitotic cells (Figure 3.15) were only observed in the MMR proficient HCT116+ch3 (*MLH1+*) but not in the MMR deficient

counterpart HCT116+ch2 (*MLH1*⁻) cells. These findings further supported our argument that cisplatin activates the antephase checkpoint via the MMR/c-Abl/MEKK1/p38MAPK pathway. Flow cytometry analysis (Figure 3.17) also revealed that there was more G2/M arrest in the MMR-proficient HCT116+ch3 cells than the MMR-deficient HCT116+ch2 cells, after a 48 hr-recovery from acute stress of cisplatin (2 hr exposure). This finding indicated that the antephase arrest in HCT116+ch3 cells contributes to the (MMR-involved) G2/M arrest induced by cisplatin.

Since the antephase checkpoint is to allow cells time for DNA damage repair and promote survival, viability after a 6-day recovery from acute cisplatin treatment was examined by MTT assay (Figure 3.18). The survival of HCT116+ch3 cells was significantly inhibited by c-Abl, p38MAPK and JNK inhibitors. JNK activation has been reported after cisplatin treatment in a MMR-dependent manner (Nehmé *et al.*, 1999). This observation was also found in HeLa cells except that c-Abl inhibitor STI571 did not show statistical significance. In fact, the synergistic effect between cisplatin and STI571 has been extensively reported (Zhang *et al.*, 2003; Yerushalmi *et al.*, 2007). Our results are also consistent with previous findings that acute treatment of TMZ activates MMR/p38MAPK to arrest U87 cells at the G2/M phase and promote survival (Hirose *et al.*, 2003). However, Wagner's group recently

observed that MNNG activates MMR/c-Abl, leading to G2 arrest and p73-mediated apoptosis (Wagner *et al.*, 2008). We believe that MMR induces G2 arrest, facilitates DNA damage repair and promotes survival in response to acute stress of genotoxic agents at low concentrations (i.e., cisplatin 5 μ M for 2 hrs), but may induce apoptosis upon sustain treatment at high concentrations when fails to repair DNA damage (i.e., cisplatin >5 μ M for 24 hrs). As observed in Figure 3.19, after a 6-day recovery from cisplatin exposure (2 hr), the survival of HCT116+ch3 cells was significantly higher than that of HCT116+ch2 cells (detected by MTT assay, Figure 3.19A); however, when these two cell lines were treated with cisplatin for a longer period of 24 hrs, HCT116+ch3 cells were, on the contrary, more sensitive to cisplatin than HCT116+ch2 cells (detected by MTT and Crystal violet staining, Figure 3.19 D and G, respectively). These results confirms our hypothesis that MMR can release both death and survival signal in response to chemotherapy, depending on the severity of DNA damage. On the other hand, we have provided evidence that DACH-containing oxaliplatin or *R,R*-5 can bypass the antepause checkpoint. This may explain that they did not show any significant difference in their cytotoxicity between these two cell lines after either acute (Figure 3.19 B and C) or sustain treatments (Figure 3.19 E, F, H and I), which is consistent with previous findings that oxaliplatin induced cell death in an MMR-independent manner (Fink *et al.*, 1997).

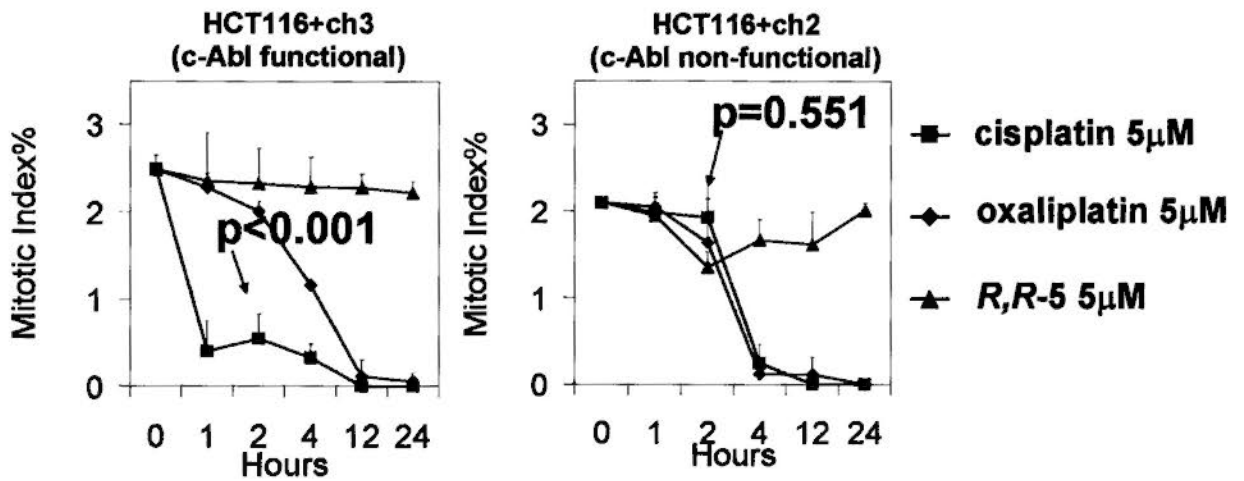


Figure 3.15: Mitotic index assay showing that MMR/c-Abl is indispensable for cisplatin-induced antephrase checkpoint activation. Mitotic indices of MMR/c-Abl-functional HCT116+ch3 cells and MMR/c-Abl-non-functional HCT116+ch2 cells were treated with cisplatin, oxaliplatin or *R,R*-5 at 5 µM. Cisplatin decreased mitotic index promptly at 2 hr after drug treatment only in HCT116+ch3 cells but not HCT116+ch2 cells. Mean \pm SD of 9 replicates from 3 independent experiments are shown. Student's t test was used to compare the mitotic indices of the two cell lines treated with cisplatin at 2 hr with control (0 hr).

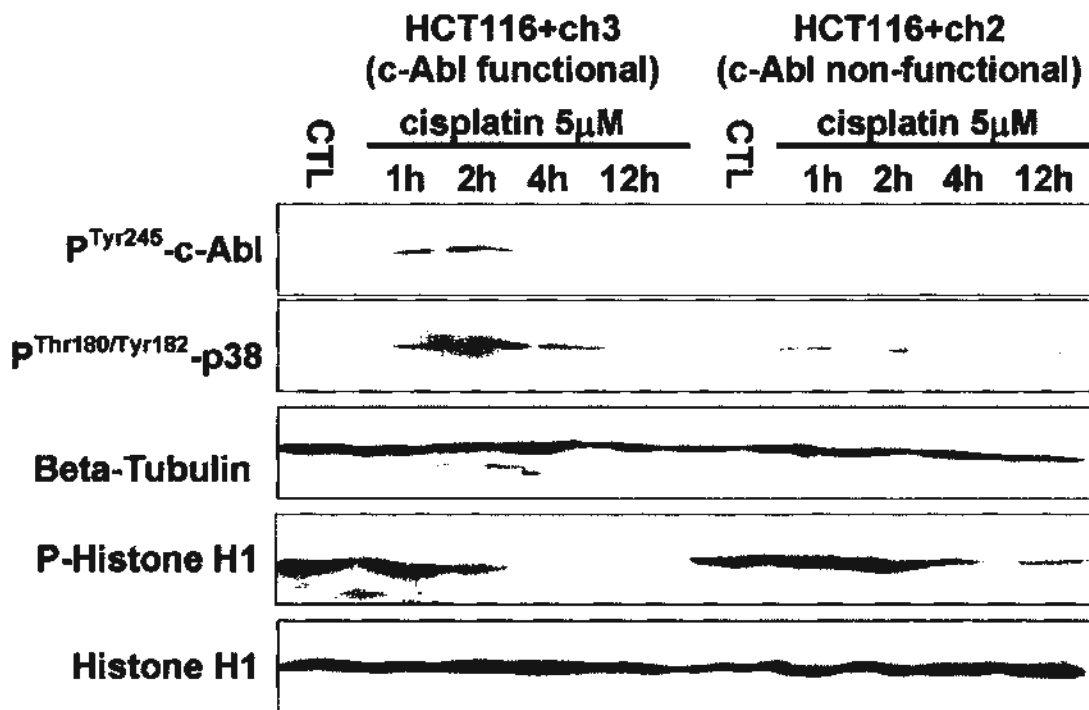


Figure 3.16: Western blot analysis showing that c-Abl is essential for cisplatin-induced antephasic checkpoint activation in HCT116+ch3 cells. Cisplatin-induced c-abl and p38MAPK activation, decreased histone H1 phosphorylation in c-Abl functional HCT116+ch3 cells but not c-Abl non-functional HCT116+ch2 cells. A representative set of result from three independent experiments is shown.

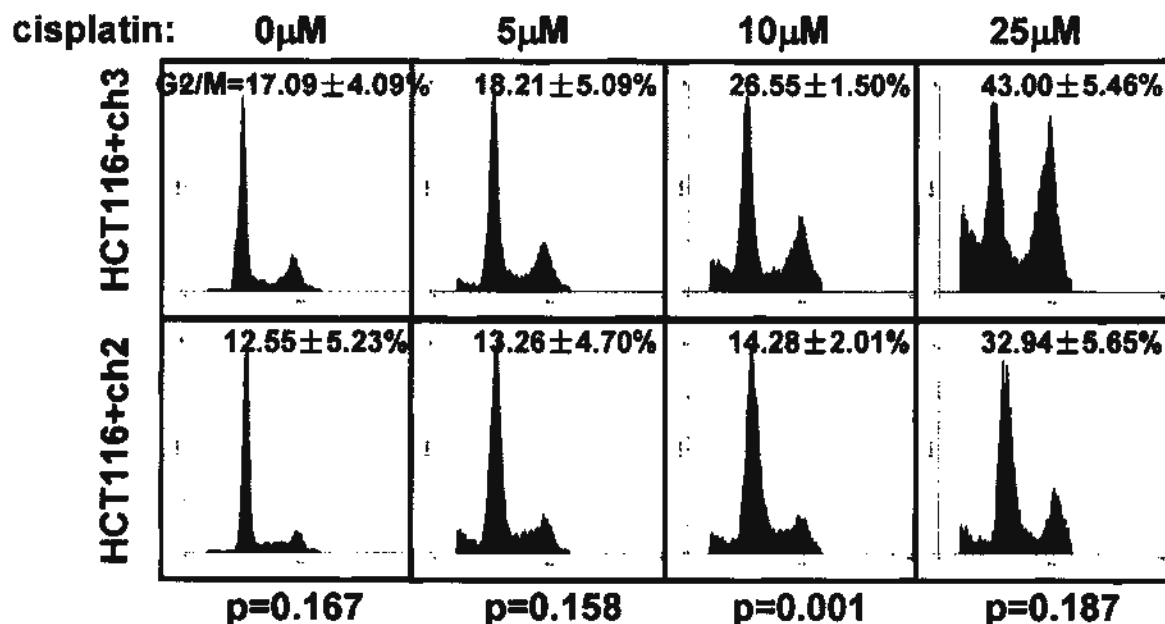


Figure 3.17: Flow cytometry analysis showing the contribution of antepause checkpoint activation to the G2/M arrest induced by cisplatin. Cells were treated with cisplatin for 2 hrs, washed by PBS once and allowed to recover in fresh medium for 2 days before fixation for flow cytometry analysis. Cisplatin treatment resulted in more G2/M arrest in MMR/c-Abl functional HCT116+ch3 cells than in MMR/c-Abl non-functional HCT116+ch2 cells. Mean \pm SD, and one representative set of result from 3 independent experiments are shown. G2/M% of these two cell lines at the same cisplatin concentration are compared using the Student's t test.

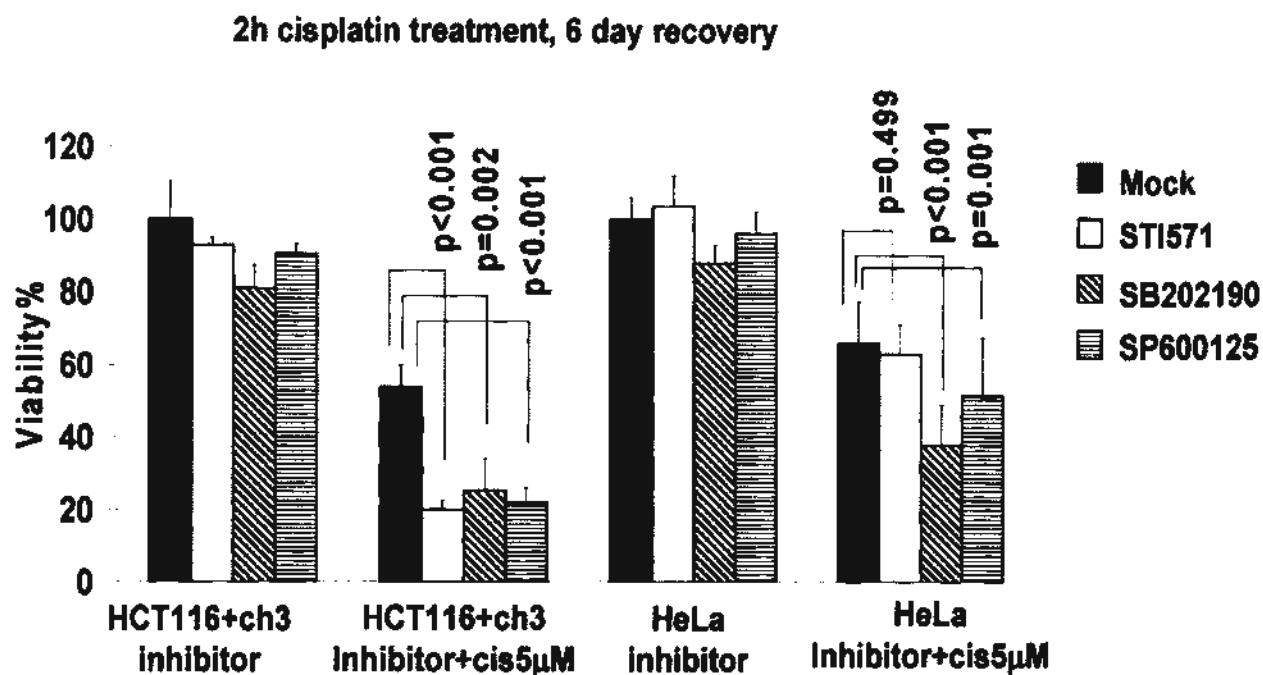


Figure 3.18: MTT assay showing that activation of the antepause checkpoint promoted cancer cell survival after acute stress to cisplatin. Cells were treated with cisplatin for 2 hrs, washed by PBS and allowed to recover in fresh medium for six days before MTT assay. Medium was changed at 48 hr after cisplatin addition. Specific inhibitors against c-Abl (STI571, 5 μ M), p38MAPK (SB202190, 20 μ M) or JNK (SP600125, 10 μ M), respectively were added at 0.5 hr before cisplatin exposure and again after treatment when fresh medium was replaced. The inhibitors were removed at 48 hr after cisplatin treatment when the medium was changed. The final concentration of DMSO was less than 0.01%. It is noted that treatment with the various inhibitors alone did not affect cell viability significantly compared with the untreated control (mock treated with water). Viability% after acute cisplatin exposure could be compromised by c-Abl (except in HeLa), p38MAPK and JNK

inhibitors. Mean \pm SD of 16 replicates from 4 independent experiments is shown.

Student's t test was used to compare the indicated groups.

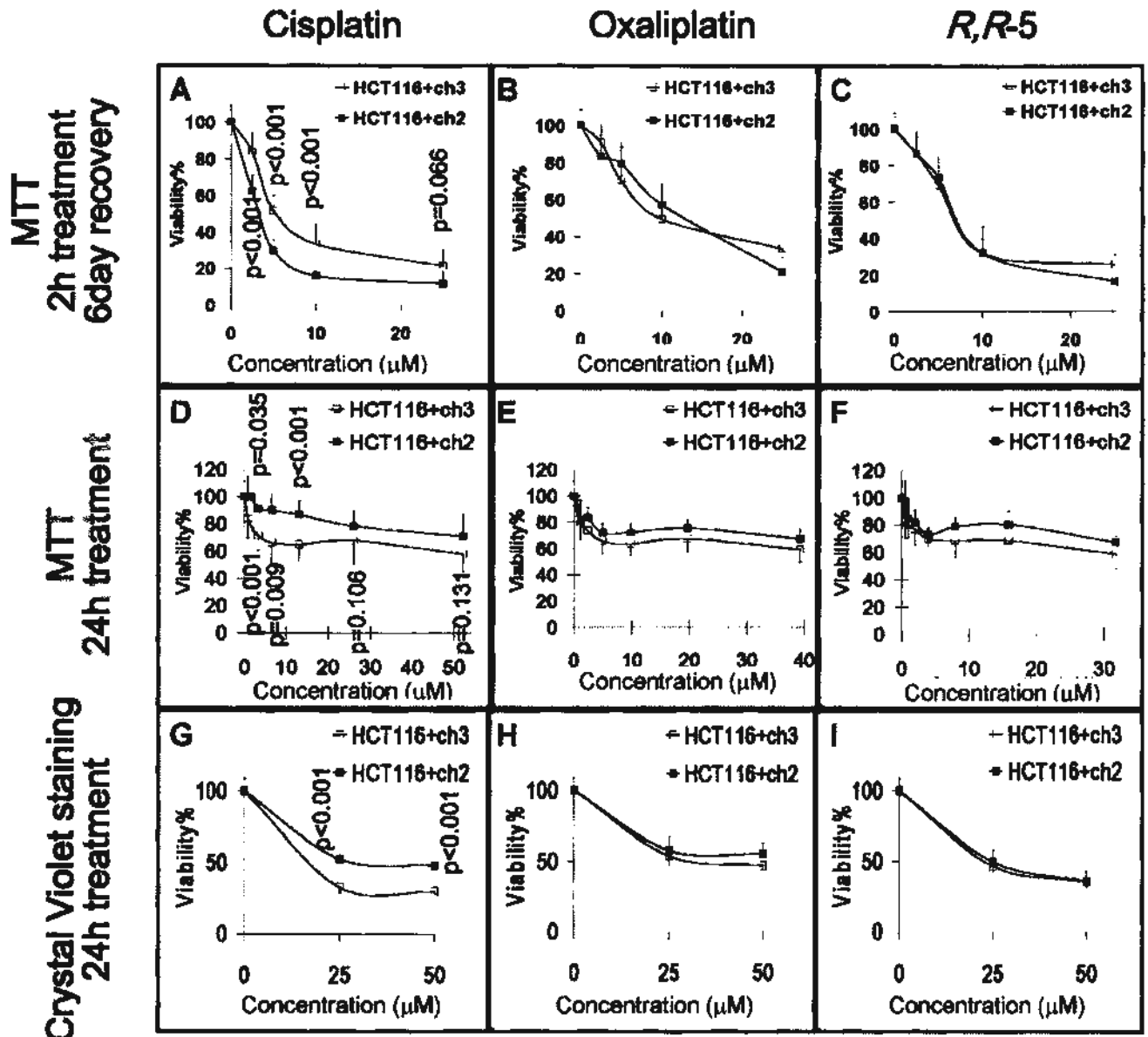


Figure 3.19: MTT and crystal violet-staining assay showing that acute cisplatin treatment promoted cell survival in HCT116+ch3 cells but sustain cisplatin treatment led to cell death. For acute treatment, HCT116+ch3 and HCT116+ch2 cells were treated with cisplatin for 2 hrs, washed by PBS and allowed to recover in fresh medium for six days before MTT assay. Fresh medium was changed at 48 hr after the start of cisplatin treatment. For sustain treatment, cells were treated with

cisplatin for 24 hrs before MTT or crystal violet-staining assay. Mean \pm SD of 16 replicates from 4 independent experiments is shown. Student's t test was used to compare the viability of these two cell lines at the same concentration.

3.5.4 Abrogation of Antephase Checkpoint Led to Prolonged and Aberrant Mitosis.

In order to amplify the effect of the activation of antephase checkpoint, cell cycle synchronization was also performed to accumulate the population of antephase cells. Six hours after the double-thymidine block, HeLa cells were synchronized and they are laboring at the antephase (because cells were entering G2/M phase, Figure 3.21). Then, cells were exposed to cisplatin in the presence or absence of various inhibitors. The mitotic transition was recorded by mitotic index assay (Figure 3.20) and mitotic exit (at 14 hr) was examined by flow cytometry analysis (Figure 3.21). In synchronized HeLa cells, cisplatin could rapidly decrease the mitotic index due to the antephase checkpoint activation (Figure 3.20). c-Abl (STI571) and p38MAPK (SB202190) but not ATM/ATR inhibitor (caffeine) could restore this mitotic transition. However, this led to a prolonged mitosis and failure in mitotic exit after antephase checkpoint abrogation. This was further confirmed by flow cytometry analysis (Figure 3.21). In untreated cells (mock treated with water at 0 μ M cisplatin), a high proportion of cells (77.42%) was found to exit mitosis and returned to the G0/G1 phase. However, in cells treated with cisplatin for 25 μ M, mitotic exit from G2/M and returning to G0 phase failed to occur, leaving only 48.36% of cells in the G0/G1 phase, thus indicating activation of mitotic checkpoint. c-Abl inhibitor

STI571 (51.08%) and p38MAPK inhibitor SB202190 (55.19%) were found to modestly reduce cisplatin-induced G2/M arrest and result in a slight increase in mitotic exit, due to the abrogation of antepause checkpoint. This suggests that abrogation of cisplatin-activated antepause checkpoint by c-Abl and p38MAPK inhibitors does not allow mitotic exit, but instead, leads to a prolonged mitosis possibly due to the activation of the mitotic spindle checkpoint, as evidenced by the mitotic index assay (Figure 3.20). Interestingly, inhibition of ATM/ATR (the well-established G2 checkpoint mediator) by caffeine could not immediately restore cisplatin-inhibited mitotic transition (Figure 3.20), implying that this rapid mitotic checkpoint was antepause checkpoint rather than G2 checkpoint; but cisplatin+caffeine did modestly promote mitotic entry (than cisplatin alone) starting from 10 hr afterwards (Figure 3.20), suggesting the abrogation of G2 checkpoint, which slightly increased cisplatin-induced G2/M arrest with appearance of sub-G1 peak (apoptosis, Figure 3.21), possibly due to the unrepairable DNA damage in mitosis.

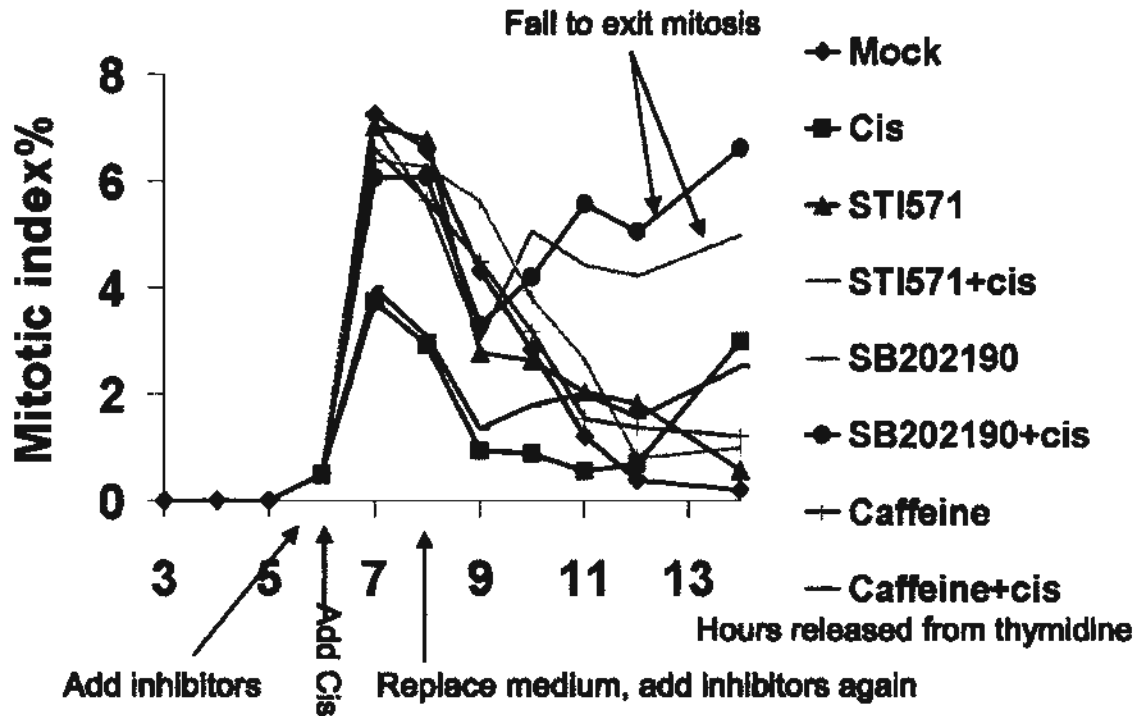


Figure 3.20: Mitotic index assay showing that abrogation of antepause checkpoint led to prolonged mitosis and failure in mitotic exit. 6 hr after release from double-thymidine block, HeLa cells were shown to be synchronized and were entering mitosis, then cisplatin was added (at 6 hr). Another 2 hours later (at 8 hr), cells were washed once, after which fresh medium (without cisplatin) was added. Various inhibitors against c-abl (STI571, 5 μ M), p38MAPK (SB202190, 20 μ M), ATM/ATR (caffeine, 5 mM) (or mock-treated with water), were added 0.5 hr before cisplatin exposure (at 5.5 hr) and again after treatment (at 8 hr). c-Abl and p38MAPK inhibitors restored cisplatin-inhibited mitotic entry and led to prolonged mitosis. Mean of 3 independent experiments is shown.

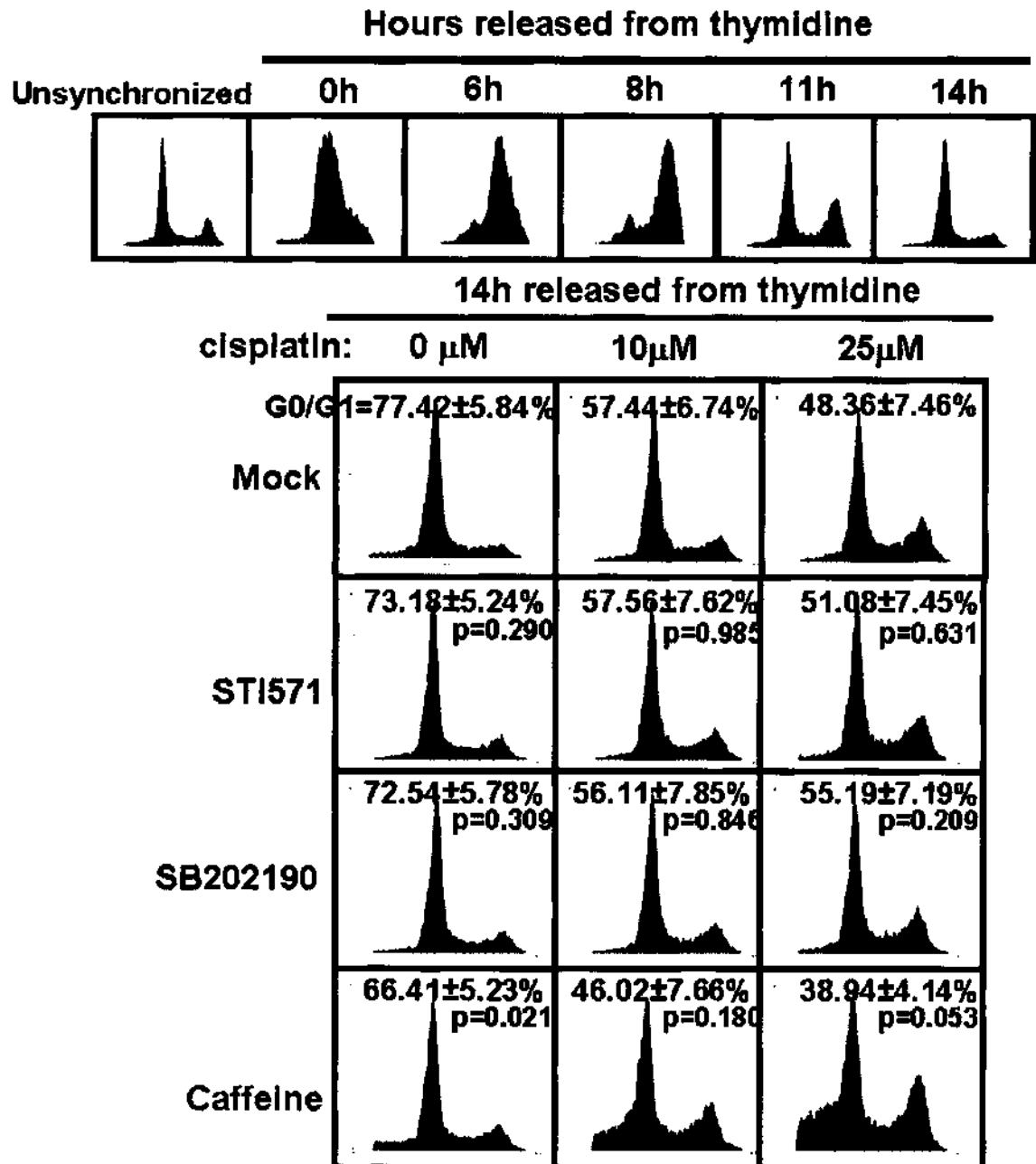


Figure 3.21: Flow cytometry analysis showing that abrogation of cisplatin-activated antepause checkpoint led to failure at mitotic exit. HeLa cells were synchronized and treated as described in Figure 3.20, and fixed at 14 hr for flow cytometry

analysis. In untreated cells (mock treated with water at 0 μ M cisplatin), 77.42% cells were able to exit mitosis and returned to G0 phase, but this transition was inhibited in cisplatin-treated cells, due to the activation of antephasic checkpoint. c-Abl and p38MAPK inhibitors attenuated cisplatin-activated antephasic checkpoint and led to mitotic defects, resulting in failure in mitotic exit. Mean \pm SD from 3 independent experiments is shown. Student's t test was used to compare the G0/G1% of "inhibitor+cisplatin" and the corresponding "inhibitor" groups under the same cisplatin concentration.

We have observed that abrogation of antephasic checkpoint will lead to prolonged mitosis and failure at mitotic exit (Figure 3.20, Figure 3.21), which is believed to result in mitotic catastrophe and consequently cell death. In fact, when HeLa cells were treated with various compounds for 2 hrs, with an additional 20 hrs to accumulate abnormal mitotic cells, mitotic catastrophe was observed in cells treated with STI571+cisplatin (2.77%) and SB202190+cisplatin (2.63%) (Figure 3.22). These treatments were previously demonstrated to inhibit the activation of

antephase checkpoint via inhibition of c-Abl and p38MAPK, respectively (Figure 3.11). In contrast, cisplatin (5 μ M) only showed 0.03% aberrant mitotic cells. On the other hand, oxaliplatin and *R,R*-5, which were also proved to bypass the antephase checkpoint (Figure 3.8), showed 1.37% and 2.10% aberrant mitosis, respectively. This finding agrees well with our earlier finding that cisplatin activates the antephase checkpoint but not oxaliplatin or *R,R*-5. Interestingly, DMC+cisplatin could also remarkably increase aberrant mitosis, when this effect was absent in cells treated with DMC and cisplatin alone. As previously observed in Figure 3.11, PP2A inhibitor DMC and okadaic acid does not attenuate cisplatin-stimulated antephase checkpoint, this aberrant-mitosis promoting effect of DMC may be generated from: a) PP2A inhibition prevents DNA damage repair, facilitates antephase-arrested cells to re-enter cell cycle (mitosis) and consequently aberrant mitosis, possibly via mechanisms illustrated in Figure 1.11; b) DMC may abrogate G2 checkpoint activation in response to cisplatin treatment (5 μ M for 2 hrs with another 20 hrs recovery) and promote mitotic catastrophe (will be further explored in Chapter Four).

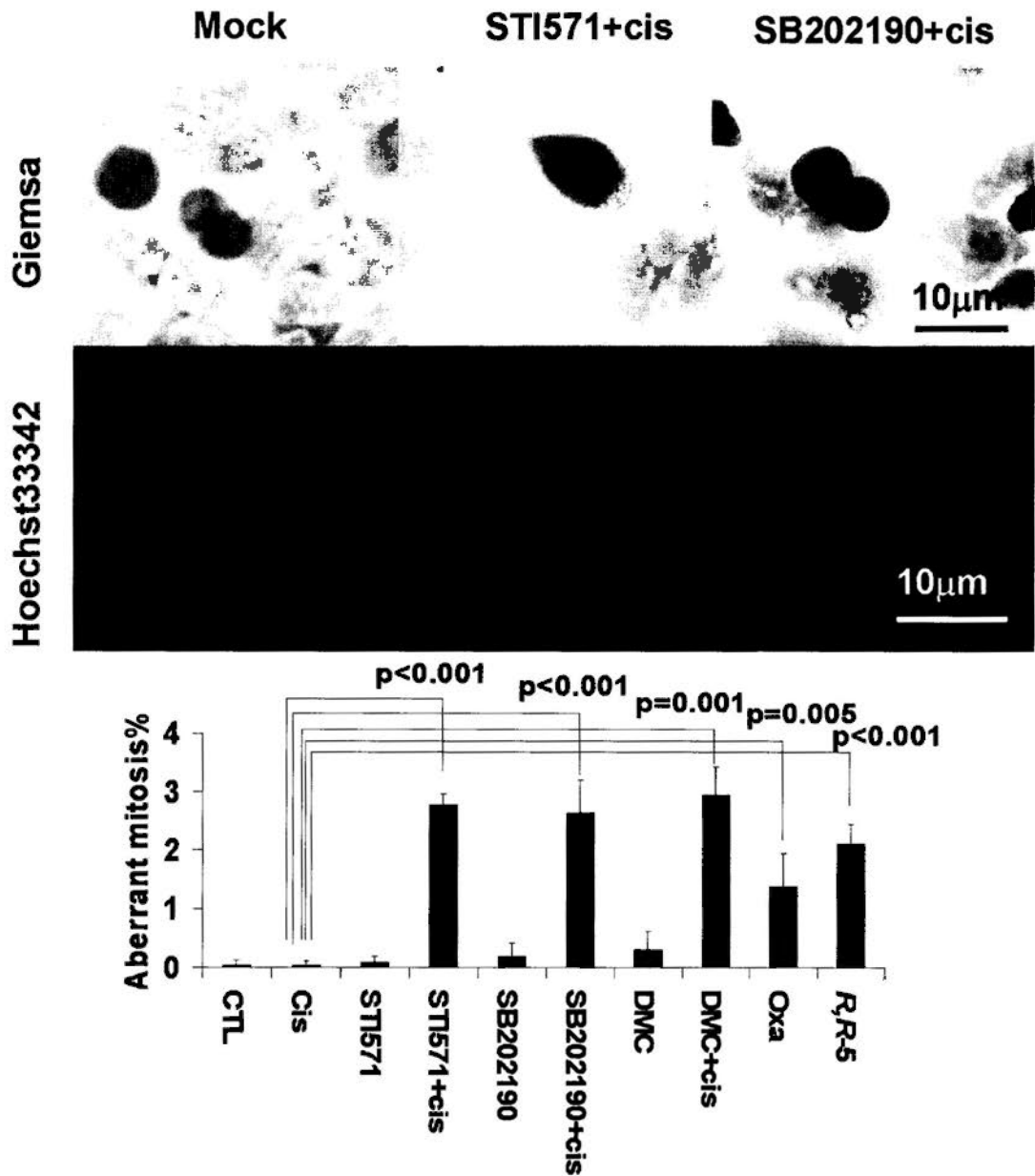


Figure 3.22: Abrogation of antepause checkpoint activation could lead to mitotic catastrophe. HeLa cells were treated with cisplatin, oxaliplatin or *R,R*-5 at 5 μM for 2 hrs, washed by PBS and allowed to recover in fresh medium for another 20 hrs, before fixation and staining for cell counting of mitotic catastrophe under a microscope. Specific inhibitors against c-Abl (STI571, 5 μM), p38MAPK (SB202190, 20 μM) or PP2A (DMC, 5 μM), respectively were added at 0.5 hr before

cisplatin treatment and stayed present until fixation at 20 hr after cisplatin treatment.

Cisplatin and inhibitors alone only showed very limited aberrant mitosis, whereas

STI571+cisplatin, SB202190+cisplatin, DMC+cisplatin, and *R,R*-5 groups exhibited

significantly higher catastrophic mitotic cells, compared with cisplatin group, using

Students' t test. Mean \pm SD of 9 replicates from 3 independent experiments is shown.

Representative images with either Giemsa- or Hoechst33342-staining are shown.

3.6 Conclusions

In summary, our working model is shown in Figure 3.23. Acute treatment of cisplatin was found to activate a MMR/c-Abl/MEKK1/p38MAPK pathway, leading to G2/M arrest associated with the activation of the antephase checkpoint (antephase arrest). This pathway allowed time for DNA damage repair before resuming cell cycle progression, thereby sparing cells from mitotic catastrophe and promoting cell survival. Failure of the antephase checkpoint resulted in genomic instability, and eventually cell death. In contrast, oxaliplatin and *R,R*-5 were unable to activate this pathway and the antephase checkpoint, due to the presence of a DACH moiety in their structures. Our findings provide the molecular basis for the superior anti-tumor activity and lack of platinum resistance demonstrated by oxaliplatin and *R,R*-5.

Since c-Abl/p38MAPK inhibitors could abrogate cisplatin-activated antephase checkpoint, they therefore can be used in combination therapy to sensitize cancer cells to platinum drugs and probably other DNA damaging agents that activate the MMR machinery. This may represent a novel strategy for the circumvention of anticancer drug resistance. To this end, the synergistic effect between STI571 (c-Abl inhibitor) and cisplatin has been proposed in a number of studies (Zhang *et al.*, 2003; Wang-Rodriguez *et al.*, 2006; Yerushalmi *et al.*, 2007).

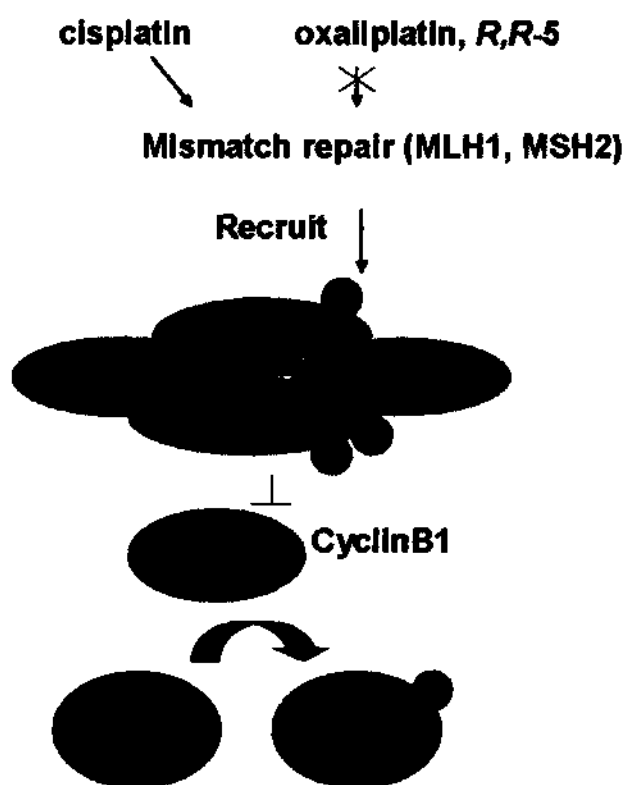


Figure 3.23: Mechanism of antepause checkpoint activation in response to acute stress of cisplatin. Acute stress of cisplatin activates the MMR/c-Abl/MEKK1/p38MAPK pathway, and stopping cells from entering mitosis. This allows time for DNA damage repair before resuming cell cycle progression and consequently promoted cancer cell survival.

Chapter Four

Demethylcantharidin abrogates oxaliplatin-activated G2 checkpoint by restoring CDK1 activity, independent of CHK1/CHK2 activation

-----Effect of *R,R*-5 at the G2 Checkpoint

4.1 Introduction

Based on the cDNA microarray analysis reported in Chapter Two, we found that 35 genes promoting G2 to M phase transition were up-regulated in HCT116 cells treated with *R,R*-5 compared with oxaliplatin (Chapter Two, Table 2.3). We therefore proposed that cells treated with *R,R*-5 may bypass the two mitotic DNA damage checkpoints: antephase and G2 checkpoints. Our findings at the antephase checkpoint have already been discussed in Chapter Three. In this chapter, the effect of cisplatin, oxaliplatin and *R,R*-5 at the G2 checkpoint will be compared. The role of DMC in the biological activities of *R,R*-5 at the G2 checkpoint will also be examined.

Compared with the recently discovered antephase checkpoint, the G2 DNA damage checkpoint is more extensively studied. When cells are exposed to

genotoxic stress, such as ionizing radiation (reactive oxygen species) and DNA damaging agents, the G2 checkpoint will be activated by either the ATM (ataxia telangiectasia mutated) and/or ATR (ATM and Rad3-related)-mediated pathways, depending on the nature of DNA damage. ATM is usually activated in response to ionizing radiation whereas ATR is important in the response to DNA alkylating agents such as methyl methanesulfonate (MMS) (Kedar *et al.*, 2008). In general, ATM and ATR are considered to be activated by double-strand and single-strand DNA breaks, respectively (Dubrana *et al.*, 2007). The recognition of DNA strand breaks by ATM/ATR involves a direct binding process, with the help of other sensor proteins such as hRAD9, hRAD1 and hHus1 (Volkmer and Karnitz, 1999). Detection of DNA damage will lead to the auto-phosphorylation and self-activation of ATM, which subsequently activate CHK2 (Figure 4.1). CHK2 directly phosphorylates CDC25C and inhibits its kinase activity, thereby decreasing the activation of CDK1/Cyclin B1. CDK1/Cyclin B1 is a critical regulator controlling cell cycle progression from G2 to M phase. As a transducer, ATM can also stimulate other effectors to activate the G2 checkpoint. ATM can activate p53, which transcribes p21 and GADD45 to inhibit CDK1. BRCA1, an important protein for homologous recombination, can also be phosphorylated by ATM, leading to G2

checkpoint activation. Similarly, ATR can signal G2 checkpoint activation through CHK1 (Bradshaw and Dennis, 2003).

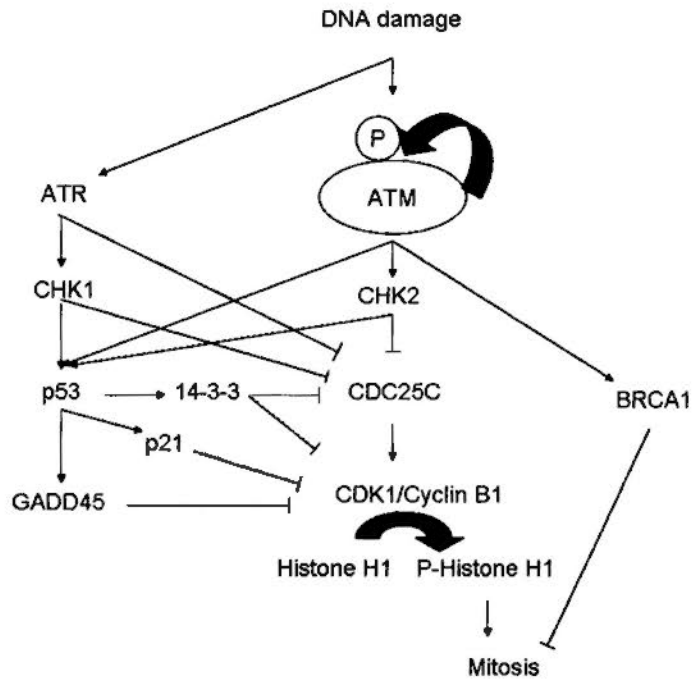


Figure 4.1: Mechanism of G2 checkpoint activation via ATM/ATR. DNA damage leads to auto-phosphorylation of ATM, thereby activating CHK2. CHK2 phosphorylates CDC25C and inhibits CDC25C kinase activity, resulting in the inhibition of CDK1/Cyclin B1 activation. This consequently leads to a decrease in histone H1 phosphorylation, and inhibition of mitosis. CHK2 can also trigger p53-mediated transcription of 14-3-3, p21 and GADD45 to inhibit mitosis. On the other hand, BRCA1 activation by ATM can also contribute to the stimulation of the G2 checkpoint. Similarly, ATR can signal G2 checkpoint activation through CHK1.

Similar to the antephasis checkpoint, the physiological significance of G2 checkpoint activation in response to DNA damage is to facilitate DNA damage repair before resuming cell cycle progression, avoid mitotic catastrophe and promote cell survival after stress exposure. As a result, abrogation of the G2 checkpoint can sensitize cancer cells to DNA damaging agents, which was observed after disruption of the antephasis checkpoint discussed in Chapter Three. In fact, the ATM/ATR inhibitor caffeine has been shown to sensitize cancer cells to radiotherapy early in 1995 (Russell *et al.*, 1995; Powell *et al.*, 1995). However, caffeine is not a specific inhibitor of ATM/ATR signaling, as it can also interact with adenosine receptors (Holtzman *et al.*, 1991). With a better understanding of the ATM/ATR-mediated G2 checkpoint signaling in recent years, more G2 checkpoint abrogators targeting different kinases have been discovered. UCN-01 (7-hydroxystaurosporine) was initially tested in a phase I clinical trial as a single compound. It was shown to exhibit anti-tumor activity, possibly due to the attenuation of protein kinase C and/or PDK1 (Sato *et al.*, 2002). As a protein kinase C inhibitor targeting both CHK1 and CHK2, UCN-01 has recently entered other clinical trials as a G2 checkpoint abrogator in combination with DNA damaging agents, such as carboplatin (ClinicalTrials.gov identifier: NCT00036777). Superior to caffeine, the IC_{50} for CHK2 inhibition by UCN-01 was around 100,000 times lower than the IC_{50} for

ATM-inhibition by caffeine (Bunch and Eastman, 1996). However, UCN-01 was found to be extensively bound to $\alpha 1$ acid glycoprotein, which severely hindered its bio-availability (Fuse *et al.*, 1998; Sausville *et al.*, 2001). Therefore, UCN-01 did not have favorable pharmacokinetic parameters to be used in combination with other chemotherapeutic drugs. Several promising G2 checkpoint abrogators are also under active investigation in recent years, such as the CHK1 inhibitors ICP-1 (Eastman *et al.*, 2002) and Go6976 (Kohn *et al.*, 2003).

We hypothesize that the novel platinum compound *R,R*-5 can bypass the G2 DNA damage checkpoint. This is supported by our results from the cDNA microarray analysis (Chapter Two, Figure 2.3, Table 2.3): 35 G2→M-promoting genes were found to be up-regulated after *R,R*-5 treatment in HCT116 cells compared with oxaliplatin. Many of the genes identified are mitotic markers, such as Cyclin B1, CDK1, CENPF, Aurora A and TPX2. Another clue supporting our hypothesis is that the PP2A inhibitor okadaic acid was reported to abrogate thymidine-induced G2 checkpoint activation (Ghosh *et al.*, 1996). It has also been shown that okadaic acid can lead to pre-mature mitosis in cancer cells (Gurland *et al.*, 1993), though the signal transduction pathway mediating this effect is still not clear. There is no evidence that okadaic acid can inhibit the kinase activity of ATM/ATR or CHK1/CHK2 directly.

On the other hand, PP2A inhibitors may affect the TPX2 signaling and facilitate mitosis (Figure 4.2). TPX2 can activate Aurora A (aurora kinase A, AURKA) and lead to phosphorylation of histone H3 (Eyers *et al.*, 2003). Histone H3 phosphorylation is a commonly used mitotic marker, though gene transcription also requires histone H3 phosphorylation (Nowak and Corces, 2000). PP2A and PP1 have been reported to inhibit the activation of Aurora A (Eyers *et al.*, 2003). Therefore, PP2A inhibitors may facilitate Aurora A activation and histone H3 phosphorylation, hence mitosis. This argument is supported by the observation that PP2A can lead to histone H3 dephosphorylation in *Drosophila melanogaster* (Nowak *et al.*, 2003). Moreover, the PP2A inhibitor okadaic acid was reported to promote histone H3 phosphorylation and DNA condensation (Takemoto *et al.*, 2007). This process required Aurora B (aurora kinase B, AURKB), another histone H3 kinase, but not Aurora A (Takemoto *et al.*, 2007). Aurora B is negatively regulated by PP2A (Sun *et al.*, 2008), but there is still no evidence suggesting that TPX2 associates with Aurora B. Since *R,R*-5 and DMC are PP2A inhibitors, they may therefore promote mitosis via activation of the TPX2 pathway. In fact, TPX2, Aurora A and Aurora B were found to be up-regulated after *R,R*-5 treatment compared to oxaliplatin in the microarray analysis in Chapter Two (Table 2.3).

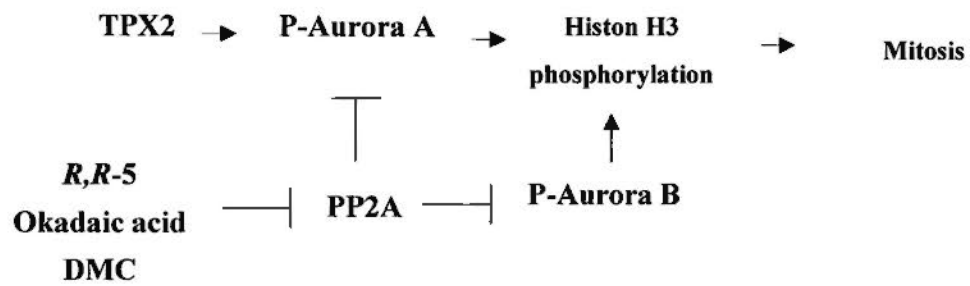


Figure 4.2: A proposed mechanism for the promotion of mitosis by PP2A inhibitors.

TPX2 can activate Aurora A, leading to the phosphorylation of histone H3, hence mitosis. Aurora B also regulates mitosis in a similar manner. Both Aurora A and B are negatively regulated by PP2A.

4.2 Objectives

The objectives of this chapter are:

- a) To compare the effect of cisplatin, oxaliplatin and *R,R*-5 at the G2 checkpoint and to find out the underlying mechanism(s);
- b) To examine if DMC abrogates oxaliplatin-activated G2 checkpoint and to elucidate the underlying mechanism(s).

4.3 Experimental Design

The potential effects of cisplatin, oxaliplatin and *R,R*-5 at the G2 checkpoint were examined. First, the mitotic index assay was used to determine if the G2 checkpoint was activated, which will be indicated by a decrease in mitotic cells. As discussed in Figure 4.1, activation of the G2 checkpoint is expected to turn on the ATR/CHK1 and/or ATM/CHK2 pathways, leading to inhibition of CDK1/Cyclin B1 (the major mitosis promoting factor), and subsequently causing the dephosphorylation of histone H1, which could be readily detected by Western blot analysis. The expected G2/M arrest upon G2 checkpoint activation (in unsynchronized HeLa and HCT116 cells) was measured by cell cycle analysis (using flow cytometry). In some cases, activation of G2 checkpoint is accompanied by the inhibition of DNA synthesis due to CHK1/CHK2 activation (S phase checkpoint), which also stops mitotic entry, and this effect was detected by BrdU incorporation assay in HeLa cells.

To examine if DMC abrogates oxaliplatin-activated G2 checkpoint by restoring CDK1 activity (CDK1 is proposed to be the molecular target by which DMC abrogates the G2 checkpoint), the change in transcription level of CDK1 was detected by real-time RT-PCR (reverse transcription polymerase chain reaction). Specific inhibition of CDK1 by roscovitine (a CDK1 inhibitor) or siRNA was also

performed, to examine whether DMC, *R,R*-5 and DMC+oxaliplatin treatments could still maintain histone H1 phosphorylation (Western blot analysis) and mitotic entry (mitotic index assay and cell cycle analysis, in synchronized HeLa cells), when CDK1 was compromised. Finally, abrogation of G2 checkpoint may induce mitotic catastrophe and consequently inhibit cell survival after drug treatment, which were investigated by cell counting (for aberrant mitosis) and MTT assay, respectively.

4.4 Materials and Methods

4.4.1 Chemicals

Roscovitrine was purchased from Cell Signaling Technology. All other chemicals used in this chapter were as described in Chapter 3.4.1.

4.4.2 Cell Lines and Cell Cultures

HeLa and HCT116 cells were obtained from the American Type Culture Collection, and maintained in RPMI1640 medium supplemented with 10% fetal bovine serum (v/v), 100U/ml penicillin and 100 U/ml of streptomycin, in a humidified CO₂ incubator (5% CO₂/95% air) at 37 °C. Cell culture was split every three or four days.

4.4.3 Mitotic Index Assay and Examination of Mitotic Catastrophe

The mitotic index assay was adapted from the method developed by Bulavin *et al.* with minor modifications. In HeLa or HCT116 cells, 2×10^4 cells/well were seeded onto a 96-well plate. Cisplatin, oxaliplatin or *R,R*-5 (at 5 μ M) were added 24 hrs later. In experiments involving drug combinations, the various inhibitors were added 0.5 hr before the treatment with Pt drugs. At 24 hr after drug addition, cells were fixed overnight with 4% paraformaldehyde and stained with 10% Giemsa or

Hoechst33342. Mitotic cells (prophase, pro-metaphase, metaphase, anaphase, telophase and cytokinesis), and aberrant mitotic cells (mitosis with irregularly arrayed and/or unequally distributed chromosomes) were counted from over 600 cells randomly picked from each well.

4.4.4 Cell Cycle Synchronization and Flow Cytometry Analysis

For unsynchronized cell cycle analysis, HCT116 cells were treated with cisplatin (4.14 μM), oxaliplatin (1.24 μM) or *R,R*-5 (0.40 μM) at their IC_{50} (72 hrs treatment, according to Yu *et al.*, 2006), DMC at 1.24 μM , or a combination of oxaliplatin (1.24 μM) and DMC (1.24 μM , added 0.5 hr before oxaliplatin) for 72 hrs. On the other hand, HeLa cells were treated with cisplatin, oxaliplatin or *R,R*-5 for 24 hrs at 5 μM , with or without DMC (5 μM) or caffeine (5 mM). DMC and caffeine were added 0.5 hr before oxaliplatin addition. After drug treatment, cells were trypsinized and fixed in 70% ethanol overnight at -20 °C before flow cytometry analysis. For synchronized cell cycle analysis, HeLa cells were synchronized using double-thymidine block as described in Chapter 3.4.6. At 3 hr after released from thymidine (when cells were progressing into G2 phase, Figure 4.14), roscovitine (a specific CDK1 inhibitor) was added; at 3.5 hr, various compounds were added with or without pre-incubation of roscovitine; at 14 hr, cells were harvested and fixed in

70% ethanol overnight at -20 °C for flow cytometry analysis. Cells were stained with 50 µg/ml propidium iodide (containing 10 mg/ml RNase A). Flow cytometry analysis was carried out using a BD FACSAria™ flow cytometer (BD Biosciences). Data were processed using the WinMDI 2.9 software (free software downloaded from <http://facs.scripps.edu/software.html>; accessed on 28 July, 2009). Analysis was performed on 10,000 cells.

4.4.5 Real-time RT-PCR

HeLa cells were treated with cisplatin, oxaliplatin or *R,R*-5 (at 5 µM) for 24 hrs with or without DMC (at 5 µM). DMC was added 0.5 hr before oxaliplatin addition. Total RNA was extracted using the RNeasy Mini Kit (Qiagen) following manufacturer's instructions. RNA was quantified using a UV-2550 spectrophotometer (Shimadzu). The Transcriptor First Strand cDNA Synthesis Kit (Roche) was used for the reverse transcription of RNA samples into cDNA. Real-time PCR detections of human CDK1 (forward primer 5'-GGGGATTCAGAAATTGATCA-3', reverse primer 5'-GGGGATTCAGAAATTGATCA-3'), Cyclin B1 (forward primer 5'-CCATTATTGATCGGTTTCATGCAGA-3', reverse primer 5'-CTAGTGCAGAATTCAGCTGTG-3') and GAPDH (forward primer 5'-

ACCACAGTCCATGCCATCAC-3', reverse primer 5'-
TCCACCACCCTGTTGCTGTA-3'), were performed on the Light Cycler 480
(Roche) using the Light Cycler 480 SYBR Green I Master Mix (Roche).

4.4.6 Western Blot Analysis

HeLa cells were treated with the platinum compounds for 24 hrs; inhibitors were added 0.5 hr before the platinum drug treatments. Details of the experiments are similar to those described in Chapter 3.4.4. Human CDK1, P^{Thr387}-CHK1 and P^{Ser19}-CHK2 antibodies were purchased from Cell Signaling Technology.

4.4.7 siRNA Transfection

Human CDK1 (sense r(GGUUAUAUCUCAUCUUUGA)dTdT, anti-sense r(UCAAAGAUGAGAUUAUAACC)dTdT) (catalog number SI02663381) siRNAs and a negative control siRNA (Alexa Fluor 488[®]-labeled siRNA, catalog number 1027280) that does not match any known gene sequences, were purchased from Qiagen. HeLa cells were transfected with these siRNAs using the Hi-PerFect transfection reagent (Qiagen) as described in Chapter 3.4.5. Both siRNAs were used at a final concentration of 20 nM. 6 to 8 hours after transfections, transfection efficiency was monitored under a fluorescence microscope. About 80% to 90% of

HeLa cells were transfected with the negative control siRNA, as indicated by a green fluorescence signal (Alexa Fluor 488[®]) upon UV excitation. Knock-down efficiency of CDK1 was further confirmed by Western blotting (Figure 4.12 B).

4.4.8 MTT Assay and BrdU Incorporation Assay

For MTT assay in HeLa and HCT116 cells, 2,000 cells/well were seeded in a 96-well plate. Twenty-four hours later, cells were treated with cisplatin, oxaliplatin or *R,R*-5 for 24 hrs. In experiments involving combination of drugs, caffeine or DMC were added 0.5 hr before oxaliplatin exposure. After drug treatment, medium containing drugs were then removed, cells were washed with PBS once and fresh medium containing no drug was added. Cells were allowed for an 8-day recovery before MTT assay. Medium was changed on the fourth day after drug treatment. To investigate cellular BrdU incorporation, the Cell Proliferation ELISA (enzyme-linked immunosorbent assay), BrdU Kit (Roche) was used following manufacturer's instructions. Briefly, cells were treated with cisplatin, oxaliplatin or *R,R*-5 for 24 hrs. In experiments involving drug combinations, caffeine or DMC were added 0.5 hr before oxaliplatin exposure. BrdU was then added at 24 hr after drug treatment for another 4-hour incubation, where BrdU will replace deoxythymidine and incorporate into DNA if cells were synthesizing DNA. Cells were then fixed and incubated with

peroxidase-linked BrdU antibody; the BrdU-labeled cells can then be quantified using a colorimetric method.

4.5 Results and Discussions

4.5.1 DMC abrogated Oxaliplatin-Stimulated G2 Checkpoint in HCT116 Cells

According to the cDNA microarray data discussed in Chapter Two, 35 mitosis-promoting genes were found to be up-regulated after *R,R*-5 treatment compared with oxaliplatin (at respective IC_{50} in HCT116 cells, Figure 4.4, also Table 2.3), with only one mitosis-inhibiting gene up-regulated. This finding suggests that *R,R*-5 may bypass the mitotic DNA damage checkpoints rather than oxaliplatin, which is believed to be due to the incorporation of DMC into its structure (Figure 4.3). In fact, under the same drug treatment (at respective IC_{50} in HCT116 cells), oxaliplatin could induce remarkable G2/M cell cycle arrest, whereas *R,R*-5 and DMC+oxaliplatin can significantly reduced G2/M arrest compared with oxaliplatin (Figure 4.5). Since HCT116 cells do not have a functional antephasis checkpoint for genotoxic stresses (due to the non-functional MMR/c-Abl status, Figure 3.9), the G2/M arrest induced by oxaliplatin is therefore considered due to G2 checkpoint activation; and the reduced G2/M arrest after *R,R*-5 or DMC+oxaliplatin exposure suggests that these treatments could bypass the G2 checkpoint. These observations may explain the higher cytotoxicity of *R,R*-5 compared with oxaliplatin in HCT116 cells (Yu *et al.*, 2006). Interestingly, *R,R*-5, but not oxaliplatin or DMC, was also found to induce G0/G1 arrest (demonstrated by the increase of G0/G1 cell

population). This is also consistent with our findings from the microarray analysis that five genes inhibiting G1 to S transition were up-regulated by *R,R*-5 relative to oxaliplatin (Table 2.2). The biological function of this G0/G1 arrest is believed to protect normal cells from DNA damage induced by *R,R*-5. Cisplatin did not exhibit appreciable G2/M arrest probably because apoptosis predominated after long hours of treatment (72 hrs).

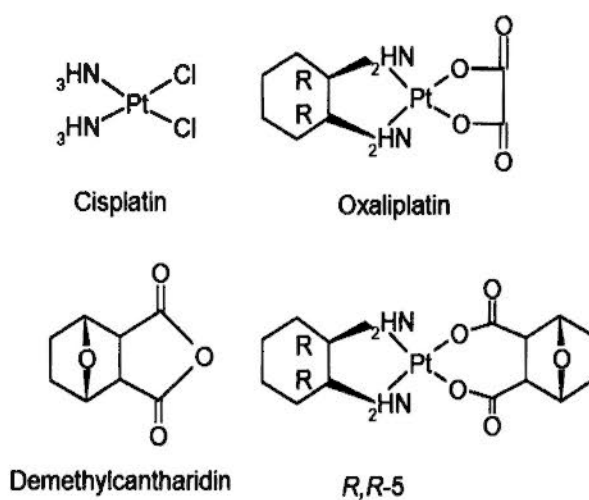


Figure 4.3: Chemical structures of cisplatin, oxaliplatin, *R,R*-5 and DMC.

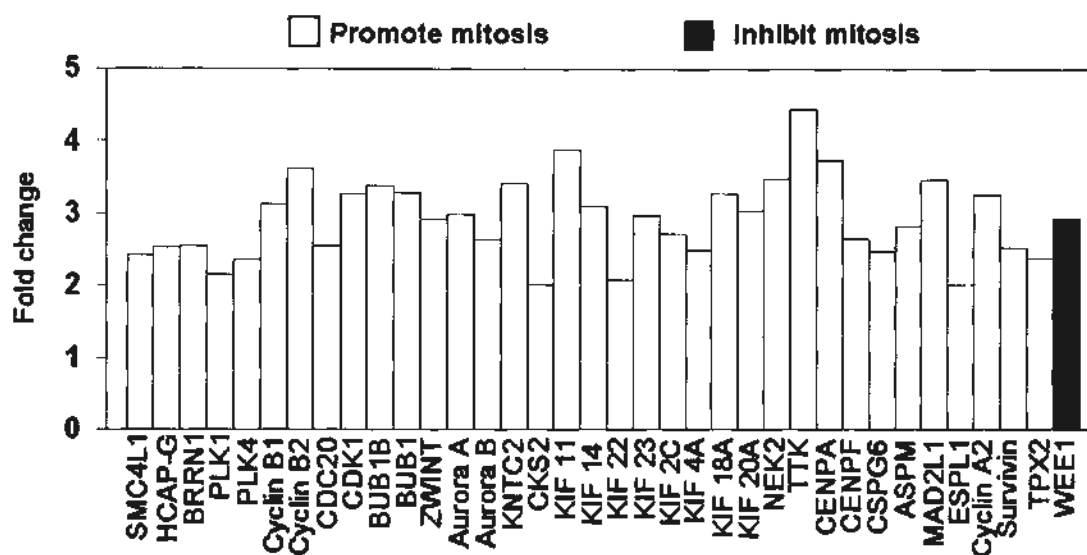


Figure 4.4: cDNA microarray analysis showing the up-regulated genes related to G2→M transition after *R,R-5* treatment compared with oxaliplatin (at respective IC_{50} in HCT116 cells). 35 mitosis-promoting and one mitosis-inhibiting gene was up-regulated whereas no gene related to G2→M transition was found down-regulated. Mean of fold changes from two independent microarray analyses are shown.

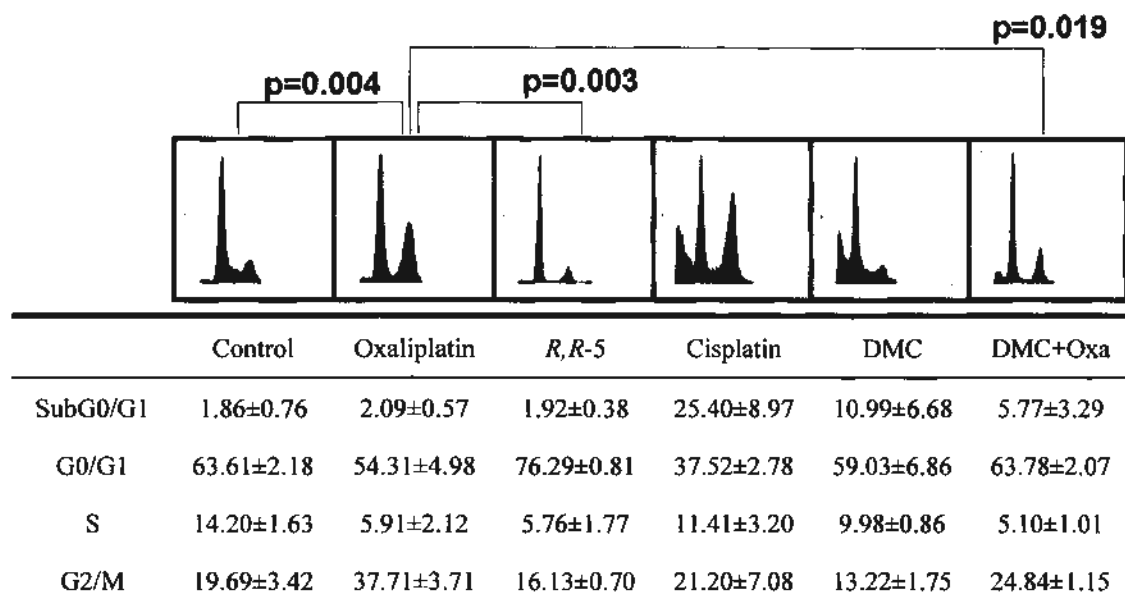


Figure 4.5: Cell cycle analysis showing the oxaliplatin-induced G2/M arrest due to G2 checkpoint activation in HCT116 cells. HCT116 cells were treated with oxaliplatin, *R,R*-5, cisplatin at their IC₅₀ for 72 hrs (as described in Chapter 4.4.4) before fixation for cell cycle analysis by PI staining. Oxaliplatin, but not *R,R*-5 or DMC+oxaliplatin treatments, resulted in significant G2/M arrest. Mean±SD and a representative set of data from 3 independent experiments are shown. Student's t test was used to compare the G2/M% arrest between the indicated groups and p values are shown.

4.5.2 DMC Restored Oxaliplatin-decreased Mitotic Index Without Altering

G2/M Arrest or DNA Synthesis

To study the effect of oxaliplatin on G2 checkpoint activation, we measured the mitotic index after sustained drug treatment (24 hr) in order to wait for vivid activation of G2 checkpoints and cell cycle arrests. This requires 24 hr of oxaliplatin-exposure at 5 μ M, as demonstrated previously in HCT116 cells (Volland *et al.*, 2006). Since the 72-hour drug treatment used in cDNA microarray analysis (at IC_{50} in HCT116 cells) might be too long for the study of G2 checkpoint regulation (50% cell death were observed after *R,R*-5 or oxaliplatin treatments), a modified drug treatment regimen (at 5 μ M for 24 hrs) was adopted for the mechanistic study of G2 checkpoint activation by oxaliplatin. Moreover, experiments were carried out in both HeLa and HCT116 cells to demonstrate the G2 checkpoint activation by oxaliplatin in cell lines with different genotypes.

In Figure 4.6, statistically significant decrease in the mitotic index was observed in HCT116 cells treated with cisplatin or oxaliplatin for 24 hrs (at 5 μ M), compared with no drug treatment respectively, suggesting G2 checkpoint activation. This effect was absent when HCT116 cells were treated with *R,R*-5, suggesting that *R,R*-5 may bypass the G2 checkpoint. Similar results were found in HeLa cells under the same drug treatment. Cisplatin and oxaliplatin could reduce the mitotic

index in HeLa cells after 24 hrs drug treatment (at 5 μ M). However, this effect could be abolished by concomitant treatment with ATM/ATR inhibitor caffeine (Figure 4.7), indicating that the decrease in mitotic cells after 24 hrs drug treatment was caused by the ATM/ATR-mediated G2 checkpoint, but not the antephase checkpoint (because oxaliplatin can bypass the antephase checkpoint, as discussed in Figure 3.8). On the other hand, the novel compound *R,R*-5 was found to bypass the G2 checkpoint because the mitotic index was not significantly changed after *R,R*-5 treatment. Interestingly, PP2A inhibitor DMC could disrupt cisplatin- and oxaliplatin-induced reduction in mitotic index (Figure 4.7), suggesting that DMC can override the G2 DNA damage checkpoint. This finding is consistent with the previous report that okadaic acid abrogates thymidine-induced G2 checkpoint (Ghosh *et al.*, 1996).

Cell cycle analysis was performed in HeLa cells to examine the change in DNA pattern after drug treatment (5 μ M for 24 hrs, Figure 4.8). Compared with the no treatment control, oxaliplatin led to remarkable G2/M cell cycle arrest, possibly due to the activation of G2 checkpoint. Interestingly, *R,R*-5, DMC+oxaliplatin and caffeine+oxaliplatin treatments, which were demonstrated to bypass the G2 checkpoint in Figure 4.7, did not show significant difference from oxaliplatin, suggesting that abrogation of G2 checkpoint does not necessary affect the G2/M population in HeLa cells. In fact, after G2 checkpoint abrogation by these

treatments, cells will undergo a prolonged mitosis possibly due to the activation of mitotic spindle checkpoint. The cells suffered from mitotic catastrophe and failed to exit mitosis (will be discussed later in Figure 4.13, Figure 4.14 and Figure 4.15). Interestingly, cisplatin exhibited less G2/M arrest compared with no drug treatment, possibly due to the activation of S phase DNA damage checkpoint that blocks DNA synthesis and G2/M entry. This is further confirmed using BrdU incorporation assay. Cisplatin and oxaliplatin did lead to a remarkable inhibition in DNA synthesis after 24 hr treatment in HeLa cells, which may consequently attenuate G2/M entry. On the other hand, caffeine+oxaliplatin increased DNA synthesis to 67.15% (mean value), which is not significantly different from oxaliplatin (64.42%), suggesting that ATM-inhibition is not sufficient to restore oxaliplatin-attenuated DNA synthesis. Interestingly, *R,R*-5 or DMC+oxaliplatin did not alter DNA synthesis compared with oxaliplatin, implying that bypassing G2 checkpoint of these treatments does not require increase in DNA synthesis. In fact, okadaic acid has been reported to lead to nuclear envelope break-down in thymidine-arrested G1 cells, suggesting that PP2A inhibitors may induce pre-mature mitosis without requirement of completing DNA synthesis (Ghosh *et al.*, 1996).

Taken together, our results demonstrated that DMC can abrogate oxaliplatin-activated G2 checkpoint and restore mitotic entry after 24 hrs treatment in HeLa cells.

This process does not require the increase in DNA synthesis, and will not decrease oxaliplatin-induced G2/M arrest. *R,R-5* bypassed the G2 checkpoint in a similar manner.

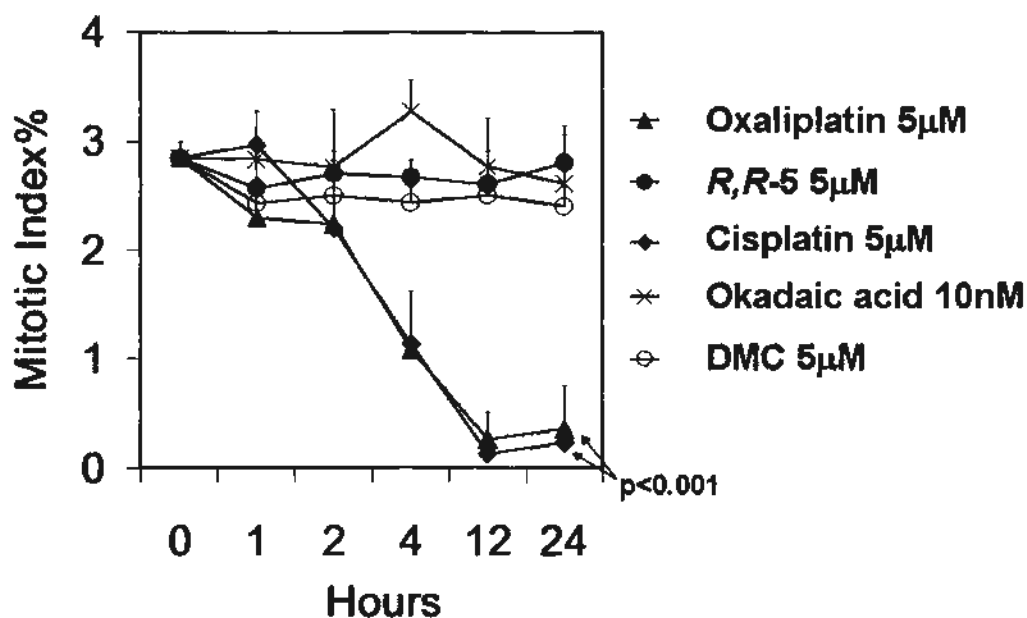


Figure 4.6: Mitotic index assay showing that cisplatin and oxaliplatin, but not *R,R-5*, DMC or okadaic acid, could decrease mitotic index in HCT116 cells. HCT116 cells were treated with various compounds indicated for various time intervals, before fixation and Giemsa-staining for mitotic cell-counting. Cisplatin and oxaliplatin were found to decrease mitotic cells after 24 hrs treatment, possibly due to the activation of the G2 checkpoint. *R,R-5* did not affect the mitotic index and therefore it bypassed the G2 checkpoint. Mean \pm SD of 9 replicates from 3 independent experiments are shown. Student's t test was used to compare the mitotic indices of cisplatin and oxaliplatin, respectively with no treatment control at 0 hr, and p values are shown.

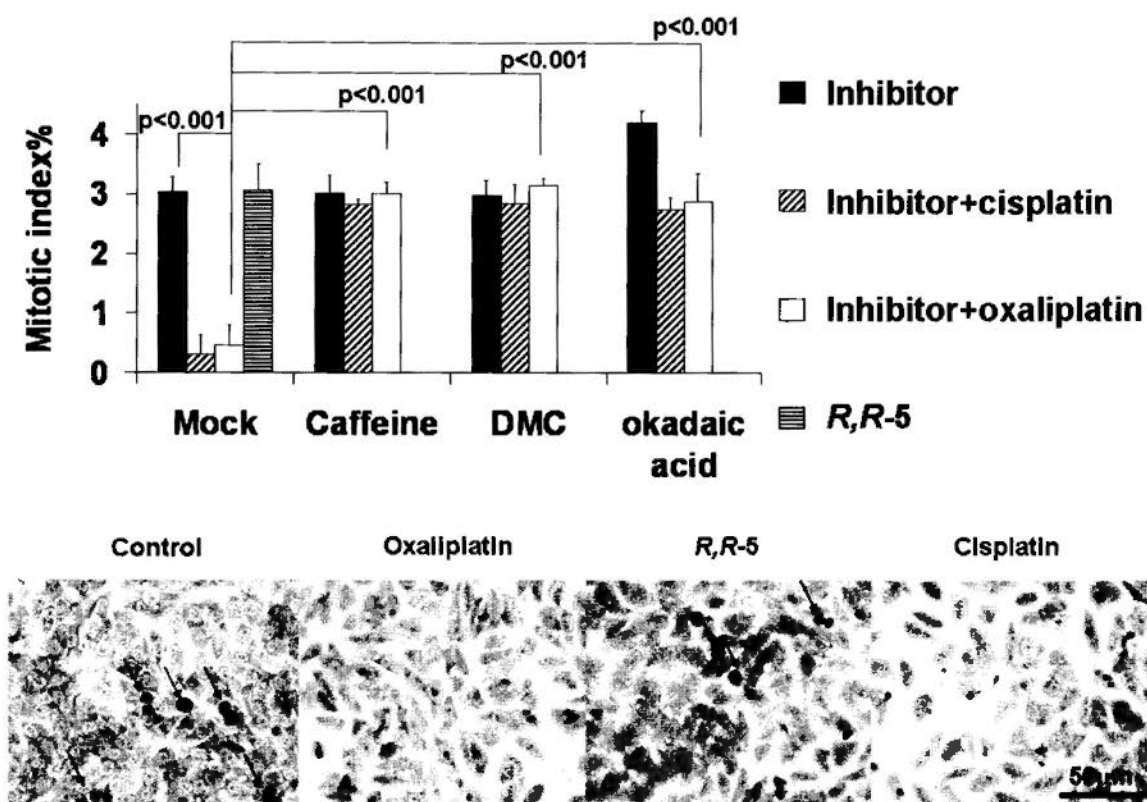


Figure 4.7: Mitotic index assay showing that cisplatin and oxaliplatin, but not *R,R-5* or DMC+oxaliplatin, decreased mitotic index due to G2 checkpoint activation in HeLa cells. HeLa cells were treated with the three platinum compounds at 5 μ M with or without the presence of various inhibitors (or mock treated with water) for 24 hrs, before fixation and Giemsa-staining for mitotic cell-counting. Cisplatin and oxaliplatin were found to decrease mitotic cells after 24 hrs treatment due to the activation of the G2 checkpoint, which could be inhibited by caffeine (an ATM/ATR inhibitor, 5 mM), DMC (5 μ M) or okadaic acid (10 nM) (PP2A inhibitors). *R,R-5* did not affect the mitotic index and therefore it bypassed the G2 checkpoint. Mean \pm SD and representative images of 9 replicates from 3 independent experiments are shown. Student's t test was used for statistical analysis to compare the indicated

treatment groups and p values are shown.

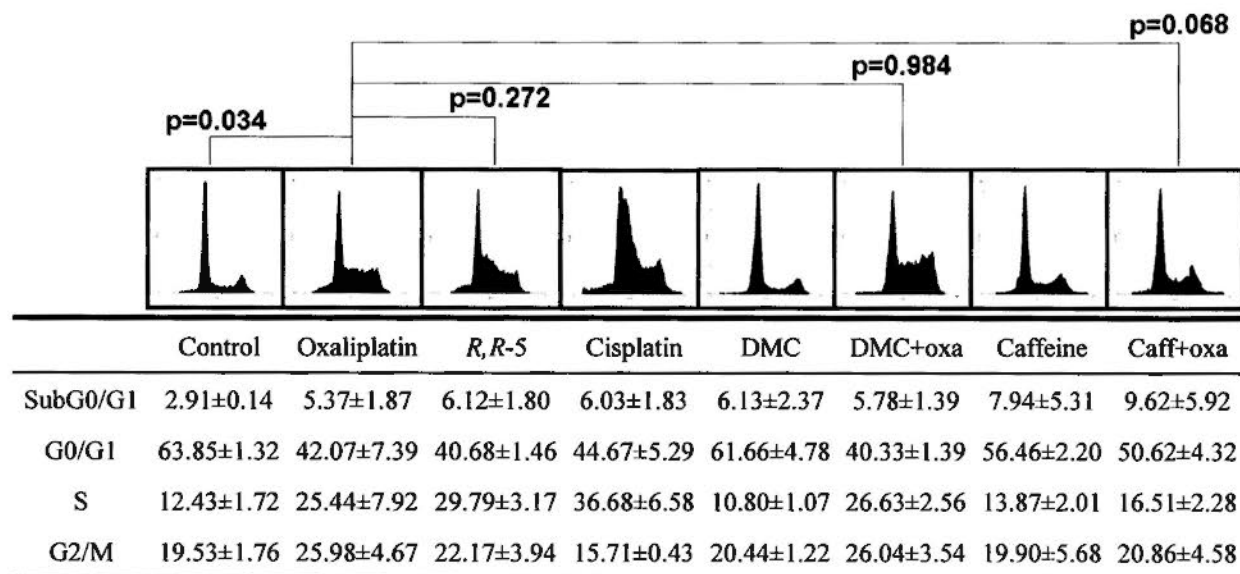


Figure 4.8: Cell cycle analysis showing that DMC did not affect oxaliplatin-induced G2/M arrest in HeLa cells. HeLa cells were treated with cisplatin, oxaliplatin or *R,R*-5 (5 μ M) for 24 hrs before fixation for cell cycle analysis by PI staining. DMC (5 μ M) or caffeine (5 mM) was added 0.5 hr before oxaliplatin treatment. Oxaliplatin resulted in obvious G2/M arrest, whereas *R,R*-5 did not accumulate G2/M arrest as pronounced as oxaliplatin. Cisplatin showed no mitotic arrest (compared with oxaliplatin). Mean \pm SD and a representative set of data from 3 independent experiments are shown. Student's t test was used to compare the G2/M% arrest between the indicated groups and p values are shown.

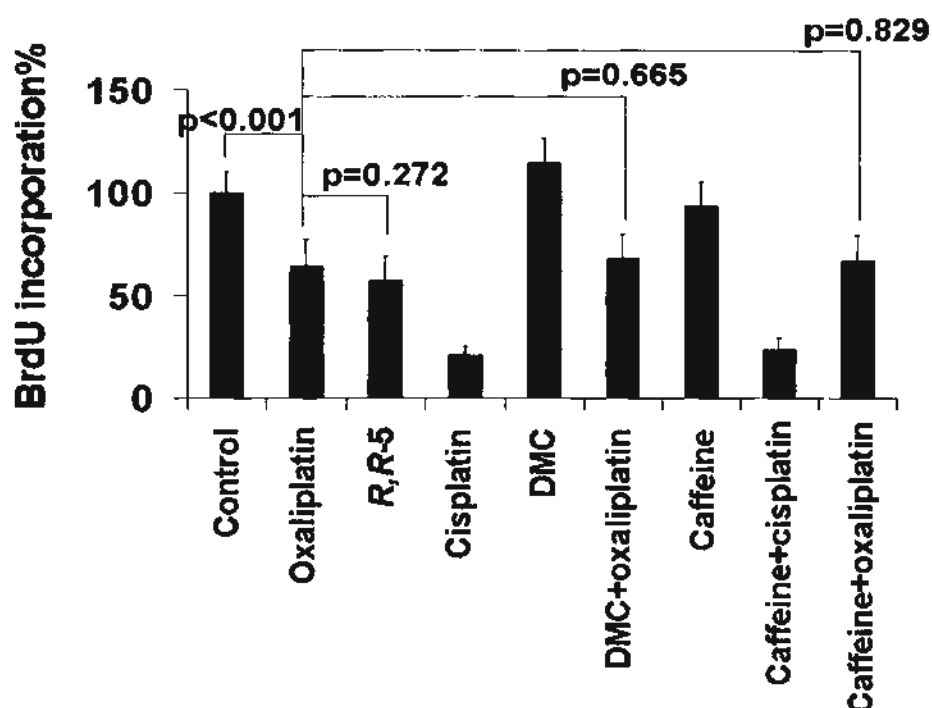


Figure 4.9: BrdU incorporation assay showing that DMC did not restore oxaliplatin-inhibited DNA synthesis. HeLa cells were treated with cisplatin, oxaliplatin or *R,R*-5 (5 μ M) for 24 hrs before BrdU-labeling for another 4 hrs (28 hrs total drug treatment). DMC (5 μ M) or caffeine (5 mM) was added 0.5 hr before cisplatin or oxaliplatin treatment. Oxaliplatin and cisplatin resulted in a remarkable decrease in DNA synthesis after 24 hrs treatment, whereas *R,R*-5, DMC+oxaliplatin and caffeine+oxaliplatin treatments did not show significant difference from oxaliplatin, suggesting that abrogation of oxaliplatin-activated G2 checkpoint by these treatments did not require increase in DNA synthesis. Mean \pm SD of 14 replicates from 3 independent experiments is shown. Student's t test was used to compare the indicated groups and p values are shown.

4.5.3 DMC Restored Oxaliplatin-Crippled CDK1 Activity Independent of

CHK1/CHK2 activation

In order to understand the underlying mechanism(s) for *R,R*-5 and DMC+oxaliplatin to bypass the G2 checkpoint, detection of histone H1 (a known substrate of CDK1/Cyclin B1) phosphorylation by Western blot analysis was employed to measure CDK1/Cyclin B1 (the major mitosis promoting factor) activity in HeLa cells. Oxaliplatin was found to remarkably decrease the phosphorylation of histone H1 after 24 hrs treatment (Figure 4.10), suggesting inhibition of CDK1/Cyclin B1 and activation of G2 checkpoint. However, the phosphorylation of histone H1 was restored by the addition of DMC to oxaliplatin treatment, suggesting that DMC can, at least partially, attenuate G2 checkpoint-mediated inhibition in CDK1/Cyclin B1 kinase activity. Interestingly, unlike oxaliplatin, *R,R*-5 (an analogy to combining oxaliplatin with DMC) did not alter histone H1 phosphorylation compared to no treatment control. The result indicated that DMC+oxaliplatin and *R,R*-5 could restore the CDK1/Cyclin B1 kinase activity and therefore bypassed the G2 checkpoint. It also provides the mechanistic evidence to support the findings that DMC+oxaliplatin and *R,R*-5 maintained the mitotic index at normal level in HeLa cells (Figure 4.7). In contrast, despite cisplatin could severely repress the mitotic index (Figure 4.7) and DNA synthesis (Figure 4.9), it did not decrease histone H1 phosphorylation compared with oxaliplatin in HeLa cells (Figure 4.10). This effect

(appearance of histone H1 phosphorylation after cisplatin treatment) is believed to be caused by the hyper-activation of CDK2, a histone H1 kinase promoting G1→S transition. It has been reported that cisplatin could activate S phase DNA damage checkpoint and strongly stimulate CDK2 activity, which lead to histone H1 hyper-phosphorylation in mouse kidney proximal tubule cells after 24 hrs treatment at 25 μ M (Price *et al.*, 2006; Yu *et al.*, 2007). In fact, according to our results, cisplatin at 5 μ M (24 hrs treatment in HeLa) can induce pronounced S phase arrest (Figure 4.8) and readily decrease DNA synthesis (Figure 4.9) and mitotic entry (Figure 4.7), with partial inhibition in histone H1 phosphorylation (Figure 4.10), compared with no treatment control.

Upon our investigation at the ATM/ATR pathway, oxaliplatin, *R,R*-5, cisplatin, and DMC+oxaliplatin were able to stimulate CHK1 (phosphorylated at Thr387) and CHK2 (phosphorylated at Ser19), suggesting that all of these treatments can lead to DNA damage that can be recognized by the ATR/CHK1 and ATM/CHK2 pathways. In fact, our previous finding has demonstrated that these treatments, including DMC alone, can induce DNA damage in HCT116 cells (Pang *et al.*, 2007). Moreover, oxaliplatin (Rakitina *et al.*, 2007) and cisplatin (Pabla *et al.*, 2008; Colton *et al.*, 2006) have been reported to activate both CHK1 and CHK2. Interestingly, despite the activation of CHK1 and CHK2 by *R,R*-5 and DMC+oxaliplatin, they did not lead to

decrease in mitotic index (Figure 4.7) or phosphorylation of histone H1 (Figure 4.10). Therefore, the abrogation of oxaliplatin-activated G2 checkpoint by DMC and bypass of the G2 checkpoint by *R,R*-5, may be independent of the CHK1/CHK2 activation. Instead, DMC and *R,R*-5 may probably maintain the CDK1 activity through PP2A inhibition, hence restoring oxaliplatin-crippled histone H1 phosphorylation. This suggests that abrogation of oxaliplatin-activated G2 checkpoint by DMC requires CDK1, which was further verified in Figure 4.12 and Figure 4.13 by the use of specific CDK1 inhibitor and siRNA. As a PP2A inhibitor, DMC may also promote mitotic entry through the mechanisms illustrated in Figure 1.11. For example, DMC may inhibit cohesin activation by attenuating Sgo1/PP2A, leading to the dissociation of sister chromatids and mitotic progression. However, since the Sgo1/PP2A/cohesin pathway is activated in metaphase (mitosis) after nuclear envelope break-down, it may not participate in the regulation of G2 checkpoint (preceding nuclear envelope break-down) by DMC; hence it can only be considered as an assisting mechanism to promote mitotic progression, not mitotic entry.

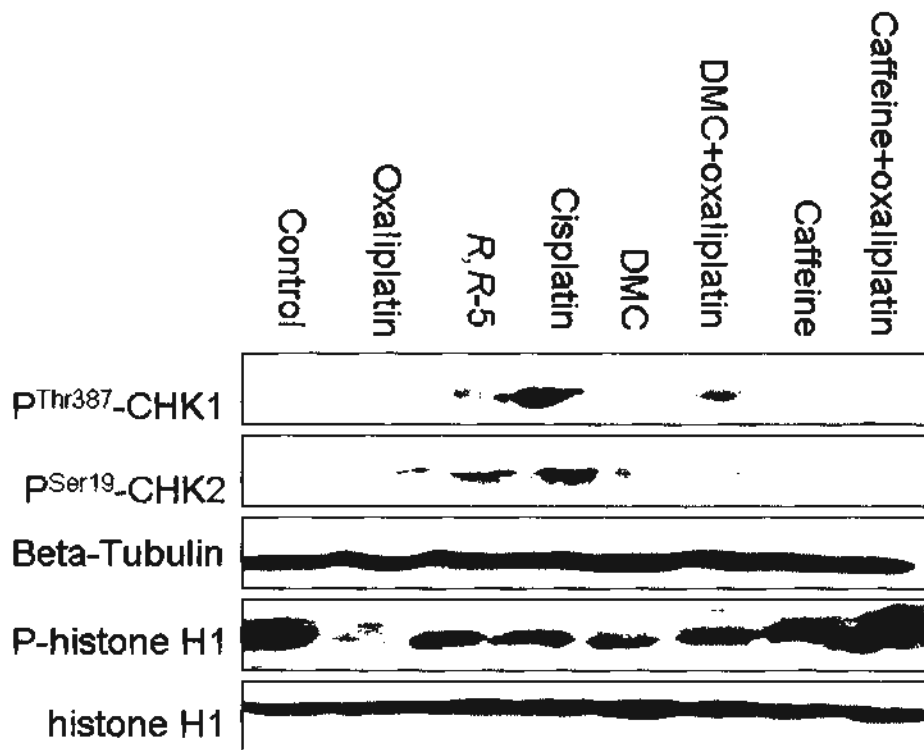


Figure 4.10: Western blot analysis showing that activation of G2 checkpoint by oxaliplatin was accompanied by CHK1 and CHK2 activation, and histone H1 dephosphorylation. HeLa cells were treated with the three platinum compounds indicated at 5 μ M for 24 hrs, with or without the presence of DMC (5 μ M) or caffeine (5 mM). Oxaliplatin was found to decrease phosphorylation of histone H1, which could be restored by DMC. *R,R*-5, cisplatin and DMC alone did not cause dephosphorylation of histone H1 as pronounced as oxaliplatin. All of these three platinum compounds, and also DMC+oxaliplatin, could activate CHK1 and CHK2. A representative set of result from three independent experiments is shown.

4.5.4 DMC Abrogated Oxaliplatin-stimulated G2 Checkpoint without Up-Regulating CDK1

Transcription of CDK1 and Cyclin B1 was also measured by real-time RT-PCR to examine if DMC up-regulates CDK1 or Cyclin B1 to restore oxaliplatin-crippled CDK1 activity. After oxaliplatin treatment, there was a reduction in the mRNA levels of two mitotic genes, Cyclin B1 and CDK1 (also known as CDC2, Figure 4.11), compared with the mRNA levels of the control group, possibly due to the activation of G2 checkpoint in HeLa cells. This finding is consistent with previously finding that oxaliplatin could decrease mitotic gene expression in HCT116 cells (5 μ M for 24 hrs; Volland *et al.*, 2006). Interestingly, the decrease in mitotic gene transcription was not observed in *R,R*-5 and DMC+oxaliplatin treated HeLa cells, which agrees well with our earlier observations that *R,R*-5 and DMC+oxaliplatin did not alter the mitotic index (Figure 4.7) and phosphorylation of histone H1 (Figure 4.10), and bypassed the G2 DNA damage checkpoint. However, there is no statistically significant difference at CDK1 and Cyclin B1 mRNA levels after *R,R*-5 or DMC+oxaliplatin treatments compared with oxaliplatin. This indicates that abrogation of G2 checkpoint by DMC does not require CDK1 transcription, but instead, DMC may maintain the phosphorylation/activation status of the available CDK1 protein and promote mitotic transition upon oxaliplatin treatment. In contrast,

cisplatin did not seem to affect the mRNA levels of CDK1 and Cyclin B1 (at 5 μ M for 24 hrs in HeLa), even when the mitotic index is significantly reduced (Figure 4.7). These findings are consistent with a previous report that cisplatin (at 5 μ M for 24 hrs) does not affect mitotic gene expressions when mitotic index is decreased in HCT116 cells (Volland *et al.*, 2006).

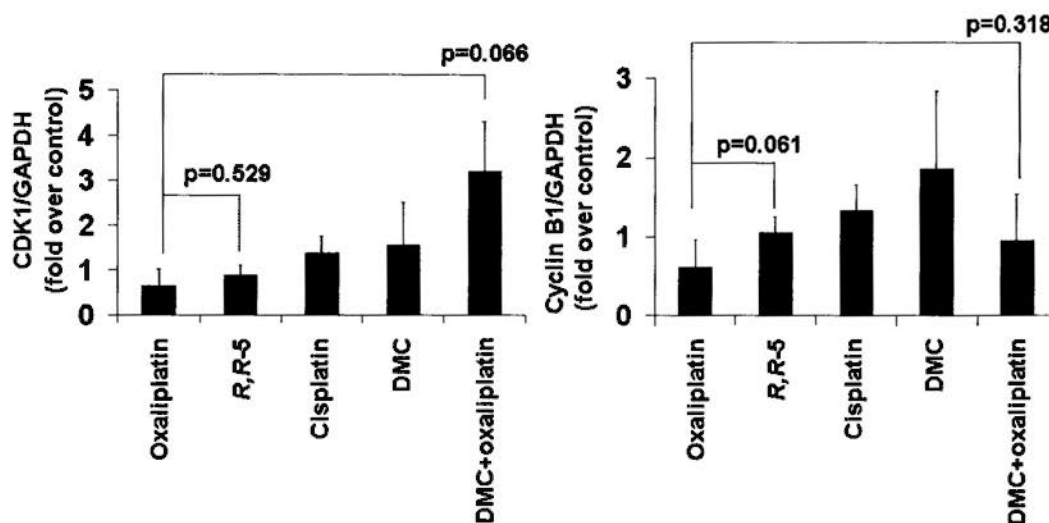


Figure 4.11: Real-time RT-PCR analysis showing that DMC abrogated oxaliplatin-stimulated G2 checkpoint without requirement of CDK1 transcription. HeLa cells were treated with cisplatin, oxaliplatin or *R,R*-5 at 5 μ M for 24 hrs, with or without the presence of DMC (5 μ M) before harvested for real-time RT-PCR analysis. Oxaliplatin treatment resulted in a decrease in CDK1 and Cyclin B1 transcriptions, whereas *R,R*-5 and DMC+oxaliplatin did not significantly increase CDK1 or Cyclin B1 transcriptions compared with oxaliplatin, respectively. Results represent the mean (\pm SD) of 9 replicates from 3 independent experiments. Student's t test was used for statistical analysis to compare oxaliplatin respectively with *R,R*-5 and DMC+oxaliplatin and p values are shown.

4.5.5 DMC Abrogated Oxaliplatin-Stimulated G2 Checkpoint by Restoring CDK1 Activity

It has been shown that the specific PP2A inhibitor, okadaic acid, could abrogate thymidine-activated G2 checkpoint (Ghosh *et al.*, 1996), though the underlying mechanism is still not well-understood. In our study, DMC, as a PP2A inhibitor, seemed to abrogate oxaliplatin-activated G2 DNA damage checkpoint, by increasing CDK1 activity (Figure 4.10) but not by up-regulating CDK1 gene level (Figure 4.11). *R,R-5* bypassed G2 checkpoint in a similar manner. These findings may suggest that DMC abrogates oxaliplatin-activated G2 checkpoint by restoring CDK1 activity. In fact, another PP2A inhibitor, fostriecin, has been reported to promote mitotic entry by enhancing CDK1 and histone H1 association (Roberge *et al.*, 1994). However, okadaic acid (a PP2A inhibitor) was reported to trigger DNA condensation through Aurora B in a cell-free system, without the requirement of Aurora A or CDK1 (Takemoto *et al.*, 2007). This may not be true in living cells because specific inhibition of Aurora B by small compound hesperidin in human epithelial ARPE-19 cells does not stop mitotic entry or the DNA condensation process, but instead, leads to mitotic catastrophe (Wang *et al.*, 2008). In contrast and importantly, CDK1 inhibition by the specific inhibitor purvalanol attenuates mitotic progression (Goga *et al.*; 2007), suggesting that CDK1 plays a more important role during G2→M

transition than Aurora B. Putting all the thoughts together, it is clear that DMC and *R,R*-5 do not inhibit the ATR/CHK1 and ATM/CHK2 pathways like caffeine does (Figure 4.10), as both CHK1/CHK2 activation are observed after DMC+oxaliplatin and *R,R*-5 treatments in Figure 4.10; and DMC is unlikely to abrogate G2 checkpoint through activation of Aurora B and Aurora A (Figure 4.2), as both of them are not gate keepers for mitotic entry, but seemingly for mitotic exit. As a result, in order to search for the target that DMC regulates for G2 checkpoint abrogation, CDK1 is finally chosen to be further studied. We believe that DMC and *R,R*-5 may counteract the CDK1-inhibiting CHK1/CHK2 pathways (Figure 4.1), and restore CDK1 activity by inhibiting PP2A. Since DMC may also inhibit other protein phosphatase isoforms besides PP1/2A, this G2 checkpoint abrogation effect of DMC may also be generated from the inhibition of other protein phosphatases.

To examine if DMC abrogates oxaliplatin-induced G2 checkpoint by restoring CDK1 activity, CDK1 was specifically inhibited by using roscovitine or siRNA. DMC, *R,R*-5 and DMC+oxaliplatin could not restore histone H1 phosphorylation when CDK1 was inhibited by roscovitine (Figure 4.12A), suggesting that DMC and *R,R*-5 could not abrogate G2 checkpoint or promote mitotic entry when CDK1 was compromised. Similar result was obtained when knocking-down CDK1 using specific siRNA. As illustrated in Figure 4.12B, CDK1 siRNA specifically down-

regulated CDK1 level at 24 hr after transfection, and this effect persisted for at least another 24 hrs (at 48 hr post-transfection). Therefore, cells at 24 hr after transfection were treated with DMC and *R,R*-5 for another 24 hrs and the drug effect was evaluated at 48 hr post-transfection. In Figure 4.12C, phosphorylation of histone H1 was reduced to about 50% after CDK1 was knocked-down by siRNA, whereas *R,R*-5 and DMC could not restore histone H1 phosphorylation when CDK1 was absent. The results indicated that restoration of histone H1 phosphorylation by DMC and *R,R*-5 requires CDK1, and that the abrogation of G2 checkpoint by DMC depends on CDK1.

Mitotic index assay using CDK1 inhibitor was also performed in synchronized HeLa cells (Figure 4.13A). *R,R*-5, DMC or DMC+oxaliplatin did not inhibit the mitotic transition when HeLa cells were released from thymidine (compared with no treatment control); instead and interestingly, they promoted mitotic entry (immature mitosis) at 6 hr (after released from thymidine), which was not observed in no treatment group. Moreover, after *R,R*-5 and DMC+oxaliplatin treatments, HeLa cells failed to exit mitosis at 14 hr (after released from thymidine), possibly due to the activation of mitotic spindle checkpoint after bypassing the G2 checkpoint. In fact, this effect was further demonstrated using cell cycle analysis in Figure 4.14A, which will consequently result in mitotic catastrophe and will be discussed in more

detail in Figure 4.15. Importantly, *R,R*-5, DMC and DMC+oxaliplatin failed to maintain mitotic entry when cells were concomitantly treated with roscovitine, suggesting that DMC could not promote mitosis or abrogate G2 checkpoint when CDK1 was compromised by roscovitine. This argument is further confirmed using cell cycle analysis in Figure 4.14A. Roscovitine could inhibit DMC+oxaliplatin-treated cells from returning to G0 phase (at 14 hr after the synchronized mitosis), suggesting that mitotic transition of DMC+oxaliplatin-treated cells requires CDK1 activity. In contrast, cisplatin and oxaliplatin inhibited mitotic transition in synchronized HeLa cells (Figure 4.13B), even when the drug exposure was less than 24 hrs. Caffeine could restore this oxaliplatin-inhibited mitotic entry, suggesting this oxaliplatin-activated mitotic checkpoint is G2 checkpoint (Figure 4.13B).

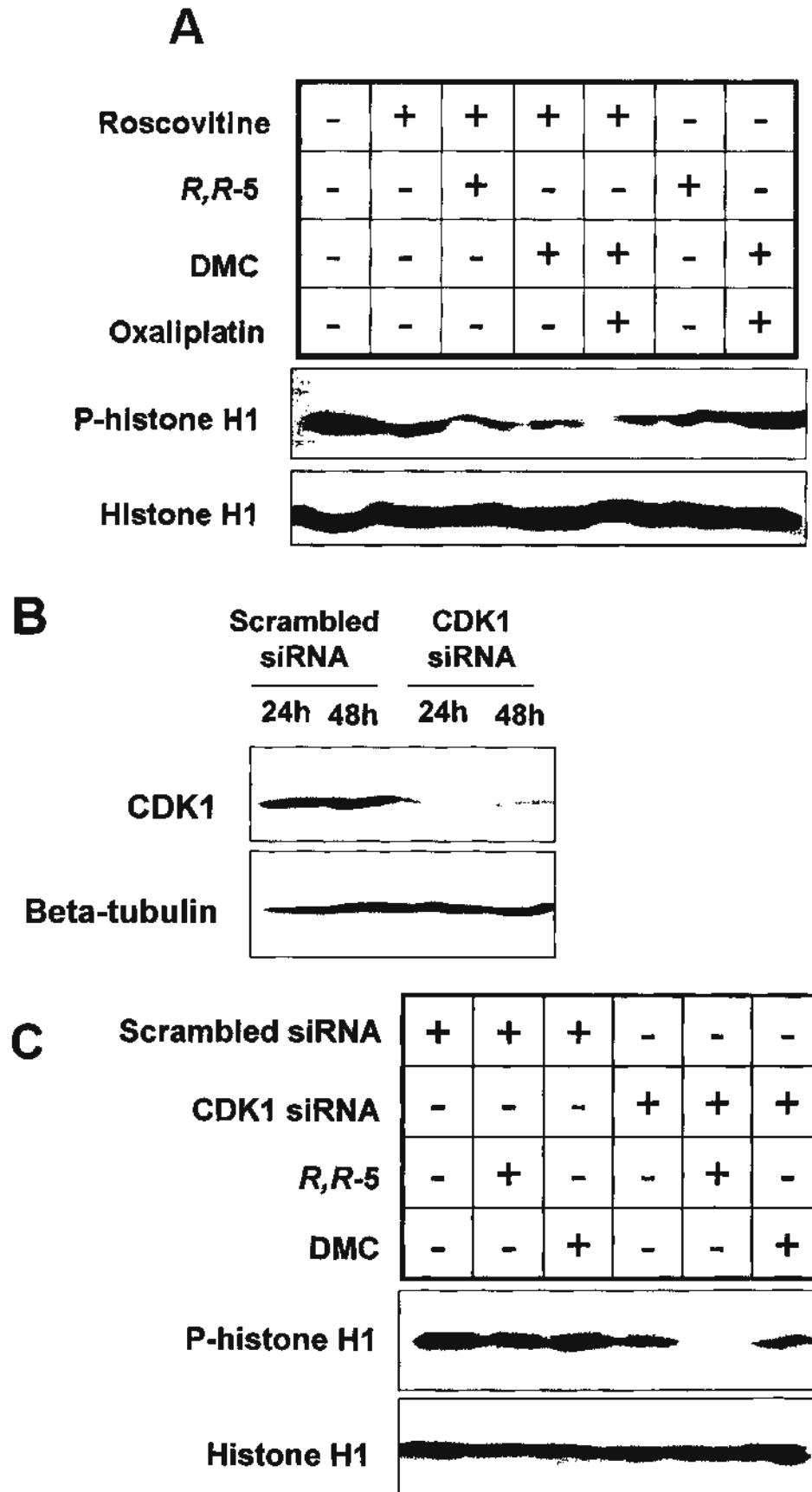
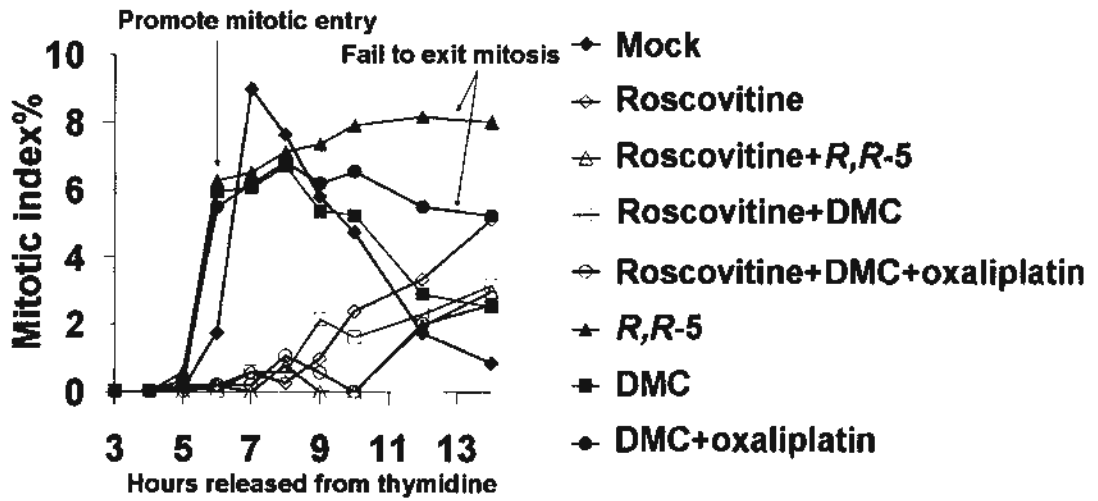


Figure 4.12: Western blot analysis showing that DMC and *R,R*-5 maintained histone

H1 phosphorylation by restoring CDK1 activity. A) HeLa cells were treated with *R,R*-5 or oxaliplatin (5 μ M) in the presence or absence of DMC (5 μ M) and/or CDK1 inhibitor roscovitine (20 μ M) for 24 hrs. Roscovitine were treated 0.5 hr before other drugs treatments. Roscovitine could reduce histone H1 phosphorylation levels of *R,R*-5, DMC and DMC+oxaliplatin by inhibiting CDK1. B) CDK1 was specifically down-regulated by siRNA at 24 hr post-transfection, and the knock-down effect persisted until at 48 hr post-transfection. C) DMC and *R,R*-5 were added at 24 hr post-transfection and another 24 hrs later (at 48 hr post-transfection) cells were harvested for Western blot analysis. DMC and *R,R*-5 could not restore histone H1 phosphorylation when CDK1 was compromised by roscovitine or siRNA. A representative set of result from three independent experiments is shown.

A



B

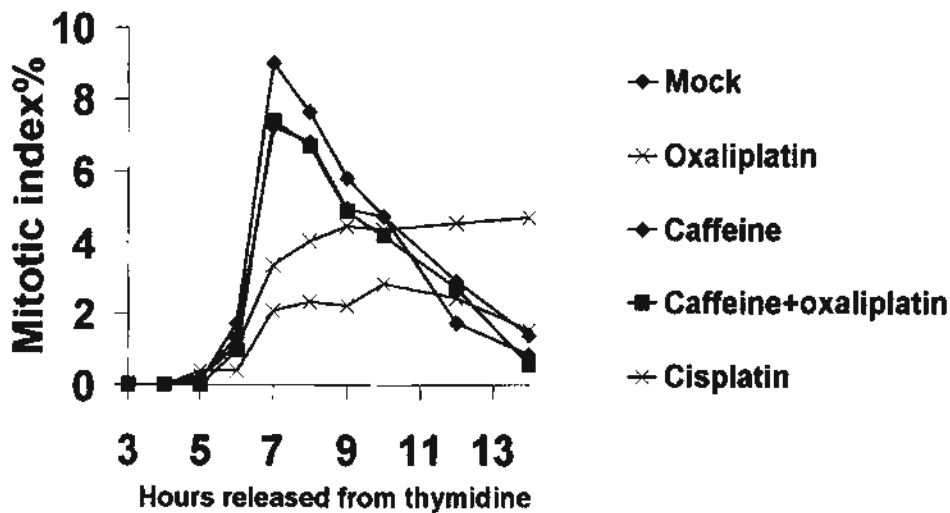


Figure 4.13: Mitotic index assay showing that DMC and *R,R*-5 promoted mitotic entry by restoring CDK1 activity. HeLa cells were synchronized using double-thymidine block. At 3.5 hr after released from thymidine, HeLa cells were treated with cisplatin, oxaliplatin or *R,R*-5 at 5 μ M, with or without the presence of DMC (5 μ M), caffeine (5 mM) or roscovitine (CDK1 inhibitor, 20 μ M). Roscovitine were

treated 0.5 hr before other drug treatments (at 3 hr after released from thymidine). A) *R,R*-5, DMC and DMC+oxaliplatin did not inhibit mitotic entry in HeLa cells, but instead, promoted mitotic entry at 6 hr (released from thymidine) compared with no treatment control (mock treated with water). However, concomitant treatment with roscovitine could abrogate this effect. Also, *R,R*-5 and DMC+oxaliplatin failed to exit mitosis at 14 hr (released from thymidine). B) Oxaliplatin could modestly inhibit mitotic entry in HeLa cells, and concomitant treatment with caffeine could abolish this effect. In contrast, cisplatin could remarkably inhibit mitotic entry. Mean of 3 replicates from 3 independent experiments is shown.

4.5.6 DMC Abrogated Oxaliplatin-Stimulated G2 Checkpoint, Leading to Aberrant Mitosis and Failure at Mitotic Exit, and Consequently Inhibition of Cell Survival

We have demonstrated that *R,R*-5 and DMC+oxaliplatin could not promote mitosis when CDK1 was compromised by roscovitine in Figure 4.13A, suggesting that *R,R*-5 and DMC+oxaliplatin bypass G2 checkpoint through restoring CDK1 activity. Interestingly, cells treated with *R,R*-5 and DMC+oxaliplatin were found to fail at mitotic exit (Figure 4.13A), which will be further confirmed using cell cycle analysis by flow cytometry. At 14 hr after released from thymidine in HeLa cells, 66.31% cells (mean value) exited mitosis and returned to G0 phase (mitotic exit, reflected by G0/G1%) in negative control group (Figure 4.14A). This process was inhibited after *R,R*-5 or DMC+oxaliplatin treatments, leaving 55.06% and 55.27% mitotic exit (mean value), respectively, which explains the failure at mitotic exit after these treatments in Figure 4.13A. In contrast, DMC did not seem to affect this process. However and importantly, despite that *R,R*-5 and DMC+oxaliplatin themselves could attenuate mitotic exit, the G0/G1% population after *R,R*-5, DMC or DMC+oxaliplatin treatments could be further and significantly inhibited by concomitant treatment with CDK1 inhibitor roscovitine (Figure 4.14A), suggesting that the mitosis-promoting effect (and mitosis transition) of these treatments required

CDK1 activity. This result confirms our argument and DMC abrogate oxaliplatin-activated G2 checkpoint by restoring CDK1 activity.

Interestingly, oxaliplatin could inhibit mitotic exit in HeLa cells, seemingly due to the activation of G2 checkpoint because concomitant treatment with caffeine could modestly abolish this effect (Figure 4.14B). In contrast, cisplatin could remarkably inhibit mitotic exit (Figure 4.14B).

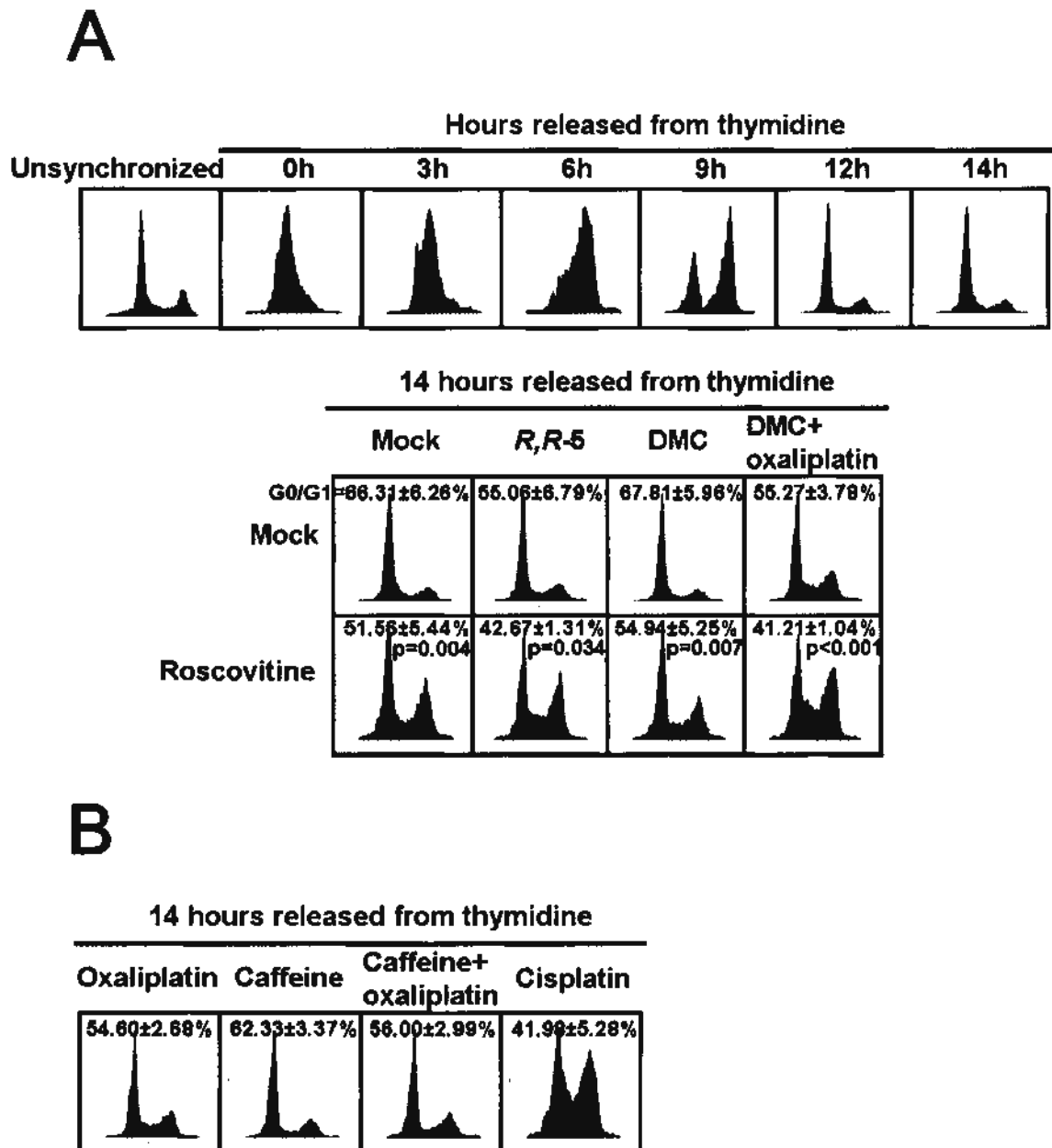


Figure 4.14: Cell cycle analysis showing that CDK1 activity was required in DMC- and *R,R*-5-induced mitosis. HeLa cells were synchronized using double-thymidine block. Drug treatment was as described in Figure 4.13. At 14 hr after released from thymidine, cells were harvested and fixed for cell cycle analysis. A) In negative control group (mock treated with water), 66.31±6.26% cells exited mitosis and returned to G0 phase (mitotic exit, reflected by G0/G1%). *R,R*-5 and

DMC+oxaliplatin could modestly inhibit this process; however, concomitant treatment with roscovitine could further and significantly decrease mitotic exit. The G0/G1 population after DMC treatment was also inhibited by roscovitine, where DMC alone did not affect the mitotic exit. B) Oxaliplatin could inhibit mitotic entry and consequently mitotic exit due to the activation of G2 checkpoint; concomitant treatment with caffeine could modestly abolish this effect. In contrast, cisplatin could remarkably inhibit mitotic exit. Mean \pm SD of mitotic exit (G0/G1%) from 3 independent experiments is shown. Mock treatment (water), *R,R*-5, DMC and DMC+oxaliplatin were compared to the respective concomitant treatment groups with roscovitine using Student's t test and p values are shown.

Abrogation of mitotic DNA damage checkpoints is expected to induce a characteristic morphology associated with mitotic catastrophe (mitosis with irregularly arrayed and/or unequally distributed chromosomes). In fact, the attenuation of 5-fluorouracil (5-FU)-activated G2 checkpoint by caffeine (Del Campo *et al.*, 2005), and the inhibition of ionizing radiation (IR)-stimulated G2 checkpoint by geldanamycin (Moran *et al.*, 2008), have been reported to induce mitotic catastrophe. In our experiments, the cells bearing mitotic catastrophe after drug treatments were quantified and the results are shown in Figure 4.15. With the activation of G2 checkpoint, oxaliplatin and cisplatin only induced 0.68% and 0.58% (mean value) aberrant mitosis, respectively; however, *R,R*-5, DMC+oxaliplatin and caffeine+oxaliplatin, the treatments that were observed to bypass G2 checkpoint in Figure 4.7 (reflected by the presence of mitotic cells), showed significant increase in mitotic catastrophe at 2.60%, 2.87% and 2.54% (mean value) (compared with oxaliplatin), respectively. DMC and caffeine alone did not seem to significantly affect the basal (no treatment) abnormal mitosis level. This result indicates that G2 checkpoint bypass of *R,R*-5 (also, DMC+oxaliplatin and caffeine+oxaliplatin) could lead to mitotic catastrophe, when G2 cells bearing unrepaired DNA damage are forced to progress into mitosis.

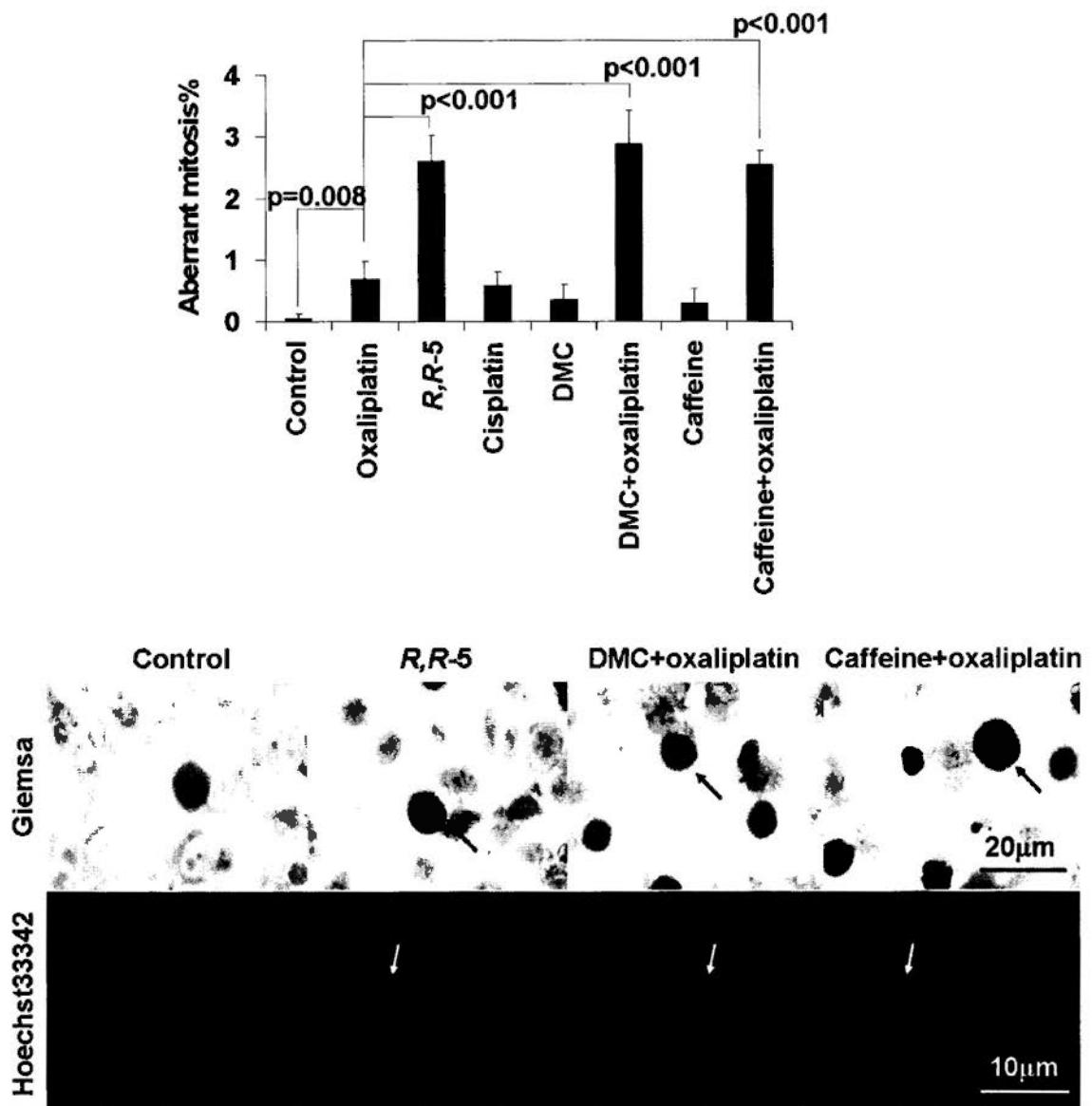


Figure 4.15: Aberrant mitosis cell-counting demonstrating that DMC abrogated oxaliplatin-stimulated G2 checkpoint and led to mitotic catastrophe. HeLa cells were treated with cisplatin, oxaliplatin or *R,R*-5 at 5 μM, with or without DMC (5 μM) or caffeine (5 mM) (added 0.5 hr before oxaliplatin treatment) for 24 hrs before fixation and Giemsa-staining for quantification of aberrant mitosis. Representative images of mitotic catastrophe using Giemsa- and Hoechst33342-staining are shown. Cisplatin

and oxaliplatin did not induce remarkable aberrant mitosis due to the activation of G2 checkpoint, whereas *R,R*-5, DMC+oxaliplatin and caffeine+oxaliplatin treatments could remarkably increase catastrophic mitosis. Mean \pm SD of 6 replicates from 3 independent experiments is shown. Student's t test was used for statistical analysis to compare the indicated groups and p values are shown.

We hypothesized that abrogation of mitotic DNA damage checkpoints can lead to mitotic catastrophe and attenuate cancer cell survival after chemotherapy. Similar to the inhibition of cell survival after the abrogation of cisplatin-stimulated anaphase checkpoint (by c-Abl and p38MAPK inhibitors, Figure 3.18), *R,R*-5, DMC+oxaliplatin and caffeine+oxaliplatin treatments were found to attenuate cancer cell survival compared with oxaliplatin after an 8-day recovery (in both HeLa and HCT116 cells, Figure 4.16), whereas oxaliplatin alone could significantly inhibit cell viability but not DMC or caffeine. This observation demonstrates that bypass of G2 checkpoint after *R,R*-5 and DMC+oxaliplatin treatments could inhibit cancer cell survival and stop cells from re-entering cell cycle after DNA damage repair, which may therefore prevent the emergence of drug resistance. This result also explains the failure at mitotic exit (Figure 4.13A and Figure 4.14A) and appearance of mitotic catastrophe (Figure 4.15) after *R,R*-5 and DMC+oxaliplatin treatments, suggesting that abrogation of oxaliplatin-activated G2 checkpoint by DMC could inhibit cancer cell survival after oxaliplatin exposure.

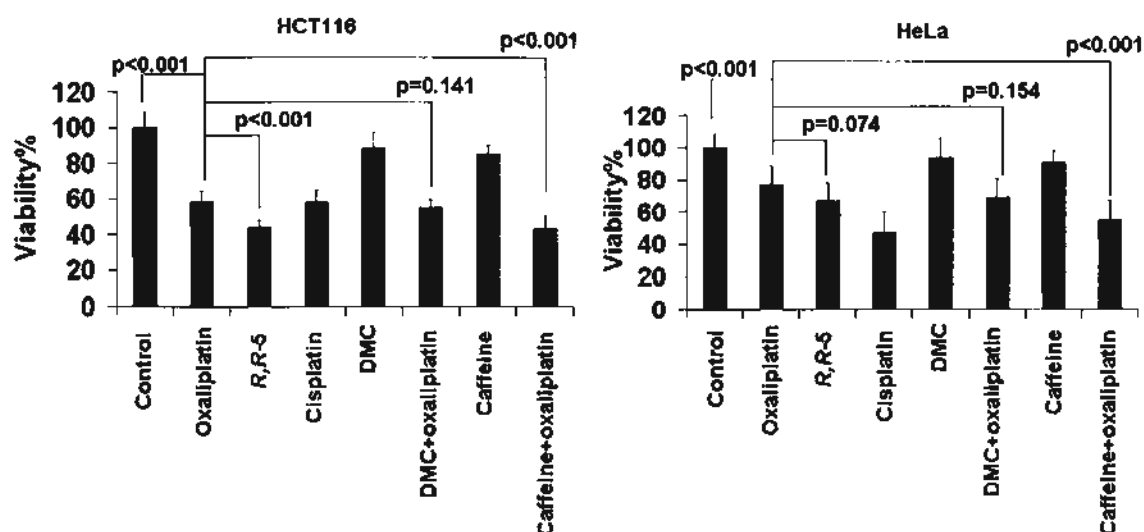


Figure 4.16: MTT assay showing that DMC abrogated oxaliplatin-stimulated G2 checkpoint and led to inhibition of cell survival. HCT116 and HeLa cells were treated with cisplatin, oxaliplatin or *R,R*-5 at 5 μ M for 24 hrs, with or without the presence of DMC (5 μ M) or caffeine (5 mM). After drug treatment, cells were washed with PBS once and then allowed for an 8-day recovery in drug-free medium before MTT assay. Medium was changed on the fourth day after drug treatment. *R,R*-5, DMC+oxaliplatin and caffeine+oxaliplatin treatments was found to reduce cell survival than oxaliplatin in both cell lines. Mean \pm SD of 24 replicates from 3 independent experiments is shown. Student's t test was used for statistical analysis to compare the indicated groups and p values are shown.

4.6 Conclusions

In this chapter, the differential effects of cisplatin, oxaliplatin and *R,R*-5 at the G2 DNA damage checkpoint are demonstrated. Collectively, the findings are summarized as follows:

- a) Oxaliplatin was found to activate the G2 DNA damage checkpoint in HeLa cells, as evidenced by the decrease in mitotic index, dephosphorylation of histone H1, appearance of G2/M cell cycle arrest and activation of CHK1 and CHK2. This avoided mitotic catastrophe and promoted cancer cell survival after oxaliplatin treatment.
- b) Cisplatin activated G2 checkpoint through CHK1 and CHK2 activation, leading to a decrease in the mitotic index in HeLa cells. This was accompanied by the activation of an S phase DNA damage checkpoint, which stopped mitotic entry.
- c) *R,R*-5 and DMC+oxaliplatin maintained the mitotic index and phosphorylation of histone H1 at normal level, even when CHK1 and CHK2 were pronouncedly stimulated. This effect did not require increase in DNA synthesis or CDK1 transcription, but instead, DMC+oxaliplatin and *R,R*-5 restored the kinase activity of the available CDK1 to promote mitotic entry, and consequently led to mitotic catastrophe, failure at mitotic exit, and inhibition of cancer cell survival compared

with oxaliplatin. Incorporation of DMC into *R,R*-5 is believed to contribute to this bypass effect at the G2 checkpoint.

A working model is shown in Figure 4.17 to illustrate the differential effects of cisplatin, oxaliplatin and *R,R*-5 at the G2 DNA damage checkpoint. Cisplatin and oxaliplatin activate CHK1 and CHK2, to inhibit CDK1/Cyclin B1, decrease histone H1 phosphorylation (not so pronounced after cisplatin treatment in Figure 4.10) and consequently stop mitotic entry. *R,R*-5 and DMC+oxaliplatin can also stimulate CHK1 and CHK2, due to the DACH moiety; however, the presence of DMC restore the activity of CDK1 that is compromised by CHK1 and CHK2 activation, probably by PP2A/PP1 inhibition, leading to the recovery in histone H1 phosphorylation and mitotic progression, hence the bypass of G2 checkpoint.

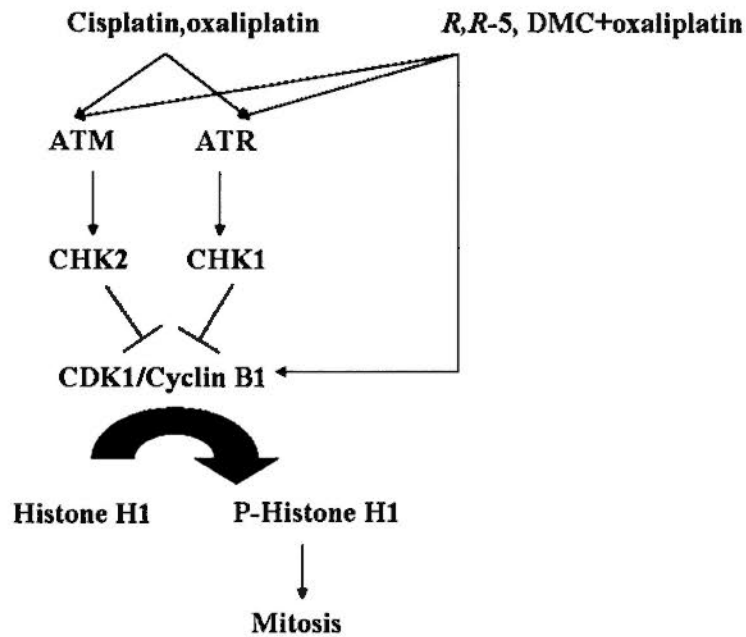


Figure 4.17: DMC abrogates oxaliplatin-activated G2 checkpoint by restoring CDK1 activity, independent of CHK1/CHK2 activation. Cisplatin and oxaliplatin can activate CHK1 and CHK2, which inhibits CDK1 and activates G2 DNA damage checkpoint. DMC+oxaliplatin and *R,R*-5 can also activate CHK1 and CHK2; however, they can restore CDK1 activity, maintain histone H1 phosphorylation and facilitate mitotic entry, hence bypassing the G2 checkpoint.

Chapter Five

Conclusions

The clinical use of the platinum anticancer agents, cisplatin and carboplatin, has been well established. However, more widespread use of these agents is limited by emergence of drug resistance. Moreover, a variety of adverse effects, such as nephrotoxicity, myelosuppression, neurotoxicity, and severe emesis, are observed in patients receiving cisplatin chemotherapy (Krakoff, 1979). These limitations reduce the efficacy of the drug and have inspired efforts to develop new agents that display improved therapeutic properties.

Oxaliplatin is a third-generation diaminocyclohexane (DACH)-containing platinum-based anti-tumor drug that is clinically used for the treatment of advanced colorectal cancer, and is able to circumvent cisplatin resistance. It is widely believed that the recognition of cisplatin-DNA adducts by the MMR system contributes to the cytotoxicity of cisplatin in tumor cells. In contrast to cisplatin-DNA adducts, the MMR protein hMutS α has a low affinity for oxaliplatin-DNA adducts, due to the integration of a novel DACH moiety into oxaliplatin's structure (Zdraves *et al.*, 2002). Therefore, an unique mechanism of drug action originating from the Pt(*R,R*-

DACH) moiety has been postulated that is different from cisplatin.

A novel series of TCM-Pt compounds has been synthesized by the School of Pharmacy and Department of Chemistry at the Chinese University of Hong Kong. The novel design involved the integration of demethylcantharidin (DMC), a modified TCM component, with a Pt moiety. To make use of the advantages brought by the DACH moiety in oxaliplatin, one of our novel Pt compounds (abbreviated as *R,R*-5) was synthesized by integrating the DMC ligand with *trans-R,R*-diaminocyclohexane (DACH). We propose that its mechanism of anti-cancer action is two-fold: (a) the *R,R*-DACH-Pt moiety alkylates DNA, and (b) the DMC ligand induces an additional cytotoxic effect in cancer cells.

This thesis focuses on the pharmacological behaviour of the novel compound *R,R*-5, and its comparison with oxaliplatin and cisplatin. *R,R*-5 can be slowly hydrolyzed into DMC that inhibits protein phosphatase 1 and 2A, and a DACH-Pt moiety that binds to DNA and results in DNA damage. Since the structural difference between *R,R*-5 and oxaliplatin is the incorporation of DMC in the former Pt compound, a cDNA microarray analysis was performed with an aim to discover the molecular targets that can differentiate between *R,R*-5 and oxaliplatin, which may be contributed by DMC (Chapter Two). Compared with oxaliplatin, *R,R*-5 resulted in up-regulation of 35 genes that can promote G2 to M cell cycle progression in

HCT116 cells. Since there are DNA damage checkpoints controlling the G2 to M transition, results from the cDNA microarray analysis therefore led us to hypothesize that *R,R*-5 may bypass these DNA damage checkpoints, subsequently resulting in mitotic catastrophe and inhibition of cell survival after drug exposure. Detailed investigation into the effects of *R,R*-5 at the antepause and G2 checkpoints were carried out. The results are discussed in Chapter Three and Four, respectively. Based on our findings, the superior anti-tumor activity of *R,R*-5, compared with oxaliplatin, could be due to the bypassing of antepause and G2 checkpoints.

5.1 Effect of *R,R*-5 at the Antephase Checkpoint (Chapter Three)

Among all cell cycle checkpoints, the antephase checkpoint is the closest to mitotic entry. Cells typically spend approximately 15 minutes to 1 hr in the antephase before entering mitosis (nuclear envelope break-down). As a result, activation of the antephase checkpoint can lead to rapid decrease in the proportion of mitotic cells within 1 hr (Figure 3.8). Antephase checkpoint can be triggered by various kinds of stresses, such as osmotic shock (Dmitrieva *et al.*, 2002), cold shock (Rieder, 1981), UV or ionizing radiation (Rieder and Cole, 1998), and microtubule disassembly (Rieder and Cole, 2000). To date, activation of the antephase checkpoint by DNA damaging agents has not been reported.

In our findings, cisplatin was observed to activate the antephase checkpoint and decrease mitotic entry in an hour in HeLa cells (Figure 3.8). And the mechanism by which cisplatin activated this antephase checkpoint was studied in detail. Interestingly, chemical inhibitor and siRNA against c-Abl (Figure 3.12 and Figure 3.13), p38MAPK inhibitor (Figure 3.12), and MEKK1 siRNA (Figure 3.13), but not ATM/ATR or protein phosphatase 2A inhibitors (Figure 3.11), were found to abrogate the activation of antephase checkpoint by cisplatin. Moreover, cisplatin was found to activate the antephase checkpoint only in MMR-proficient HCT116+ch3 cells but not MMR-deficient HCT116+ch2 cells (Figure 3.15 and

Figure 3.16), reinforcing the involvement of the MMR system in the antephasis checkpoint regulation. An MMR/c-Abl/MEKK1/p38MAPK pathway is therefore demonstrated to be involved in this checkpoint regulation. In contrast, DACH-containing Pt drugs, oxaliplatin and *R,R*-5, bypassed the antephasis checkpoint as evidenced by their negligible effect on the mitotic index (Figure 3.8). They also did not have significant effect on c-Abl or p38MAPK activation (Figure 3.10).

An increase in cancer cell survival was observed in HCT116+ch3 cells after acute cisplatin treatment (Figure 3.19A), compared with HCT116+ch2 cells, which could be inhibited by c-Abl, p38MAPK and JNK inhibitors (Figure 3.18). On the other hand, acute treatments of oxaliplatin and *R,R*-5 did not have significant difference in the survival profiles of HCT116+ch3 and HCT116+ch2 cells (Figure 3.19B and C). Taken together, acute stress to cisplatin can activate the MMR/c-Abl/MEKK1/p38MAPK pathway, leading to inhibition of the CDK1/Cyclin B1 activity, and stopping cells from entering mitosis rapidly, thereby avoiding mitotic catastrophe and promoting cancer cell survival. In contrast, *R,R*-5 and oxaliplatin bypass the antephasis checkpoint, deprive cancer cells of the time for DNA damage repair, result in mitotic catastrophe and consequently inhibit cancer cell survival after acute drug treatment. Since the differential activation of the antephasis checkpoint by cisplatin was found to endow the cells with survival benefit, this observation could

explain the superior anti-tumor activity of oxaliplatin and *R,R*-5 over cisplatin.

In this study, the mechanisms for the activation of antephasis checkpoint in response to DNA damage is elucidated. For the first time, DNA damaging agent cisplatin is observed to activate the antephasis checkpoint and oxaliplatin and *R,R*-5 are demonstrated to bypass it. According to our findings, addition of c-Abl or p38MAPK inhibitors to the cisplatin regimen could allow the cells to abrogate the antephasis checkpoint and cells are thus more sensitive to cisplatin treatment, thereby representing a new means of circumventing cisplatin resistance. Our theory also explains the mechanisms for the synergistic effect that was found between cisplatin and c-Abl inhibitor (Zhang *et al.*, 2003; Yerushalmi *et al.*, 2007). Applying these findings to the clinic, the use of oxaliplatin or *R,R*-5 can bypass the antephasis checkpoint and may inhibit cancer cell survival after chemotherapy, therefore may have a less re-occurrence rate than cisplatin.

5.2 Effect of *R,R*-5 at the G2 checkpoint (Chapter Four)

The differential regulation of the antephasis checkpoint by cisplatin, oxaliplatin and *R,R*-5 has already been discussed in Chapter Three. However, the G2→M-promoting effect of *R,R*-5 in the cDNA microarray analysis (Chapter Two) can not be due to the bypass of antephasis checkpoint, because HCT116 cells do not have a functional antephasis checkpoint (Figure 3.9). As a result, the effect of *R,R*-5 at the G2 checkpoint, another mitotic DNA damage checkpoint, was explored in Chapter Four. It is noted that a longer duration of drug treatment (24 hrs) was used in our experiments to wait for a vivid activation of G2 checkpoint by oxaliplatin (than the rapid detection of antephasis checkpoint activation in Figure 3.8). Also, the G2 phase cells require more time for progression into mitosis than antephasis (late G2 phase) cells; hence G2 checkpoint activation takes more time to show reduction in mitotic index, which is in contrast to the quick response at the antephasis checkpoint (within an hour).

In Chapter Four, oxaliplatin were found to activate CHK1 and CHK2 in HeLa cells after 24 hrs drug treatment, leading to the inhibition of CDK1/Cyclin B1 activity and phosphorylation of histone H1 (Figure 4.10), which consequently attenuated mitotic entry (Figure 4.7) and cells were arrested at the G2/M phase (Figure 4.8). These observations suggested the activation of G2 checkpoint by

oxaliplatin, which could be inhibited by concomitant treatment with ATM/ATR inhibitor caffeine (Figure 4.7, Figure 4.10). On the other hand, *R,R*-5 and DMC+oxaliplatin treatments were found to maintain phosphorylation of histone H1 and the mitotic index at normal level (Figure 4.7, Figure 4.10), implying that these treatments could bypass the G2 checkpoint, supposedly due to the presence of DMC. This G2 checkpoint-bypass effect of *R,R*-5 and DMC+oxaliplatin did not require increase in S phase entry (Figure 4.9), CDK1 and Cyclin B1 transcriptions (Figure 4.11), and would not decrease the G2/M population (Figure 4.8). On the other hand, surprisingly, CHK1 and CHK2 activation was observed in *R,R*-5 and DMC+oxaliplatin treated cells (Figure 4.10), indicating the DNA damage induced by these treatments could be recognized by the ATM/CHK2 and ATR/CHK1 pathways. Therefore, the abrogation of oxaliplatin-induced G2 checkpoint by DMC and bypass of the G2 checkpoint by *R,R*-5, do not require the inhibition of CHK1/CHK2 activation. Since the phosphorylation status of histone H1 was unchanged after *R,R*-5 and DMC+oxaliplatin treatments (Figure 4.10), we therefore hypothesized the G2 checkpoint-bypass effect of these treatments requires CDK1. In fact, *R,R*-5 and DMC+oxaliplatin failed to promote mitotic entry (Figure 4.13A) or maintain the phosphorylation of histone H1 (Figure 4.12A) when CDK1 was compromised by roscovitine (a specific CDK1 inhibitor). These observations demonstrate that DMC

counteracts the CDK1-inhibiting CHK1/CHK2 pathways and abrogates oxaliplatin-activated G2 checkpoint by restoring CDK1 activity. Interestingly, after bypassing the G2 checkpoint, *R,R*-5 and DMC+oxaliplatin treatments led to a prolonged mitosis (Figure 4.13A) and mitotic catastrophe (Figure 4.15), which was not observed in oxaliplatin treatment. And after an 8-day recovery, *R,R*-5 and DMC+oxaliplatin (less promising than *R,R*-5) could inhibit cell survival in both HCT116 and HeLa cells, suggesting that bypass of G2 checkpoint contributes to the cytotoxicity of DNA damaging agents.

Collectively, activation of G2 checkpoint by cisplatin and oxaliplatin stops cells from entering mitosis; cells can then repair DNA damage before re-entering cell cycle, thereby avoiding mitotic catastrophe and promoting cancer cell survival. In contrast, *R,R*-5 and DMC+oxaliplatin can bypass this G2 checkpoint by restoring CDK1 activity, independent of CHK1/CHK2 activation. According to these findings, DMC can be clinically used as a novel G2 checkpoint abrogator in combination treatment with oxaliplatin, which may help circumventing the emerging of drug resistance. Also, the mechanism for DMC to abrogate oxaliplatin-activated G2 checkpoint, and for *R,R*-5 to bypass the G2 checkpoint, was demonstrated to be unique from all the discovered G2 checkpoint activators. DMC+oxaliplatin and *R,R*-5 do not inhibit the recognition of DNA damage by ATM/CHK2 and

ATR/CHK1 pathways like other G2 checkpoint abrogators do. Instead, they stop the inhibition of CDK1 by CHK1/CHK2 and maintain the kinase activity of CDK1, possibly by inhibiting PP1/2A, and restore mitotic entry. It seems that DMC and *R,R*-5 interfere many cellular signalling pathways and stop many inhibition processes that involve protein dephosphorylation, including CDK1 inhibition during G2 checkpoint activation. Since this mechanism of action is demonstrated for the first time and is different from the biological behaviour of other G2 checkpoint abrogators, it would be interesting to look at the effect of DMC in combination with other DNA damaging agents in clinical trials, compared with typical G2 checkpoint abrogators.

5.3 Summary of the Thesis

Summarizing the findings in this thesis, we have proven that cisplatin activates both the antephasis and G2 checkpoints (Figure 5.1); oxaliplatin has no effect at the antephasis checkpoint because of the DACH-Pt moiety, but activates the G2 checkpoint; *R,R*-5 leads to the bypass of both antephasis (due to the DACH-Pt moiety) and G2 checkpoint (due to the incorporation of DMC). The experimental data support our hypothesis emphatically, for using DMC and DACH moieties in the design of the new Pt compound, *R,R*-5, in attaining a dual mechanism of anti-tumor action, higher potency, and lack of cross-resistance.

From a drug design point of view, it appears that *R,R*-5 is the optimum structure that demonstrates the highest potency among the novel TCM-Pt compounds and has even greater cytotoxic effect than oxaliplatin. Since the activation of cell cycle checkpoints may be involved in the induction of drug resistance, cancer cells could be the least likely to acquire drug resistance from *R,R*-5 because of its ability to bypass the mitotic DNA damage checkpoints. It will be interesting to find out if *R,R*-5 could maintain its anti-tumor activity in oxaliplatin-resistant cancer cell lines.

Our study also bring forth with a very important concept: to inhibit cancer cell survival after radiation or chemotherapy, which is completely neglected in current cancer treatment. The ability to induce cell death can vary from different cancer

treatments. For example, cisplatin was shown to have strong anti-tumor activity in clinical use at the very beginning. However, despite the fact that cisplatin and other cancer chemotherapeutic drugs are highly potent in inducing cell death during initial treatment, recurrence does occur. Cancer cells are usually equipped with DNA repair and survival mechanisms, eventually exhibiting resistance to various anti-tumor drugs. As a result, cancer cells can repair DNA damage and survive after cisplatin treatment and lead to drug resistance. Therefore, clinical use of cisplatin should be concomitantly treated with antephasis and G2 checkpoint abrogators to inhibit cancer cell survival and the generation of drug resistance. This was neglected in cisplatin treatment for a long time. In contrast, *R,R-5* can bypass both the antephasis and G2 checkpoint and deprive cancer cells of the time for DNA damage repair, resulting in the inhibition of cancer cell survival after chemotherapy. Therefore we would expect a better therapeutic effect of *R,R-5* than cisplatin.

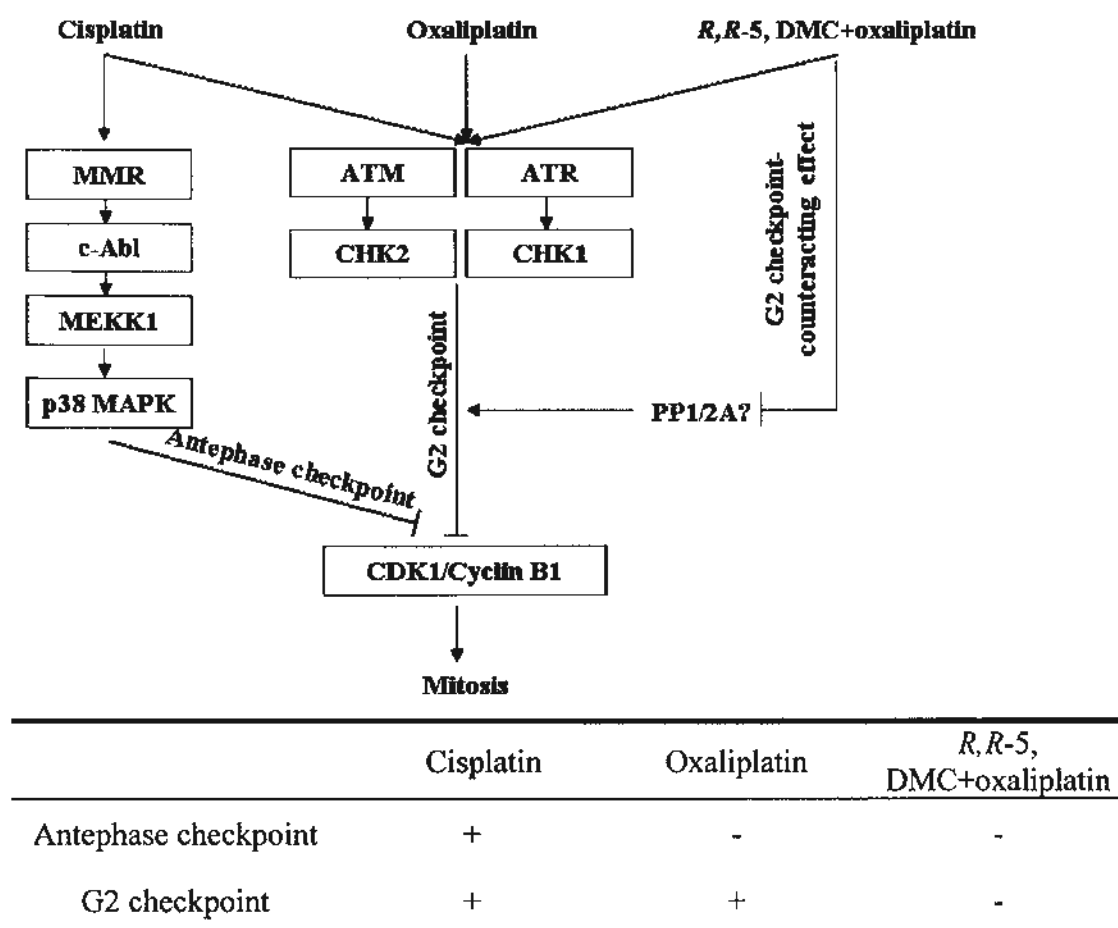


Figure 5.1: Effect of platinum compounds at mitotic DNA damage checkpoints.

Cisplatin can activate the MMR/c-Abl/MEKK1/p38MAPK pathway and consequently the antephase checkpoint. Also, cisplatin can activate the G2 checkpoint by stimulating CHK1 and CHK2 pathways. In contrast, oxaliplatin does not affect the antephase checkpoint because of the DACH-Pt moiety, but activates the G2 checkpoint. Cancer cells treated with *R,R-5* or DMC+oxaliplatin can bypass not only the antephase checkpoint (due to the DACH-Pt moiety), but also the G2 checkpoint (DMC can counteract G2 checkpoint and restoring CDK1 activity, possibly by inhibiting PP1/2A).

5.4 Future Work

This thesis has provided the molecular evidence for the differential effects of cisplatin, oxaliplatin and *R,R*-5 at the two mitotic DNA cell cycle checkpoints. In the cDNA microarray analysis, besides the mitotic genes that we have discussed earlier in the thesis, another 25 genes related to DNA replication were also found to be up-regulated by *R,R*-5 (Table 2.1). This observation suggests that cancer cells treated with *R,R*-5 may activate the S phase checkpoint and arrest cells at the S phase (or onset of S phase), possibly because the incorporation of DMC in *R,R*-5 induces severe DNA damage that hinders S phase progression. It will be interesting to explore this effect in the therapeutic response to *R,R*-5.

We have also found that inhibitors against c-Abl or p38MAPK could be used to sensitize cancer cells to cisplatin (or other DNA damaging agents) because of abrogation of the antephase checkpoint. However, according to the difference in cell death between HCT116+ch3 and HCT116+ch2 cells after cisplatin treatment, the percentage of cells at the antephase is estimated to be less than 10% (Figure 3.19A). It follows that abrogation of the antephase checkpoint could only lead to a maximum of 10% enhancement of cytotoxicity. Likewise, cells in each of the S and G2 phase contributed to about 15% of the total cell population. Theoretically, when one of these checkpoints is abrogated, the drug sensitization effect will only be about 15%.

Therefore, to achieve the maximal therapeutic benefit from this approach of abrogating DNA damage checkpoints in cancer chemotherapy, it may be necessary to disrupt all the undesired cell cycle checkpoints. To sensitize cancer cells to cisplatin treatment, for example, a potential combination with UCN-01 (ATM/ATR or CHK1/CHK2 inhibitors that inhibit the S and G2 checkpoints) and STI571 (c-Abl inhibitor that abolishes the antephasis checkpoint) may be useful. And these novel combinations of drug use in chemotherapy deserve to be confirmed in future studies. To bring it closer to clinical trials, animal studies could also be launched based on our findings, to evaluate the combination effects of DNA damaging agents and cell cycle checkpoint abrogators, under the examination of a live entity.

Bibliography

Abbott, D. W.; Thompson, M. E.; Robinson-Benion, C.; Tomlinson, G.; Jensen, R. A.;

Holt, J. T. BRCA1 expression restores radiation resistance in BRCA1-defective cancer cells through enhancement of transcription-coupled DNA repair. *The Journal of Biological Chemistry*, **1999**; *274*, 18808–12.

Abraham, D.; Podar, K.; Pacher, M.; Kubicek, M.; Welzel, N.; Hemmings, B.A.;

Dilworth, S.M.; Mischak, H.; Kolch, W.; Baccharini, M. Raf-1-associated protein phosphatase 2A as a positive regulator of kinase activation. *The Journal of Biological Chemistry*, **2000**; *275*, 22300-04.

American Cancer Society, Inc. 2009. Webpage:

(<http://www.cancer.org/downloads/STT/500809web.pdf>)

Ariza, R.R.; Keyse, S.M.; Moggs, J.G.; Wood, R.D. Reversible protein

phosphorylation modulates nucleotide excision repair of damaged DNA by human cell extracts. *Nucleic Acids Res.*, **1996**, *24*, 433-40.

Ayad, N.G. CDKs give CDC6 a license to drive into S phase. *Cell*, **2005**, 825-7.

Bai, F.; Pei, X.H.; Pandolfi, P.P.; Xiong, Y. p18^{Ink4c} and PTEN constrain a positive

regulatory loop between cell growth and cell cycle control. *Molecular And Cellular Biology*, **2006**; *26*, 4564–76.

Bannon, J.H.; Fichtner, I.; O'Neill, A.; Pampillo'n, C.; Sweeney, N.J.; Strohfeltdt, K.;

- Watson, R.W.; Tacke, M.; McGee, M.M. Substituted titanocenes induce caspase-dependent apoptosis in human epidermoid carcinoma cells in vitro and exhibit antitumour activity in vivo. *British Journal of Cancer*, **2007**; *97*, 1234–41.
- Bennin, D.A.; Don, A.S.A.; Brake, T.; McKenzie, J.L.; Rosenbaum, H.; Ortiz, L.; DePaoli-Roach, A.A.; Horne, M.C. Cyclin G2 associates with protein phosphatase 2A catalytic and regulatory β subunits in active complexes and induces nuclear aberrations and a G1/S phase cell cycle arrest. *The Journal of Biological Chemistry*, **2002**; *277*, 27449-67.
- Bialojan, C.; Takai, A. Inhibitory effect of a marine-sponge toxin, okadaic acid, on protein phosphatases. *The Journal of Biological Chemistry*, **1988**; *256*, 283-90.
- Boeckman, H. J.; Trego, K. S.; Turchi, J. J. Cisplatin sensitizes cancer cells to ionizing via inhibition of nonhomologous end joining. *Mol. Cancer Res.*, **2005**; *3*, 277-85.
- Boudreau, R.T.M.; Conrad, D.M.; Hoskin, D.W. Apoptosis induced by protein phosphatase 2A (PP2A) inhibition in T leukemia cells is negatively regulated by PP2A-associated p38 mitogen-activated protein kinase. *Cellular Signalling*, **2007**; *19*, 139-51.

Bradshaw, R.; Dennis, E. Handbook of Cell Signaling. Elsevier science USA.

2003, 3, 230-1.

Brimfield, A.A. Possible protein phosphatase inhibition by bis(hydroxyethyl)sulfide,

a hydrolysis product of mustard gas. *Toxicology Letters*, 1995; 78, 43-8.

Brown, K. D.; Rathi, A.; Kamath, R.; Beardsley, D.; Zhan, Q.; Mannino, J. L.;

Baskaran R. The mismatch repair system is required for s-phase checkpoint activation. *Nature Genetics*, 2003; 33, 80-4.

Bulavin, D.V.; Higashimoto, Y.; Popoff, I.J.; Gaarde, W.A.; Basrur, V.B.; Potapova,

O.; Appella, E.; Fornace Jr, A.J. Initiation of a G2/M checkpoint after ultraviolet radiation requires p38 kinase. *Nature*, 2001, 411, 102-7.

Bunch, R.T.; Eastman, A. Enhancement of cisplatin induced cytotoxicity by

7-hydroxystaurosporine (UCN-01), a new G2-checkpoint inhibitor. *Clin. Cancer Res.*, 1996; 2, 791-7.

Cabello, O.A.; Eliseeva, E.; He, W.G.; Youssoufian, H.; Plon, S.E.; Brinkley, B. R.;

Belmont, J.W. Cell cycle-dependent expression and nucleolar localization of hCAP-H. *Molecular Biology of the Cell*, 2001; 12, 3527-37.

Calvert, A.H.; Harland, S.J.; Newell, D.R.; Siddik, Z.H.; Jones, A.C.; Mcelwain, T.J.;

Raju, S.; Wiltshaw, E.; Smith, I.E.; Baker, J.M.; Peckham, M.J.; Harrap, K.R. Early clinical studies with cis-diammine-1,1-cyclobutane dicarboxylate

Platinum II. *Cancer Chemoth. Pharm.*, **1982**, *9*, 140-7.

Chabner, B.A.; Roberts Jr, T.G. Chemotherapy and the war on cancer. *Nature Rev. Cancer*, **2005**, *5*, 65-72.

Chinami, M.; Yano, Y.; Yang, X.; Salahuddin, S.; Moriyama, K.; Shiroishi, M.; Turner, H.; Shirakawa, T.; Adra, C.N. Binding of HTm4 to cyclin-dependent kinase (CDK)-associated phosphatase (KAP).CDK2.Cyclin A complex enhances the phosphatase activity of KAP, dissociates Cyclin A, and facilitates KAP dephosphorylation of CDK2. *The Journal Of Biological Chemistry*, **2005**; *280*, 17235–42.

Choi, S. Y.; Kim, M. J.; Kang, C. M.; Bae, S.; Cho, C. H.; Soh, J. W.; Kim, J. H.; Kang S., Chung H. Y., Lee, Y. S.; Lee, S. J. Activation of Bak and Bax through c-Abl-protein Kinase C-p38 MAPK signaling in response to ionizing radiation in human non-small cell lung cancer cells. *The Journal of Biological Chemistry*, **2006**; *281*, 7049–59.

Chou, D.M.; Petersen, P.; Walter, J.C.; Walter, G. Protein phosphatase 2A regulates binding of cdc45 to the prereplication complex. *The Journal of Biological Chemistry*, **2002**; *277*, 40520–7.

Chowdhury, D.; Keogh, M.C.; Ishii, H.; Peterson, C.L.; Buratowski, S.; Lieberman, J. Gamma-H2AX dephosphorylation by protein phosphatase 2A facilitates DNA

- double-strand break repair. *Molecular Cell*, **2005**; *20*, 801–9.
- Cicchillitti, L.; Fasanaro, P.; Biglioli, P.; Capogrossi, M.C.; Martelli, F. Oxidative stress induces protein phosphatase 2A-dependent dephosphorylation of the pocket proteins pRb, p107, and p130. *The Journal of Biological Chemistry*, **2003**; *278*, 19509–17.
- Cohen, P.; Holmes, C.F.; Tsukitani, Y. Okadaic acid: a new probe for the study of cellular regulation. *Trends Biochem Sci.*, **1990**; *15*, 98-102.
- Colton, S.L.; Xu, X.S.; Wang, Y.A.; Wang, G. The involvement of ataxia-telangiectasia mutated protein activation in nucleotide excision repair-facilitated cell survival with cisplatin treatment. *The Journal of Biological Chemistry*, **2006**; *281*, 27117–25.
- Cong, F. and Goff, S.P. c-Abl-induced apoptosis, but not cell cycle arrest, requires mitogen-activated protein kinase kinase 6 activation. *Proc. Natl. Acad. Sci. U.S.A.*, **1999**; *96*, 13819-24.
- Corcoran, M.M.; Hammarsund, M.; Zhu, C.; Lerner, M.; Kapanadze, B.; Wilson, B.; Larsson, C.; Forsberg, L.; Ibbotson, R.E.; Einhorn, S.; Oscier, D.G.; Grande'r, D.; Sangfelt, O. DLEU2 encodes an antisense RNA for the putative bicistronic RFP2/LEU5 gene in humans and mouse. *Genes, Chromosomes & Cancer*, **2004**; *40*, 285–97.

- Cortez, D. Caffeine inhibits checkpoint responses without inhibiting the ataxia-telangiectasia-mutated (ATM) and ATM- and Rad3-related (ATR) protein kinases. *The Journal of Biological Chemistry*, **2003**; *39*, 37139–45.
- Cude, K.; Wang, Y.; Choi, H.J.; Hsuan, S.L.; Zhang, H.; Wang, C.Y.; Xia, Z. Regulation of the G2-M cell cycle progression by the ERK5-NF{ κ }B signaling pathway. *Journal of Cell Biology*, **2007**; *177*, 253-64.
- Dasika, G.K.; Lin, S.C.J.; Zhao, S.; Sung, P.; Tomkinson, A.; Lee, E.Y.H.P. DNA damage-induced cell cycle checkpoints and DNA strand break repair in development and tumorigenesis. *Oncogene*, **1999**; *18*, 7883-99.
- Davenport, J.W.; Fernandes, E.R.; Harris, L.D.; Neale, G.A.M.; Goorha, R. The mouse mitotic checkpoint gene bub1b, a novel bub1 family member, is expressed in a cell cycle-dependent manner. *Genomics*, **1999**; *55*, 113–7.
- Del Campo, A.; Bracho, M.; Marcano, L.; Guñiez, J.; De la Torre, C. DNA injury induced by 5-aminouracil and caffeine in G2 checkpoints path of higher plant cells. *Biocell*, **2005**; *29*, 169-76.
- DelloRusso, C.; Welch, P. L.; Wang, W.; Garcia, R. L.; King, M. C.; Swisher, E. M. Functional characterization of a novel BRCA1-null ovarian cancer cell line in response to ionizing radiation. *Mol. Cancer Res.*, **2007**; *5*, 35-45.

- Desbiens, K.M.; Deschesnes, R.G.; Labrie, M.M.; Desfoss'Es, Y.; Lambert, H.; Landry J.; Bellmann, J. c-Myc Potentiates The mitochondrial pathway of apoptosis by acting upstream of apoptosis signal-regulating kinase 1 (ASK1) in the p38 signalling cascade. *Biochem. J.*, **2003**, *372*, 631–41.
- Di Francesco, A.M.; Ruggiero, A.; Riccardi, R. Cellular and molecular aspects of drugs of the future: oxaliplatin. *Cell. Mol. Life Sci.*, **2002**, *59*, 1914-27.
- Dubrana, K.; Van Attikum, H.; Hediger, F.; Gasser, S.M. The processing of double-strand breaks and binding of single-strand-binding proteins RPA and Rad51 modulate the formation of ATR-kinase foci in yeast. *Journal of Cell Science*, **2007**, *120*, 4209-20.
- Eastman, A.; Kohn, E. A.; Brown, M.K.; Rathman, J.; Livingstone, M.; Blank, D.H.; Gribble, G.W. A novel indolocarbazole, ICP-1, abrogates dna damage induced cell cycle arrest and enhances cytotoxicity: similarities and differences to the cell cycle checkpoint abrogator UCN-01. *Molecular Cancer Therapeutics*, **2002**, *1*, 1067–78.
- Eckerdt, F.; Strebhardt, K. Polo-like kinase 1: target and regulator of anaphase-promoting complex/cyclosome-dependent pro-teolysis. *Cancer Res.*, **2006**; *66*, 6895-8.
- Eichhorst, S. T.; Mu"ller, M.; Li-Weber, Min; Schulze-Bergkamen, H.; Angel, P.;

- Krammer, P. H. A novel AP-1 element in the CD95 ligand promoter is required for induction of apoptosis in hepatocellular carcinoma cells upon treatment with anticancer drugs. *Molecular And Cellular Biology*, **2000**; *20*, 7826–37.
- Espinosa, M.; Martinez, M.; Aguilar, J.L.; Mota, A.; Garza, J.G.; Maldonado, V. Melendez, Z.J. Oxaliplatin activity in head and neck cancer cell lines. *Cancer Chemother. Pharm.*, **2005**, *55*, 301-5.
- Extra, J. M.; Espie, M.; Calvo, F.; Ferme, C.; Mignot, L.; Marty, M. Phase I study of oxaliplatin in patients with advanced cancer. *Cancer Chemother. Pharmacol.*, **1990**, *25*, 299-303.
- Eyers, P.; Erikson, E.; Chen, L.; Maller, J. A novel mechanism for activation of the protein kinase aurora A. *Current Biology*, **2003**; *13*, 691–7.
- Fang, G.; Yu, H.; Kirschner, M.W. Direct binding of CDC20 protein family members activates the anaphase-promoting complex in mitosis and G1. *Mol. Cell*, **1998**; *2*,163-71.
- Fink, D.; Zheng, H.; Nebel, S.; Norris, P.S.; Aebi, S.; Lin, T.P.; Nehme, A.; Christen, R.D.; Haas, M.; Macleod, C.L.; Howell, S.B. *In vitro* and *in vivo* resistance to cisplatin in cells that have lost dna mismatch repair. *Cancer Research*, **1997**, *57*, 1841-5.

Fisk, H.A.; Mattison, C.P.; Winey, M. A field guide to the Mps1 family of protein kinases. *Cell Cycle*, **2004**; *3*, 439-42.

Foray, N.; Marot, D.; Randrianarison, V.; Venezia, N.D.; Picard, D.; Perricaudet, M.; Favaudon, V.; Jeggo, P. Constitutive Association of BRCA1 and c-Abl and Its ATM-Dependent Disruption after Irradiation. *Molecular and Cellular Biology*, **2002**; *22*, 4020-32.

Foulkes, W. D. BRCA1 and BRCA2: chemosensitivity, treatment outcomes and prognosis. *Familial Cancer*, **2006**; *5*, 135-42.

Fritz, G.; Kaina, B. Late activation of stress kinases (SAPK/JNK) by genotoxins requires the dna repair proteins DNA-PKcs and CSB. *Molecular Biology of the Cell*, **2006**; *17*, 851–61.

Fujie, Y.; Yamamoto, H.; Ngan, C. Y.; Takagi, A.; Hayashi, T.; Suzuki, R.; Ezumi, K.; Takemasa, I.; Ikeda, M.; Sekimoto, M.; Matsuura, N.; Monden, M. Oxaliplatin, a potent inhibitor of survivin, enhances paclitaxel-induced apoptosis and mitotic catastrophe in colon cancer cells. *Jpn. J. Clin. Oncol.* **2005**, *35*, 453–63.

Fuse, E.; Tanii, H.; Kurata, N.; Kobayashi, H.; Shimada, Y.; Tamura, T.; Sasaki, Y.; Tanigawara, Y.; Lush, R.D.; Headlee, D.; Figg, W.D.; Arbutk, S.G.; Senderowicz, A.M.; Sausville, E.A.; Akinaga, S.; Kuwabara, T.; Kobayashi, S.

- Unpredicted clinical pharmacology of UCN-01 caused by specific binding to human α 1-acid glycoprotein. *Cancer Res.*, **1998**; *58*, 3248–53.
- Goga, A.; Yang, D.; Tward, A.D.; Morgan, D.O.; Bishop, J.M. Inhibition of CDK1 as a potential therapy for tumors over-expressing MYC. *Nature medicine*, **2007**; *13*, 820-7.
- Gao, Y.; Chaudhuri, J.; Zhu, C.; Davidson, L.; Weaver, D. T.; Alt, F. W. A targeted DNA-PKcs-null mutation reveals DNA-PK-independent functions for Ku in V(D)J recombination. *Immunity*, **1998**; *9*, 367–76.
- Ghosh P.; Kornfeld, S. AP-1 binding to sorting signals and release from clathrin-coated vesicles is regulated by phosphorylation. *The Journal of Cell Biology*, **2003**; *160*, 699–708.
- Ghosh, S.; Paweletz, N.; Schroeter, D. CDC2-independent induction of premature mitosis by okadaic acid in hela cells. *Experimental Cell Research*, **1998**; *242*: 1–9.
- Ghosh, S.; Paweletz, N.; Schroeter, D. Effects of okadaic acid on mitotic HeLa cells. *Journal of Cell Science*, **1992**; *103*: 117-24.
- Ghosh, S.; Schroeter, D.; Paweletz, N. Okadaic acid overrides the S-phase check point and accelerates progression of G2-phase to induce premature mitosis in HeLa cells. *Experimental Cell Research*, **1996**, *227*, 165–9.

Giaccone, G. Clinical prospective on platinum resistance. *Drugs*, 2000, 59 (Suppl. 4), 9-17.

Gil-Bernabe, A.M.; Romero, F.; Limo'n-Morte's, M.C.; Tortolero, M. Protein phosphatase 2A stabilizes human securin, whose phosphorylated forms are degraded via the SCF ubiquitin ligase. *Molecular and cellular biology*. 2006; 26, 4017-27.

Gilmore, P. M.; McCabe, N.; Quinn, J. E.; Kennedy, R. D.; Gorski, J. J.; H. N. Andrews; Mcwilliams, S.; Carty, M.; Mullan, P. B.; Duprex, W. P.; Liu, E. T.; Johnston, P.G; Harkin, D. P. BRCA1 interacts with and is required for paclitaxel-induced activation of mitogen-activated protein kinase kinase kinase 3. *Cancer Research*, 2004; 64, 4148-54.

Goff, S.P.; Gilboa, E.; Witte, O.N.; Baltimore, D. Structure of the Abelson murine leukemia virus genome and the homologous cellular gene: studies with cloned viral DNA. *Cell*, 1980; 22, 777-85.

Goldbaum O.; Richter-Landsberg, C. Activation of PP2A-like phosphatase and modulation of tau phosphorylation accompany stress-induced apoptosis in cultured oligodendrocytes. *GLIA*, 2002; 40, 271-82.

Gong, J.G; Costanzo, A.; Yang, H.Q.; Melino, G.; Kaelin, W.J. Jr; Levrero, M.; Wang, J.Y.J. The tyrosine kinase c-Abl regulates p73 in apoptotic response

- to cisplatin-induced DNA damage. *Nature*, **1999**; *399*, 806-9.
- Goodarzi, A.A.; Jonnalagadda, J.C.; Douglas, P.; Young, D.; Ye, R.; Moorhead, G.B.G.; Lees-Miller, S.P.; Khanna, K.K. Autophosphorylation of ataxia-telangiectasia mutated is regulated by protein phosphatase 2A. *The EMBO Journal*, **2004**; *23*, 4451-61.
- Gorbsky, G.J. The mitotic spindle checkpoint. *Current Biology*, **2001**; *11*, R1001-R1004.
- Gowdy, P.M.; Anderson, H.J.; Roberge, M. Entry into mitosis without CDC2 kinase activation. *Journal of Cell Science*, **1998**; *111*: 3401-10.
- Graves, P.R.; Yu, L.; Schwarz, J.K.; Gales, J.; Sausville, E.A.; O'Connor, P.M.; Piwnicka-Worms, H.. The CHK1 protein kinase and the CDC25C regulatory pathways are targets of the anticancer agent UCN-01. *The Journal of Biological Chemistry*, **2000**; *275*, 5600-5.
- Grethe, S.; Poern-Ares, M.I. p38 MAPK regulates phosphorylation of Bad via PP2A-dependent suppression of the MEK1/2-ERK1/2 survival pathway in TNF- α induced endothelial apoptosis. *Cellular Signalling*. **2006**; *18*, 531-40.
- Gudmundsson, K.O.; Thorsteinsson, L.; Sigurjonsson, O.E.; Keller, J.R.; Olafsson, K.; Egeland, T.; Gudmundsson, S.; Rafnar, T. Gene expression analysis of hematopoietic progenitor cells identifies DLG7 as a potential stem cell gene. *Stem Cells*, **2007**; *25*, 1498-506.

Guo, M.; Li, J.; Wan, D.; Gu, J. KIAA0101 (OEACT-1), an expressionally down-regulated and growth-inhibitory gene in human hepatocellular carcinoma. *BMC Cancer*, **2006**; *6*, 1-8.

Guo, X.W.; Th'ng, J.R.H.; Swank, R.A.; Anderson, H.J.; Tudan, C.; Bradbury, E.M.; Roberge, M. Chromosome condensation induced by fostriecin does not require p34Cdc2 kinase activity and histone H1 hyperphosphorylation, but is associated with enhanced histone H2A and H3 phosphorylation. *The EMBO Journal*. **1995**; *14*, 976-85.

Gurland, G.; Gundersen, G.G. Protein phosphatase inhibitors induce the selective breakdown of stable microtubules in fibroblasts and epithelial cells. *Proc. Natl. Acad. Sci. U.S.A.*, **1993**; *90*, 8827-31.

Habedanck, R.; Stierhof, Y.D.; Wilkinson, C.J.; Nigg, E.A. The Polo kinase PLK4 functions in centriole duplication. *Nature Cell Biology*, **2005**; *7*, 1140-6.

Hartman, A. R.; Ford, J. M. BRCA1 induces DNA damage recognition factors and enhances nucleotide excision repair. *Nature Genetics*, **2002**; *32*, 180-4.

Hayward, D.G.; Fry, A.M. NEK2 kinase in chromosome instability and cancer. *Cancer Letters*, **2006**; *237*, 155–66.

Healy, A.M.; Zolnierowicz, S.; Stapleton, A.E.; Goebel, M.; DePaoli-Roach, A.A.; Pringle, J.R. CDC55, a *Saccharomyces cerevisiae* gene involved in cellular

morphogenesis: identification, characterization, and homology to the B subunit of mammalian type 2A protein phosphatase. *Mol. Cell Biol.*, **1991**; *11*, 5767–80.

Herman, M.; Ori, Y.; Chagnac, A.; Weinstein, T.; Korzets, A.; Zevin, D.; Malachi, T.; Gafter, U. DNA repair in mononuclear cells: Role of serine/threonine phosphatases. *Journal of Laboratory and Clinical Medicine*, **2002**; *140*, 255-62.

Hirose Y.; Katayama, M.; Stokoe, D.; Haas-Kogan, D.A.; Berger, M.S.; and Pieper, R.O. The p38 mitogen-activated protein kinase pathway links the DNA mismatch repair system to the G2 checkpoint and to resistance to chemotherapeutic DNA-methylating agents. *Molecular and Cellular Biology*, **2003**; *23*, 8306-15.

Ho, Y.P.; To, K.K.W.; Au-Yeung, S.C.F.; Wang, X.; Lin, G.; Han, X. Potential new antitumor agents from an innovative combination of demethylcantharidin, a modified traditional chinese medicine, with a platinum moiety. *J. Med. Chem.*, **2001**, *44*, 2065-8.

Holtzman, S.G.; Mante, S.; Minneman, K.P. Role of adenosine receptors in caffeine tolerance. *The Journal of Pharmacology and Experimental Therapeutics*, **1991**, *256*, 62-8.

- Hwang, H.C.; Clurman, B.E. Cyclin E in normal and neoplastic cell cycles. *Oncogene*, **2005**; *24*, 2776–86.
- Jackson, J.R.; Gilmartin, A.; Imburgia, C.; Winkler, J.D.; Marshall, L.A.; Roshak, A. An indolocarbazole inhibitor of human checkpoint kinase (Chk1) abrogates cell cycle arrest caused by DNA damage. *Cancer Res.*, **2000**; *60*, 566-72.
- Jakupec, M.A.; Galanski, M.; Keppler, B.K. Tumor-inhibiting platinum complexes-state of the art and future perspectives. *Rev. Physiol. Biochem. Pharmacol.*, **2003**, *146*, 1-53.
- Jin, S.; Inoue, S.; Weaver, D. T. Differential etoposide sensitivity of cells deficient in the Ku and DNA-PKcs components of the DNA-dependent protein kinase. *Carcinogenesis*, **1998**; *19*, 965–71.
- Jin, S.; Antinore, M. J.; Lung, F. T.; Dong, X.; Zhao, H.; Fan, F.; Colchagie, A. B.; Blanck, P.; Roller, P. P.; Fornace, A. J., Jr.; Zhan, Q. The GADD45 inhibition of CDC2 kinase correlates with GADD45-mediated growth suppression. *The Journal of Biological Chemistry*, **2000**; *275*, 16602–8.
- Jin, S.; Zhao, H.; Fan, F.; Blanck, P.; Fan, W.; Colchagie, A. B.; Fornace, A. J., Jr.; Zhan, Q. BRCA1 activation of the GADD45 promoter. *Oncogene*, **2000**; *19*, 4050-7.
- Jung, H. J.; Kim, E. H.; Mun, J. Y.; Park, S.; Smith, M. L.; Han, S. S.; Seo, Y. R.

- Base excision DNA repair defect in GADD45a-deficient cells. *Oncogene*, **2007**; 26, 1–9.
- Kawabe, T. G2 checkpoint abrogators as anticancer drugs. *Mol. Cancer Ther.*, **2004**; 3, 513–9.
- Kedara, P.S.; Stefanicka, D.F.; Hortona, J.K.; Wilson, S.H. Interaction between PARP-1 and ATR in mouse fibroblasts is blocked by PARP inhibition. *DNA Repair*, **2008**; 7, 1787-98.
- Kennedy, R. D.; Quinn, J. E.; Mullan, P. B.; Johnston, P. G.; Harkin, D. P. The role of BRCA1 in the cellular response to chemotherapy. *Journal of the National Cancer Institute*, **2004**; 96, 1659-68.
- Kharbanda, S.; Pandey, P.; Jin, S.; Inoue, S.; Bharti, A.; Yuan, Z. M.; Weichselbaum, R.; Weaver, D.; Kufe, D. Functional interaction between DNA-PK and c-Abl in response to DNA damage. *Nature*, **1997**; 386, 732-5.
- Kharbanda, S.; Pandey, P.; Yamauchi, T.; Kumar, S.; Kaneki, M.; Kumar, V.; Bharti, A.; Yuan, Z. M.; Ghanem, L.; Rana, A.; Weichselbaum, R.; Johnson, G.; Kufe, D. Activation of MEK kinase 1 by the c-abl protein tyrosine kinase in response to dna damage. *Molecular and Cellular Biology*, **2000**, 20, 4979–89.

- Kim, S.O.; Jing, Q.; Hoebe, K.; Beutler, B.; Duesbery, N.S.; Han, J. Sensitizing anthrax lethal toxin-resistant macrophages to lethal toxin-induced killing by tumor necrosis factor-alpha. *The Journal of Biological Chemistry*, **2003**, *278*, 7413-21.
- Kitajima, T.S.; Sakuno, T.; Ishiguro, K.; Iemura, S.; Natsume, T.; Kawashima, S.A.; Watanabe, Y. Shugoshin collaborates with protein phosphatase 2A to protect cohesion. *Nature*, **2006**; *441*, 46-52.
- Kohn, E.A.; Yoo, C.J.; Eastman, A. The protein kinase C inhibitor G—6976 is a potent inhibitor of DNA damage-induced S and G2 cell cycle checkpoints. *Cancer Res.*, **2003**; *63*, 31–5.
- Krakoff, I.H. Nephrotoxicity of cis-dichlorodiammineplatinum(II). *Cancer Treat. Rep.*, **1979**, *63*, 1523-5.
- Kumar, S.; Pandey, P.; Bharti, A.; Jin, S.; Weichselbaum, R.; Weaver, D.; Kufe, D.; Kharbanda, S. Regulation of DNA-dependent protein kinase by the Lyn tyrosine kinase. *The Journal Of Biological Chemistry*, **1998**; *273*, 25654–8.
- Kufer, T.A.; Silljé, H.H.W.; Körner, R.; Gruss, O.J.; Meraldi, P.; Nigg, E.A. Human TPX2 is required for targeting Aurora-A kinase to the spindle. *The Journal of Cell Biology*, **2002**; *158*, 617–23.
- Lankoff, A.; Bialczyk, J.; Dziga, D.; Carmichael, W.W.; Gradzka, I.; Lisowska, H.;

- Kuszeowski, T.; Gozdz, S.; Piorun, I.; Wojcik, A. The repair of gamma-radiation-induced DNA damage is inhibited microcystin-LR, the PP1 and PP2A phosphatase inhibitor. *Mutagenesis*, **2006**; *21*, 83–90.
- Lankoff, A.; Bialczyk, J.; Dziga, D.; Carmichael, W.W.; Lisowska, H.; and Wojcik, A. Inhibition of nucleotide excision repair (NER) by microcystin-LR in CHO-K1 cells. *Toxicol*, **2006**; *48*, 957-65.
- Lee, S. A.; Dritschilo, A.; Jung, M. Impaired ionizing radiation-induced activation of a nuclear signal essential for phosphorylation of c-Jun by dually phosphorylated c-Jun amino-terminal kinases in ataxia telangiectasia fibroblasts. *The Journal of Biological Chemistry*, **1998**; *273*, 32889–94.
- Lee, S. A.; Dritschilo, A.; Jung, M. Role of ATM in oxidative stress-mediated c-Jun phosphorylation in response to ionizing radiation and CDC12. *The Journal of Biological Chemistry*, **2001**; *276*, 11783–90.
- Li, Z.; Tu, X.; Wang, C.C. Okadaic acid overcomes the blocked cell cycle caused by depleting CDC2-related kinases in *Trypanosoma brucei*. *Experimental Cell Research*, **2006**; *312*, 3504-16.
- Lim, H.H.; Surana, U. Tome-1, weel, and the onset of mitosis: coupled destruction. *Molecular Cell*, **2003**; *11*, 845–46.
- Lin, J.; Raouf, D.A.; Wang, Z.; Lin, M.Y.; Thomas, D.G.; Greenon, J.K.; Giordano,

- T.J.; Orringer, M.B.; Chang, A.C.; Beer, D.G.; Lin, L. Expression and effect of inhibition of the ubiquitin-conjugating enzyme E2C on esophageal adenocarcinoma. *Neoplasia*, **2006**; *12*, 1062-71.
- Lippard, S.J.; Hoeschele, J.D. Binding of cis- and trans-dichlorodiammineplatinum(ii) to the nucleosome core. *Proc. Natl. Acad. Sci. U.S.A.*, **1979**, *76*, 6091-5.
- Liu, Q.; Hofmann, P.A. Protein phosphatase 2A-mediated cross-talk between p38 MAPK and ERK in apoptosis of cardiac myocytes. *Am. J. Physiol. Heart Circ. Physiol.*, **2004**; *286*, 2204-12.
- Ma, L.; Zhao, X.; Zhu, X. Mitosin/CENP-F in mitosis, transcriptional control, and differentiation. *Journal of Biomedical Science*, **2006**; *13*, 205-13.
- Maeda, T.; Espino, R. A.; Chomey, E. G.; Luong, L.; Bano, A.; Meakins, D.; Tron, V. A. Loss of p21WAF1/Cip1 in GADD45-deficient keratinocytes restores DNA repair capacity. *Carcinogenesis*, **2005**; *26*, 1804-10.
- Maiti, B.; Li, J.; Bruin, A.; Gordon, F.; Timmers, C.; Opavsky, R.; Patil, K.; Tuttle, J.; Cleghorn, W.; Leone, G. Cloning and characterization of mouse E2F8, a novel mammalian E2F family member capable of blocking cellular proliferation. *The Journal of Biological Chemistry*, **2005**; *280*, 18211-20.
- Mak, S. K.; Kultz, D. GADD45 proteins induce G2/M arrest and modulate

- apoptosis in kidney cells exposed to hyperosmotic stress. *The Journal of Biological Chemistry*, **2004**; 279, 39075–84.
- Mansouri, A.; Ridgway, L. D.; Korapati, A. L.; Zhang, Q.; Tian, L.; Wang, Y.; Siddik, Z. H.; Mills, G. B.; Claret, F. X. Sustained activation of JNK/p38 MAPK pathways in response to cisplatin leads to fas ligand induction and cell death in ovarian carcinoma cells. *The Journal of Biological Chemistry*, **2003**; 278, 19245–56.
- Mante, S.; Minneman, K.P. Caffeine inhibits forskolin-stimulated cyclic AMP accumulation in rat brain. *Eur. J. Pharmacol.*, **1990**; 175, 203–5.
- Masai, H.; Arai, K. CDC7 kinase complex: a key regulator in the initiation of DNA replication. *J. Cell Physiol.*, **2002**, 190, 287-96.
- Matsusaka, T.; Pines, J. Chfr acts with the p38 stress kinases to block entry to mitosis in mammalian cells. *J. Biol. Chem.*, **2004**, 166, 507–16.
- Messner, D.J.; Ao, P.; Jagdale, A.B.; Boynton; A.L. Abbreviated cell cycle progression induced by the serine/threonine protein phosphatase inhibitor okadaic acid at concentrations that promote neoplastic transformation. *Carcinogenesis*, **2001**; 22, 1163-72.
- Messner, D.M.; Romeo, C.; Boynton, A.; Rossie, S. Inhibition of PP2A, but not PP5, mediates p53 activation by low levels of okadaic acid in rat liver

- epithelial cells. *Journal of Cellular Biochemistry*, **2006**; *99*, 241–55.
- Mikhailov, A.; Shinohara, M.; Rieder, C.L. The p38-mediated stress-activated checkpoint: a rapid response system for delaying progression through antepause and entry into mitosis. *Cell Cycle*, **2005**, *4*, 57-62.
- Miki, H.; Setou, M.; Kaneshiro, K.; Hirokawa, N. All kinesin superfamily protein, KIF, genes in mouse and human. *Proc. Natl. Acad. Sci. U.S.A.*, **2001**; *98*, 7004–11.
- Minshull, J.; Straight, A.; Rudner, A.D.; Dernburg, A.F.; Belmont, A.; Murray, A.W. Protein phosphatase 2A regulates MPF activity and sister chromatid cohesion in budding yeast. *Current Biology*, **1996**; *6*, 1609–20.
- Mistry, S.J.; Li H.C.; Atweh, G.F. Role for protein phosphatases in the cell-cycle-regulated phosphorylation of stathmin. *The Journal of Biological Chemistry*, **1998**; *334*, 23-9.
- Mita, A.C.; Mita, M.M.; Nawrocki, S.T.; Giles, F.J. Survivin: key regulator of mitosis and apoptosis and novel target for cancer therapeutics. *Clin. Cancer Res.*, **2008**; *14*, 5000-5.
- Miyake, Z.; Takekawa, M.; Ge, Q.; Saito, H. Activation of MTK1/MEKK4 by GADD45 through induced N-C dissociation and dimerization-mediated trans

autophosphorylation of the MTK1 kinase domain. *Molecular and Cellular Biology*, **2007**; *27*, 2765–76.

Moran1, D.M.; Gawlak, G.; Jayaprakash, M.S.; Mayar, S.; Maki, C.G. Geldanamycin promotes premature mitotic entry and micronucleation in irradiated p53/p21 deficient colon carcinoma cells. *Oncogene*, **2008**; *27*, 5567–77.

Narasimhaiah, R.; Tuchman, A.; Lin, S. L.; Naegele, J. R. Oxidative damage and defective DNA repair is linked to apoptosis of migrating neurons and progenitors during cerebral cortex development in Ku70-deficient mice. *Cerebral Cortex*, **2005**; *15*, 696-707.

Nasmyth, K. Segregating sister genomes: the molecular biology of chromosome separation. *Science*, **2002**, *297*, 559-65.

Nehmé, A.; Baskaran, R.; Nebel, R.; Fink, D.; Howell, S.B.; Wang, J.Y.J.; Christen, R.D. Induction of JNK and c-Abl signalling by cisplatin and oxaliplatin in mismatch repair-proficient and –deficient cells. *British Journal of Cancer*, **1999**, *79*, 1104–10.

Nowak, S.J.; Corces, V.G. Phosphorylation of histone H3 correlates with transcriptionally active loci. *Genes & Dev.*, **2000**; *14*, 3003-13.

- Nowak, S.J.; Pai, C.Y.; Corces, V.G. Protein Phosphatase 2A Activity Affects Histone H3 Phosphorylation and Transcription in *Drosophila melanogaster*. *Molecular and Cellular Biology*, **2003**; 23, 6129-38.
- Ohi, R.; Gould, K.L. Regulating the onset of mitosis. *Curr. Opin. Cell. Biol.*, **1999**; 11, 267-73.
- Pabla, N.; Huang, S.; Mi, Q.S.; Daniel, R.; Dong, Z. ATR-Chk2 Signaling in p53 activation and DNA damage response during cisplatin-induced apoptosis. *The Journal of Biological Chemistry*, **2008**; 283, 6572–83.
- Pandey, P.; Raingeaud, J.; Kaneki, M.; Weichselbaum, R.; Davis, R.J.; Kufe, D.; Kharbanda, S. Activation of p38 mitogen-activated protein kinase by c-Abl-dependent and -independent mechanisms. *J. Biol. Chem.*, **1996**; 271, 23775-9.
- Pang, S.K.; Yu, C.W.; Au-Yeung, S.C.F.; Ho, Y.P. DNA damage induced by novel demethylcantharidin-integrated platinum anticancer complexes. *Biochemical And Biophysical Research Communications*, **2007**; 363, 235–40.
- Pendyala, L.; Kidani, Y.; Perez, R.; Wilkes, J.; Bernacki, R.J.; Creave, P.J. Cytotoxicity, cellular accumulation and DNA binding of oxaliplatin isomers. *Cancer Lett.*, **1995**; 97, 177-84.
- Percy, M.J.; Myrie, K.A.; Neeley, C.K.; Azim, J.N.; Ethier, S.P.; Petty, E.M.

Expression and mutational analyses of the human MAD2L1 gene in breast cancer cells. *Genes Chromosomes Cancer*, **2000**; *29*, 356-62.

Perfettini, J. L.; Castedo, M.; Nardacci, R.; Ciccocanti, F.; Boya, F.; Roumier, T.; Larochette, N.; Piacentini, M.; Kroemer, D. Essential role of p53 phosphorylation by p38 MAPK in apoptosis induction by the HIV-1 envelope. *The Journal of Experimental Medicine*, **2005**; *10*, 1084.

Petersen, P.; Chou, D.M.; You, Z.; Hunter, T.; Walter, J.C.; Walter, G. Protein phosphatase 2A antagonizes ATM and ATR in a CDK2- and CDC7-independent DNA damage checkpoint. *Molecular and cellular biology*, **2006**; *26*, 1997–2011.

Petritsch, C.; Beug, H.; Balmain, A.; Oft, M. TGF- β inhibits p70^{S6} kinase via protein phosphatase 2A to induce G1 arrest. *Genes and Development*, **2000**; *14*, 3093–101.

Potts, P.R.; Porteus, M.H.; Yu, H. Human SMC5/6 complex promotes sister chromatid homologous recombination by recruiting the SMC1/3 cohesin complex to double-strand breaks. *The EMBO Journal*, **2006**; *25*, 3337-88.

Powell, S.N.; DeFrank, J.S.; Connell, P.; Eogan, M.; Preffer, F.; Dombkowski, D.; Tang, W.; Friend, S. Differential sensitivity of p53(-) and p53(+) cells to caffeine-induced radiosensitization and override of G2 delay. *Cancer*

Research, 1995; 55, 1643–8.

Price, P.M.; Yu, F.; Kaldis, P.; Aleem, E.; Nowak, G.; Safirstein, R.L.; Megyesi, L.

Dependence of cisplatin-induced cell death *in vitro* and *in vivo* on cyclin-dependent kinase 2. *J. Am. Soc. Nephrol.*, 2006; 17: 2434–42.

Quinn, J. E.; Kennedy, R. D.; Mullan, P. D.; Gilmore, P. M.; Carty, M.; Johnston, P. G.;

Harkin, D. P. BRCA1 functions as a differential modulator of chemotherapy-induced apoptosis. *Cancer Research*, 2003; 63, 6221–8.

Rakitina, T.V.; Vasilevskaya, I.A.; O'Dwyer, P.J. Inhibition of G1/S transition

potentiates oxaliplatin-induced cell death in colon cancer cell lines. *Biochemical pharmacology*, 2007; 73, 1715–26.

Ramírez, C.J.; Haberbush, J.M.; Soprano, D.R.; Soprano, K.J. Retinoic acid

induced repression of AP-1 activity is mediated by protein phosphatase 2A in ovarian carcinoma cells. *Journal of Cellular Biochemistry*, 2005; 96, 170–82.

Rauh, R.; Kahl, S.; Boechzelt, H.; Bauer, R.; Kaina, B.; Efferth, T. Molecular

biology of cantharidin in cancer cells. *Chin. Med.*, 2007, 4, 2-8.

Ray, R.M.; Bhattacharya, S.; Johnson, L.R. Protein phosphatase 2A regulates

apoptosis in intestinal epithelial cells. *The Journal of Biological Chemistry*, 2005; 280, 31091–100.

- Reithofer, M.R.; Valiahdi, S.M.; Jakupec, M.A.; Arion, V.B.; Egger, A.; Galanski, M.; Keppler, B.K. Novel Di- and Tetracarboxylatoplatinum(IV) Complexes. Synthesis, Characterization, Cytotoxic Activity, and DNA Platination. *J. Med. Chem.*, **2007**; *50*, 6692–9.
- Rivera, T.; Losada, A. Shugoshin and PP2A, shared duties at the centromere. *BioEssays*, **2006**; *28*, 775–9.
- Roberge, M.; Tudan, C.; Hung, S.M.F.; Harder, K.W.; Jirik, F.R.; Anderson, H. Antitumor drug fostriecin inhibits the mitotic entry checkpoint and protein phosphatases 1 and 2A. *Cancer Research*, **1994**, *54*, 6115-21.
- Rubin, C.I.; Atweh, G.F. The Role of Stathmin in the Regulation of the Cell Cycle. *Journal of Cellular Biochemistry*, **2004**; *93*, 242-50.
- Russell, K.J.; Wiens, L.W.; Demers, G.W.; Galloway, D.A.; Plon, S.E.; Groudine, M. Abrogation of the G₂ checkpoint results in differential radiosensitization of G₁ checkpoint-deficient and G₁ checkpoint-competent cells. *Cancer Research*, **1995**, *55*, 1639-42.
- Sarkaria, J.N.; Busby, E.C.; Tibbetts, R.C.; Roos, P.; Taya, Y.; Karnitz, L.M.; Abraham, R.T. Inhibition of ATM and ATR kinase activities by the radiosensitizing agent, caffeine. *Cancer Research*, **1999**; *59*, 4375–82.
- Sato, S.; Fujita, N.; Tsuruo, T. Interference with PDK1-Akt survival signaling

pathway by UCN-01 (7-hydroxystaurosporine). *Oncogene*, **2002**; *21*, 1717–38.

Sausville, E.A.; Arbuck, S.G.; Messmann, R.; Headlee, D.; Bauer, K.S.; Lush, R.M.; Murgo, A.; Figg, W.D.; Lahusen, T.; Jaken, S.; Jing, X-X.; Roberge, M.; Fuse, E.; Kuwabara, T.; Senderowicz, A.M. Phase I trial of 72-hour continuous infusion UCN-01 in patients with refractory neoplasms. *J. Clin. Oncol.*, **2001**; *19*, 2319–33.

Saxena, A.; Saffery, R.; Wong, L.H.; Kalitsis, P.; Choo, K.H.A. Centromere proteins Cenpa, Cenpb, and Bub3 interact with poly(ADP-ribose) polymerase-1 protein and are poly(ADP-ribosyl)ated. *The Journal of Biological Chemistry*, **2002**; *277*, 26921–6.

Scolnick, D.M.; Halazonetis, T.D. Chfr defines a mitotic stress checkpoint that delays entry into metaphase. *Nature*, **2000**, *406*, 430-5.

Seeling, J.M.; Miller, J.R.; Gil, R.; Moon, R.T.; White, R.; Virshup, D.M. Regulation of β -catenin signaling by the B56 subunit of protein phosphatase 2A. *Science*, **1999**; *283*, 2089 – 91.

Shafman, T.; Khanna, K.K.; Kedar, P.; Spring, K.; Kozlov, S.; Yen, T.; Hobson, K.; Gatei, M.; Zhang, N.; Watters, D.; Egerton, M.; Shiloh, Y.; Kharbanda, S.; Kufe, D.; Lavin, M.F. Interaction between ATM protein and c-Abl in

- response to DNA damage. *Nature*, **1997**; *387*, 520–3.
- Shao, X.; Xue, J.; Van der Hoorn, F.A. Testicular protein SPAG5 has similarity to mitotic spindle protein Deepest and binds outer dense fiber protein Odfl. *Mol. Reprod. Dev.*, **2001**; *59*, 410-6.
- Shiotani, B.; Zou, L. Single-stranded DNA orchestrates an ATM-to-ATR switch at DNA breaks. *Molecular Cell*, **2009**; *33*, 547–58.
- Silverstein, A.M.; Barrow, C.A.; Davis, A.J.; Mumby, M.C. Actions of PP2A on the MAP kinase pathway and apoptosis are mediated by distinct regulatory subunits. *Proc. Natl. Acad. Sci. U.S.A.*, **2002**; *99*, 4221–6.
- Simizu, S.; Tamura, Y.; Osada, H. Dephosphorylation of Bcl-2 by protein phosphatase 2A results in apoptosis resistance. *Cancer Sci.*, **2004**; *95*, 266–70.
- Smith, M. L.; Ford, J. M.; Hollander, M. C.; Bortnick, R. A.; Amundson, S. A.; Seo, Y. R.; Deng, C. X.; Hanawalt, P. C.; Fornace, A. J., Jr. p53-mediated DNA repair responses to UV radiation: studies of mouse cells lacking *p53*, *p21*, and/or *gadd45* genes. *Molecular and Cellular Biology*, **2000**; *20*, 3705–14.
- Sontag, E.; Nunbhakdi-Craig, V.; Lee, G.; Bloom, G.S.; Mumby, M.C. Regulation of the phosphorylation state and microtubule-binding activity of tau by protein phosphatase 2A. *Neuron*, **1996**; *17*, 1201–7.

- Spruck, C.H.; De Miguel, M.P.; Smith, A.P.L.; Ryan, A.; Stein, P.; Schultz, R.M.; Lincoln, A.J.; Donovan, P.J.; Reed, S.I. Requirement of Cks2 for the First Metaphase/Anaphase Transition of Mammalian Meiosis. *Science*, **2003**; *300*, 647-50.
- Spunt, S.L.; Freeman, B.B.; Billups, C.A.; Mcpherson, V.; Khan, R.B.; Pratt, C.B.; Stewart, C.F. Phase I clinical trial of oxaliplatin in children and adolescents with refractory solid tumors. *Journal of Clinical Oncology*, **2007**, *25*, 2274-80.
- Sun, L.; Gao, J.; Dong, X.; Liu, M.; Li, D.; Shi, X.; Dong, J.T.; Lu, X.; Liu, C.; Zhou, J. EB1 promotes Aurora-B kinase activity through blocking its inactivation by protein phosphatase 2A. *Proc. Natl. Acad. Sci. U.S.A.*, **2008**; *105*, 7153-8.
- Surveillance, Epidemiology, and End Results Program, 1975-2005. Division of Cancer Control and Population Sciences, National Cancer Institute, 2008.
- Takai, A.; Bialojan, C.; Troschka, M.; Ruegg, J.C. Smooth muscle myosin phosphatase inhibition and force enhancement by black sponge toxin. *FEBS Lett.*, **1987**; *217*, 81-4.
- Takekawa, M.; Saito, H. A family of stress-inducible GADD45-like proteins mediate activation of the stress-responsive MTK1/MEKK4 MAPKKK. *Cell*,

1998; 95, 521–30.

Takemoto, A.; Murayama, A.; Katano, M.; Urano, T.; Furukawa, K.; Yokoyama, S.;

Yanagisawa, J.; Hanaoka, F.; Kimura, K. Analysis of the role of Aurora B on the chromosomal targeting of condensin I. *Nucleic Acids Research*, 2007; 35, 2403–12.

Terret, M.E.; Jallepalli, P.V. Meiosis: separase strikes twice. *Nature Cell Biology*, 2006; 8, 910-1.

Terzoudi, G.T.; Manola, K.N.; Pantelias, G.E.; Iliakis, G. Checkpoint abrogation in G₂ compromises repair of chromosomal breaks in ataxia telangiectasia cells. *Cancer Research*, 2005, 65, 11292-6.

Theis, S.; Roemer, K. c-Abl tyrosine kinase can mediate tumor cell apoptosis independently of the Rb and p53 tumor suppressors. *Oncogene*, 1998; 17, 557-64.

Thottassery, J. V.; Westbrook, L.; Someya, H.; Parker, W. B. c-Abl-independent p73 stabilization during gemcitabineor 4V-thio-B-D-arabinofuranosylcytosine-induced apoptosis in wild-type and p53-null colorectal cancer cells. *Mol. Cancer Ther.*, 2006; 5, 400-10.

To, K.K.W.; Au-Yeung, S.C.F.; Ho, Y.P. Differential nephrotoxicity of cisplatin and a novel series of traditional Chinese medicine–platinum anticancer agents

- correlates with their chemical reactivity towards sulfur-containing nucleophiles. *Anti-Cancer Drugs*, **2006**; *17*, 673-83.
- To, K.K.W.; Ho, Y.P.; Au-Yeung, S.C.F. Determination of the release of hydrolyzed demethylcantharidin from novel traditional Chinese medicine-platinum compounds with anticancer activity by gas chromatography. *Journal of Chromatography A*, **2002**; *947*, 319-26
- To, K.K.W.; Ho, Y.P.; Au-Yeung, S.C.F. Synergistic interaction between platinum-based antitumor agents and demethylcantharidin. *Cancer Letters*, **2005**; *223*, 227-37.
- To, K.K.W.; Wang, X.; Yu, C.W.; Ho, Y.P.; Au-Yeung, S.C.F. Protein phosphatase 2a inhibition and circumvention of cisplatin cross-resistance by novel TCM-platinum anticancer agents containing demethylcantharidin. *Bioorganic & Medicinal Chemistry*, **2004**; *12*, 4565-73.
- Toh, W. H.; Siddique, M. M.; Boominathan, L.; Lin, K. W.; Sabapathy, K. c-Jun Regulates The stability and activity of the p53 homologue, p73. *The Journal of Biological Chemistry*, **2004**; *279*, 44713-22.
- Tritarelli, A.; Oricchio, E.; Ciciarello, M.; Mangiacasale, R.; Palena, A.; Lavia, P.; Soddu, S., Cundari, E. p53 localization at centrosomes during mitosis and postmitotic checkpoint are atm-dependent and require serine 15

- phosphorylation. *Molecular Biology of the Cell*, **2004**, *15*, 3751–7.
- Tsuchiya, A.; Tashiro, E.; Yoshida, M.; Imoto, M.. Involvement of protein phosphatase 2A nuclear accumulation and subsequent inactivation of activator protein-1 in leptomycin B-inhibited cyclin D1 expression. *Oncogene*, **2007**, *26*, 1522–32.
- Urien, S. and Lokiec, F. Population pharmacokinetics of total and unbound plasma cisplatin in adult patients. *British Journal of Clinical Pharmacology*, **2004**; *57*, 756-63.
- Utrera, R.; Collavin, L.; Lazarevic', D.; Delia, D.; Schneider, C. A novel p53-inducible gene coding for a microtubule-localized protein with G2-phase-specific expression. *The EMBO Journal*, **1998**; *17*, 5015–25.
- Voland, C.; Bord, A.; Pe' leraux, A.; Pe' narier, G.; Carrie` re, D.; Galie` gue, S.; Cvitkovic, E.; Jbilo, O.; Casellas, P. Repression of cell cycle-related proteins by oxaliplatin but not cisplatin in human colon cancer cells. *Mol. Cancer Ther.*, **2006**; *5*, 2149-57.
- Volkmer, E.; Karnitz, L. Human homologs of *Schizosaccharomyces pombe* Rad1, Hus1, and Rad9 form a DNA damage-responsive protein complex. *The Journal of Biological Chemistry*, **1999**; *274*, 567–70.
- Voorhoeve, P.M.; Hijmans, E.M.; Bernards, R. Functional interaction between a

- novel protein phosphatase 2A regulatory subunit, PR59, and the retinoblastoma-related p107 protein. *Oncogene*, **1999**; *18*: 515-24.
- Voorhoeve, P.M.; Watson, R.J.; Farlie, P.G.; Bernards, R.; Lam, E.W.F. Rapid dephosphorylation of p107 following UV irradiation. *Oncogene*, **1999**; *18*, 679-88.
- Wang, B.; Zou, J. X.; Ek-Rylander, B.; Ruoslahti, E. R-Ras contains a proline-rich site that binds to SH3 domains and is required for integrin activation by r-Ras. *The Journal of Biological Chemistry*, **2000**; *275*, 5222-7.
- Wang, H.; Hu, X.; Ding, X.; Dou, Z.; Yang, Z.; Shaw, A.W.; Teng, M.; Cleveland, D.W.; Goldberg, M.L.; Niu, L.; Yao, X. Human zwint-1 specifies localization of zeste white 10 to kinetochores and is essential for mitotic checkpoint signaling. *The Journal of Biological Chemistry*, **2004**; *279*, 54590-8.
- Wang, W.; Stukenberg, P.T.; Brautigan, D.L. Phosphatase inhibitor-2 balances protein phosphatase 1 and Aurora B kinase for chromosome segregation and cytokinesis in human retinal epithelial cells. *Molecular Biology of the Cell*, **2008**; *19*, 4852-62.
- Wang, X.; Gorospe, M.; Holbrook, N. J. GADD45 is not required for activation of c-jun n-terminal kinase or p38 during acute stress. *The Journal of Biological*

Chemistry, **1999**; 274, 29599–602.

Wang, Y.; Burke, D.J. CDC55p, the B-type regulatory subunit of protein phosphatase 2A, has multiple functions in mitosis and is required for the kinetochore/spindle checkpoint in *Saccharomyces cerevisiae*. *Mol. Cell Biol.*, **1997**, 17, 620–6.

Wang, Y.; Li, J.; Booher, R.N.; Kraker, A.; Lawrence, T.; Leopold, W.R.; Sun, Y. Radiosensitization of p53 mutant cells by PD0166285, a novel G(2) checkpoint abrogator. *Cancer Research*, **2001**; 61, 8211–7.

Wagner, M.W.; Li, L.S.; Morales, J.C.; Galindo, C.L.; Garner, H.R.; Bornmann, W.G.; Boothman, D.A. Role of c-Abl kinase in dna mismatch repair-dependent g2 cell cycle checkpoint arrest responses. *The Journal of Biological Chemistry*, **2008**; 283, 21382–93.

Wei, G.; Li, A. G.; Liu, X. Insights into selective activation of p53 DNA binding by c-Abl. *The Journal of Biological Chemistry*, **2005**; 280, 12271–8.

Wiltshaw, E.; Subramarian, S.; Alexopoulos, C.; Barker, G.H. Cancer of the ovary: a summary of experience with cis-dichlorodiammineplatinum(ii) at the royal marsden hospital. *Cancer Treat. Rep.*, **1979**, 63, 1545-8.

Wolgemuth, D.J.; Lele, K.M.; Jobanputra, V.; Salazar, G. The A-type cyclins and the meiotic cell cycle in male germ cells. *International Journal of Andrology*,

2004; 27, 192–9.

Wong, E.; Giandomenico, C.M. Current status of platinum-based antitumor drugs.

Chem. Rev., 1999, 99, 2451-66.

Xie, W.; Herschman, H. R. V-Src induces prostaglandin synthase 2 gene expression by activation of the c-jun n-terminal kinase and the c-jun transcription factor.

The Journal of Biological Chemistry, 1995; 270, 27622–8.

Xin, M.; Deng, X. Protein phosphatase 2A enhances the proapoptotic function of

Bax through dephosphorylation. *The Journal of Biological Chemistry*, 2006;

281, 18859–67.

Yamashita, K.; Yasuda, H.; Pines, J.; Yasumoto, K.; Nishitani, H.; Ohtsubo, M.;

Hunter, H.; Sugimura, T.; Nishimoto, T. Okadaic acid, a potent inhibitor of type 1 and type 2A protein phosphatases, activates CDC2/H1 kinase and transiently induces a premature mitosis-like state in BHK21 cells. *The*

EMBO Journal, 1990; 9, 4331-8.

Yan, Z.; Fedorov, S.A.; Mumby, M.C.; Williams, R.S. PR48, a novel regulatory

subunit of protein phosphatase 2a, interacts with cdc6 and modulates dna replication in human cells. *Mol. Cell Biol.*, 2000; 20, 1021–9.

Yang, H.; Burke, T.; Dempsey, J.; Diaz, B.; Collins, E.; Toth, J.; Beckmann, R.; Ye, X.

Mitotic requirement for aurora A kinase is bypassed in the absence of aurora B

- kinase. *FEBS Letters*, **2005**; *579*, 3385–91.
- Yen, C.C.; Chen, Y.J.; Pan, C.C.; Lu, K.H.; Chen, P.C; Hsia, J.Y.; Chen, J.T.; Wu, Y.C.; Hsu, W.H.; Wang, L.S.; Huang, M.H.; Huang, B.S.; Hu, C.P.; Chen, P.M.; Lin, C.H. Copy number changes of target genes in chromosome 3q25.3-qter of esophageal squamous cell carcinoma: TP63 is amplified in early carcinogenesis but down-regulated as disease progressed. *World J. Gastroenterol*, **2005**; *11*, 1267-72.
- Yeong, F.M.; Hombauer, H.; Wendt, K.S.; Hirota, T.; Mudrak, I.; Mechtler, K.; Loregger, T.; Marchler-Bauer, A.; Tanaka, K.; Peters, J.M.; Ogris, E. Identification of a subunit of a novel Kleisin-beta/SMC complex as a potential substrate of protein phosphatase 2A. *Current Biology*, **2003**; *13*, 2058–64.
- Yerushalmi, R.; Nordenberg, J.; Beery, E. Combined antiproliferative activity of imatinib mesylate (STI-571) with radiation or cisplatin *in vitro*. *Exp. Oncol.*, **2007**; *29*, 126-31.
- Yoshida, K.; Miki, Y. Role of BRCA1 and BRCA2 as regulators of DNA repair, transcription, and cell cycle in response to DNA damage. *Cancer Sci.*, **2004**; *95*, 866–71.
- Yoshida, K.; Weichselbaum, R.; Kharbanda, S.; Kufe, D. Role of Lyn tyrosine kinase as a regulator of stress-activated protein kinase activity in response to

- DNA damage. *Molecular and Cellular Biology*, **2000**; *20*, 5370–80.
- Yu, C.W.; Li, K.K.W.; Pang, S.K.; Au-Yeung, S.C.F.; Ho, Y.P. Anticancer Activity of a series of platinum complexes integrating demethylcantharidin with isomers of 1,2-diaminocyclohexane. *Bioorganic & Medicinal Chemistry Letters*, **2006**, *16*, 1686–91.
- Yu, F.; Megyesi, J.; Safirstein, R.L.; Price, P.M. Involvement of the CDK2-E2F1 pathway in cisplatin cytotoxicity in vitro and in vivo. *Am. J. Physiol. Renal. Physiol.*, **2007**; *293*: F52–F59.
- Yu, P.; Huang, B.; Shen, M.; Lau, C.; Chan, E.; Michel, J.; Xiong, Y.; Payan, D.G.; Luo, Y. p15(PAF), a novel PCNA associated factor with increased expression in tumor tissues. *Oncogene*, **2001**; *20*, 484-9.
- Yu, Q.; La Rose, J.; Zhang, H.; Takemura, H.; Kohn, K.W.; Pommier, Y. UCN-01 inhibits p53 up-regulation and abrogates g-radiation-induced G(2)-M checkpoint independently of p53 by targeting both of the checkpoint kinases, Chk2 and Chk1. *Cancer Research*, **2002**; *62*, 5743–8.
- Zdraveski, Z.Z.; Mello, J.A.; Farinelli, C.K.; Essigmann, J.M.; Marinus, M.G. MutS preferentially recognizes cisplatin- over oxaliplatin-modified DNA. *The Journal of Biological Chemistry*, **2002**, *277*, 1255–60.

Zhang, P.; Gao, W.Y.; Turner, S.; Ducatman, B.S. Gleevec (STI-571) inhibits lung cancer cell growth (A549) and potentiates the cisplatin effect *in vitro*.

Molecular Cancer, **2003**, 2, 1-9.

Zhong, X.; Liu, L.; Zhao, A.; Pfeifer, G.P.; Xu, X. The abnormal spindle-like, microcephaly-associated (ASPM) gene encodes a centrosomal protein. *Cell*

Cycle, **2005**; 4, 1227-9.

Zhang, Y.; Zhou, J.; Cao, X.; Zhang, Q; Lim, C. U. K.; Ullrich, R. L.; Bailey, S. M.;

Liber, H. J. Partial deficiency of DNA-PKcs increases ionizing radiation-induced mutagenesis and telomere instability in human cells.

Cancer Letters, **2007**; 250, 63-73.

Impact of oxaliplatin and a novel DACH-platinum complex in the gene expression of HCT116 colon cancer cells

SIU-KWONG PANG^{1,2}, CHUN-WING YU¹, HUAJI GUAN¹, STEVE C.F. AU-YEUNG² and YEE-PING HO¹

¹School of Pharmacy and ²Department of Chemistry, The Chinese University of Hong Kong, Shatin, New Territories, Hong Kong SAR, P.R. China

Received May 6, 2008; Accepted June 27, 2008

DOI: 10.3892/or_00000140

Abstract. Novel demethylcantharidin-platinum (DMC-Pt) complexes have been found to have superior *in vitro* anticancer activity against a number of human colon cancer cell lines when compared with oxaliplatin. One complex where the DMC-Pt moiety was integrated with *trans*-*R,R*-diaminocyclohexane (DACH), exhibited the most pronounced cytotoxicity. To ascertain the mechanistic contribution of the DMC component, microarray analysis was conducted to compare the effect of the novel (*R,R*-DACH)-Pt-(DMC) complex and oxaliplatin, on the gene expression of human colorectal cancer (HCT116) cells. The Affymetrix HG-U133A oligonucleotide microarray was used, and the data allowed for the discrimination of genes that were specifically affected by the DMC ligand. One hundred and forty-one genes were found to be up-regulated. Of these, 48 can be classified according to different cellular responses including DNA repair, DNA synthesis, cell adhesion, cell cycle regulation, mitotic spindle checkpoint and apoptosis/antiapoptosis. The DMC ligand is likely to have caused damage to DNA bases and/or strands, and nucleotide mismatch, as highlighted by the recruitment of the repairing genes from the BER, HR and MMR. Antiapoptotic genes such as *survivin*, *BRCA1* and *ITGB3BP* were up-regulated, and it is proposed that the inherent defense mechanism of the cell may have been triggered, creating potential resistance to apoptosis. This study is the first to demonstrate the impact of the DMC ligand on the gene expression profile of HCT116 colon cancer cells and further substantiates its inclusion in the design of novel platinum-based anticancer complexes.

Introduction

Oxaliplatin is a third generation diaminocyclohexane (DACH)-containing platinum-based antitumour drug that is clinically

used for the treatment of advanced colorectal cancer and is able to circumvent cisplatin resistance (1). In general, the cytotoxicity of oxaliplatin is comparable to, and occasionally greater than that of cisplatin, but neurotoxicity is a significant side effect (1).

Demethylcantharidin (DMC) (or norcantharidin) is an analogue of cantharidin, an active principle derived from traditional Chinese medicine (*Mylabris*) that has anticancer properties (2). Utilizing a dual mechanism of the drug action approach in designing a novel platinum-based anticancer agent, the complex (*R,R*-DACH)-Pt-(DMC) has been synthesized (3), so that it has the same *R,R*-diaminocyclohexane (DACH)-Pt moiety as oxaliplatin, and DMC as the released ligand (Fig. 1a). We propose that the mechanism of anticancer action is two-fold: i) the *R,R*-DACH-Pt moiety alkylates DNA, and ii) the DMC ligand induces an additional cytotoxic effect in cancer cells. In support of the latter effect, we have demonstrated that (*R,R*-DACH)-Pt-(DMC) generated more DNA lesions when compared with oxaliplatin, and confirmed that the DMC ligand released from (*R,R*-DACH)-Pt-(DMC) participates in DNA damage (4).

DMC has separately been reported to cause loss of cell adhesion (5), inhibition of DNA synthesis (6), cell cycle distortion (3) and apoptosis (3,6,7) (Fig. 1b). Furthermore, cantharidin has been found to be capable of inducing an aberrant mitotic spindle in human lung epithelial carcinoma A549 cells (8).

This study aimed to compare the effect of oxaliplatin and the novel complex (*R,R*-DACH)-Pt-(DMC) on the gene expression of human colorectal cancer (HCT116) cells using microarray technology. The Affymetrix HG-U133A oligonucleotide microarray was used, allowing for the simultaneous examination of a large number of genes by measuring mRNA levels. As the structures of the two test compounds have a common *R,R*-DACH-Pt moiety, the analysis should be able to discriminate the effect due to the DMC ligand. The strategy used for the microarray analysis is shown in Fig. 1b, and the detected genes were sorted according to the observed differences in gene expression levels in cells treated with either (*R,R*-DACH)-Pt-(DMC) or oxaliplatin.

Materials and methods

Chemicals and reagents. Oxaliplatin was supplied by W.C. Heraeus GmbH & Co. KG (Hanau, Germany). DMC was

Correspondence to: Dr Yee-Ping Ho, School of Pharmacy, The Chinese University of Hong Kong, Hong Kong SAR, P.R. China
E-mail: yeepingho@cuhk.edu.hk

Key words: gene expression, diaminocyclohexane-platinum complexes, demethylcantharidin, oxaliplatin, colon cancer

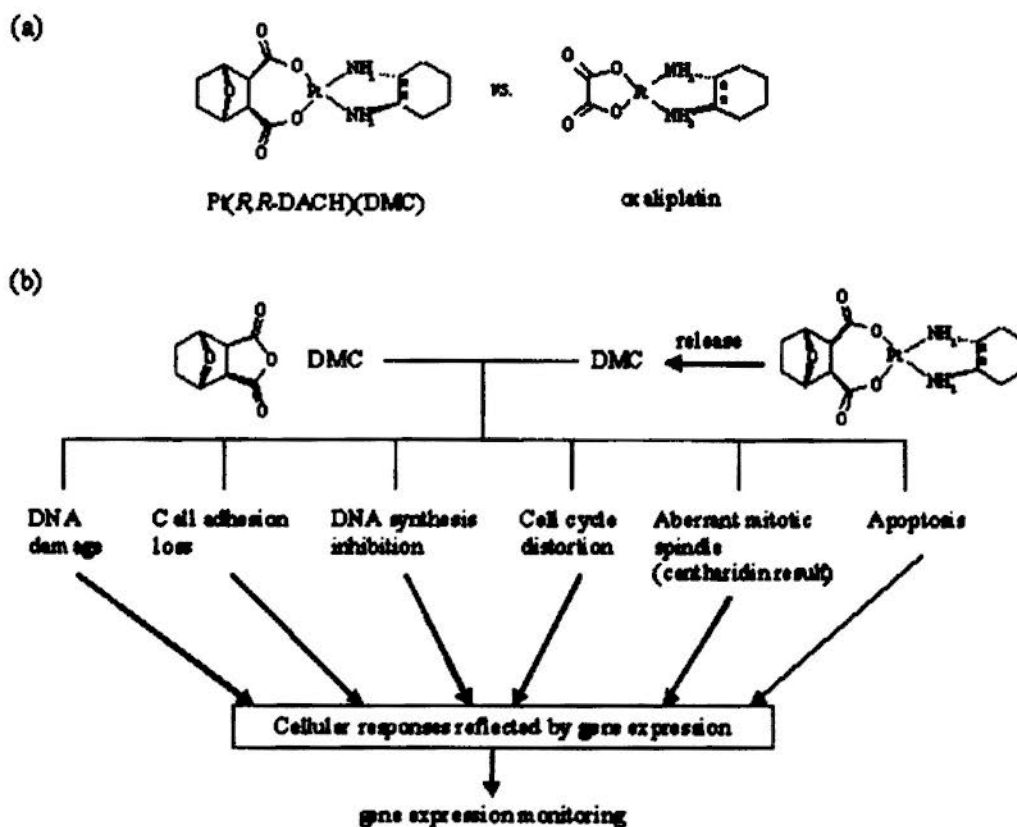


Figure 1. (a) DACH-containing Pt compounds compared in the microarray analysis. (b) Strategy used in the analysis of gene expression changes in response to DMC released from Pt (*R,R*-DACH) (DMC), using the Affymetrix HG-U133A oligonucleotide microarray.

synthesized from the Diels-Alder reaction between furan and maleic anhydride, and (*R,R*-DACH)-Pt-(DMC) was synthesized according to procedures described previously (3).

Cell culture and drug treatment. HCT116 cells from the American Type Culture Collection (ATCC, Rockville, MD, USA) were grown in RPMI-1640 medium, supplemented with 10% fetal bovine serum, 100 U/ml penicillin and 100 μ M/ml streptomycin. Cells were plated in tissue culture dishes and incubated (37°C, 5% CO₂) for 18-24 h before drug treatment. Oxaliplatin and (*R,R*-DACH)-Pt-(DMC) at their IC₅₀ values in HCT116 cells (i.e. 1.24 and 0.40 mM, respectively) were exposed to cells for 72 h (3).

Determination of relative gene expression. After drug treatment, adherent cell populations were harvested for subsequent expression profile analysis. Total RNAs were extracted with TriReagent according to the manufacturer's protocol (Molecular Research Center, USA), and purified and cleaned by passing through an RNeasy column (Qiagen, Valencia, USA). The differential expression of genes in HCT116 cells treated with (*R,R*-DACH)-Pt-(DMC) and oxaliplatin was examined by microarray analysis according to the Affymetrix microarray protocol (Affymetrix, Santa Clara, USA). The samples were subjected to oligonucleotide array analysis using the human HG-U133A GeneChip that contains ~54,000 probe sets including 38,500 well-characterized human genes. Cells treated with (*R,R*-DACH)-Pt-(DMC) or oxaliplatin were compared. Experiments were duplicated and

data analyzed with the GeneChip Operating Software (GCOS). The criterion for gene selection was a fold-change of ≥ 2.0 in the two experiments.

Results

Microarray analysis. The effect on the gene expression of HCT116 cells treated with either oxaliplatin or (*R,R*-DACH)-Pt-(DMC) was compared by microarray technology, where the analysis was able to differentiate genes influenced by the DMC ligand. The results showed that 141 genes were up-regulated and 4 were down-regulated (data not shown). The classification of the function of each gene was according to the information provided by the NetAffx Analysis Center (www.affymetrix.com). Forty-eight genes were classified into different categories based on the cellular responses induced by DMC, and summarized in sub-sections, as shown in Table 1: DNA repair (Table 1a), DNA synthesis (Table 1b), cell adhesion (Table 1c), cell cycle regulation (Table 1d), mitotic spindle checkpoint (Table 1e) and apoptosis/anti-apoptosis (Table 1f). The average fold changes ranged from 2.1 to 3.8. No down-regulated genes were found among the 48 genes. The results from each category will be discussed in detail.

Genes involved in DNA repair. Sixteen genes associated with DNA repair were found to be up-regulated, and a summary of their involvement in the relevant sub-groups is shown in Table 1a. Specific genes included *TOP2A*, which is involved

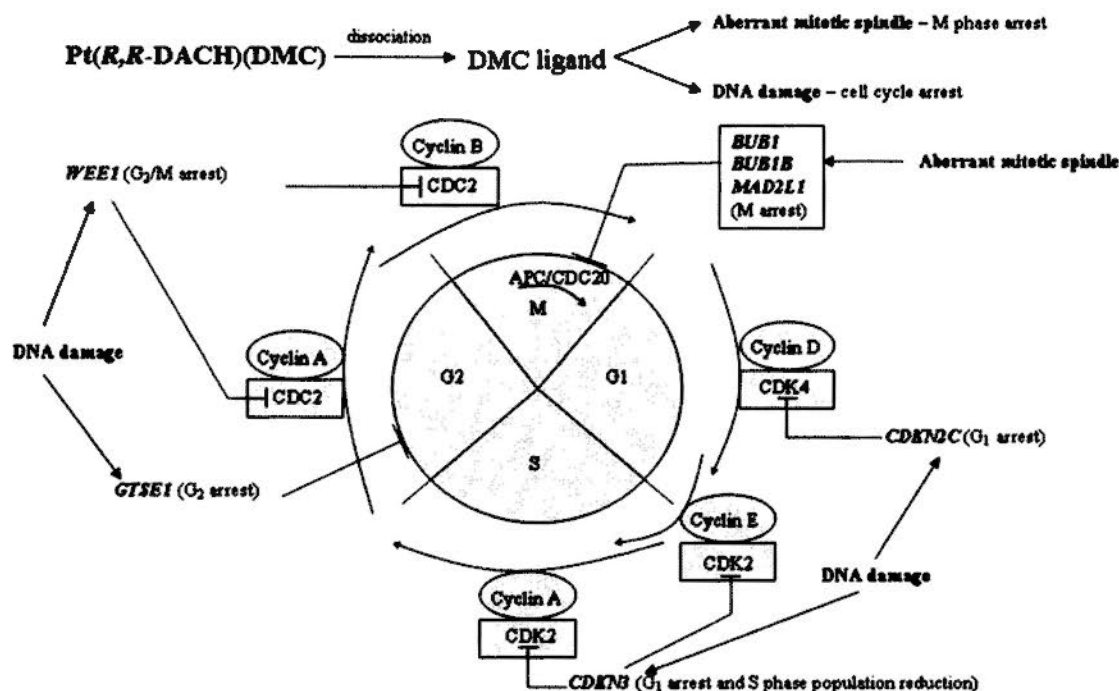


Figure 2. The cell cycle regulation controlled by the expression of cyclin-dependent kinase inhibitor genes induced by the DMC ligand is shown.

in the cleavage and ligation of phosphodiester bonds; *USP1*, which inhibits PCNA activity; *RFC3*, 4 and 5, involved in the loading of PCNA; *RAD51AP1* and *RAD51*, important for strand transfers in homologous recombination (HR); *RAD54B*, which interacts with DNA damage sites in HR; *BRCA1*, a gene that facilitates HR and non-homologous end-joining (NHEJ) processes; *CSPG6*, which contains damaged and undamaged chromatids; *FEN1*, involved in flap cleavages in base excision repair (BER) and the elimination of divergent sequences in HR (9); *POLE2*, involved in DNA synthesis; *HMGB1* and *HMGB2*, important for recognition of the DNA cross-links; and *MSH2* and *MSH1*, for recognition of mismatch in mismatch repair (MMR). Among this group of genes, the expression of *HMGB2* was found to be the most affected (average fold change: 3.6).

Genes involved in DNA synthesis. Twenty-eight genes related to DNA synthesis were found to be up-regulated and summarized (Table 1b). Among this group, 8 genes are linked to DNA repair: *TOP2A*, *RFC3*, 4, and 5, *FEN1*, *HMGB1*, *HMGB2* and *POLE2*. Seven of these are linked to nucleotide synthesis: *RRM1* and 2, involved in the production of deoxyribonucleotides; *TK1*, which converts thymidine to TMP; *DUT*, which converts dUTP to dUMP; *DCK*, which converts deoxycytidine to dCMP; *PRPS2*, which converts ribose 5-phosphate to 5'-phosphoribosyl-1-pyrophosphate; and *DHFR*, involved in the reduction of folic acid to tetrahydrofolate. Eleven of the 28 genes are related to initiation of DNA replication: *ORC1L*, *MCM2*, 4, 5, 6 and 7, which form the pre-replication complex; *GINS1* and 2, involved in the unwinding of the replication fork; *PRIM1*, a primer; *CDC6*, involved in the loading of the MCM complex; and *CDC7*, important for the phosphorylation of the MCM complex. From this latter group, *MCM4* appears to be the most significant gene as

three probe sets (212141_at, 212142_at and 222036_s_at) were identified, of which one (212141_at) had the highest gene expression (average fold change: 3.6).

Genes involved in cell adhesion. Two genes associated with cell adhesion were up-regulated (Table 1c). *ITGB3BP* activates $\beta 3$ integrin, whereas *KITLG* promotes cell adhesion directly and activates integrins (10,11). *KITLG* is the more significant gene due to the two probe sets (207029_at and 211124_s_at) being expressed. The average fold change for the 211124_s_at probe set was 2.8.

Genes involved in cell cycle regulation. Eight up-regulated genes involved in cell cycle regulation were detected and summarized (Table 1d and Fig. 2). These include *CDKN2C* which causes G_1 arrest and *CDKN3* which inhibits the G_1/S transition and reduces the S-phase population, *WEE1* which induces G_2/M arrest, and *GTSE1* which causes G_2 arrest and is also a DNA damage response gene. Others include mitotic checkpoint genes *BUB1*, *BUB1B* and *MAD2L1* which cause M-phase arrest. The most prominent gene was *BUB1*, as two probe sets (209642_at and 215509_s_at) were detected where the average gene expression fold change for the 209642_at probe set was the highest at 3.8. The three mitotic checkpoint genes are induced when the mitotic spindle becomes aberrant.

Genes involved in apoptosis and antiapoptosis. The three genes involved in antiapoptosis were: *BIRC5*, *ITGB3BP* and *BRCA1* (Table 1e and Fig. 3). *ITGB3BP* participates in cell adhesion, and *BRCA1* is involved in DNA repair as described previously. The role of *HMGB1* remains unclear as there are reports that it facilitates apoptosis by activating p53 (12), but it has also been suggested that it can act as an antiapoptotic protein (13). The most notable gene was *BIRC5* where two

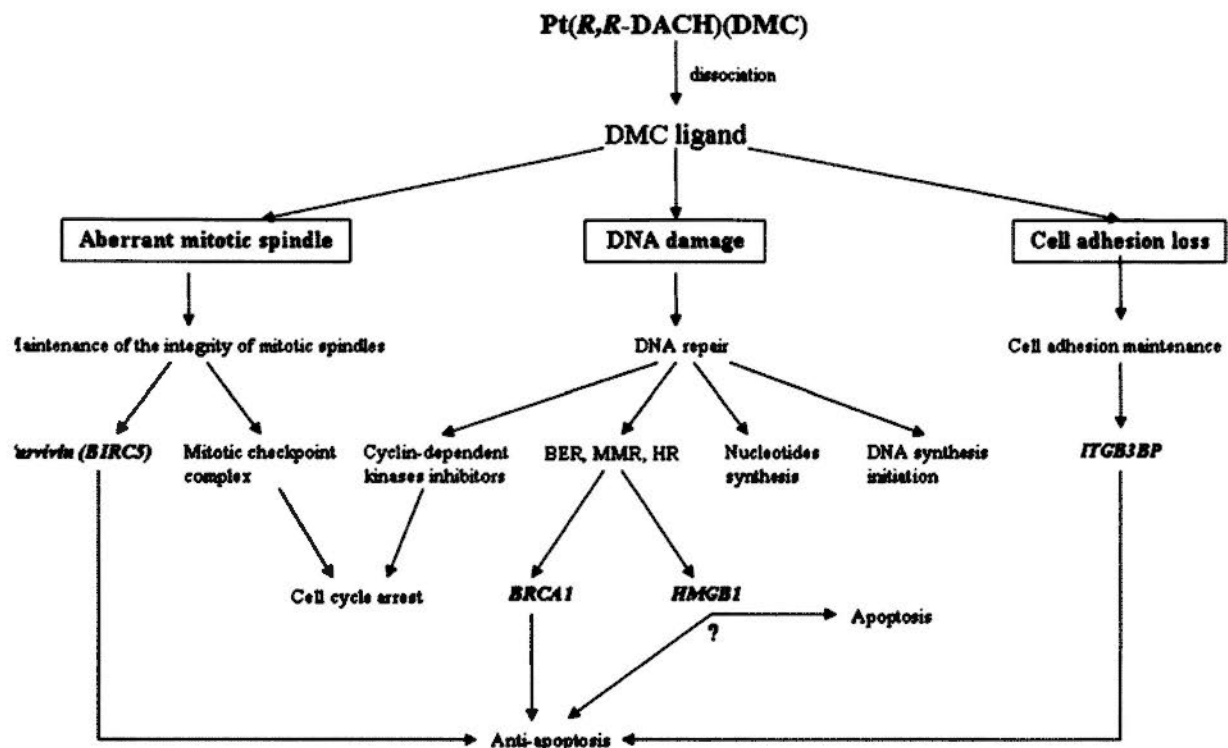


Figure 3. Apoptosis and antiapoptosis genes apparently induced by the DMC ligand.

probe sets (202094_at and 202095_s_at) were observed and the average fold change for the 202095_s_at probe set was the highest (3.6). *BIRC5* is triggered when defects are present in the mitotic spindle assembly.

Discussion

The microarray data revealed that changes in the expression of specific genes can distinguish cellular responses due to the DMC ligand. The results provided further insight into DMC contribution to the overall mechanism of cytotoxicity in HCT116 cells. Selection of the genes was based on their appearance in two experimental trials with a difference in expression of ≥ 2 -fold. Thus, the reliability of the results in this study is significantly increased. The impact of this study is that it has demonstrated that 48 out of 145 genes (one-third of the data) can be correlated with cellular responses induced by DMC (Fig. 1b), as opposed to that of oxaliplatin.

In this study, cells were subjected to drug treatment for 72 h, which was sufficient exposure time to enable the triggering of the DNA repair mechanisms to restore DMC-induced DNA damage. The genes likely to be involved in DNA repair are shown in Table 1a. *POLE2*, *RFC3*, 4 and 5, and *TOP2A* are recruited in most DNA repair mechanisms, and are found to be overexpressed in cells treated with (R,R-DACH)-Pt-(DMC) rather than oxaliplatin. This finding implied that more DNA lesions were formed which required additional repairing units. These observations concurred with our recent report that (R,R-DACH)-Pt-(DMC) caused more serious DNA damage when compared with oxaliplatin (4). The results also showed that *FEN1* in BER, *BRCA1*, *RAD51*, *RAD51AP1*, *RAD54B* and *CSPG6* in HR, and *MSH2* and *MSH6* in MMR were overexpressed. Therefore, we conclude

that the DMC ligand can damage DNA bases, induce DNA strand breaks and cause nucleotide mismatch, which are then repaired by the BER, HR and MMR mechanisms, respectively.

NER is generally believed to be involved in the removal of Pt-DNA adducts (14). However, no changes in the expression of genes directly related to NER were found in this analysis. This is consistent with the NCI (National Cancer Institute) microarray data for cantharidin (15). It is noteworthy that the HMGB1 protein, which protects Pt-DNA adducts from recognition by the NER proteins (repair shielding model) and blocks the removal of Pt-DNA adducts (12), and the HMGB1 gene were found to be up-regulated in this study. The implication is that the over-expression of *HMGB1*, induced by the DMC ligand, may assist or enhance the drug action originating from the platinum (Pt-DACH) moiety. However, a recent report showed that introducing a foreign *HMGB1* gene did not influence the cytotoxicity of platinum drugs (16).

The *USP1* gene blocks all DNA repair mechanisms through the deubiquitination of PCNA (17), and its expression in (R,R-DACH)-Pt-(DMC)-treated cells was found to be higher than oxaliplatin. Thus, it may be that the DMC ligand is able to disrupt DNA repair.

In this study, GMNN (*Geminin*) was found to be over-expressed in (R,R-DACH)-Pt-(DMC)-treated cells. Geminin binds to Cdt1 and prevents its association with the MCM complex, leading to the inhibition of the initiation of DNA synthesis (18). This is supported by a report that DMC inhibited DNA replication, which was tentatively attributed to the cleavage of the Cdc6 protein (6).

Genes facilitating nucleotide synthesis (*RRM1*, *RRM2*, *TK1*, *DUT*, *PRPS2*, *DCK* and *DHFR*), and initiation of DNA replication (*ORC1L*, *CDC6*, *MCM2*, *MCM4*, *MCM5*, *MCM6*,

Table I. Microarray analysis of HCT116 cells treated with Pt (*R,R*-DACH) (DMC) vs. oxaliplatin.^a

Probe set ID	Gene symbol	Fold change 1	Fold change 2
(a) DNA repair genes			
201291_s_at	<i>TOP2A</i>	2.8	3.7
201292_at	<i>TOP2A</i>	2.6	2.8
202412_s_at	<i>USP1</i>	2.3	2.6
202911_at	<i>MSH6</i>	2.0	2.5
203209_at	<i>RFC5</i>	2.3	2.6
203210_s_at	<i>RFC5</i>	2.3	2.1
204023_at	<i>RFC4</i>	2.0	2.3
204127_at	<i>RFC3</i>	2.1	3.0
204128_s_at	<i>RFC3</i>	2.1	2.1
204146_at	<i>RAD51API</i>	2.8	3.2
204531_s_at	<i>BRCA1</i>	2.3	2.6
204767_s_at	<i>FEN1</i>	2.6	2.8
204768_s_at	<i>FEN1</i>	2.6	2.5
205024_s_at	<i>RAD51</i>	2.1	2.5
205909_at	<i>POLE2</i>	2.8	3.5
208808_s_at	<i>HMGB2</i>	3.7	3.5
209257_s_at	<i>CSPG6</i>	2.3	2.6
209421_at	<i>MSH2</i>	2.1	2.1
216508_x_at	<i>HMGB1</i>	2.3	2.1
	<i>HMG1L1</i>		
	<i>LOC644380</i>		
219494_at	<i>RAD54B</i>	2.3	2.5
(b) DNA synthesis genes			
48808_at	<i>DHFR</i>	2.1	2.8
	<i>LOC643509</i>		
201291_s_at	<i>TOP2A</i>	2.8	3.7
201292_at	<i>TOP2A</i>	2.6	2.8
201477_s_at	<i>RRM1</i>	2.3	2.3
201890_at	<i>RRM2</i>	2.3	2.8
201930_at	<i>MCM6</i>	2.5	2.8
202107_s_at	<i>MCM2</i>	2.3	2.3
202532_s_at	<i>DHFR</i>	2.0	3.2
	<i>LOC643509</i>		
202534_x_at	<i>DHFR</i>	2.3	2.6
	<i>LOC643509</i>		
202338_at	<i>TK1</i>	2.8	2.5
203209_at	<i>RFC5</i>	2.3	2.6
203302_at	<i>DCK</i>	2.6	2.6
203210_s_at	<i>RFC5</i>	2.3	2.1
203401_at	<i>PRPS2</i>	2.0	2.5
203967_at	<i>CDC6</i>	3.0	2.1
203968_s_at	<i>CDC6</i>	2.6	2.5
204023_at	<i>RFC4</i>	2.0	2.3
204127_at	<i>RFC3</i>	2.1	3.0

Table I. Continued.

Probe set ID	Gene symbol	Fold change 1	Fold change 2
204128_s_at	<i>RFC3</i>	2.1	2.1
204510_at	<i>CDC7</i>	2.0	3.0
204767_s_at	<i>FEN1</i>	2.6	2.8
204768_s_at	<i>FEN1</i>	2.6	2.5
205053_at	<i>PRIM1</i>	2.1	2.3
205085_at	<i>ORC1L</i>	2.3	2.0
205909_at	<i>POLE2</i>	2.8	3.5
206102_at	<i>GINS1</i>	2.6	2.6
208795_s_at	<i>MCM7</i>	2.6	3.0
208808_s_at	<i>HMGB2</i>	3.7	3.5
208956_x_at	<i>DUT</i>	2.1	2.0
209773_s_at	<i>RRM2</i>	2.6	2.5
210983_s_at	<i>MCM7</i>	2.5	2.3
212141_at	<i>MCM4</i>	4.6	2.6
212142_at	<i>MCM4</i>	3.2	2.0
216237_s_at	<i>MCM5</i>	3.0	2.5
216508_x_at	<i>HMGB1</i> <i>HMGIL1</i> <i>LOC644380</i>	2.3	2.1
218350_s_at	<i>GMNN</i>	2.5	2.6
221521_s_at	<i>GINS2</i>	2.6	3.2
222036_s_at	<i>MCM4</i>	2.8	2.6
(c) Cell adhesion genes			
205176_s_at	<i>ITGB3BP</i>	2.6	2.0
207029_at	<i>KITLG</i>	2.6	2.1
211124_s_at	<i>KITLG</i>	2.8	2.8
(d) Cell cycle regulation genes			
203362_s_at	<i>MAD2L1</i>	3.7	3.2
203755_at	<i>BUB1B</i>	3.0	3.7
204159_at	<i>CDKN2C</i>	3.2	3.5
204318_s_at	<i>GTSE1</i>	2.5	3.0
209642_at	<i>BUB1</i>	4.0	3.5
209714_s_at	<i>CDKN3</i>	2.3	2.5
212533_at	<i>WEE1</i>	2.8	3.0
215509_s_at	<i>BUB1</i>	2.5	3.2
(e) Apoptosis and anti-apoptosis genes			
202094_at	<i>BIRC5</i>	3.5	2.6
202095_s_at	<i>BIRC5</i>	4.0	3.2
204531_s_at	<i>BRCA1</i>	2.3	2.6
205176_s_at	<i>ITGB3BP</i>	2.6	2.0
216508_x_at	<i>HMGB1</i> <i>HMGIL1</i> <i>LOC644380</i>	2.3	2.1

Table I. Continued.

Probe set ID	Gene symbol	Fold change 1	Fold change 2
(f) Aberrant mitotic spindle response genes			
202094_at	<i>BIRC5</i>	3.5	2.6
202095_s_at	<i>BIRC5</i>	4.0	3.2
203362_s_at	<i>MAD2L1</i>	3.7	3.2
203755_at	<i>BUB1B</i>	3.0	3.7
209642_at	<i>BUB1</i>	4.0	3.5
215509_s_at	<i>BUB1</i>	2.5	3.2

Genes appearing in the two trials with a difference in expression ≥ 2 -fold were considered to be significant in this microarray analysis. ^aGenes are related to (a) DNA repair, (b) DNA synthesis, (c) cell adhesion, (d) cell cycle regulation, (e) apoptosis and antiapoptosis, and (f) aberrant mitotic spindle.

MCM7, *CDC7*, *PRIM1*, *GINS1* and *GINS2*) were over-expressed. It is assumed that the up-regulation of these genes is necessary in order to synthesize new strands during the process of repairing DMC-induced DNA lesions (Table 1b). Similarly, overexpression of the DNA replication initiation genes is presumed to be involved in DNA repair with the aim of synthesizing new strands. There is supporting evidence for the correlation of DNA replication initiation with DNA repair, where human Rad51 and Rad52, which participate in HR, have been reported to interact with MCM proteins which are a component of the pre-replicative complex in DNA replication (19). In this regard, *RAD51* and *MCM2*, 4, 5, 6 and 7 were found to be up-regulated in this study.

The microarray data revealed that the expression of *ITGB3BP* and *KITLG* was elevated, and it is suggested that this is essential in order to maintain cell adhesion capacity during the slow release of DMC from (*R,R*-DACH)-Pt-(DMC) (Table 1c).

The progression of a cell cycle is promoted by the activity of cyclin/cyclin-dependent kinase (CDK) complexes, generally regarded as engines driving this process, whereas cell cycle regulation is controlled by cyclin-dependent kinase inhibitors (20). The microarray data indicated that the CDK inhibitor genes such as *CDKN2C*, *CDKN3* and *WEE1* were all up-regulated, thus blocking the activities of CDK4, CDK2 and CDC2, respectively (Fig. 2). G_1 arrest should occur as a result of the up-regulation of *CDKN2C* and *CDKN3*. A reduction of the S-phase population is likely to be caused by an overexpression of *CDKN3*, while an overexpression of *WEE1* leads to G_2/M arrest. It is reasonable to assume that the release of DMC from the (*R,R*-DACH)-Pt-(DMC) complex causes more serious DNA damage that results in overexpression of the three cyclin-dependent kinase inhibitor genes, leading to the reinforcement of cell cycle arrest and subsequent DNA repair. The *GTSE1* gene, which induces G_2 arrest on DNA damage (21), was also found to be up-regulated. These observations are in agreement with our previous results of the cell cycle distribution where G_1 arrest, S-phase population reduction and G_2/M arrest were clearly demonstrated for

HCT116 cells treated with (*R,R*-DACH)-Pt-(DMC) or DMC alone (3).

A recent study has indicated that the mitotic spindles were aberrant after cantharidin treatment (8). From this microarray analysis, *MAD2L1*, *BUB1B* and *BUB1* were highly expressed in cells treated with Pt (*R,R*-DACH) (DMC). *MAD2L1* and *BUB1B* are components of the mitotic checkpoint complex that cause mitotic arrest when defects are present in the spindle assembly, and in the bipolar attachment of chromosomes (Fig. 2) (22). *BUB1* is located on the kinetochores during mitosis, and recruits other mitotic checkpoint proteins (23). An important function of survivin (*BIRC5*) is to maintain mitotic arrest in response to defects in the mitotic machinery (24), and in this study, expression of *BIRC5* was found to be up-regulated. Therefore, it is proposed that DMC can disrupt the organization of the mitotic spindles. As a result, genes related to the mitotic checkpoint complex are up-regulated.

A summary of the apoptotic and antiapoptotic genes apparently induced by the DMC ligand is shown in Fig. 3. Overexpression of several genes [*ITGB3BP* (25), *BRCA1* (26) and *BIRC5* (24)] involved in the antiapoptotic process was found. The role of the *HMGB1* gene in apoptosis remains unclear as previous reports have indicated that it may facilitate apoptosis by activating p53 (12). However, *HMGB1* has been reported as an antiapoptotic protein (13).

In conclusion, the influence of the DMC ligand on the gene expression in HCT116 cells is multi-faceted, and competently demonstrated using microarray technology. For example, the increase in the expression of genes related to DNA repair was triggered by DNA lesions caused by the DMC ligand that is released from the parent complex. The DMC ligand is likely to have caused DNA base damage, DNA strand break, and nucleotide mismatch as exemplified by the BER, HR and MMR genes, respectively, being recruited to repair these lesions. Moreover, the ligand may cause an aberrant mitotic spindle with a subsequent overexpression of genes related to the mitotic checkpoint complex and survivin. Due to further damage induced by the DMC ligand, genes related to the cyclin-dependent kinase inhibitors and the mitotic checkpoint

complex were overexpressed in order to reinforce cell cycle arrest and allow the cells to repair damage. Finally, anti-apoptotic genes were also up-regulated and it is proposed that the inherent defense mechanism of the cell is triggered. These genes may contribute towards resistance against apoptosis which is induced by the DMC ligand, allowing the cells to survive. This study has highlighted the possibility of a dual mechanism of anticancer action exerted by the novel (*R,R*-DACH)-Pt-(DMC) complex, but further studies are required to determine the exact role of DMC.

Acknowledgements

Financial assistance from the Research Grant Council of Hong Kong SAR (RGC Ref: 4357/04M) is gratefully acknowledged. We thank The Chinese University of Hong Kong (CUHK) for the provision of studentships to C.W. Yu and H. Guan. Technical assistance from the Gene Company Limited (Hong Kong) and GeneTech Biotechnology Limited Company (Shanghai, China) is acknowledged.

References

1. Raymond E, Faivre S, Chaney S, Woynarowski J and Cvitkovic E: Cellular and molecular pharmacology of oxaliplatin. *Mol Cancer Ther* 1: 227-235, 2002.
2. Massicot F, Dutertre-Catella H, Pham-Huy C, Liu XH, Due HT and Warnet JM: *In vitro* assessment of renal toxicity and inflammatory events of two protein phosphatase inhibitors cantharidin and nor-cantharidin. *Basic Clin Pharmacol Toxicol* 96: 26-32, 2005.
3. Yu CW, Li KKW, Pang SK, Au-Yeung SCF and Ho YP: Anti-cancer activity of a series of platinum complexes integrating demethylcantharidin with isomers of 1,2-diaminocyclohexane. *Bioorg Med Chem Lett* 16: 1686-1691, 2006.
4. Pang SK, Yu CW, Au-Yeung SCF and Ho YP: DNA damage induced by novel demethylcantharidin-integrated platinum anti-cancer complexes. *Biochem Biophys Res Commun* 363: 235-240, 2007.
5. Chen YJ, Shieh CJ, Tsai TH, Kuo CD, Ho LT, Liu TY and Liao HF: Inhibitory effect of norcantharidin, a derivative compound from blister beetles, on tumor invasion and metastasis in CT26 colorectal adenocarcinoma cells. *Anti-cancer Drugs* 16: 293-299, 2005.
6. Li JL, Cai YC, Liu XH and Xian LJ: Norcantharidin inhibits DNA replication and induces apoptosis with the cleavage of initiation protein Cdc6 in HL-60 cells. *Anti-cancer Drugs* 17: 307-314, 2006.
7. Chen YN, Chen JC, Yin SC, Wang GS, Tsauer W, Hsu SF and Hsu SL: Effector mechanisms of norcantharidin-induced mitotic arrest and apoptosis in human hepatoma cells. *Int J Cancer* 100: 158-163, 2002.
8. Bonness K, Aragon IV, Rutland B, Ofori-Acquah S, Dean NM and Honkanen RE: Cantharidin-induced mitotic arrest is associated with the formation of aberrant mitotic spindles and lagging chromosomes resulting, in part, from the suppression of PP2Aa. *Mol Cancer Ther* 5: 2727-2736, 2006.
9. Kikuchi K, Taniguchi Y, Hatanaka A, Sonoda E, Hochegger H, Adachi N, Matsuzaki Y, Koyama H, van Gent DC, Jasin M and Takeda S: Fen-1 facilitates homologous recombination by removing divergent sequences at DNA break ends. *Mol Cell Biol* 25: 6948, 2005.
10. Liu S, Calderwood DA and Ginsberg MH: Integrin cytoplasmic domain-binding proteins. *J Cell Sci* 113: 3563-3571, 2000.
11. Ashman LK: The biology of stem cell factor and its receptor C-kit. *Int J Biochem Cell Biol* 31: 1037-1051, 1999.
12. Widlak P, Pietrowska M and Lanuszewska J: The role of chromatin proteins in DNA damage recognition and repair. *Histochem Cell Biol* 125: 119-126, 2006.
13. Müller S, Ronfani L and Bianchi ME: Regulated expression and subcellular localization of HMGB1, a chromatin protein with a cytokine function. *J Intern Med* 255: 332-343, 2004.
14. Wang D and Lippard SJ: Cellular processing of platinum anti-cancer drugs. *Nat Rev Drug Discov* 4: 307-320, 2005.
15. Efferth T, Rauh R, Kahl S, Tomacic M, Böchzelt H, Tome ME, Briehl MM, Bauer R and Kaina B: Molecular modes of action of cantharidin in tumor cells. *Biochem Pharmacol* 69: 811-818, 2005.
16. Jung Y and Lippard SJ: Direct cellular responses to platinum-induced DNA damage. *Chem Rev* 107: 1387-1407, 2007.
17. Friedberg EC: Reversible monoubiquitination of PCNA: a novel slant on regulating translesion DNA synthesis. *Mol Cell* 22: 150-152, 2006.
18. Saxena S and Dutta A: Geminin-Cdt1 balance is critical for genetic stability. *Mutat Res* 569: 111-121, 2005.
19. Shukla A, Navadgi VM, Mallikarjuna K and Rao BJ: Interaction of hRad51 and hRad52 with MCM complex: a cross-talk between recombination and replication proteins. *Biochem Biophys Res Commun* 329: 1240-1245, 2005.
20. Malumbres M and Barbacid M: Mammalian cyclin-dependent kinases. *Trends Biochem Sci* 30: 630-641, 2005.
21. Taylor WR and Stark GR: Regulation of the G2/M transition by p53. *Oncogene* 20: 1803-1815, 2001.
22. Taylor SS, Scott MIF and Holland AJ: The spindle checkpoint: a quality control mechanism which ensures accurate chromosome segregation. *Chromosome Res* 12: 599-616, 2004.
23. Hoffmann I: Protein kinase involved in mitotic spindle checkpoint regulation. In: *Cell Cycle Regulation: Results and Problems in Cell Differentiation*. Kaldis P (ed). Vol. 4, Springer, New York, p31-63, 2006.
24. Castedo M, Perfettini JL, Roumier T, Andreau K, Medema R and Kroemer G: Cell death by mitotic catastrophe: a molecular definition. *Oncogene* 23: 2825-2837, 2004.
25. Damiano JS: Integrins as novel drug targets for overcoming innate drug resistance. *Curr Cancer Drug Targets* 2: 37-43, 2002.
26. Deng CX: BRCA1: cell cycle checkpoint, genetic instability, DNA damage response and cancer evolution. *Nucleic Acids Res* 34: 1416-1426, 2006.